Synthesis of Structure Determining Agents (SDAs) for zeolites with extra-large pore size

Jawad Fayek

Normandie Université

UNIVERSITÉ CAEN NORMANDIE

THÈSE

Pour obtenir le diplôme de doctorat

Spécialité **CHIMIE**

Préparée au sein de l'**Université de Caen Normandie**

Synthesis of Structure Determining Agents (SDAs) for Zeolites with Extra-large Pore Size

Présentée et soutenue par

JAWAD FAYEK

Thèse soutenue le 05/01/2024

devant le jury composé de :

M. SAMI LAKHDAR	Chercheur au CNRS - UNIVERSITE TOULOUSE 3 PAUL SABATIER	Rapporteur du jury
MME LOUWANDA LAKISS	Ingénieur de recherche - CNRS	Membre du jury
M. PAUL-ALAIN JAFFRES	Professeur des universités - UNIVERSITE BRET. OCCIDENTALE UBO	Président du jury
M. BERNHARD WITULSKI	Directeur de recherche au CNRS - ENSICAEN	Directeur de thèse

Thèse dirigée par **BERNHARD WITULSKI** (Laboratoire de chimie moléculaire et thio-organique (Caen))

ED 508 NC Normande de Chimie

lcmt

Acknowledgments

This section is dedicated to all individuals who have been part of this journey in one way or another.

The research presented in this work was carried out at the Laboratoire de Chimie Moléculaire et Thio-organique (LCMT) from October 2020 to October 2023. Throughout this journey, I extend my sincere appreciation to Dr. Bernhard Witulski for his invaluable support, assistance, and guidance.

I would also like to express my heartfelt gratitude to the members of my thesis committee: M. Sami Lakhdar, M. Paul-Alain Jaffres and MMe. Louwanda Lakiss. I am truly grateful to have them as jury members, evaluating my thesis dissertation, and being part of this special day.

Furthermore, I wish to thank the LCMT family, starting with Prof. Thiery LEQUEUX, the director of the LCMT laboratory, Dr. Jean Luc Renaud, and Dr. Carole Witulski Alyrac. Special thanks go to my referent teacher, Prof. Loïc LE PLUART, for his assistance and guidance throughout this thesis.

I extend my appreciation to the administrative team, particularly Mme. Marie-Cecile Helaine and Mme. Janine Amice, for their unwavering dedication, professionalism, and ability to handle any issues, ensuring a smooth and efficient administrative process. Also, special thanks goes to Dr. Isabelle Dez for her help and support.

Likewise, I would like to express my gratitude to the LCS family, especially my colleague Mohamad Fahda, for his efforts in our project. I also like to thank Prof. Valentin for his supervision alongside Dr. Bernhard.

I am incredibly grateful for my colleagues at the BW group, namely Igor Bożek, Andrii Byrka, Nela Beytlerová, and Illia Lenko. I also want to thank my closest friend, Fatima, for her invaluable presence and the cherished memories we shared during these three years. Additionally, I would like to thank my colleagues from other groups for the valuable discussions and pleasant memories. Special thanks go to my friends Abdel Aziz Wayzani,

Malak Qassab, Nicolas Joly, Mohammed Waquaruddin Siddiqui, Yougourthen Boumekla, Aimar Gonzalo-Barquero, and Lilia Anani.

Gratitude is also extended to the personnel in charge of the NMR service, namely Rémi Legay and Hussein El Siblani, and to Karine Jarsale for mass spectroscopy. I appreciate Guillaume MORCEL for his efficiency in handling the reception and distribution of products and materials.

Throughout the ups and downs of these three years, I owe a huge debt of thanks to my fiancée, my support system, for easing my difficult times and for her care and assistance in pursuing my dreams. Moreover, I am thankful to my parents for shaping me into the person I am today. I will always strive to make you proud.

List of abbreviations

A

Å	Angstrom
Ac	Acetyl
Aq	Aqueous
Ar	Argon
Ac_2O	Acetic anhydride

B

BBU	Basic Building Unit
Bn	Benzyl
Bu	Butyl
Boc	tert-butyloxycarbonyl

C

°C	Degree Celsius
CBU	Composite Building Units
$CsCO_3$	Cesium carbonate
CH_3CN	Acetonitrile
$CHCl_3$	Chloroform
Cy	Cyclohexyl

D

D_2O	Deuterated water
DCE	Dichloroethane
DCM	Dichloromethane
DIPEA	N,N-Diisopropylethylamine
DMF	Dimethylformamide
DMSO	Dimethylsulfoxide

E

E	Electrophile
Equiv.	Equivalents
Et	Ethyl
Et_2O	Diethylether
EtOAc	Ethyl acetate
EG	Ethylene glycol
EWG	Electron withdrawing group
ELP	Extra-Large Pore

H

HCl	Hydrochloric acid
Hz	Hertz

I

IR	Infrared spectroscopy

M

Me	Methyl
$MgSO_4$	Magnesium sulfate
mg	Milligram
min	Minute
ml	Millilitre
mmol	Millimole
MR	Member ring

N

NMR	Nuclear magnetic resonance
Nu	Nucleophile

P

Pd	Palladium
$Pd(PPh_3)_4$	Tetrakis(triphenylphosphine)palladium
$Pd(OAc)_2$	Palladium acetate
$Pd(PPh_3)_2Cl_2$	Bis(triphenylphosphine)palladium
Ph	Phenyl
ppm	Parts per million

R

r.t.	Room temperature
R	General alkyl group

S

SM	Starting material

T

T	Temperature
TCE	Tetrachloroethane
TEA	Triethylamine
Tf	Trifluoromethanesulfonate
TMS	Trimethylsilyl
TS	Transition state

X

X-phos	Ligand
XRD	X-Ray Diffraction

Table of Contents

General Introduction

Zeolites represent a class of naturally occurring or synthetically produced crystalline minerals with a unique porous structure. They belong to a class of silicate and substituted silicate minerals, formed of one, two, or three-dimensional frameworks characterized by pores and channels. In addition to pores and channel systems, zeolites are also defined by their chemical composition.

In recent years, research is more oriented toward the synthesis of zeolites with extra-large pore size. These unique zeolites offer significant advantages, especially in industrial sector, as they can enhance bulky molecule accessibility and reduce diffusion limitations. Consequently, there is a considerable demand for extra-large pore zeolites in industries such as petrochemicals and pharmaceuticals. Also, they find many applications in environmental procedures like water purification. However, the synthesis of zeolites with extra-large pores poses many challenges. As of now, only 23 extra-large pore size zeolites have been reported, and many of them encounter stability issues due to the presence of elements like germanium in their framework, thereby limiting their use.

The use of structure-directing agents (SDAs) play an important role in controlling the pore size of zeolites during their synthesis. Usually, the SDAs used for synthesizing zeolites with extra-large pore sizes are mainly based on ammonium salts. Nevertheless, an emerging alternative for preparing such zeolites involves the use of phosphonium salts as promising structure-directing agents.

In this thesis, our aim was to synthesize a set of ammonium and phosphonium salts with different alkyl and aryl chains based on size expansion approach. The prepared salts were tested as possible SDAs in the synthesis of extra-large pore size zeolites by our colleague in the LCS laboratory. Zeolites with silicate and alumino-silicate frameworks were targeted due to their stability and promising character in industry. Moreover, our second target was to resynthesize ZEO-1 zeolite, a new discovered zeolite with interesting characteristics, for spectroscopic examination of its stability and acid site accessibility.

This manuscript is structured into four chapters:

- Chapter 1 provides an overview about zeolites, their synthesis, and the criteria required by structure directing agents (SDAs) to facilitate their formation with unique frameworks. This chapter focus mainly on the use of ammonium and phosphonium salts as structure directing agents (SDAs) in zeolite synthesis. Moreover, it describes the methodologies used for designing structure directing agents specifically used for the preparation of zeolites with extra-large pore sizes. Additionally, this chapter include a comprehensive listing of the discovered

extra-large pore size along with the corresponding ammonium and phosphonium based SDAs. A special focus is given to ZEO-1 zeolite, a new alumino-silicate extra-large pore-size zeolite with interesting structure, synthesized using phosphonium based SDA.

- Chapter 2 (results and discussion), shows the different categories of ammonium and phosphonium salts that we synthesized and purified, also highlighting the encountered challenges during their preparation process. Additionally, this chapter provides the experimental procedures applied in the synthesis of the salts with their characterization.

- Chapter 3 (results and discussion), shows the attempts carried out by our collaboators in the LCS laboratory, in which they used the prepared salts in chapter 2 for zeolite synthesis. Moreover, this chapter provides an interpretation account of the obtained results and their significance.

Parallel to this project , a new approach for the synthesis of indoles and aryl phosphine oxides starting from *N*-aryl ynamide is reported in this manuscript. This approach shows the effect of substituents on the ynamide and their role in either obtaining indole or aryl phosphine oxides. Furthermore, this chapter contains a detailed experimental part for the prepared molecules.

Chapter One

1. Introduction to zeolites

It all started in 1756, when a Swedish mineralogist A. F. Cronstedt discovered zeolite or in Greek words zeôlithos (the boiling stone).[1] Zeolites are uniformly crystalline porous materials formed of a vertex sharing TO_4 units (T = Si, P, Al, Ge, Ga, B etc.; O = oxygen). Moreover, Zeolites can be found naturally in the environment, for example chabazite ($|Ca_6\ (H_2O)_{40}\ |_{1/3}\ [Al_{12}Si_{24}O_{72}]_{1/3}$-CHA), erionite ($|(Ca,Na_2)_{3.5}\ K_2\ (H_2O)_{27}|\ [Al_9Si_{27}O_{72}]$-ERI), mordenite ($|Na_8\ (H_2O)_{24}\ |\ [Al_8Si_{40}O_{96}]$-MOR), and clinoptilolite ($|Ca_4\ (H_2O)_{24}\ |\ [Al_8Si_{28}O_{72}]$-HEU); or can be synthesized under hydrothermal conditions. The arrangement of TO_4 units result in the formation of unique pore and channel network with different potential uses. For example, zeolites are used in the petrochemical industry: petroleum cracking, petroleum product dewaxing, and methanol convergent.[2] They are also used as ingredients in detergents,[3] ion exchange [3, 4] catalysis,[5] and in purifying water from nuclear,[6] and house wastes[7].

1.1. Zeolite Nomenclature, Classification and Construction

- Zeolite nomenclature:

The International Union of Pure and Applied Chemistry (IUPAC) defines zeolite as follow:[8]

|guest composition| [host composition] (Sym)-IZA

The International Zeolite Association has designated the three-letter code "IZA" to denote the structural framework (topology) of zeolites. The framework designation is usually derived from the name of the zeolite or type material, with examples such as FAU zeolite from Faujasite, LTA zeolite from Linde Type A (LTA), and MFI zeolite from ZSM-5 (Zeolite Secony Mobil-five). Currently, there are 260 structural codes accepted (accessed on 25/03/2023).[9] The following is an illustration of this terminology:[8]

$|Na_{12}(H_2O)_{27}|\ [Al_{12}Si_{12}O_{48}]$ (8-ring)-LTA

- Zeolite classification:

In 1970, Meier and Olson introduced the classification of zeolite materials according to their framework type. The term framework describes the shape and dimension of zeolite referring to the connectivity of tetrahedral coordinated atoms (TO_4) at the highest possible symmetry.[10] Moreover, the framework structure does not take into account the framework's chemical

composition (T = Si, P, Al, Ge, Ga, B, etc.). Therefore, this allows many different zeolites to be categorized under one type of framework, such as ZSM-5,[11] AMS-1B,[12] AZ-1,[13] BOR-C,[14] and NU-5[15], all sharing the MFI framework type regardless of their chemical composition. Zeolite frameworks are primarily divided into groups based on their channel system[16] and microporosity.[17] The zeolite channel systems are categorized as one-dimensional (such as AEL type), two-dimensional (such as MRT), or three-dimensional (such as MEL).[9] Furthermore, the pore openings found in a zeolite are characterized by the number of T-atoms or O-atoms in the ring connected to each other. For example, Figure 1 shows the MFI framework with 10 blue dots. Each blue dot represents a T or oxygen atom, so if there are 10 T atoms (10 blue dots) it means that the number of tetrahedral (TO_4) is 10 or it is a 10-member ring zeolite. Moreover, zeolite microporosity is more defined by the size of the largest ring found in the framework. As a result, based on the number of T atoms, zeolites are divided into four groups (Table 1): [9]

- Small pore-size zeolites, with 8 member ring (TO_4 = 8), their pore diameter is around 4 Å, for example, AlPO-18 with AEI topology (Framework)
- Medium pore-size zeolites, with 10 member ring (TO_4 = 10), their pore diameter is around 4.99 Å, for example, EU-1 with EUO topology (Framework)
- Large pore-size zeolites, with 12 member ring (TO_4 = 12), their pore diameter around 7.03 Å, for example, ITQ-27 with IWV topology (Framework)
- Extra-large pore-size zeolites, with pore size greater than 12 member ring (TO_4 >12), their pore diameter greater than 7.5 Å, for example, ZEO-1 with JZO topology (Framework).

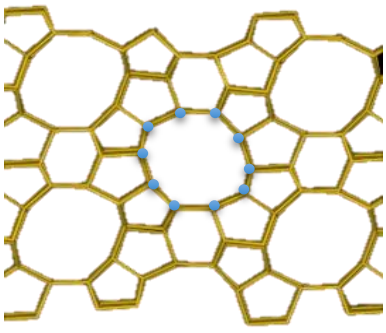

Figure 1. MFI Framework[9]

Pore Size	Number of Tetrahedra (MR)	Pore Diameter (Å)	Example
Small	8	3.84	AlPO-18 (AEI)
Medium	10	4.99	EU-1 (EUO)
Large	12	7.03	ITQ-27 (IWV)
Extra Large	>12	>7.5	ZEO-1 (JZO)

Table 1: Classification of zeolites according to their pore size; [9] MR: Members of the ring

- Zeolite construction

The TO_4 tetrahedron, known as the Basic Building Unit (BBU), is the fundamental building block of all zeolites.[18] The spatial connection of a certain number of BBU up to 16 atoms (T =16) forms a larger building unit called Secondary Building Unit (SBUs). Subsequently, a group of SBU forms a Composite Building Unit (CBUs) that reflects the zeolitic framework's properties. A zeolite framework may contain CBUs of various types. Therefore, different zeolites can share the same CBUs. An example to explain zeolite construction is shown in Figure 2, the union of BBUs forms SBUs (e.g. 4 and 4-4), and the union of SBUs forms CBUs (e.g. d4r (t-cub), clo (t-rpa), and lta (t-grc)), each edge refer to a T atom, and their combination describes the zeolite (e.g. Gloverite).[9]

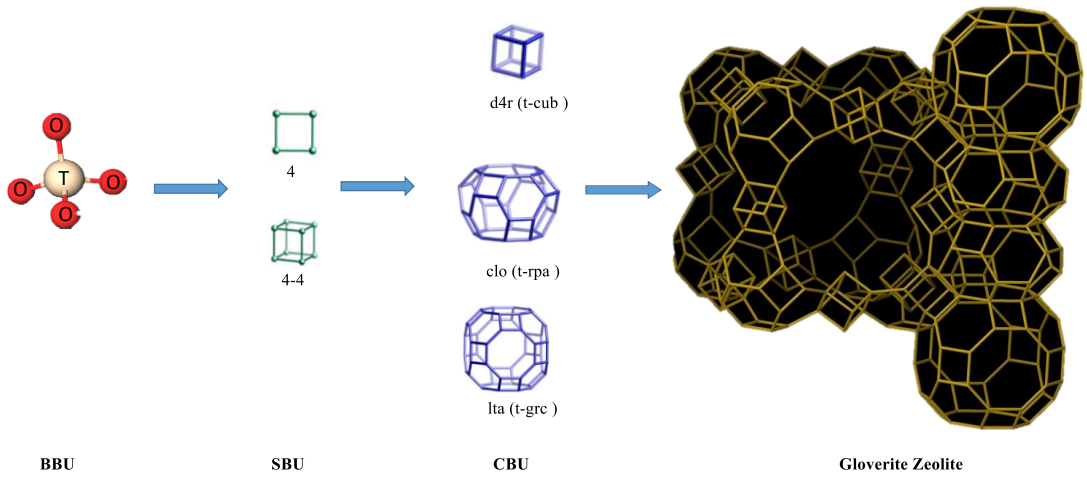

Figure 2. Construction of Gloverite Zeolite (Adapted from the IZA Database website)[9]

1.2. Zeolite Preparation

The most general approach for zeolite synthesis is the use of hydrothermal conditions. At first, hydrated alumino-silicate gel is formed by adding an aluminium (Al) source. For example Al(i-PrO)$_3$ is added to a basic aqueous solution containing organic structure-directing agents (OSDA), followed by stirring until the reactants undergo total hydrolysis (Step 1, Figure 3). Then, a silica (Si) source, such as Si(OEt)$_4$, is added and the solution is further stirred (Step 2, Figure 3). The resulting solution is heated at 85 ^{o}C in an oven to remove any excess water, until the desired H_2O:Si ratio is achieved. Secondly, the crystallization stage begins when the prepared gel-like solution is transferred to an autoclave and placed in an oven at a specific temperature for a certain time, to favor the zeolite's crystallization (Step 3, Figure 3).[19]

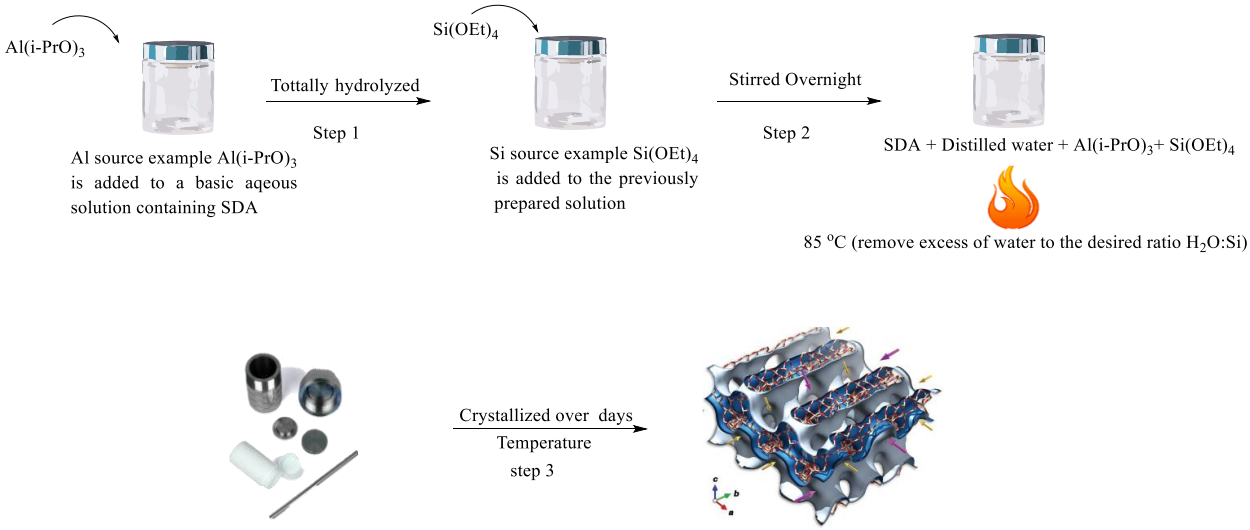

Figure 3. Steps for the preparation of aluminosilicate gel followed by its crystallization within specific time at certain temperature to afford a zeolite.

After the crystallization process, the use of organic species as structure-directing agents (SDA) for the synthesis of zeolites, is considered as the most important factor in controlling the topology of a zeolite. These organic species organize the inorganic units present in the solution, such as silica and alumina, via hydrophobic/hydrophilic interactions. At specific pH and temperature, the SDA induces nucleation and seed formation (Scheme 1 Steps 1 and 2).[20] Followed by crystal growth to obtain a zeolite with specific size, shape, and dimension (Steps 3 and 4). Finally, the last step in this process is the removal of SDAs from zeolite pores by calcination.

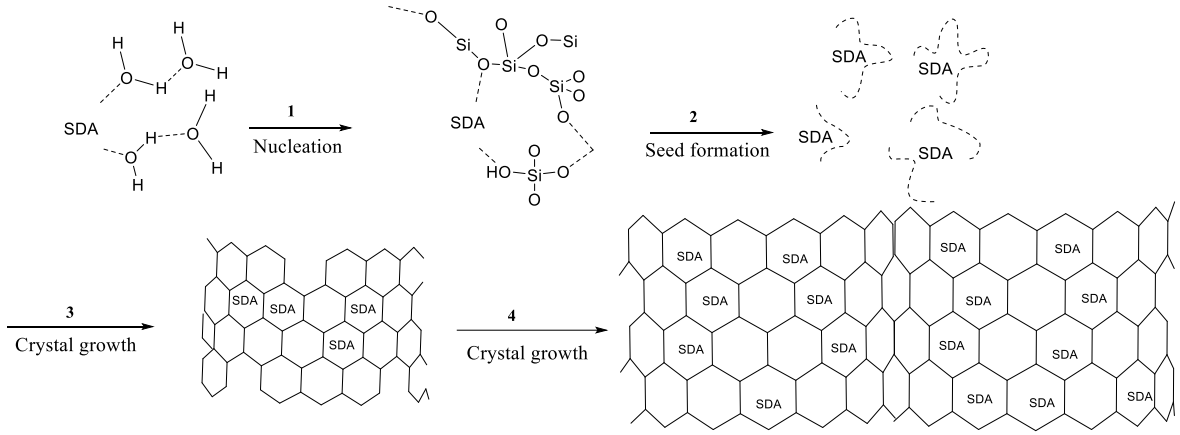

Scheme 1. Zeolite crystallization[20]

2. Use of structure-directing agents (SDAs) in zeolite synthesis

2.1. General introduction

The use of structure-directing agents in the preparation of zeolites was first introduced in 1961. [21, 22] Researchers used tetramethylammonium salt **(1)** as an organic SDA in the synthesis of ZK-4 zeolite with small pore size (Scheme 2). The use of such organic cations instead of inorganic minerals, for instance Na^+ or K^+, favor the synthesis of zeolites with lower amounts of Al due to small charge-to-volume ratio of SDA's. This was a significant discovery because low aluminium content in zeolites provides high hydrothermal stability and strong brønsted acidity. After the successful use of tetramethylammonium salt **(1)** as an SDA, researchers investigated more about organic SDAs, and another larger tetraalkyl ammonium salt was introduced. In 1967, researchers reported the discovery of the first high-silica zeolite Beta (BEA) using tetraethylammonium salt **(2)** (Scheme 2).[23] Soon after, in 1972, another important zeolite in the chemical industry,[24] the (ZSM-5), was discovered using tetrapropylammonium salt **(3)** (Scheme 2).[25] And finally, increasing the number of carbons of the alkyl substituent to four, tetrabutylammonium salt **(4)** favored the synthesis of ZSM-11 zeolite (Scheme 2).[26]

The use of tetramethylammonium cation **(1)** as SDA in the beginning resulted in the formation of zeolites with small cavities that were proportional to the size of the pores accommodated within (Scheme 2). This was the first indication of the correlation between the size and shape of the organic SDA and the pore volume of the zeolite that serves as its host. However, the correlation between the two is not always a clear-cut. This is explained by the fact that extra-large pore-size zeolite BEA, which features 12-membered rings (12 MR) and 3-dimensional

channels with a high pore volume, was discovered through the use of tetraethylammonium salt **(2)**. while, the use of larger cations such as tetrapropylammonium salt **(3)** and tetrabutyl ammonium salt **(4)** resulted in the development of medium pore size zeolites with 10-MR channels, ZSM-5 and ZSM-11, respectively (Scheme 2). The reason behind the formation of an open zeolite framework beta (BEA) when using relatively small ammonium salt **(2)**, was later linked to the clustering mode of these small ammonium salts inside the BEA framework.[27]

The synthesis of zeolites using structure directing agents goes through three possible mode of actions. The first mode of action is called Templating, the term "Templating" refers to the process wherein an organic molecule arranges oxides tetrahedra in a specific pattern around itself during gelation or nucleation. This pattern serves as a primary unit for constructing a particular type of structure. In simpler terms, structural correlations exist between the molecular size and shape of the SDA and the zeolite framework that forms during crystallization of the zeolite nuclei.[28]

The second mode of actions is called "structure-directing effect" which refers to the fact that the addition of organic species induces the crystallization of a specific framework type that would not have occurred otherwise, with no direct relation with molecular size and shape of the SDA. And the final term "pore-filling effect", it refers to the organic SDAs becoming trapped within the porous zeolite crystal lattice, creating non-bonded host-guest interactions that provide stability to the open zeolite framework with no direct relation between size and shape of the SDA and the pores dimension. Although these terms (Templating, Structure-directing, and Pore-filling) have been used separately to emphasize specific roles of organic species during the structure-directing phenomenon, but the truth is that these three modes occur simultaneously during the structural-directing phenomenon by organic species in any zeolite synthesis procedure.[29 30]

In addition to the role played by structure-directing agents SDAs in zeolite crystallization, other factors, such as the quantity of silica, alumina, or heteroatoms, etc., can affect the zeolite crystallization process. Furthermore, performing the synthesis in a medium containing fluoride, employing different water concentrations, or using aluminophosphate ($AlPO_4$), etc., are all factors that can affect the zeolitic outcome. Further description for these variables can be found here.[31]

However, in this bibliographic part, the focus is more oriented toward the role of SDAs in promoting zeolite synthesis, particularly SDAs with ammonium and phosphonium units.

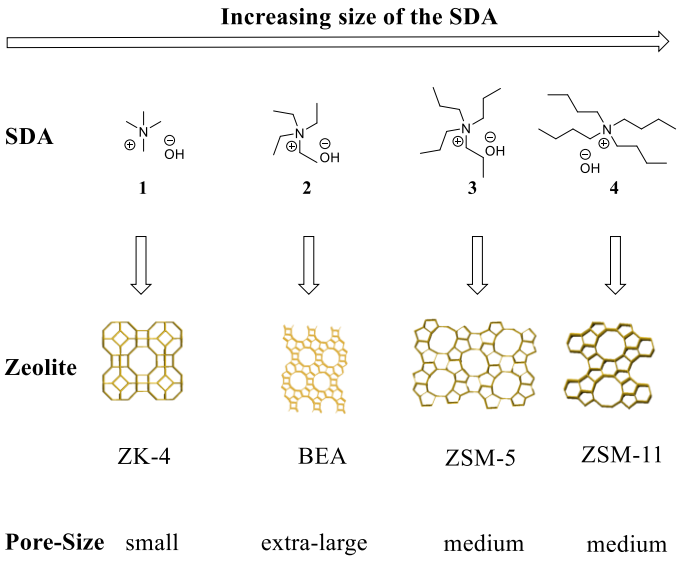

Scheme 2. Early reported synthesized zeolites using ammonium salt based SDA's with different alkyl chains.[9]

2.2 Use of Ammonium Salts as Structure-Directing Agents (SDAs) in Zeolite Synthesis

2.2.1 Recent Advances in the Use of Ammonium Salts: Size and Shape Effects in Zeolite Synthesis

The use of an organic salt as structure directing agent requires some conditions to fullfill. Starting by zeolite synthesis, it occurs in aqueous medium (water) to favor the condensation process between alumino-silicate, therefore the SDA should be soluble in aqueous media to interact with alumino-silicate species. As a result they should have a hydrophilic character. Moreover, zeolite frame works, which are formed of high silica, are considerably hydrophobic. Thus, close interaction between the organic and alumino –silicate required to promote the structure-directing phenomena. As a consequence, organic species must have a specific hydrophobic property to favor such contact.

The first example in this series describes the use of imidazole base ammonium salts with increasing size through some structure modification in the preparation of zeolites with increasing pore size (Scheme 3). The imidazole-based ammonium salt **(5)**, which is the smallest SDA among them, favored the crystallization of medium pore size zeolite called ZSM-22 (TO_4 = 10) with TON framework. [32] Moreover, increasing the size of the SDA and including two

cationic center with a spacer n = 5 (SDA **6**), favored the crystallization of large pore size zeolite called ECNU-36 (TO_4 = 12) with BEA framework. [33] And finally, similar to the concept of SDA **6**, a new SDA **7** was synthesized with two imidazole cationic centers having different alkyl groups with n = 10 spacer, the used SDA favored the crystallization of extra-large pore size zeolite HPM-8 with TO_4 = 30.[34] These examples emphasize that using ammonium salts with imidazole units having different alkyl substituents and spacers favored the crystallization of zeolites with correlated pore size.

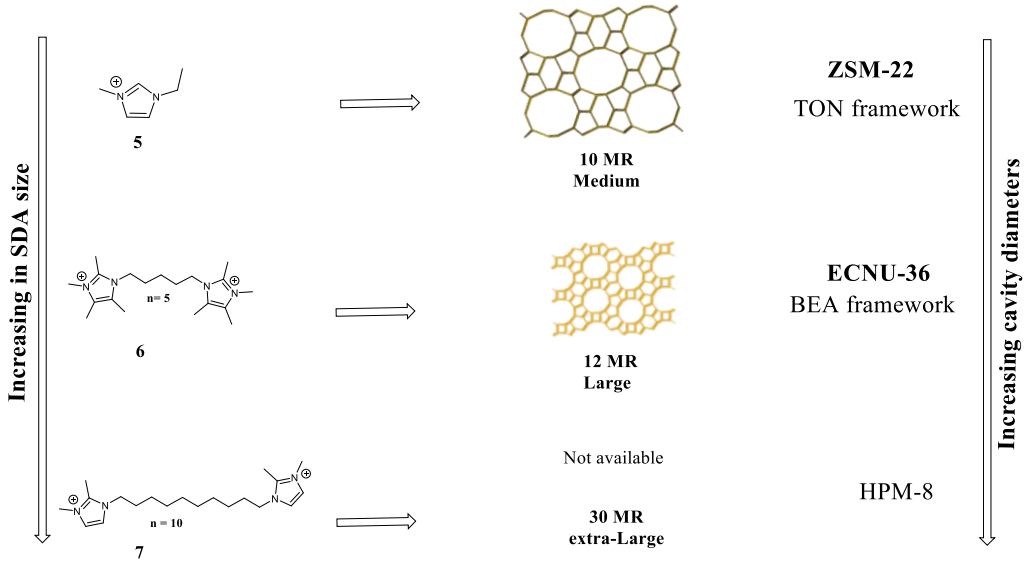

Scheme 3. The use of ammonium salts with different sizes and shapes in the preparation of zeolite frameworks with correlated dimensions [9]

The second example explains the effect of expanding the size of the same molecule on the formed topology of a zeolite. Tetrapropyl ammonium salt **(3)**, is a known SDA used in the synthesis of medium pore size zeolite ZSM-5 with MFI topology (TO_4 = 10) (Scheme 4). Recently, Villaescua, Sun and Camblor designed a new silica zeolite (IDM-1) containing medium and extra-large pores which is an expansion version of the mentioned ZSM-5 zeolite with MFI topology. The research group prepared SDA **8** having two cationic groups similar to the SDA used in the preparation of MFI. The two cationic groups are separated by an aromatic group to enhance rigidity and the size of the SDA (Scheme 4). What is special about the zeolite formed is that several medium/large zeolites have been reported before. However, the synthesis of high silica zeolites with medium and extra-large are still rare. IDM-1 is one of these examples which has high silica content,[35] therefore, high thermal stability, up to 1000 ^{o}C. The presence of stable zeolites with medium and extra-large pore size may improve the catalytic activity. For example, it helps in controlling the molecular movement for reactants and products

across different channel system. This, along with several other examples in the literature, demonstrates the geometrical relation between the size and shape of the SDA and the zeolite framework that crystallizes around.

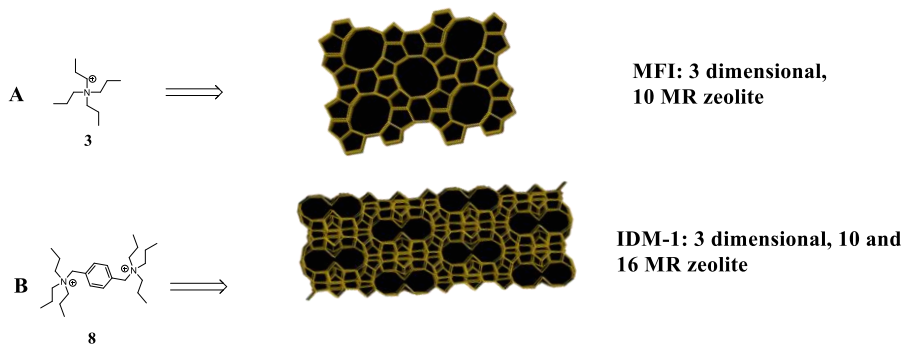

Scheme 4. Rational design of structure directing agent (SDA) for the synthesis of zeolites with both 10-ring and 16-ring multi-dimensional channel system.[9]

Over the years, zeolites were synthesized with different chemical compositions. For instance, heteroatoms like germanium favor the synthesis of zeolites with different pore sizes. One of these examples of zeolites containing germanium hetero atom is ITQ-34 with ITR topology. The ITQ-34 zeolite is a unique three-dimensional medium pore size zeolite synthesized by Corma et al.[36] The prepared ITR zeolite containing germanium (Ge) was synthesized using propane-1,3-bis(trimethylphosphonium) **(10)** (scheme 5). The ITR zeolite synthesis was always performed in the presence of Ge species by using a hazardous and costly organic template of propane-1,3-bis(trimethylphosphonium) **(10)**. Moreover, the use of Ge species in zeolite structure is costly, and reduces its stability especially upon calcination. Furthermore, researchers found that ITH zeolite could be synthesized without the addition of Ge by the help of several SDAs, one of them is SDA **9**, which is a known cheap SDA suitable for the synthesis of pure silica ITH (Scheme 5). Moreover, from a topological point of view the ITH and ITR framework are "twins" with very similar structures. Taking what mentioned into consideration and understanding the similarities and the differences in the structures of ITH and ITR zeolites. A minor modification of SDA **9** characterized by increasing the size of organic template favored the synthesis of pure silicate, alumino silicate, and borosilicate ITR zeolites with no Ge species (Scheme 5). The synthesis of such zeolites with high crystallinity and in the absence of Ge atoms, especially in the case of the synthesized ITR with aluminosilicate framework,

offers high catalytic activity in the process of converting methanol to propylene. The ITR framework exhibits excellent propylene selectivity and long life time when compared to other zeolites such as alumini silicate ZSM-5 with MFI topology.[37]

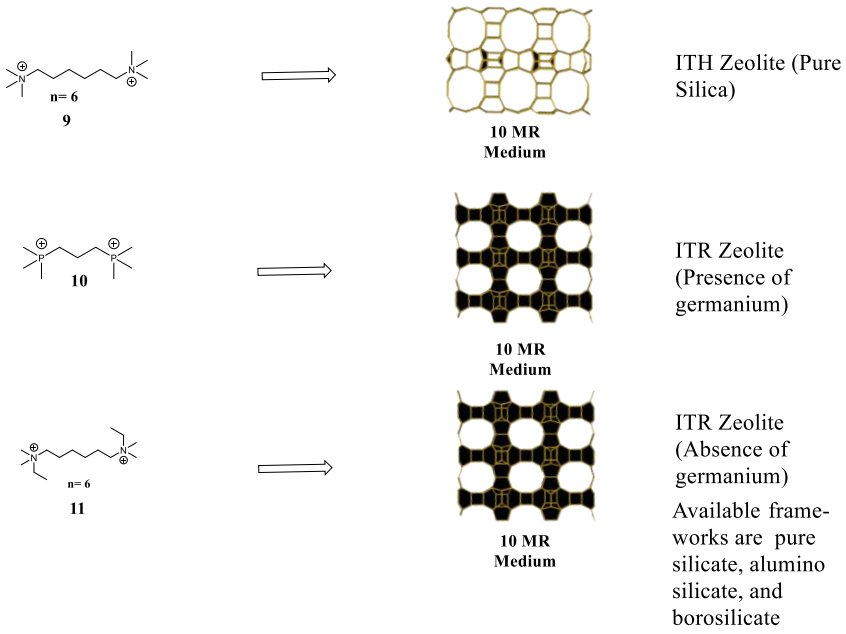

Scheme 5. Designing an ammonium salt for the synthesis of Free-Ge ITR Zeolites

The Diels–Alder (DA) reaction is one of the famous methods used for the preparation of complex cyclic and polycyclic organic compounds by reacting 1,3-dienes with dienophiles . The use of a designed catalyst for the Diels-Alder reaction can have many advantages as it can favor the formation of the transition state TS, stabilize it, and minimize the reaction's activation energy. One good option for this reaction is using solid catalysts that have pores, like zeolites. Some researchers have already looked into using zeolites for the Diels-Alder reaction. Their early results showed that a zeolite called ZSM-5 could help with this reaction when heated between 250 °C and 500 °C. However, the zeolite catalysts were selected on the bases of the already available materials with no correlation with the transition state formed.

Taking the Diels–Alder (DA) reaction as a starting point, researchers had developed a method to make pure silica zeolite using an organic structure directing agent (OSDA) mimicking the transition state (TS) of the Diels Alder reaction. Following this principle, and taking into consideration that the transition state and reaction product are very close. An organic SDA **12** that represent the product of reaction between 1,3-cyclohexadiene and N-methylmaleimide

was used in zeolite crystallization and indeed it favored the crystallization of zeolite with BEC framework (Scheme 6). [38]

The use of BEC zeolite as catalyst for the Diels alder reaction showed a 2–2.5 fold increase of the initial reaction rate at 60 °C compared to the use of ZSM-5 at 250-500 °C. The reason behind these results is the stabilization of the transition state inside the pores and the decrease in activation energy. More precisely, the decrease in enthalpy and entropy of activation energy as calculated by Eyring-Polanyi equation. These results support the importance of the stabilization effect achieved by the catalyst structure and which also depends on the reaction temperature. Finally, the reaction rate of the Diels Alder process can also be remarkably increased by introducing single metal atom to zeolite pores, such as Ti. This example and other examples describes the effectiveness of this new approach to enhance reaction-specific catalysts through imprinting SDA size and shape.[39]

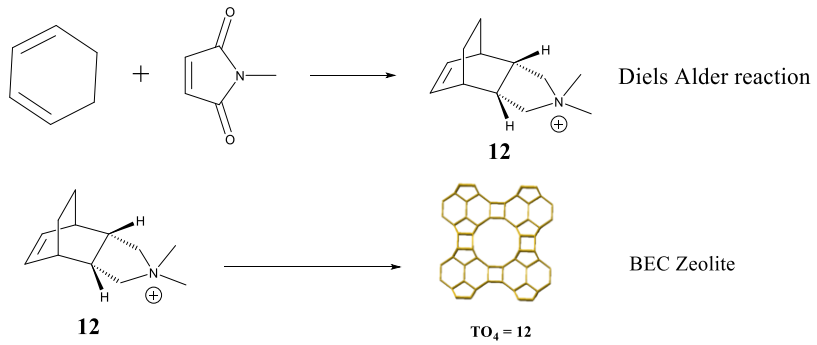

Scheme 6. Customizing Zeolite Catalysts for Diels-Alder Reactions: Imprinting SDAs Size and Shape into Pore Structures[9, 38]

Nano sheet zeolites are a category of zeolites having a unique two-dimensional structure with few nanometer thick. Such materials are prepared using SDAs with long alkyl chains. An example illustrating the synthesis of nano sheets using bifunctional surfactants is highlighted here. In which bifunctional surfactants were systematically synthesized with a long hydrophobic alkyl chain with 22 carbon atoms on one side and two quaternary ammonium groups joined by a C6 spacer on the other, almost equivalent to the distance between two successive MFI unit cells.[40, 30] The bis-ammonium head groups served as two successive tetrapropylammonium SDA **(3)** of the MFI framework, while the long hydrophobic tails prevented further crystal formation of the zeolite in one direction, thus encouraging the formation of a thin layer of zeolite (Scheme 7). The intelligent construction of this SDA **13** possessing specific hydrophilic/hydrophobic characteristics enables the production of extremely thin (2 nm) zeolite with MFI topology. This approach will improve the catalytic

efficiency because of their remarkable ability to prevent catalyst deactivation caused by coke deposition in methanol-to-gasoline conversion. For additional examples check [41].[41]

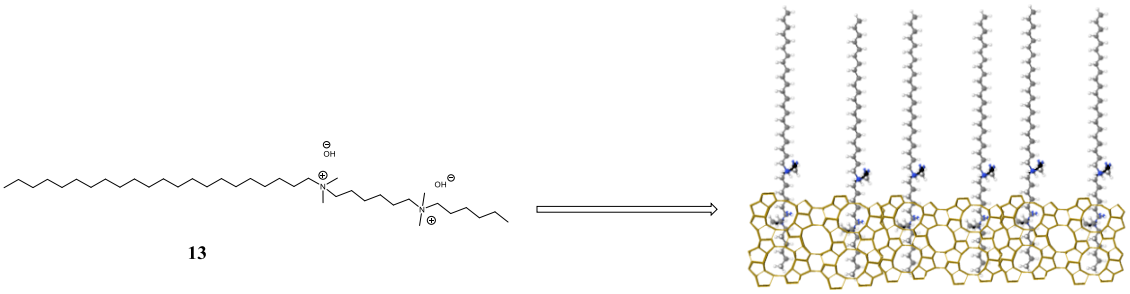

13

Scheme 7: Synthesis of thin (2 nm) MFI zeolite using hydrophobic SDA.[9]

2.2.2 The impact of Rigidity vs Flexibility of Ammonium-Based SDAs on Zeolite Crystallization and Cavity Formation

The rigidity or flexibility of organic cations play a crucial factor in determining their ability to create zeolite structures. For example, large and rigid molecules with limited flexibility, including those with multiple rings, are the most effective for creating new zeolite frameworks with large cavities. Moreover, a tight lock-and-key type of interaction between large and rigid SDA from one side and the formed zeolite from the other is found. Such SDAs play the role of templates, as they imprint their shape and size in the zeolite cavities.

Several examples of these polycyclic ammonium cations, along with the resulting zeolite frameworks were summarized in a recent review.[39] Some examples are highlighted in scheme 8, the use of large and rigid ammonium-based SDAs **14-19** favored the crystallization of the corresponding zeolites, with a direct correlation between their dimension and the zeolite cavities obtained.

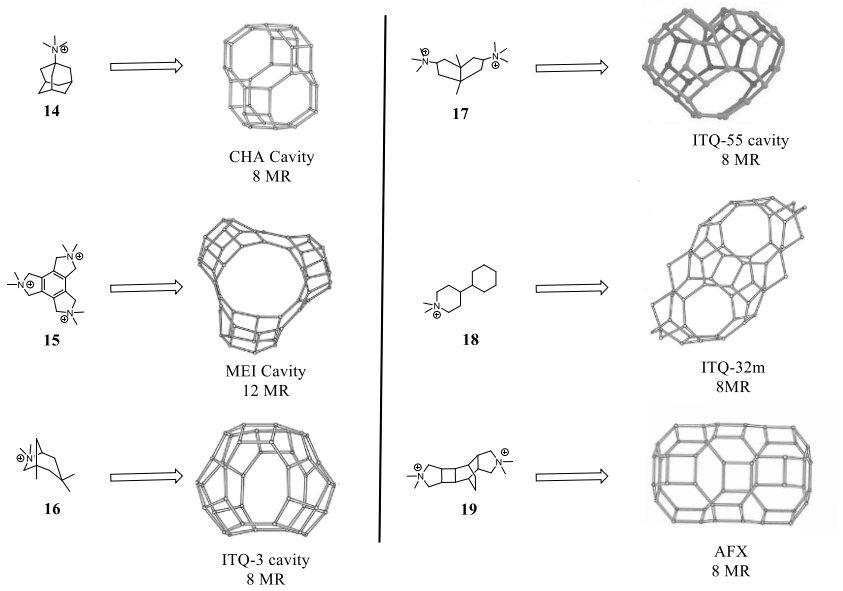

Scheme 8. The use of rigid SDAs in the synthesis of zeolites with identical cavities. [39]

On the other hand, the SDAs that are flexible and have more methylene groups can adopt a wide range of shapes, and any of these shapes could potentially favor specific zeolite structures. Therefore, flexible cations are generally viewed as less selective SDAs, since they can result in various frameworks depending on the specific shape they adopt. This can be seen as a disadvantage since it often produces a mixture of phases. However, the ability of SDA to take different conformations increases the chances of discovering suitable crystallization conditions that lead to the formation of zeolite materials. For instance, hexamethonium cations **(9)** have been used recently to synthesize three zeolites having medium pore size, which are RFE, [42] ITH, [43] and EUO [44] framework (Scheme 9).

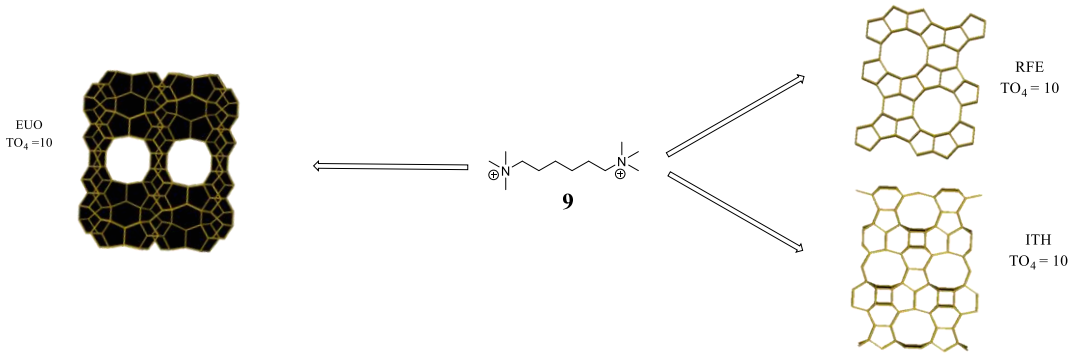

Scheme 9. The use of Flexible SDAs (hexamethonium) in the synthesis of different medium pore size zeolites.[9]

2.2.3. Preparation of Zeolites with Extra-Large Pore Size

2.2.3.1 Introduction to extra-large pore-size zeolites

The Structure Commission of the International Zeolite Association (IZA-SC) has compiled a database of zeolite structures that currently lists 260 distinct zeolite types, including 23 extra-large pore zeolites (ELP) zeolites with unique structural topologies. This represents a doubling of the number of ELP zeolites found in the database over the past decade. Despite this increase, ELP zeolites account for a relatively small proportion (23/260) of the discovered zeolites, in comparison to small pore (82/260), medium pore (54/260), and large pore zeolites (70/260) (Figure 4).[9] The extra-large pore size zeolites with pore aperture larger than 0.75 nm, aroused increasing interest from researchers because these zeolites have a wide range of applications: for example, in processing bulkier molecules, improving diffusion rate, prolonging catalyst lifetimes and changing product selectivity.

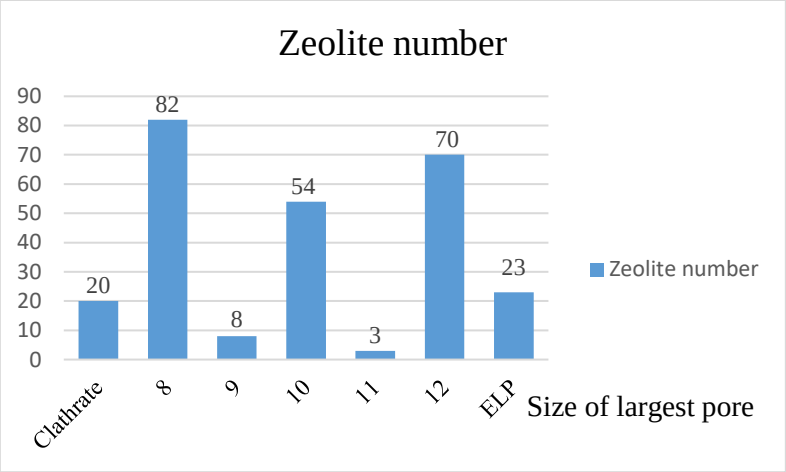

Figure 4. The classification of zeolites based on their largest pore as shown in the database of zeolite structure [9]

2.2.3.2 Approaches for Choosing Suitable Ammonium Salts as Structure-Directing Agents (OSDA) for Extra-Large Pore- Size Zeolite Synthesis

The formation of extra-large pore-size zeolites is mainly dependent on the structure-directing agent used. The choice of large, rigid, and polar organic SDAs, in addition to suitable gels and media containing fluoride, will favor the formation of low framework density zeolites with a multi-dimensional channel system. Moreover, the presence of some secondary building units, such as Ge heteroatom will favor the formation of zeolites with extra-large pore sizes. To

discover new ELP zeolites, successful SDA design strategies are followed, including SDA size expansion and SDAs π–π stacking.

2.2.3.2.1.The Use of Size Expansion Approach in the Synthesis of Extra-Large Pore Size Zeolites

The size expansion approach is a method used in the synthesis of extra-large pore-size zeolites using modified structure-directing agents. It involves enlarging the size of the organic molecule used as an SDA by adding extra carbons or other groups during resynthesis. This approach resulted in the formation of larger pore zeolites, allowing for the synthesis of novel zeolite frameworks. For example, the use of SDA **20** favored the crystallization of three dimensional large pore size zeolite MCM-68 with a 12-member ring (Scheme 10).[45] However, when using SDA **21** having two extra methyl groups favored the crystallization of a three dimensional extra-large pore size zeolite ITQ-37 (30-member ring (ITQ-37) >12-member ring (MCM-68)).[46]

Moreover, the presence of halogenated groups on the used SDA and its position, can also play an important role on the outcome of the crystallization process. For example, the use of SDA **22** having fluorine on meta position favored the crystallization of a one dimensional large pore size zeolite SSZ-55 with 12-member ring (Scheme 10).[47] Using similar SDA **23** having fluorine atom on para instead of meta position favored the synthesis of a one dimensional extra-large pore size zeolite SSZ-53 having 14-member ring (14-member ring (SSZ-53) >12-member ring (SSZ-55)).[48]

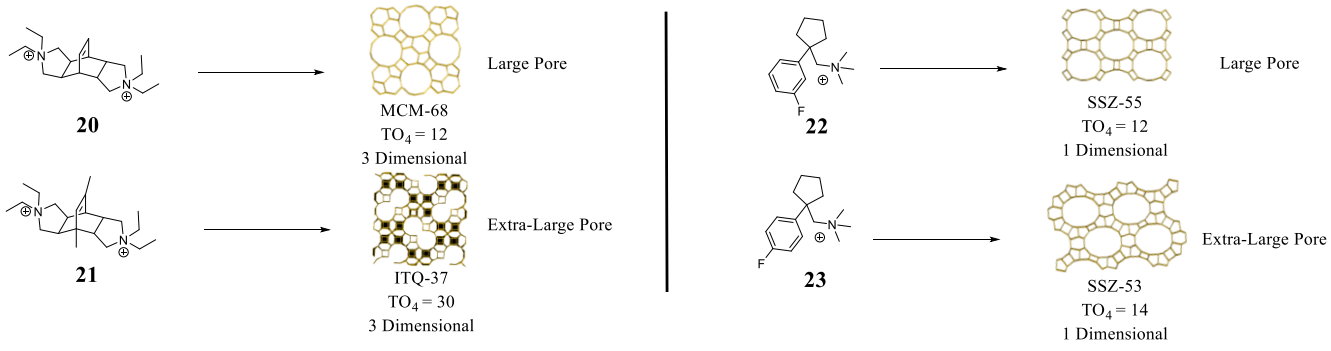

Scheme 10. The use of size expansion approach for the synthesis of extra-large pore size zeolites. [9]

Furthermore, the use of isoindoline-based SDA **24** having two methyl groups on the nitrogen atom favored the crystallization of a three dimensional large pore size zeolite BEC having a 12 member ring (Scheme 11). The use of similar SDA **25** having two cyclohexyl group instead of

the two methyl groups favored the crystallization of three dimensional extra-large pore zeolite ITQ-54 with 20 member rings [49] (20 member ring (ITQ-54) > 12-member ring (BEC)). Researchers at Chevron also demonstrated another case when using SDA **27** having two ethyl groups instead of SDA **26** having two methyl groups (Scheme 11). A one dimensional extra-large pore size zeolite SSZ-61[50] with 21-member ring was obtained instead of extra-large pore size zeolite SSZ-35,[51] having 16-member ring (21-member ring (SSZ-61) > 16-member ring (SSZ-35)). It is quite worthy that SSZ-61 is the first pure silica zeolite with a 21-member ring.

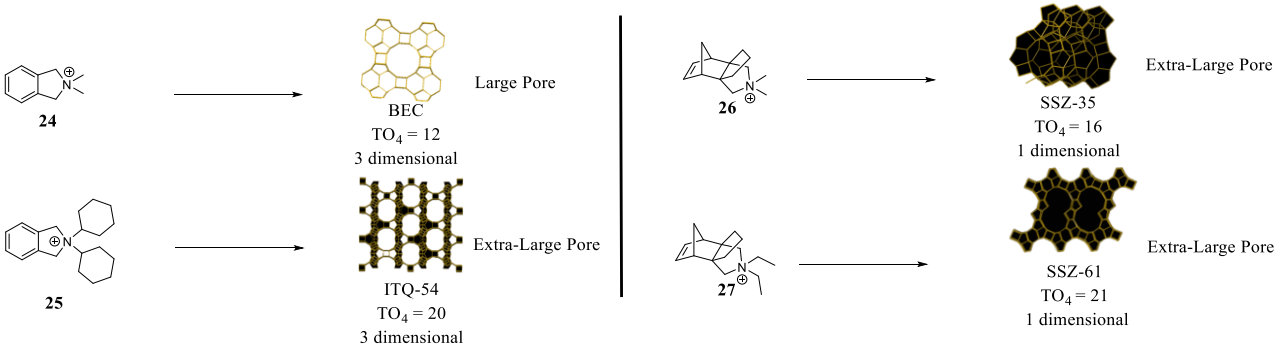

Scheme 11. The use of size expansion approach for the synthesis of extra-large pore size zeolites.[9]

Last example in this section shows, the use of trimethyladammantammonium **(14)** which favored the crystallization of a three dimensional small pore size zeolite SSZ-13 with 8-member ring. However, replacing SDA **14** with SDA **28,** which has additional two methyl groups, favored the crystallization of three dimensional extra-large pore size ITQ-56 zeolite with 22-member ring (22-member ring (ITQ-56) > 8-member ring (SSZ-13)). [52]

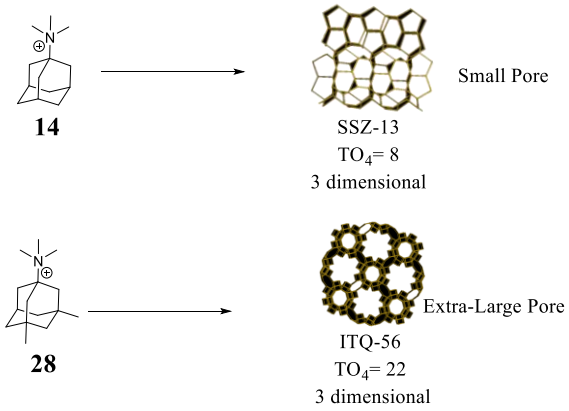

Scheme 12. The use of size expansion approach for the synthesis of extra-large pore size zeolites.[9]

2.2.3.2.2.The Use of π–π Stacking Phenomenon in the Synthesis of Extra-Large Pore Size Zeolites

The π–π stacking phenomenon refers to the non-covalent interaction between aromatic molecules, where the aromatic rings align in parallel to each other with a distance of 3.4-3.5 Å. In the synthesis of zeolites using SDAs, π–π stacking can occur between the aromatic rings of the SDA molecules. This phenomena can influence the size and shape of the formed zeolite pores. For example, Du and his colleagues built upon this idea by using imidazole-based aromatic derivatives. They used SDAs having different groups at different positions as supramolecular SDAs, to produce NUD-1 with 18 member rings using SDA **29**,[53] NUD-2 with 14-member ring using SDA **30**,[54] and ITQ-37 with 30 member rings using SDA **31** (Scheme 13).[55] This shows that π-π supramolecular stacking, which uses planar shape SDAs having aromatic groups that build up above each other fitting in one pore, is a promising strategy to direct the crystallization process of extra-large pore size zeolites.

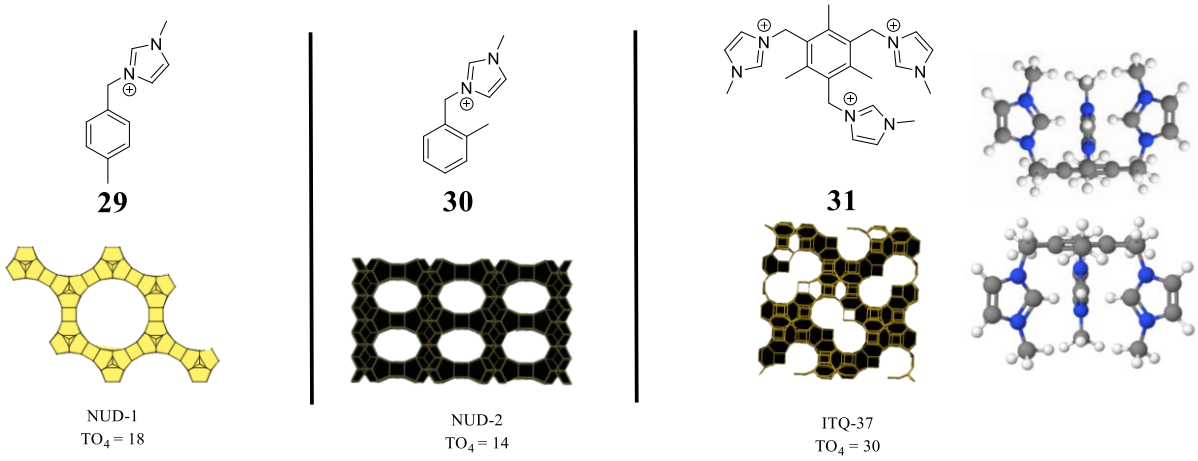

Scheme 13. The use of π–π Stacking phenomenom in synthesis of zeolites with extra large pore size.[9]

2.2.4.Ammonium Salts Used in the Preparation of Extra-Large Pore Size Zeolites.

2.2.4.1. Ammonium Salts Used as SDAs in the Synthesis of Aluminophosphate/ Gallophosphate Extra-Large Pore Size Zeolites with the Resulting Topology

In this category, the first reported extra-large pore size zeolite was VPI-5 in 1988.[56] The VPI-5 is a one dimensional 18-member ring zeolite with aluminophosphate VFI framework and pore size larger than 1 nm. The synthesized VPI-5 was obtained when using SDA **32** (Table 2, Entry 1). Similarly to SDA **32**, the two SDAs **33**[57] and **34**[58] have directed the synthesis of zeolites with VFI Framework. Two years later, in 1990, a one dimensional 14-member ring zeolite named AlPO-8 was reported with aluminophosphate AET framework when using SDA **35** (Table 2, Entry 2).[59] One year later in 1991, a novel zeolite, Gloverite, was reported with CLO topology having phosphorus and gallium atoms in its framework. Gloverite zeolite is an extra-large zeolite with three dimensional framework and 20-rings, it was prepared by a cage like SDA **36** (Table 2, Entry 3)[60]. Later, different procedures using SDAs **37-41** were used for the preparation of zeolites with CLO topology.[61] After 22 years, in 2013, the last extra-large pore size zeolite belonging to alumino phosphate family was reported. The prepared extra-large pore size zeolite ITQ-51, was synthesized with IFO topology with the help of a proton sponge-based SDA **42** (Table 2, Entry 4) .[62] So far, only three extra-large pore size zeolite with aluminophosphates have been reported (VFI, AET, and IFO). The SDAs used in their preparation belong to the ammonium salt family. Protonated aliphatic ammonium salts with two or three alkyl chains appear to favor the crystallization of aluminophosphate zeolites. Ammonium salts with aromatic substituents having a shared proton sponge and 3 positive charges work as well. The gallophosphate extra-large pore zeolite seems to be favored by a quite different range of SDAs (imidazole, ammonium salts with two positive charges, bicyclic ammonium salts, tetra alkyl and di alkyl ammonium salts).

Entry	Year	Zeolite (topology)	Channel dimension	Framework composition	SDA used
1	1988	VPI-5 (VFI)	1D 18-ring	Al, P	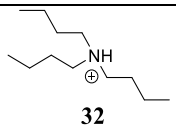 **32** 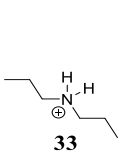 **33** 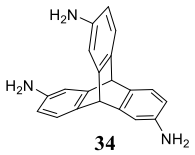 **34**
2	1990	AlPO-8 (AET)	1D 14-ring	Al, P	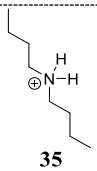 **35**
3	1991	Gloverite (CLO)	3D 20-ring	Ga, P	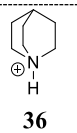 **36** 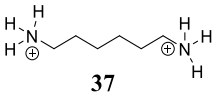 **37** 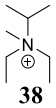 **38**  **39** 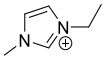 **40**  **41**
4	2013	ITQ-51 (IFO)	1D 16-ring	Al, P	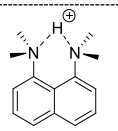 **42**

Table 2. The ammonium salts used as SDA's in the synthesis of aluminophosphate / gallophosphate extra-large pore size zeolites with the resulted topology.

2.2.4.2. Ammonium Salts Used in the Synthesis of Pure and Substituted Silicates (excluding Ge) Extra-Large Pore Size Zeolites with the Resulting Topology

UTD-1, a pure silicate extra-large pore size zeolite, was synthesized in 2019 with DON topology having one dimensional channel with a 14-member ring using imidazole based SDA **43** (Table 3a, Entry 1).[63] This UTD-1 was first reported in 1996 using cobalt based SDA . One year later, in 1997, another interesting extra-large pore size zeolite was synthesized from pure silicate, having one dimension with 14-member ring named CIT-5 with CFI topology.[64] It was synthesized using SDA **44** based on natural product derivative sparteine as mentioned before (Table 3a, Entry 2). In 2003, after 6 years, two extra-large pore size zeolites having a mixture of boron and silica in their framework were reported. The extra-large pore zeolites SSZ-53[48] with SFH topology and SSZ-59[65] with SFN topology were synthesized, both having a one dimensional framework with a 14- member rings. SSZ-53 was synthesized using fluoro aromatic SDA **23** (Table 3a, Entry 3) and SSZ-59 was synthesized using a quite similar SDA **45** having a non-flourinated aromatic and 1-methylpiperidine groups (Table 3a, Entry 4). In the same year, a three dimensional 18-member ring extra-large pore size zeolite ECR-34 was synthesized with an ETR topology having a mixture of Ga, Al, and Si in the framework (Table 3a, Entry 5).[66] The synthesis of ECR-34 zeolite proceeded when using tetraethylammonium hydroxide SDA **2**.

Entry	Zeolite (topology)	Year	Channel dimension	Framework composition	SDA used
1	UTD-1 (DON)	1996	1D 14-ring	Si	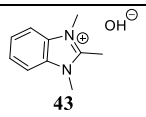 **43**
2	CIT-5 (CFI)	1997	1D 14-ring	Si	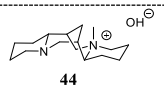 **44**
3	SSZ-53 (SFH)	2003	1D 14-ring	B, Si	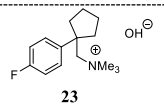 **23**
4	SSZ-59 (SFN)	2003	1D 14-ring	B, Si	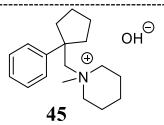 **45**
5	ECR-34 (ETR)	2003	3D 18-ring	Ga, Al, Si	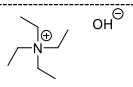 **2**

Table 3a.The ammonium salts used as SDA's in the synthesis of pure and substituted silicates (excluding Ge) extra-large pore size zeolites with the resulted topology between 1996 and 2003.

After 13 years, in 2014, a one dimensional 18-member ring extra-large pore zeolite SSZ-61[50] with SSO topology was synthesized, having only Si in the framework composition. The synthesis of this zeolite was done using bicyclic SDA **27** (Table 3b, Entry 6). Another extra-large pore size zeolite, EMM-23 with EWT topology, also having three dimensional channel with 21-member ring, was reported in the same year. In this case, the SDA **46** used was based on a bisquaternary ammonium salt having 2 heterocycles linked with an *n*-pentyl group[67] (Table 3b, Entry 7). Additionally, cyclic bisammonium SDA **47** also favored the synthesis of zeolite with EWT framework.[68] Three years later, in 2017, an imidazole based ammonium salt **48** favored the synthesis of two dimensional, 14 member ring extra-large pore size zeolite SSZ-70 with SYV topology (Table 3b, Entry 8).[69] In 2020, extra-large pore size zeolites with silica content NUD-6[70] and IDM-1[35] were synthesized from imidazole-based ammonium salt SDA **43** (Table 3b, Entry 9) and aromatic SDA **8**, respectively. (Table 3b, Entry 10).

Entry	Zeolite (topology)	year	Channel dimension	Framework composition	SDA used
6	Ssz-61 (SSO)	2014	1D 18-ring	Si	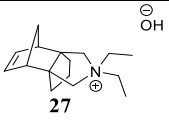 **27**
7	EMM-23 (EWT)	2014	3D 21-ring	Si	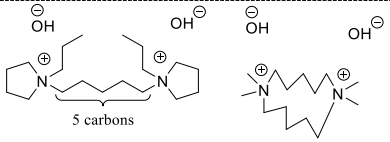 5 carbons **46** **47**
8	SSZ-70 (SVY)	2017	2D 14-ring	Si	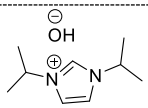 **48**
9	NUD-6	2020	3D 16-ring	Si	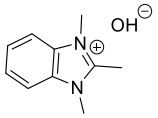 **43**
10	IDM-1	2020	-	Si	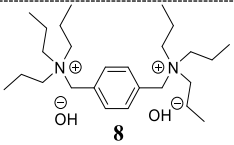 **8**

Table 3b.The ammonium salts used as SDA's in the synthesis of pure and substituted silicates (excluding Ge) extra-large pore size zeolites with the resulted topology between 2014 and 2020.

2.2.4.3. Ammonium Salts Used in the Synthesis of Germanosilicate Extra-Large Pore Size Zeolites with the Resulting Topology

Extra-large pore size zeolite having germanium atoms in their framework composition was first synthesized in 2004. An ITQ-15 zeolite with UTL topology was obtained, having two dimensional channel with 14-member ring when using SDA **49** (Table 4a, Entry 1).[71] Two years later, in 2006, a three dimensional 18-member ring extra-large pore zeolite ITQ-33 was synthesized with ITT framework by the help of diquaternary salt **9** (Table 4a, Entry 2).[72] Three years later, in 2009 another germanium containing extra-large pore size zeolite ITQ-37 was prepared with ITV topology, having a three dimensional channel with 30-member ring.[46] It was synthesized using diquaternary compound **50** as SDA (Table 4a, Entry 3). In 2010, an extra-large pore size zeolite ITQ-44 was also reported with IRR topology by the use of SDA **51** (Table 4a, Entry 4).[73]

Entry	Zeolite (topology)	Year	Channel dimension	Framework composition	SDA used
1	ITQ-15 (UTL)	2004	2D 14-ring	Ge, Si	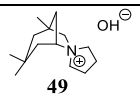 **49**
2	ITQ-33 (ITT)	2006	3D 18-ring	Ge, Si	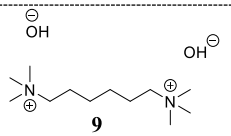 **9**
3	ITQ-37 (ITV)	2009	3D 30-ring	Ge, Si	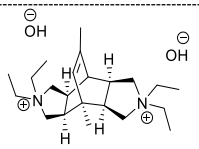 **50**
4	ITQ-44 (IRR)	2010	3D 18-ring	Ge, Si	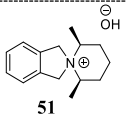 **51**

Table 4a. The ammonium salts used as SDA's in the synthesis of germanosilicate extra-large pore size zeolites with the resulted topology between 2004 and 2010.

The same SDA **51** was used one year later in the preparation of three dimensional 18-member ring ITQ-43 with IRT topology (Table 4b, Entry 5).[74] Three years later, in 2014, an imidazole-based SDA favored the synthesis of three dimensional extra-large pore sized NUD-1 with three dimensional having 18 member ring using SDA **29** (Table 4b, Entry 6).[53]

In 2015, a zeolite containing germanium was reported, ITQ-54 a three dimensional extra-large

pore size zeolite with 20 member ring was synthesized with IFU topology using SDA **25** (Table 4b, Entry 7)[49] The last reported example in the germanium series, is the extra-large pore size zeolite SYSU-3 with SYT topology. The extra-large pore size zeolite SYSU-3 was prepared using SDA **52** derived from traditional Chinese medicine (Sophoridine) (Table 4b, Entry 8).[75]

Entry	Zeolite (topology)	year	Channel dimension	Framework composition	SDA used
5	ITQ-43 (IRT)	2011	3D 28-ring	Ge, Si	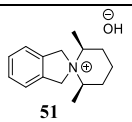 **51**
6	NUD-1	2014	3D 18-ring	Ge, Si	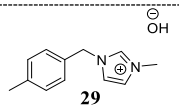 **29**
7	ITQ-54 (IFU)	2015	3D 20-ring	Ge, Si	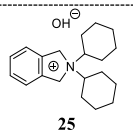 **25**
8	SYSU-3 (SYT)	2018	3D 24-ring	Ge, Si	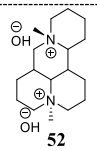 **52**

Table 4b. The ammonium salts used as SDA's in the synthesis of germanosilicate extra-large pore size zeolites with the resulted topology between 2011 and 2018.

2.2.5.Hydrothermal Stability of the Ammonium Based SDAs in Zeolite Synthesis

In order for the organic cations to withstand the harsh conditions applied by the hydrothermal synthesis of zeolites, characterized by high temperatures, pressures, and basic pHs, SDA species must exhibit a high hydrothermal stability. When ammonium cations are exposed to high pH and temperature in aqueous media, they frequently undergo Hofmann elimination reaction to produce the corresponding alkenes and tertiary amines. As a result, these fragments will cancel or at least change the structure-directing mode of an SDA. Degradation of SDAs during zeolite crystallization may affect the molecule's potential to crystalize a zeolite, not only because of the lower concentration of the SDA, but also because of the ability of creating other organic species with their own structure-directing potential. For example, The use of N,N,N-trimethyl-*tert*-butylammonium (TMTBA) **(53)**, under specific conditions, caused its interaction with its own Hofmann elimination side product, that is trimethylamine **(57)**, thus generating a smaller tetramethylammonium cation **(1)** (Scheme 14).[76] [30] Despite the fact that the original and newly produced cations are different in size and shape, both have been proven to structure-direct the crystallization of AST zeolites in fluoride media.[77] However, the unit cell dimensions of the synthesized AST zeolites were substantially different containing smaller unit cells. For additional examples check [78].[78]

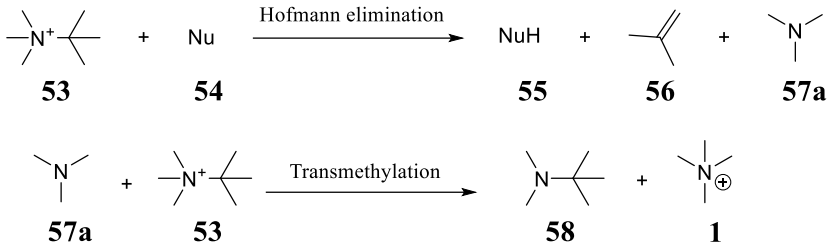

Scheme 14. Formation of trimethylamine **(21)** via hoffmen elimination followed by transmethylation to give SDA **1**.

2.3. Use of phosphonium salts in zeolite synthesis:

2.3.1. Summary of the Prepared Phosphonium Salts with the Corresponding Zeolites.

The use of phosphonium cations as SDAs in the preparation of zeolite materials has been discovered in the beginning of 2000. These phosphonium cations were introduced as promising alternatives to ammonium cations as they have higher stability, even though the synthesis may be carried out under more harsh conditions. In fact, the use of these phosphonium cations has allowed for the creation of zeolite frameworks with different pore sizes. Below is a list covering almost all phosphonium based SDAs with the corresponding zeolite frameworks. The results shows that zeolites with small (GIS, PTH) [7980], medium (ITR),[36] Large (GME, ITQ-27)[81] and extra-large (IFT and ITQ-40) [82] were prepared using a wide set phosphonium salts (Scheme 15). The size expansion approach is also applicable in case of phosphonium salts, for instance, Corma and his co-workers reported the use of phosphonium-based SDA **62** in the preparation of two dimensional large pore zeolite ITQ-27 with a 12-member ring. Using similar SDA **63** having two ethyl groups instead of two methyl groups or using the SDA **64** having two phosphonium groups connected with a 3 carbon linker, favored the crystallization of 3 dimensional extra-large pore size zeolite ITQ-40 with 16-member ring (16-member ring (ITQ-40) > 12-member ring (ITQ-27)).

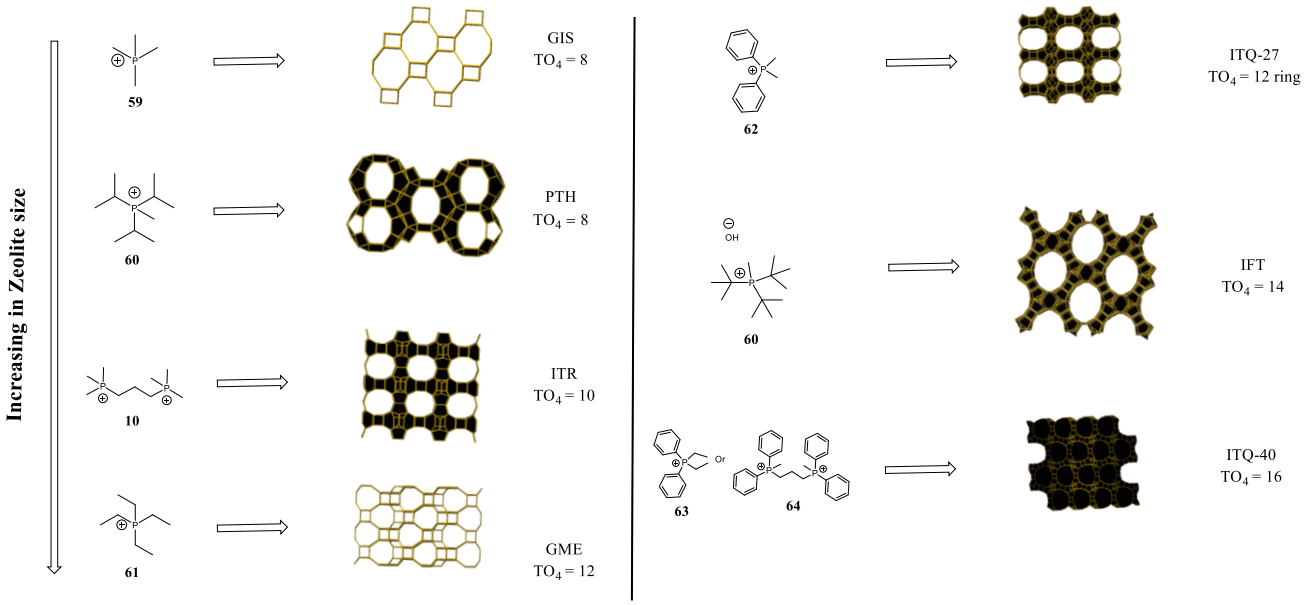

Scheme 15. The use of phosphonium salts in the synthesis of zeolites with different pore sizes

2.3.2. ZEO-1 zeolite

Over the past three decades, there has been significant progress in synthesizing zeolites with extra-large pores, as previously shown in Tables 2, 3 and 4. Since the beginning of the zeolite synthesis journey in 1940, around 22 extra-large pore-size zeolites were reported. However, these prepared zeolites suffered from stability issues concerning their use in the industry due to the presence of expensive heteroatoms such as germanium, given for example, the multidimensional extra-large pores zeolites with -ITV,-CLO,-IFU,-IRY, and -IFT frameworks. Moreover, some of these extra-large pore-size zeolites suffer from low multidimensionality and have interrupted frameworks. As a result, only stable fully connected aluminosilicate large-pore zeolites such as BEA, FAU, and EMT were discovered and used in industry

Lately, a fully connected non-interrupted three-dimensional aluminosilicate extra-large pore-size zeolite with an interesting mixture of extra-large and large pore-size named ZEO-1 was discovered.[83] The ZEO-1 zeolite was synthesized using Tricyclohexyl methyl phosphonium (TCyMP) **(65a)** as the organic structure-directing agent (OSDA). The framework composition contains an alumino-silicate ratio of 14.5. Additionally, it showed high thermal and hydro-thermal stability up to at least 1000°C and possess a good potential as a catalytic cracking catalyst.

The pore system of ZEO-1 contains both three-dimensional extra-large 16MR and large 12MR channels with high interconnectivity. Therefore three types of super cages with four windows of 16MR (A), 16-12 MR (B), and 12MR (C) are present (Scheme 16). The presence of alumina in the framework composition forms active acid sites which in its turn enable good heavy-oil conversion and fluid catalytic cracking (FCC), competing with the used zeolites in such processes.

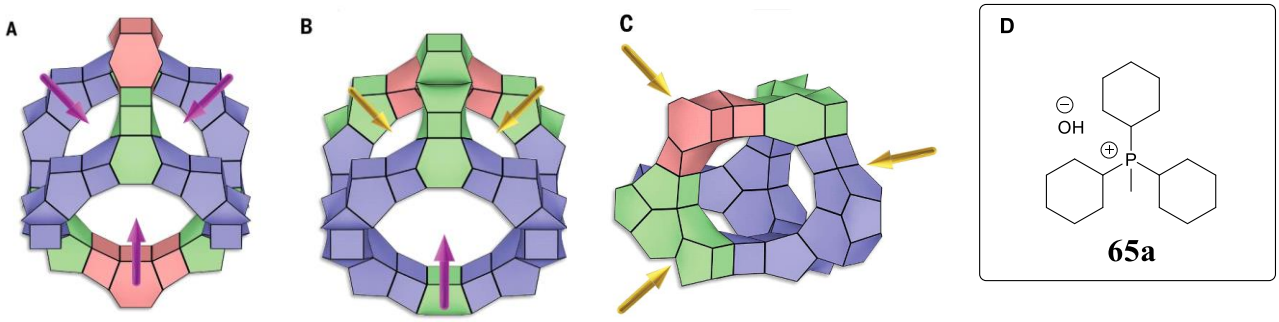

Scheme 16. The ZEO-1 pore system containing three super cages with (A) 16MR, (B) 16-12MR, and (C) 12MR apertures. The phosphonium based SDA **79a** used in ZEO-1 synthesis is shown to the right (D).

In conclusion the meta stability of a zeolite and the complexity of their formation mechanisms, make it hard to understand the real effect of the synthetic variables on the mechanism of formation. Understanding the mode of action of organic structure-directing agents at the molecular level is still a matter of debate and the ability of SDA to favor zeolite formation, in most of the time, is based on trial and error concept. A general conclusion has not yet been reached. However, it is supposed that using large, rigid, and polar organic structure directing agents (OSDAs), in addition to suitable gels and fluoride containing media, will favor the formation of low framework density zeolites with multi-dimensional channel system. Moreover, the presence of some secondary building units, such as Ge heteroatom will favor the formation of zeolites with extra-large pore sizes.

3. Project description

The aim of this doctoral thesis was to synthesize rigid, polar, and hydrophilic organic salts. At first, our interest is devoted to the synthesis of ammonium salts that have alkyl chains similar to the structure directing agents (SDAs) found in Scheme 2. Herein, a new set of ammonium salts **66** having a single alkyne substituent were prepared. The use of ammonium salts with alkyne units in zeolite synthesis, can enable their use in introducing metals to zeolite frameworks through the formation of metal-π-complexes. Additionally, a second set of ammonium salts **67** featuring two alkyne moieties are prepared and some of them tested in zeolite synthesis. Moreover, ammonium salts **67** can serve as building block to form larger molecules through the size expansion approach for example, by trimerization.

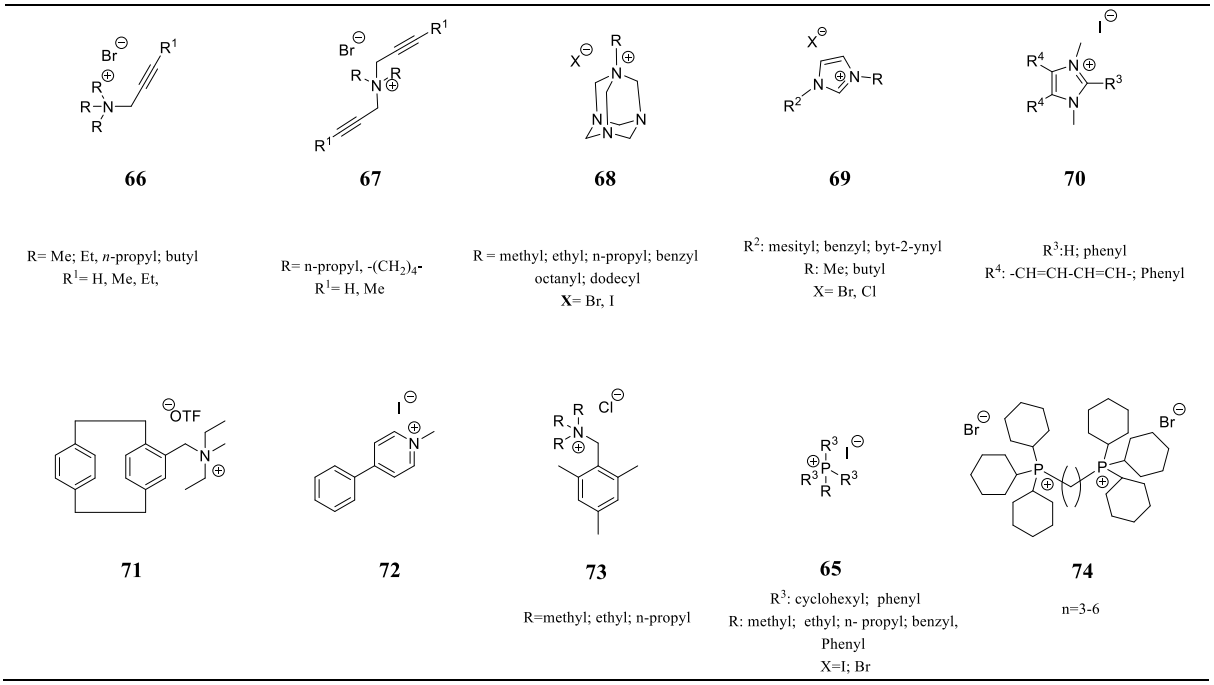

Scheme 17. The ammonium and phosphonium salts prepared in the thesis

As demonstrated before, ball-shaped SDAs like SDA **14**, **28**, and **36**, favored the crystallization of zeolites with distinct frameworks and pore sizes. In this study, a new series of ammonium salts, based on hexamethylenetetramine **68**, was synthesized with different alkyl groups and tested as a potential candidate to favor crystallization of zeolites. Two ammonium salts with long-carbon chains based on hexamethylenetetramine **68** were prepared as possible candidates for the synthesis of thin layer zeolites. Moreover, it has been proven that ammonium salts with imidazole units are among the most successful SDAs for zeolite synthesis, with over

59 imidazole-based SDAs directing the crystallization of zeolites with various frameworks and pore sizes.[84] Nonetheless, five of these SDAs favored the crystallization of extra-large pore size zeolites, more preciously, three out of these five SDAs (Table 3, SDA **43**, **48** and **43**) demonstrated the ability to preferentially induce the formation of extra-large pore size zeolites with silicate and substituted silicate frameworks. To this end, an expanded series of ammonium salts **69** and **70**, with imidazole substituents, were synthesized and tested for its ability to enhance the synthesis of zeolites with alumino-silicate frameworks.

SDAs containing aromatic units were also used in the synthesis of zeolites with diverse framework compositions, as detailed in Tables 2, 3, and 4. Herein, a new ammonium salt **71** incorporating a [2.2] paracyclophane unit was developed, which possesses two aromatic units, one of the two benzene rings is situated at a sufficiently distant location from the cation. This structural configuration may promote π-π stacking similar to the example described in Scheme 13 by SDA **31**. The incorporation of two connected rings, as in the case of [2.2] paracyclophane, is expected to support the crystallization of zeolites with extra-large pores, compared to the reported example of ITQ-37 Scheme 13. Additionally, another aromatic compound, the 4-phenylpyridinium salt **(72)** was synthesized, the presence of two aromatic rings may facilitate the formation of extra-large pore zeolites featuring a channel system, potentially favoring π-π stacking. Finally, the last prepared ammonium salts in the aromatic category are those containing the mesityl group **73**, which were generated by the alkylation of (Chloromethyl)-1,3,5-trimethylbenzene-based ammonium salts using tertiary amines.

Apart from the use of ammonium salts in zeolites synthesis, SDAs based on phosphorous are emerging as promising contenders for zeolite synthesis. This class of SDAs exhibits remarkable thermal stability and is impervious to Hoffman elimination. Although just one example was presented in Table 3 and two in Table 4, these preliminary results indicate a new area of SDAs with great potential. Accordingly, the first target in this series is to reproduce alumino silicate zeolite ZEO-1 using tricyclohexyl(methyl)phosphonium hydroxide **(65a)**. ZEO-1, a new type of zeolites, having an extra-large pore size and excellent stability up to 1000 ^{o}C, making it as a prime target for researchers. This process will enable a spectroscopic examination of its stability and acid site accessibility. Following the size expansion strategy, a new set of SDAs employing different alkyl chains based on tricyclohexyl phosphine and triphenyl phosphine **(65)** are prepared and some of them tested using the same conditions employed for the preparation of ZEO-1

Furthermore, the phosphonium salts series is extended to include the preparation of bisphosphonium **74** salts having two tricyclohexyl phosphonium units with various alkyl chain

spacers. As shown in Table 3 Entry 7 and 10 and Table 4 Entry 2, bis salts featuring two ammonium units is well-known and has been employed in the synthesis of zeolites with extra-large pore size. Here in, a new set of bisphosphonium salts instead of ammonium salts featuring tricyclohexyl ohosphine is synthesized.

The different ammonium and phosphonium salts prepared are used in several zeolite synthesis trials in the LCS laboratory and the resulted outcomes are shown in chapter 3.

4. References

[1] A. Cronstedt, Beschreibung und untersuchung einer unbekannten Bergart, *Zheolites gennant. Abh. Schwed. Akad. Wiss*. **1756**, *18*, 111–113

[2] (a) E. Vogt, G. Whiting, A. Chowdhury, B. Weckhuysen in Advances in Catalysis, Vol. 58 (Ed.: F.C. Jentoft), Elsevier: Amsterdam, **2015**, pp. 221-260. (b) U. Olsbye, S. Svelle, M. Bjørgen, P. Beato, T. V. W. Janssens, F. Joensen, S. Bordiga, K. P. Lillerud, Conversion of Methanol to Hydrocarbons: How Zeolite Cavity and Pore Size Controls Product Selectivity. *Angew. Chem. Int. Ed.* **2012**, *51*, 5810–5831. https://doi.org/10.1002/anie.201103657. (c) C. Chizallet, C. Bouchy, K. Larmier, G. Pirngruber, Molecular Views on Mechanisms of Brønsted Acid-Catalyzed Reactions in Zeolites. *Chem. Rev.* **2023**, *123*, 6107–6196. https://doi.org/10.10 21/acs.chemrev.2c00896. (d) B. K. Singh, Y. Kim, S. Kwon, K. Na, Synthesis of Mesoporous Zeolites and Their Opportunities in Heterogeneous Catalysis. *Catalysts* **2021**, *11*, 1541-1571 https://doi.org/10.3390/catal111215 4 1.

[3] E. Koohsaryan, M. Anbia, M. Maghsoodlu, Application of Zeolites as Non-phosphate Detergent Builders: A Review. *J. Environ. Chem. Eng.* **2020**, *8*, 104287. https://doi.or g/10.1016/j.jece.2020. 104287.

[4] (a) T. Maesen, B. Marcus, Chapter 1 The Zeolite Scene—An Overview. In *Studies in Surface Science and Catalysis*; H. van Bekkum, E. M. Flanigen, P. A. Jacobs, J. C. Jansen, Eds.; Introduction to Zeolite Science and Practice; Elsevier, **2001**; Vol. 137, pp 1–9. https://doi.org /10.1016/S0167-2991(01)80242-1. (b) G. Confalonieri, G. Vezzalini, L. Maletti, F. Di Renzo, V. Gozzoli, R. Arletti, Ion Exchange Capacity of Synthetic Zeolite L: A Promising Way for Cerium Recovery. *Environ. Sci. Pollut. Res.* **2022**, *29*, 65176–65184. http s://doi.org/10.1007 /s11356-022-20429-1.

[5] (a) B. Yilmaz, U. Müller, Catalytic Applications of Zeolites in Chemical Industry. *Top Catal.* **2009**, *52*, 888–895. https://doi.org/10.1007/s11244-009-9226-0. (b) Y. Li, J. Yu, Emerging Applications of Zeolites in Catalysis, Separation and Host–Guest Assembly. *Nat. Rev. Mater.* **2021**, *6*, 1156–1174. https://doi.org/10.1038/s41578-021-00347-3.

[6] S. Kwon, C. Kim, E. Han, H. Lee, H. S. Cho, M. Choi, Relationship between Zeolite Structure and Capture Capability for Radioactive Cesium and Strontium. *J. Hazard. Mater.* **2021**, *408*, 124419. https://doi.org/ 10.1016/j.jhazmat.2020.124419.

[7] L. F. de Magalhães, G. R. da Silva, A. E. C. Peres, Zeolite Application in Wastewater Treatment. *Adsorp. Sci. Technol.* **2022**, *2022*, e4544104. https://doi.org/10.1155/2022/454410 4.

[8] L. B. McCusker, F. Liebau, G. Engelhardt, Nomenclature of Structural and Compositional Characteristics of Ordered Microporous and Mesoporous Materials with Inorganic Hosts: (IUPAC Recommendations 2001). *Microporous Mesoporous Mater.* **2003**, *58*, 3–13. https://d oi.org/10.1016/S1387-1811(02)00545-0.

[9] C. Baerlocher, L. McCusker, Database of Zeolite Structures: Paloma Vinaches http://www.Izastruc ture.org/data-bases/.

[10] W. M. Meier, D. H. Olson, Zeolite Frameworks *Adv. Chem. Ser.* **1971**, *101*, 155-170. https://doi.org/1 0.1 021/ba-1971-0101.ch014.

[11] (a) G. T. Kokotailo, S. L. Lawton, D. H. Olson, W. M. Meier, Structure of Synthetic Zeolite ZSM-5. *Nature*, **1978**, *272*, 437–438. https://doi.org/10.1038/272437a0. (b) D. H. Olson, G. T. Kokotailo, S. L. Lawton, W. M. Meier, Crystal Structure and Structure-Related Properties of ZSM-5. *J. Phys. Chem.* **1981**, *85*, 2238–2243. https://doi.org/10.1021/j150615a020.
(c) H. van Koningsveld, H. van Bekkum, J. C. Jansen, On the Location and Disorder of the Tetrapropylammonium (TPA) Ion in Zeolite ZSM-5 with Improved Framework Accuracy. *Acta Cryst. B* **1987**, *43*, 127–132. https://doi.org/10.1107/S0108768187098173.

[12] M. R. Klotz, U.S. Patent 4,269,813 (1981)

[13] M. Chono, and H. E. Ishida, Patent B-113,116 (1984)

[14] M. Taramasso, G. Perego, B. Notari, Proc. 5th Int. Zeolite Conf., pp. 40-48 (1980)

[15] T.V. E. Whittam, Patent B-54,386 (1982)

[16] C. SANCHEZ, J. Pérez-Pariente, *Zeolites and Ordered Porous Solids: Fundamentals and Applications*, **2011**.

[17] M. A. Camblor, S. Bong Hong, Synthetic Silicate Zeolites: Diverse Materials Accessible through Geoinspiration in *Porous Materials*, (Eds.: D. W. Bruce, D. O'Hare, R. I. Walton) John Wiley & Sons, Ltd, **2010**, pp. 265–325. https://doi.org/10.1 002/9780470711385.ch5.

[18] Y. Li, J. Yu, New Stories of Zeolite Structures: Their Descriptions, Determinations, Predictions, and Evaluations. *Chem. Rev.* **2014**, *114*, 7268–7316. https://doi.org/10.1021/cr 500010r.

[19] (a) M. Moshoeshoe, M. S. Nadiye-Tabbiruka, V. Obuseng, A Review of the Chemistry, Structure, Properties and Applications of Zeolites. *Am. j. mater. sci.* **2017**, *7*, 196–221. doi:10.5923/j.materials.20170705.12 (b) E. Nyankson, J. K. Efavi, A. Yaya, G. Manu, K. Asare, J. Daafuor, R. Y. Abrokwah, Synthesis and Characterization of Zeolite-A and Zn-Exchanged Zeolite-A Based on Natural Aluminosilicates and Their Potential Applications. *Cogent Eng.* **2018**, *5*, 1440480. https://doi.org/10.1080/23311916.2018.1440480.

[20] S. L. Burkett, M. E. Davis, Mechanisms of Structure Direction in the Synthesis of Pure-Silica Zeolites. 1. Synthesis of TPA/Si-ZSM-5. *Chem. Mater.* **1995**, *7*, 920–928. https://doi.org/10.1021/cm00053a017.

[21] R. M. Barrer, P. J. Denny, 201. Hydrothermal Chemistry of the Silicates. Part IX. Nitrogenous Aluminosilicates. *J. Chem. Soc.* **1961**, 971–982. https://doi.org/10.10 39/JR 9610000971.

[22] G. T. Kerr, G. T. Kokotailo, SODIUM ZEOLITE ZK-4, A NEW SYNTHETIC CRYSTALLINE ALUMINOSILICATE. *J. Am. Chem. Soc.* **1961**, *83*, 4675–4675. https://doi. org/10.1021/ja01483a052.

[23] RL. Wadlinger, GT. Kerr, EJ. Rosinski (1967) US Patent 3, 308, 069

[24] L. Zhang, N. Liu, C. Dai, R. Xu, G. Yu, B. Chen, N. Wang, Recent advances in shape selectivity of MFI zeolite and its effect on the catalytic performance, Chem. Synth. **2023**, 3, 1-26. https://dx.doi.org/10.20517/cs.2022.31

[25] RJ. Argauer, GR. Landolt (1972) US Patent 3,702, 886

[26] G. T. Kokotailo, P. Chu, S. L. Lawton, W. M. Meier, Synthesis and Structure of Synthetic Zeolite ZSM-11. *Nature*, **1978**, *275*, 119–120. https://doi.org/10.1038/275119a0.

[27] T. Ikuno, W. Chaikittisilp, Z. Liu, T. Iida, Y. Yanaba, T. Yoshikawa, S. Kohara, T. Wakihara, T. Okubo, Structure-Directing Behaviors of Tetraethylammonium Cations toward Zeolite Beta Revealed by the Evolution of Aluminosilicate Species Formed during the Crystallization Process. *J. Am. Chem. Soc.* **2015**, *137*, 14533–14544. https://doi.org/10.1021/jacs.5b11046.

[28] B. M. Lok, T. R. Cannan, C. A. Messina, The Role of Organic Molecules in Molecular Sieve Synthesis. *Zeolites*, **1983**, *3* , 282–291. https://doi.org/10.1016/0144-2449(83)90169-0

[29] J. Perez-Pariente, L. Go´mez-Hortigüela (2008) The role of templates in the synthesis of zeolites. In: C˘ejka J, Pere´z-Pariente J, Roth WJ (eds) Zeolites: from model materials to industrial catalysts. Trans world Research Network, pp 33–62. ISBN: 978-81-7895-330-4

[30] L. Gómez-Hortigüela, M. Á. Camblor, in *Insights into the Chemistry of Organic Structure-Directing Agents in the Synthesis of Zeolitic Materials* (Ed.: L. Gómez-Hortigüela), Springer International Publishing, Cham, **2018**, pp. 1–41. https://doi-org.inc.bib.cnrs.fr/10.1007/430_2017_8

[31] (a) S. Li, J. Li, M. Dong, S. Fan, T. Zhao, J. Wang, W. Fan, Strategies to control zeolite particle morphology, *Chem. Soc. Rev.* **2019**, *48*, 885–907. DOI: 10.1039/c8cs00774h. (b) H. Xu, P. Wu, New progress in zeolite synthesis and catalysis, *Natl. Sci. Rev.* **2022**, *9*, nwac045. DOI: 10.1093/nsr/nwac045 (c) J. Čejka, R. Millini, M. Opanasenko, D. P. Serrano, W. J. Roth, Advances and challenges in zeolite synthesis and catalysis, *Catalysis Today* **2020**, *345*, 2–13. https://doi.org/10.1016/j.cattod.2019.10.021

[32] (a) X. Li, S. -T. Tsai, K. C. W. Wu, O. J. Curnow, J. Choi, A. C. K. Yip, Morphology control of ionic-liquid-templated ZSM-22 and ZSM-5 zeolites using a step process and its effect on toluene methylation, Microporous Mesoporous Mater. **2021**, *328*, 111475 https://doi.org/10.1016/j.micr omeso.2021.111475. (b) X. Li, C. Ku, Y. Jeong, O. J. Curnow, P. H. L. Sit, Z. Wu, J. Choi, A. C. K. Yip, Ionic liquid-templated synthesis of 10-MR zeolites and its origin disclosure, *Microporous Mesoporous Mater.* **2020**, *305*, 110346. https://doi.org/10.1016/j.micromeso.2020.110346. (c) X. Li, T. H. Li, W. Zhou, Y. P. Li, P. H. L. Sit, Z. Wu, O. J. Curnow, K. C. W. Wu, J. Choi, A. C. K. Yip, Unveiling the elusive role of tetraethyl orthosilicate hydrolysis in ionic-

liquid-templated zeolite synthesis, *Mater, Today Chem* **2022**, *23*, 100658. https://doi.org/10.1016/j.mtchem.2021.1 00658

[33] M. Jiao, J. Huang, H. Xu, J. Jiang, Y. Guan, Y. Ma, P. Wu, ECNU-36: a quasi-pure polymorph CH beta silicate composed of hierarchical nanosheet crystals for effective VOCs, Adsorption, **2020**, *59*, 17291e17296 DOI: 10.1002/anie.202008327

[34] P. Lu, A. Mayoral, L. Gomez-Hortigüela, Y. Zhang, M. A. Camblor, Synthesis of 3D large-pore germanosilicate zeolites using imidazolium-based long dications, Chem. Mater. **2019**, *31*, 5484e5493. https://doi-org.inc.bib.cnrs.fr/10.1021/acs.chemmater.9b00959

[35] L. A. Villaescusa, J. Li, Z. Gao, J. Sun, M. A. Camblor, IDM-1: A Zeolite with Intersecting Medium and Extra-Large Pores Built as an Expansion of Zeolite MFI. *Angew. Chem. Int. Ed.* **2020**, *59*, 11283–11286. https://doi.org/10.1002/anie.202001740

[36] A. Corma, M. J. Diaz-Cabanas, J. L. Jorda, F. Rey, G. Sastre, K. G. Strohmaier, A Zeolitic Structure (ITQ-34) with Connected 9- and 10-Ring Channels Obtained with Phosphonium Cations as Structure Directing Agents *J. Am. Chem. Soc.* **2008**, *130*, 16482–16483. https://doi-org.inc.bib.cnrs.fr/10.1021/ja806903c

[37] Y. Ma, J. Hu, K. Fan, W. Chen, S. Han, Q. Wu, Y. Ma, A. Zheng, E. Kunkes, T. De Baerdemaeker, A.-N. Parvulescu, N. Bottke, T. Yokoi, D. E. De Vos, X. Meng, F.-S. Xiao, Design of an Organic Template for Synthesizing ITR Zeolites under Ge-Free Conditions *J. Am. Chem. Soc.* **2023**, *145*, 17284–17291. https://doi-org.inc.bib.cnrs.fr/10.1021/jacs.3c04652

[38] E. M. Gallego, C. Paris, Á. Cantín, M. Moliner, A. Corma, Conceptual similarities between zeolites and artificial enzymes *Chem. Sci.* **2019**, *10*, 8009–8015. https://doi-org.inc.bib.cnrs.fr/10.1039/C9SC02477H

[39] M. Moliner, M. Boronat, Towards "enzyme-like" zeolite designs to maximize the efficiency of catalysts by molecular recognition: Fine-tuning confinement and active site location *Microporous Mesoporous Mater.* **2023**, *358*, 112354. https://doi.org/10.1016/j.micromeso.2022.112354

[40] M. Choi, K. Na, J. Kim, Y. Sakamoto, O. Terasaki, R. Ryoo, Stable Single-Unit-Cell Nanosheets of Zeolite MFI as Active and Long-Lived Catalysts. *Nature*, **2009**, *461*, 246–249. https://doi.org/10.1038/nature08288.

[41] (a) R. Peng, S. Li, Z. Wan, Z.-Q. Wang, X. Si, J. Tuo, H. Xu, Y. Guan, J. Jiang, Y. Ma, X. He, X.-Q. Gong, P. Wu, Directing Highly a-Axis-Oriented ZSM-5 Nanosheets with Pre-estimated Bifunctional Imidazole Cations, *ACS Appl. Mater. Interfaces* **2023**, *15*, 28116–28124. https://doi-org.inc.bib.cnrs.fr/10.1021/acsami.3c04317 (b) G. T. M. Kadja, N. J. Azhari, S. Mardiana, N. T. U. Culsum, A. Maghfirah, Recent advances in the development of nanosheet zeolites as heterogeneous catalysts, *Results in Engineering* **2023**, *17*, 100910. https://doi.o rg/10.1016/j.rineng.2023.100910 (c) Y. Nan, S. Ma, F. Zha, H. Tian, X. Tang, Y. Chang, X. Guo, Facile surfactant-assisted synthesis of nanosheet-like mesoporous SAPO-34 zeolites and catalysis performance for methanol to olefins *Reac. Kinet. Mech. Cat.* **2022**, *135*, 1987–1998. https://doi-org.inc.bib.cnrs.fr/10.1007/s11144-022-02233-7.

[42] J. Meng, C. Li, X. Chen, C. Song, C. Liang, Seed-assisted synthesis of ZSM-48 zeolite with low SiO_2/Al_2O_3 ratio for n-hexadecane hydroisomerization *Microporous and Mesoporous Mater.* **2020**, *309*, 110565. https://doi.org/10.1016/j.micromeso.2020.110565

[43] C. Lei, Z. Dong, C. Martínez, J. Martínez-Triguero, W. Chen, Q. Wu, X. Meng, A.-N. Parvulescu, T. De Baerdemaeker, U. Müller, A. Zheng, Y. Ma, W. Zhang, T. Yokoi, B. Marler, D. E. De Vos, U. Kolb, A. Corma, F.-S. Xiao, A Cationic Oligomer as an Organic Template for Direct Synthesis of Aluminosilicate ITH Zeolite, *Angew. Chem. Int. Ed.* **2020**, *59*, 15649–15655. https://doi-org.inc.bib.cnrs.fr/10.1002/anie.202003282

[44] P. Wei, W. Liu, J. Li, Y. Wang, Q. Yu, Z. Yang, X. Liu, L. Xu, X. Li, X. Zhu, Synthesis and crystallization mechanism of EUO zeolite, *Microporous and Mesoporous Mater.* **2022**, *337*, 111911. https://doi.org/10.1016/j.micromeso.2022.111911

[45] D. L. Dorset, S. C. Weston, S. S. Dhingra, Crystal Structure of Zeolite MCM-68: A New Three-Dimensional Framework with Large Pores. *J. Phys. Chem. B* **2006**, *110*, 2045–2050. https://doi.org/10.1021/jp0565352.

[46] J. Sun, C. Bonneau, Á. Cantín, A. Corma, M. J. Díaz-Cabañas, M. Moliner, D. Zhang, M. Li, X. Zou, The ITQ-37 Mesoporous Chiral Zeolite. *Nature,* **2009**, *458*, 1154–1157. https://doi .org/10.1038/nature07957.

[47] S. A. Elomari, S. I. Zones, 03-O-03-Synthesis of Novel Zeolites SSZ-53 and SSZ-55 Using Organic Templating Agents Derived from Nitriles. In *Studies in Surface Science and Catalysis*; Galarneau, A., Fajula, F., Di Renzo, F., Vedrine, J., Eds.; Zeolites and Mesoporous Materials at the dawn of the 21st century; Elsevier, 2001; Vol. 135, p 167. https://doi.org/10.1016/S0167-2991(01)81296-9.

[48]A. Burton, S. Elomari, C. –Y. Chen, R. C. Medrud, I. Y. Chan, L. M. Bull, C. Kibby, T. V. Harris, S. I. Zones, E. Vittoratos, E. S. SSZ-53 and SSZ-59: Two Novel Extra-Large Pore Zeolites. *Chem. Eur. J.* **2003**, *9*, 5737–5748. https://doi.org/10.1002/chem.200305238.

[49] J. Jiang, Y. Yun, X. Zou, J. L. Jorda, A. Corma, ITQ-54: A Multi-Dimensional Extra-Large Pore Zeolite with 20 × 14 × 12-Ring Channels. *Chem. Sci.* **2014**, *6*, 480–485. https://doi.org/10.1039/C4SC02577F.

[50] S. Smeets, D. Xie, C. Baerlocher, L. B. McCusker, W. Wan, X. Zou, S. I. Zones, High-Silica Zeolite SSZ-61 with Dumbbell-Shaped Extra-Large-Pore Channels. *Angew. Chem. Int. Ed.* **2014**, *53*, 10398–10402. https://doi.org/10.1002/anie.201405658.

[51] P. Wagner, S. I. Zones, M. E. Davis, R. C. Medrud, SSZ-35 and SSZ-44: Two Related Zeolites Containing Pores Circumscribed by Ten- and Eighteen-Membered Rings. *Angew. Chem. Int. Ed.* **1999**, *38*, 1269–1272. https://doi.org/10.1002/(SICI)1521-3773(19990503)38:9 <1269::AID-ANIE1269>3.0.CO;2-3.

[52] E. Kapaca, J. Jiang, J. Cho, J. L. Jordá, M. J. Díaz-Cabañas, X. Zou, A. Corma, T. Willhammar, Synthesis and Structure of a 22 × 12 × 12 Extra-Large Pore Zeolite ITQ-56 Determined by 3D Electron Diffraction. *J. Am. Chem. Soc.* **2021**, *143* , 8713–8719. https://do i.org/10.1021/jacs.1c02654.

[53] F. –J. Chen, Y. Xu, H. –B. Du, An Extra-Large-Pore Zeolite with Intersecting 18-, 12-, and 10-Membered Ring Channels. *Angew. Chem. Int. Ed.* **2014**, *53*, 9592–9596. https://doi.org/10.1002/anie.201404608.

[54] Z. –H. Gao, F. –J. Chen, L. Xu, L. Sun, Y. Xu, H. –B. Du, A Stable Extra-Large-Pore Zeolite with Intersecting 14- and 10-Membered-Ring Channels. *Chem. Eur. J.* **2016**, *22*, 14367–14372. https://doi.org/10.1002/chem.201602419.

[55] F. –J. Chen, Z. –H. Gao, L. –L. Liang, J. Zhang, H. –B. Du, Facile Preparation of Extra-Large Pore Zeolite ITQ-37 Based on Supramolecular Assemblies as Structure-Directing Agents. *Cryst. Eng. Comm.* **2016**, *18*, 2735–2741. https://doi.org/10.1039/C5CE02312B.

[56] M. E. Davis, C. Saldarriaga, C. Montes, J. Garces, C. Crowdert, A Molecular Sieve with Eighteen-Membered Rings. *Nature* **1988**, *331*, 698–699. https://doi.org/10.1038/331698a0.

[57] E. G. Derouane, L. Maistriau, Z. Gabelica, A. Tuel, J. B. Nagy, R. Von Ballmoos, Synthesis and Characterization of the Very Large Pore Molecular Sieve MCM-9. *Appl. Catal.* **1989**, *51*, L13–L20. https://doi.org/10.1016/S0166-9834(00)80218-3.

[58] B. W. Boal, S. I. Zones, M. E. Davis, Triptycene Structure-Directing Agents in Aluminophosphate Synthesis. *Microporous and Mesoporous Mater.* **2015**, *208*, 203–211. https://doi.org/10.1016/j.micromeso.2015.01.045.

[59] R. M. Dessau, J. L. Schlenker, J. B. Higgins, Framework Topology of AlPO4-8: The First 14-Ring Molecular Sieve. *Zeolites*, **1990**, *10*, 522–524. https://doi.org/10.1016/S0144-2449(05)80306-9.

[60] M. Estermann, L. B. McCusker, C. Baerlocher, A. Merrouche, H. Kessler, A Synthetic Gallophosphate Molecular Sieve with a 20-Tetrahedral-Atom Pore Opening. *Nature*, **1991**, *352*, 320–323. https://doi.org/10.1038/352320a0.

[61] (a) Y. Wei, Z. Tian, H. Gies, R. Xu, H. Ma, R. Pei, W. Zhang, Y. Xu, L. Wang, k. Li, B. Wang, G. Wen, L. Lin, Ionothermal Synthesis of an Aluminophosphate Molecular Sieve with 20-Ring Pore Openings. *Angew. Chem. Int. Ed.* **2010**, *49*, 5367–5370. https://doi.org/10.1002/anie.201000320. (b) J. Su, Y. Wang, J. Lin, J. Liang, J. Sun, X. Zou, A Silicogermanate with 20-Ring Channels Directed by a Simple Quaternary Ammonium Cation. *Dalton Trans.* **2013**, *42*, 1360–1363. https://doi.org/10.1039/C2DT32231E. (c) S. Tao, R. Xu, X. Li, H. Ma, D. Wang, Y. Xu, Z. Tian, Synthesis of Discrete Aluminophosphate –CLO Nanocrystals in a Eutectic Mixture. *J. Colloid Interface Sci.* **2015**, *451*, 117–124. https://doi.org/10.1016/j.jci s.2015.04.011.(d) Y. Lin, L. Zhang, K. Guo, M. Wang, Y. Wei, Co-Structure-Directing Effect in Ionothermal Synthesis of Extra-Large-Pore Aluminophosphate Zeotype with −CLO Topology. *Chem. Eur. J.* **2018**, *24*,

2410–2417. https://doi.org/ 10.1002/chem.201705038. (e) S. Tao, X. Li, X. Wang, Y. Wei, Y. Jia, J. Ju, Y. Cheng, H. Wang, S. Gong, X. Yao, H. Gao, C. Zhang, Q. Zang, Z. Tian, Facile Synthesis of Hierarchical Nanosized Single-Crystal Aluminophosphate Molecular Sieves from Highly Homogeneous and Concentrated Precursors. *Angew. Chem. Int. Ed.* **2020**, *59*, 3455–3459. https://doi.org/10.1 002/anie.201915144.

[62] R. Martínez-Franco, M. Moliner, Y. Yun, J. Sun, W. Wan, X. Zou, A. Corma, Synthesis of an Extra-Large Molecular Sieve Using Proton Sponges as Organic Structure-Directing Agents. *Proc. Natl. Acad. Sci.* **2013**, *110*, 3749–3754. https://doi.org/10.1073/pnas.1220733110.

[63] W. –W. Zi, Z. Gao, J. Zhang, J. –H. Lv, B. –X. Zhao, Y. –F. Jiang, H. –B. Du, F. –J Chen, Designed Synthesis of an Extra-Large Pore Zeolite with a 14-Membered Ring Channel via Supramolecular Assembly Templating Approach. *Microporous and Mesoporous Mater.* **2019**, *290*, 109654. https://doi. org/10.10 16 /j . micromeso.2019.109654.

[64] P. Wagner, M. Yoshikawa, K. Tsuji, M. E. Davis, P. Wagner, M. Lovallo, M. Taspatsis, CIT-5: A High-Silica Zeolite with 14-Ring Pores *Chem. Commun.* **1997**, 2179–2180. https:// doi.org/10 .1039/A704774F.

[65] A. Burton, S. Elomari, C. Y, Chen, T. V. Harris, E. S. Vittoratos SSZ-53 and SSZ-59: Two Novel Extra-Large Pore Zeolites. In *Studies in Surface Science and Catalysis*; van Steen, E., Claeys, I. M., Callanan, L. H., Eds.; Recent Advances in the Science and Technology of Zeolites and Related Materials; Elsevier, 2004; Vol. 154, pp 126–132. https://doi.org/10.101 6/S0167-2991(04)80792-4.

[66] K. G. Strohmaier, D. E. W. Vaughan, Structure of the First Silicate Molecular Sieve with 18-Ring Pore Openings, ECR-34. *J. Am. Chem. Soc.* **2003**, *125*, 16035–16039. https://doi.org/10 .1021/ja0371653.

[67] T. Willhammar, A. W. Burton, Y. Yun, J. Sun, M. Afeworki, K. G. Strohmaier, H. Vroman, X. Zou, EMM-23: A Stable High-Silica Multidimensional Zeolite with Extra-Large Trilobe-Shaped Channels. *J. Am. Chem. Soc.* **2014**, *136*, 13570–13573. https://doi.org/10.1021/ja507 615b.

[68] Y. Wang, J. Zhu, M. Sun, L. Wang, J. Yang, Q. Wu, X. Wang, C. Liu, J. Sun, X. Mu, X. Shu, The Synthesis of RZM-3 Zeolite with EWT Topology Structure Using 1,1,6,6-Tetramethyl-1,6-Diazacyclododecane-1,6-Diium Dihydroxide as Structure-Directing Agent. *Microporous and Mesoporous Mater.* **2019**, *275*, 87–94. https://doi.org/10.1016/j.micromeso. 2018.08.012.

[69] S. Smeets, Z. J. Berkson, D. Xie, S. I. Zones, W. Wan, X. Zou, M. –F Hsieh, B. F. Chmelka, L. B. McCusker, C. Baerlocher, Well-Defined Silanols in the Structure of the Calcined High-Silica Zeolite SSZ-70: New Understanding of a Successful Catalytic Material. *J. Am. Chem. Soc.* **2017**, *139*, 16803–16812. https://doi. Or g/10.1021/jacs.7b08810.

[70] W. –W. Zi, Z. Gao, J. Zhang, B. –X. Zhao, X. –S. Cai, H. –B. Du, F. –J. Chen, An Extra-Large-Pore Pure Silica Zeolite with 16×8×8-Membered Ring Pore Channels Synthesized Using an Aromatic Organic Directing Agent. *Angew. Chem. Int. Ed.* **2020**, *59*, 3948–3951. https:// doi.org/10.1002/anie.201915232.

[71] (a) J. –L. Paillaud, B. Harbuzaru, J. Patarin, N. Bats, Extra-Large-Pore Zeolites with Two-Dimensional Channels Formed by 14 and 12 Rings. *Science*, **2004**, *304*, 990–992. https://doi.org/10.1126/science.1098242. (b) A. Corma, M. J. Díaz-Cabañas, F. Rey, S. Nicolopoulus, K. Boulahya, ITQ-15: The First Ultralarge Pore Zeolite with a Bi-Directional Pore System Formed by Intersecting 14- and 12-Ring Channels, and Its Catalytic Implications. *Chem. Commun.* **2004**, No. 12, 1356–1357. https://doi.org/10.1039/B406572G.

[72] A. Corma, M. J. Díaz-Cabañas, J. L. Jordá, C. Martínez, M. Moliner, High-Throughput Synthesis and Catalytic Properties of a Molecular Sieve with 18- and 10-Member Rings. *Nature*, **2006**, *443*, 842–845. https://doi.org/10.1038/nature05238.

[73] J. Jiang, J. L. Jorda, M. J. Diaz-Cabanas, J. Yu, A. Corma, The Synthesis of an Extra-Large-Pore Zeolite with Double Three-Ring Building Units and a Low Framework Density. *Angew. Chem. Int. Ed.* **2010**, *49*, 4986–4988. https://doi.org/10.1002/anie.201001506.

[74] J. Jiang, J. L. Jorda, J. Yu, L. A. Baumes, E. Mugnaioli, M. J. Diaz-Cabanas, U. Kolb, A. Corma, Synthesis and Structure Determination of the Hierarchical Meso-Microporous Zeolite ITQ-43. *Science*, **2011**, *333*, 1131–1134. https://doi.org/10.1126/science.1208652.

[75] C. Zhang, E. Kapaca, J. Li, Y. Liu, X. Yi, A. Zheng, X. Zou, J. Jiang, J. Yu, An Extra-Large-Pore Zeolite with 24×8×8-Ring Channels Using a Structure-Directing Agent Derived from Traditional Chinese Medicine, *Angew. Chem. Int. Ed.* **2018**, *57*, 6486–6490. DOI:10.1002/anie.201801386

[76] L. A. Villaescusa, M. A. Camblor, Time Evolution of an Aluminogermanate Zeolite Synthesis: Segregation of Two Closely Similar Phases with the Same Structure Type. *Chem. Mater.* **2016**, *28*, 3090–3098. https://doi.org/10.1021/acs.chemmater.6b00507.

[77] (a) P. Caullet, J. L. Guth, J. Hazm, J. M. Lamblin, H. Gies, Characterization, and Crystal Structure of the New Clathrasil Phase Octadecasil. *ChemInform* **2010**, *22*, https://doi.org/10.1002/chin.199124028. (b) L. A. Villaescusa, P. A. Barrett, M. A. Camblor, Calcination of Octadecasil: Fluoride Removal and Symmetry of the Pure SiO_2 Host. *Chem. Mater.* **1998**, *10*, 3966–3973. https://doi.org/10.1021/cm9804113.

[78] (a) P. Caullet, J. –L. Paillaud, Y. Mathieu, N. Bats, Synthesis of Zeolites in the Presence of Diquaternary Alkylammonium Ions as Structure-Directing Agents. *Oil & Gas Science and Technology – Rev. IFP*, **2007**, *62*, 819-825 https://doi.org/10.2516/ogst:2007079. (b) S. –H. Lee, C. –H. Shin, D. –K. Yang, S.-D. Ahn, I. –S. Nam, S. B. Hong, Reinvestigation into the Synthesis of Zeolites Using Diquaternary Alkylammonium Ions $(CH_3)_3N^+(CH_2)NN^+(CH_3)_3$ with N = 3–10 as Structure-Directing Agents. *Microporous and Mesoporous Mater.* **2004**, *68*, 97–104. https://doi.org/10.1016/j.micromeso.2003.12.011. (c) A. Rojas, L. Gómez-Hortigüela, M. A. Camblor, Benzylimidazolium Cations as Zeolite Structure-Directing Agents. Differences in Performance Brought about by a Small Change in Size. *Dalton Trans.* **2013**, *42*, 2562–2571. https://doi.org/10.1039/C2DT32230G. (d) P. Emily, R. Morris, 1-Alkyl-3-Methyl Imidazolium Bromide Ionic Liquids in the Ionothermal Synthesis of Aluminium Phosphate Molecular Sieves. *Chem. Mater.* **2006**, *18*, 4882-4887 https://doi.org/10.1021/cm0615929. (e) E. R. Parnham, E. A.

Drylie, P. S. Wheatley, A. M. Z. Slawin, R. E. Morris, Ionothermal Materials Synthesis Using Unstable Deep-Eutectic Solvents as Template-Delivery Agents. *Angew. Chem. Int. Ed.* **2006**, *45*, 4962–4966. https://doi.org/10.1002/anie.200600290. (f) Y. Li, X. Gong, L. Liu, J. Dong, Co-templating Ionothermal Synthesis and Crystal Structure of a New Layered Aluminophosphate from a Protic Deep Eutectic Solvent *Chinese Journal of Chemistry* **2016**, *34*, 419–424. https://doi-org.inc.bib.cnrs.fr/10.1002/cjoc.201600023

[79] Y. Yamasaki, N. Tsunoji, Y. Takamitsu, M. Sadakane, T. Sano, Synthesis of phosphorus-modified small-pore zeolites utilizing tetraalkyl phosphonium cations as both structure-directing and phosphorous modification agents, *Microporous and Mesoporous Mater*. **2016**, *223*, 129–139. https://doi.org/10.1016/j.micromeso.2015.10.038.

[80] T. Lemishko, J. Simancas, M. Hernández-Rodríguez, M. Jiménez-Ruiz, G. Sastre, F. Rey, An INS study of entrapped organic cations within the micropores of zeolite RTH *Phys. Chem. Chem. Phys.* **2016**, *18*, 17244–17252. https://doi-org.inc.bib.cnrs.fr/10.1039/C6CP00971A

[81] (a) E. Mitani, N. Tsunoji, M. Sadakane, T. Sano, Synthesis of GME zeolite with high porosity by hydrothermal conversion of FAU zeolite using a dual-template method with tetraethylphosphonium and N,N-dimethyl-3,5-dimethylpiepridinium hydroxides *J Porous Mater* **2019**, *26*, 1345–1352. https://doi-org.inc.bib.cnrs.fr/10.1007/s10934-019-00725-x (b) D. L. Dorset, G. J. Kennedy, K. G. Strohmaier, M. J. Diaz-Cabañas, F. Rey, A. Corma, P-Derived Organic Cations as Structure-Directing Agents: Synthesis of a High-Silica Zeolite (ITQ-27) with a Two-Dimensional 12-Ring Channel System. *J. Am. Chem. Soc.* **2006**, *128*, 8862–8867. https://doi.org/10.1021/ja061206o.

[82] (a) Y. Yun, M. Hernández, W. Wan, X. Zou, J. L. Jordá, A. Cantín, F. Rey, A. Corma, The first zeolite with a tri-directional extra-large 14-ring pore system derived using a phosphonium-based organic molecule, *Chem. Commun.* **2015**, *51*, 7602–7605. DOIhttps://doi-org.inc.bib.cnrs.fr/10.1039/C4C C10317C. (b) A. Corma, M. J. Díaz-Cabañas, J. Jiang, M. Afeworki, D. L. Dorset, S. L. Soled, K. G. Strohmaier, Extra-Large Pore Zeolite (ITQ-40) with the lowest Framework Density Containing Double Four- and Double Three-Rings. *Proc. Natl. Acad. Sci. U.S.A.* **2010**, *107*, 13997–14002. https://doi.org/10.1073/pnas.100300910.

[83] Q. -F. Lin, Z. R. Gao, C. Lin, S. Zhang, J. Chen, Z. Li, X. Liu, W. Fan, J. Li, X. Chen, M. A. Camblor, F.-J. Chen, A stable aluminosilicate zeolite with intersecting three-dimensional extra-large pores, *Science* **2021**, *374*, 1605–1608. DOI: 10.1126/science.abk3258

[84] (a) P. Vinaches, K. Bernardo-Gusmão, S. B. C. Pergher, An Introduction to Zeolite Synthesis Using Imidazolium-Based Cations as Organic Structure-Directing Agents. *Molecules* **2017**, *22*, 1307. https://doi.org/10.3390/molecules22081307. (b) X. Li, O. J. Curnow, J. Choi, A. C. K. Yip, Recent Advances in the Imidazolium-Based Ionic Liquid-Templated Synthesis of Microporous Zeolites. *Materials Today Chemistry* **2022**, *26*, 101133. https://doi.org/10.1016/ j.mtchem.2022.101133

Chapter Two

1. Synthesis of ammonium salts.

1.1. Ammonium salts containing terminal and non-terminal alkyne unit(s).

- Ammonium salts containing one alkyne group substituent **66(a-g)**:

At first, in the series of ammonium salts containing one alkyne group substituent, two ammonium salts with terminal alkyne groups **66(a,b)** were synthesized by reacting 1.2 equiv. of triethylamine **(57b)** or tripropylamine **(57c)** with 1 equiv. of propargylbromide **(75a)**. Following a procedure described by McLndoe group for the alkylation of trioctylamine with propargyl bromide, the reaction proceeded at room temperature in diethyl ether (Et_2O) within 48h (Scheme 18).[85] A total of 9g of **66a** and 10.5 g of **66b** were prepared. The colored impurities of the obtained ammonium salts **66a** and **66b** were removed by triturating in acetone. For purification, the salts were dissolved in distilled water and washed with pentane several times to afford the final products **66a** and **66b** in 93% and 83% yield, respectively. The **^{1}H NMR** spectra for ammonium salts with terminal alkynes showed special pattern. For example, in the case of **66a** (Scheme 18), when the **^{1}H NMR** analysis was run in deuterated DMSO, four different peaks were observed: 4.33 ppm (d, J = 2.6 Hz, 2H, H-3), 4.01 ppm (t, J = 2.6 Hz, 1H, H-1), 3.32 ppm (q, J = 7.2 Hz, 6H, H-4), and 1.2 ppm (t, J = 7.2 Hz, 9H, H-5). However, when the **^{1}H NMR** analysis was run in deuterium oxide (D_2O) instead of deuterated DMSO, only three peaks were observed: 4.11 ppm (s, 2H, H-3), 3.40 ppm (q, J = 7.3 Hz, 6H, H-4), and 1.29 ppm (t, J = 7.3 Hz, 9H, H-5). The reason behind the disappearance of the H-1 peak was the acidic character of H and the lability of deuterium in D_2O.

The set of ammonium salts, which have one alkyne group substituent, was extended to include ammonium salts with non-terminal alkyne units **66c-f** (Scheme 18). Based on the size expansion approach, ammonium salts with different alkyl chains were prepared quantitatively (94-99 %) following the same experimental procedure. A total of 3g of **66c**, 4.2g of **66d**, 12.9g of **66e**, and 6g of **66f** were synthesized. All of these salts were dissolved in water and washed with pentane several times for purification. The last example in this series was synthesized by reacting tri-n-propyl amine **(57c)** with 1-bromo-2-pentyne **(75c)**, and 2g of **66g** were obtained after purification with a 99% yield. All of these reported ammonium salts are new except for the first ammonium salt **66a** it was synthesized before but not used as SDA.

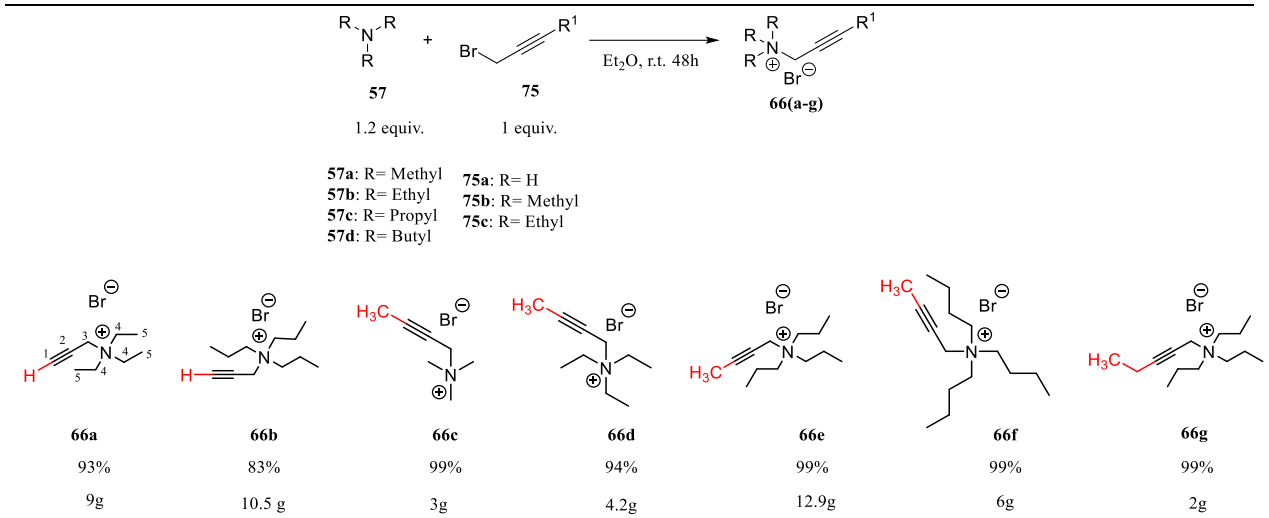

Scheme 18. Synthesis of terminal and non-terminal alkyne based ammonium salts

- Ammonium salts containing two alkyne group substituents **67(a-b)**:

Ammonium salts containing two alkyne group substituents were also synthesized and tested as possible candidates in zeolite synthesis (Schemes 19 and 21). At first, ammonium salt **67a** was prepared by a two-step reaction (Scheme 19). In step 1, tertiary amine **77** was obtained by reacting 2.5 equiv. of pyrrolidine **(76)** with 1 equiv. of propargyl bromide **(75a)** in acetonitrile at 60 ^{o}C. The reaction proceeded within 48h, and the obtained product **77** was purified by removing the excess of pyrrolidine salt using column chromatography (alumina oxide 95:5 (v/v) pentane-ethyl acetate). The combined fractions were then concentrated not to dryness to avoid the loss of tertiary amine **77** and further alkylated with propargyl bromide **(75a)** (1.3 equiv.) in dry diethylether (Et_2O) at room temperature. The reaction proceeded within 48h to afford final product with a 45 % yield. The obtained product was further washed with pentane to remove the traces of pyrrolidine **(76)**. For clarification, the reaction was done over two steps to avoid having a mixture of protonated pyrrolidinium salt and product **67a** that are hard to separate.

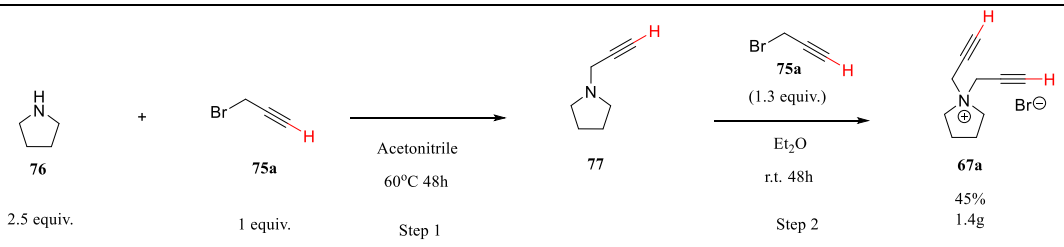

Scheme 19. Synthesis of ammonium salt **67a** using a two step reaction.

In order to minimize the use of excess pyrrolidine **(76)** and eliminate the need of purifying through column chromatography, another approach was followed for synthesizing ammonium salts with two alkyne units. Propargyl bromide **(75a)** was added to a solution containing dipropylamine **(78)** and potassium carbonate (1.2 equiv.) in acetonitrile (Scheme 20). The reaction was heated at 60°C for 48h. However, the reaction did not proceed as expected, resulting in the formation of different side products and impurities. This outcome may be due to the instability of terminal alkynes under basic conditions at high temperatures.

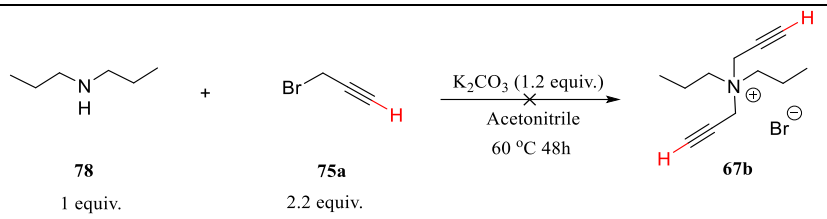

Scheme 20. Attempt to prepare ammonium salt **67b**

As an alternative, acetylene **75(a** or **b)** was added to a solution containing secondary amines **76** or **78** and potassium carbonate (2 equiv.) in DMF (Scheme 21).[86] Following a procedure reported by Nakamura's group for the preparation of propargylic amines, the reaction proceeded within 48 h at room temperature. The resulting mixture was filtered over celite and washed with diethyl ether (Et_2O), followed by washing with distilled water to remove the excess of DMF. The obtained tertiary amine **79** was dissolved again in dry diethylether (Et_2O) and further alkylated with bromo alkyne **75** (1.2 equiv.) to afford ammonium salts **67c** (43%, 1.3g), **67d** (86%, 2.4g), and **67b** (87%, 1.6g). The reason behind using a two-step reaction instead of one is the use of DMF as a polar solvent with a base to favor the occurrence of reaction at room temperature. Thus, when DMF is present, tertiary amine can be extracted by diethyl ether and washed with water to remove traces of DMF. However, if the product **67** is formed in the first step, it will be challenging to isolate it from DMF as they are both soluble in distilled water. From the reported ammonium salts **67a-d,** the ammonium salt **67a** was synthesized before but not used as SDA.

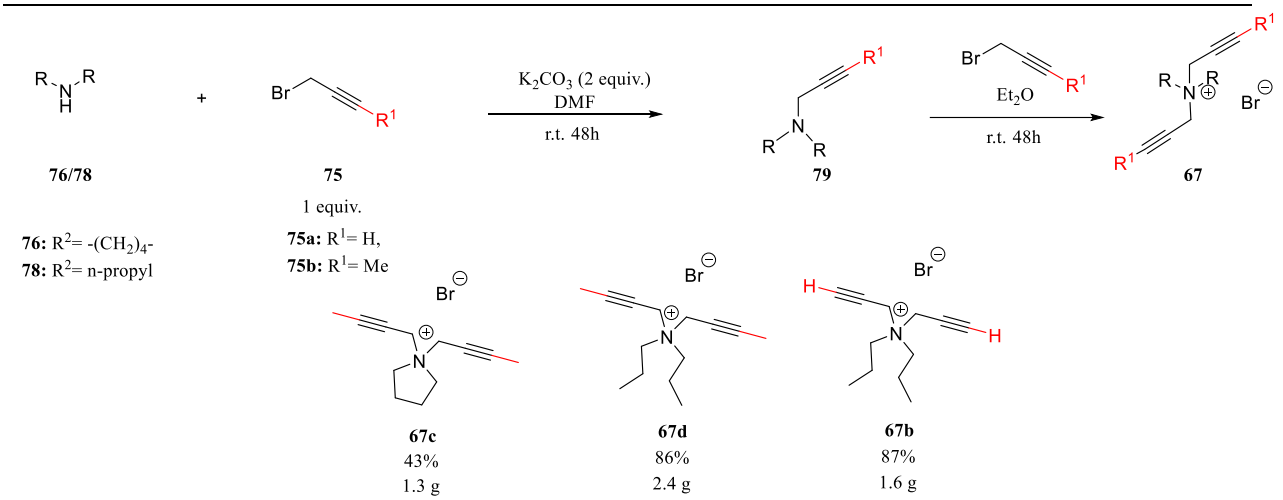

Scheme 21. Synthesis of ammonium salts **67c**, **67d** and **67b** through a 2 step reaction

To investigate the effect of having two alkyl groups instead of alkyne groups in zeolite synthesis, ammonium salt **82** was proposed. An attempt to synthesize ammonium salt based on pyrrolidine with two alkyl chains (propyl) following the same procedure mentioned in scheme 21 was made. Pyrrolidine **(76)** and bromopropane **(80c)** (1 equiv.) were added to a DMF solution containing potassium carbonate (2 equiv.). However, The reaction didn't proceed even after stirring at room temperature for 48h (Scheme 22).

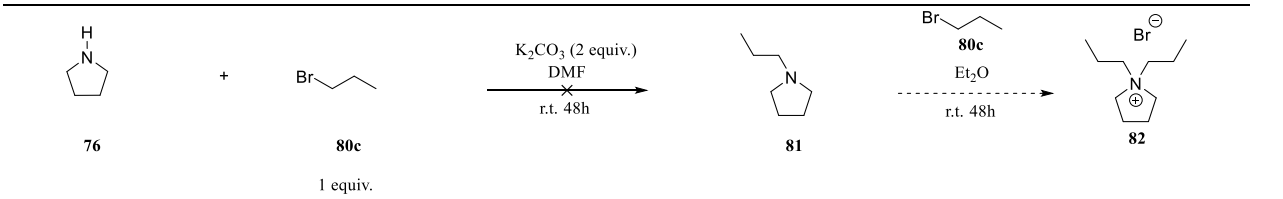

Scheme 22. Attempt to synthesize ammonium salt **82** following a 2 step reaction

As an alternative, the reaction conditions found in scheme 20 were repeated again in scheme 23 on different substrates. Pyrrolidine **(76)** (1 equiv.) and bromopropane **(80c)** (3 equiv.) were added to a solution containing K_2CO_3 (1.2 equiv.) dissolved in acetonitrile. The reaction proceeded at 60 ^oC within 48h. The resulting solution was condensed under reduced pressure, dissolved in ethanol, and filtered to remove the remaining insoluble potassium carbonate to afford 2g of ammonium salt **82** with a 98 % yield.

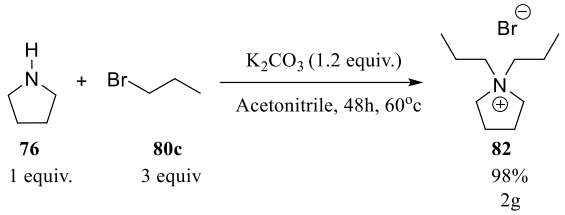

Scheme 23. Synthesis of ammonium salt **82** in one step reaction

1.2. Hexamethylenetetramine based ammonium salts 87(a-f).

As demonstrated previously in chapter 1, ball-shaped SDAs like SDA **14**, **28** and **36** favored the crystallization of zeolites with distinct frameworks and pore sizes. In this part, a new set of ammonium salts with different nitrogen to carbon ratios based on hexamethylenetetramine **68a-f** were prepared (Scheme 24). These salts were prepared following a procedure reported by Ma's group for the synthesis of N- benzyl hexamethylenetetranium bromide **68d** (yield reported by the group: 84%), the alkylation reaction between RX **80** (5 equiv.) and hexamethylenetetramine **(83)** proceeded in ethyl acetate at 60 °C within 12h.[87] The hexamethylenetetramine-based ammonium salts **68a-f** were obtained in quantitative yields after washing with ethyl acetate (**68a** (1.9 g, 42%), **68b** (3g, 93%), **68c** (17.2 g, 86%), **68d** (4 g, 64%), **68e** (1.2 g, 50%), and **68f** (1.6 g, 54%)). All of these ammonium salts **68a-e** were synthesized before except the last one **68f**. However, these ammonium salts were never used in zeolite synthesis. Extra information about these molecules is given in the experimental part.

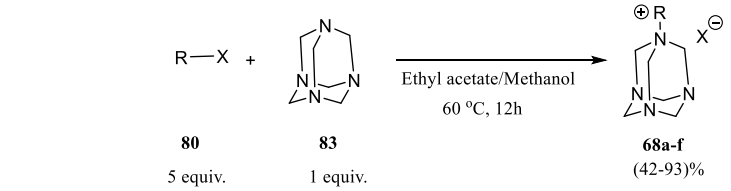

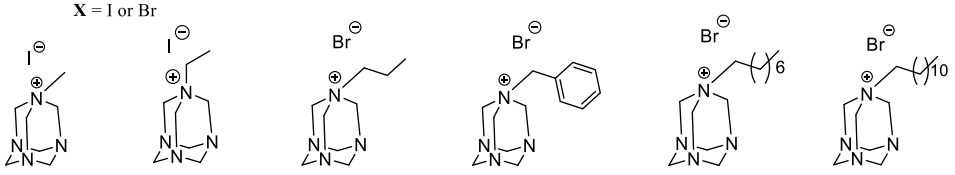

68a	68b	68c	68d	68e	68f
92%	93%	86%	64% (84%)	50%	54%
1.9 g	3 g	17.2 g	4 g	1.2 g	1.6 g

Scheme 24. Synthesis of hexamethylenetetramine based ammonium salts **68a-f**.

1.3. Imidazole based ammonium salts 69a-d and 70a-c.

SDAs with different imidazole units are quite famous ammonium salts that favor the crystallization of zeolites with different frameworks.[88] Here, four different imidazole-based ammonium salts were synthesized, having acetylene, benzyl, and mesitylene units **69a-d** (Scheme 25). The alkylation reaction between R_2X (**75b**, **80d**, or **80g**) and N-alkylimidazole **84a** or **84b** in THF at 66 ^oC proceeded within 48 h to afford the salts **69a** (1.5g, 80%), **69b** (2g, 99%), **69c** (4.5g, 64%), and **69d** (5.3 g, 92%) (Scheme 25). The procedure used was reported by Li and Camblor's group for the synthesis of ammonium salt **69c** (Reported yield: 92 %). [89] For purification, the imidazole-based ammonium salts were dissolved in water and washed with diethyl ether (Et_2O) several times. Ammonium salt **69d** had an ionic liquid character, so it was heated more under reduced pressure to remove the traces of starting material. All of these ammonium salts **69a-d** were synthesized before, however only **69c** was used in the synthesis of extra-large germanosilicate zeolite HPM-14.

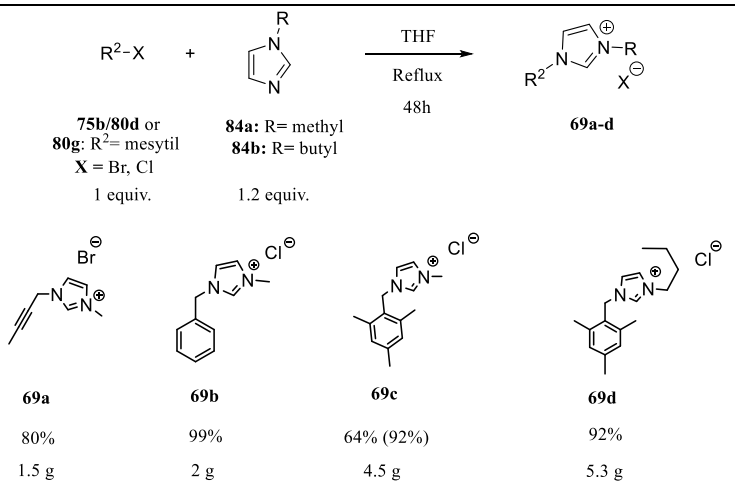

Scheme 25. Synthesis of imidazole based ammonium salts **69a-d**

The set of ammonium salts having imidazole units was extended, and another three imidazole based ammonium salts were prepared with extra aromatic substituents **70(a-c)** (Scheme 26). The reaction between imidazole **85** and methyl iodide (MeI, 3 equiv.) in the presence of potassium

carbonate (3 equiv.) proceeded at 60 ^{o}C within 48 h. The first attempt to purify the products by dissolving the crude in ethanol and then filtering the insoluble potassium carbonate was not efficient. So, another method was followed in which distilled water was added to the crude, the solution was heated to 50 ^{o}C to dissolve all potassium carbonate, and the un soluble imidazole salts were collected by filtration. The procedure was repeated several times until the pH of the filtered distilled water was around 7. The imidazole-based ammonium salts **70a-c** were obtained quantitatively (Scheme 26). These three ammonium salts **70a-c** were synthesized before but not used in zeolite synthesis.

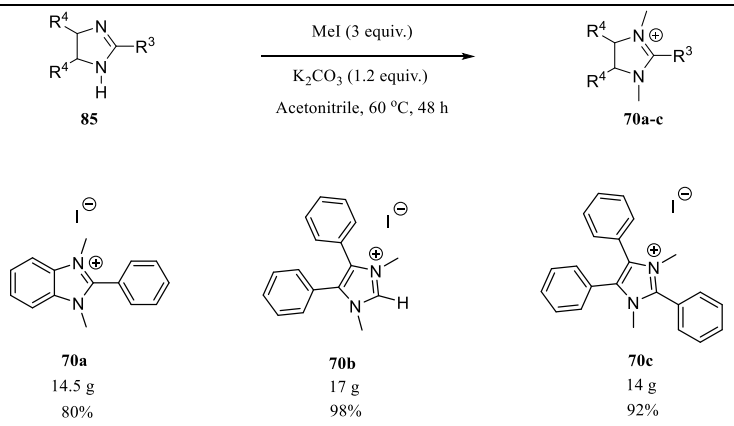

Scheme 26. Synthesis of imidazole based ammonium salts **70 (a-c)**

1.4. Ammonium salts containing aromatic units.

1.4.1. Synthesis of [2.2] paracyclophane ammonium salt using different approaches.

Ammonium salts with aromatic units showed great potential in the synthesis of zeolites with different pore sizes. The combination of hydrophobic planar part and hydrophilic polar part, tends to be efficient in the synthesis of extra-large pore sizes zeolites with different topologies (Chapter 1, Table: 2, Entry 1 and 4; Table: 3, Entry 1, 3, 4, and 10; and Table: 4, Entry 4, 6, and 7). The first target in this section was the preparation of an ammonium salt with a [2.2] paracyclophane unit. The reason behind this choice was the rigidity of this compound, the presence of two aromatic rings phasing each other would favor π–π stacking between two pairs of molecules, thus forming pores with larger dimensions. For the preparation of ammonium salt with [2.2] paracyclophane unit, amide **91** should be prepared first (Scheme 27). Initially, [2.2] paracyclophane **(86)** reacts

with acetyl chloride (2 equiv.) in the presence of Lewis acid aluminum chloride (1.8 equiv.) as shown in path 1 (Scheme 27). Following the procedure described by Cram for the synthesis of Ketone **87** (yield reported 74%), the reaction proceeded at room temperature in dichloromethane within 17 h to yield the final product with a 66% yield.[90] Following a procedure reported by Cram and Allinger for the syntheses of carboxylic acid **88** from **87** using potassium hydroxide (KOH, 7.3 equiv.) and bromine (Br_2, 3.3 equiv.) in a mixture of water and Dioxane (Reported yield 90%). The attempt to synthesize carboxylic acid **88** starting from ketone **87** using the same haloform reaction wasn't successful.[91] So, another approach was followed (path 2). Compound **89** was also synthesized using a Frieldel-Crafts acylation reaction from [2.2] paracyclophane **(86)** (1 equiv.) and oxalyl chloride (1.8 equiv.) with a 99% yield. Then, the obtained product **89** undergoes a decarbonylation reaction when refluxed in chlorobenzene within 48 h to afford acyl chloride compound **90** following a procedure described by Psiorz for the synthesis of **90** from **89**.[92] Then, to the obtained mixture containing acyl chloride **90** and chlorobenzene, dichloromethane and diethyl amine were added. The reaction proceeded at room temperature within 48 h to yield amide **91** with a 26% yield. To increase the yield of the amide **91** and to avoid the moisture sensitivity of the acyl chloride **90**, path 3 was followed. Ketone **92** was prepared from [2.2] paracyclophane **(86)** and 2-cloroacetyl chloride (2 equiv.) using a Friedel-Crafts acylation reaction. The reaction proceeded within 17h to afford the final product **92** with an 80% yield (Scheme 27). In step 2, compound **92** was added to a pyridine solution and heated at 60 ^{o}C for 20h following Kings reaction.[93] After that, the pyridine was evaporated from the solution, and the remaining salt was dissolved in a 14% NaOH solution. The solution was stirred for 24 h at 60 ^{o}C and the obtained carboxylic acid **88** was isolated and purified by acid-base workup with an 86% yield. In step 3, following Richards approach for the preparation of compound similar to **91** but having two methyl instead of ethyl groups, oxalyl chloride (1.1 equiv.) was added to a solution of carboxylic acid **88** and DMF (0.8 equiv.) in dichloromethane. The solution was stirred for 5h at room temperature, followed by the addition of diethyl amine to the acyl chloride compound formed in situ. The reaction was further stirred for 16h and the final amide product **91** was obtained with a 65% yield after purification.[94]

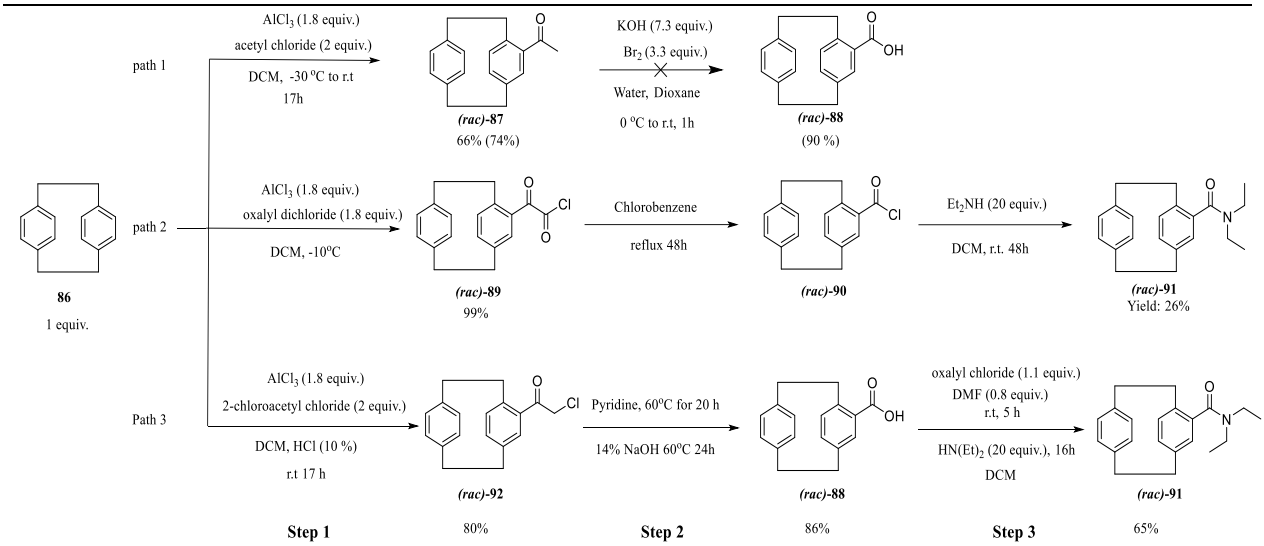

Scheme 27. Attempts to synthesis amide **91** using different paths.

The obtained amide **91** was reduced to the tertiary amine compound **93** using $LiAlH_4$ (7 equiv.) in THF within 24h at room temperature (Scheme 28).[94] This reaction was used by Richards group for the preparation of a similar compound to **93**, but having two methyl instead of two ethyl groups (yield: 80%). The crude was isolated by an acid base workup. The obtained mixture after treatment showed the target product **93** with another side product **94**. The reason behind obtaining side product **94** could be caused during the reduction step by the cleavage of the amine group as shown in scheme 28c. To isolate the targeted product **93**, a column chromatography using alumina oxide with 90:10 (v/v) pentane-ethyl acetate was applied. The final product **93** was obtained with a 65% yield, and the alcohol **94** was isolated with a 17% yield.

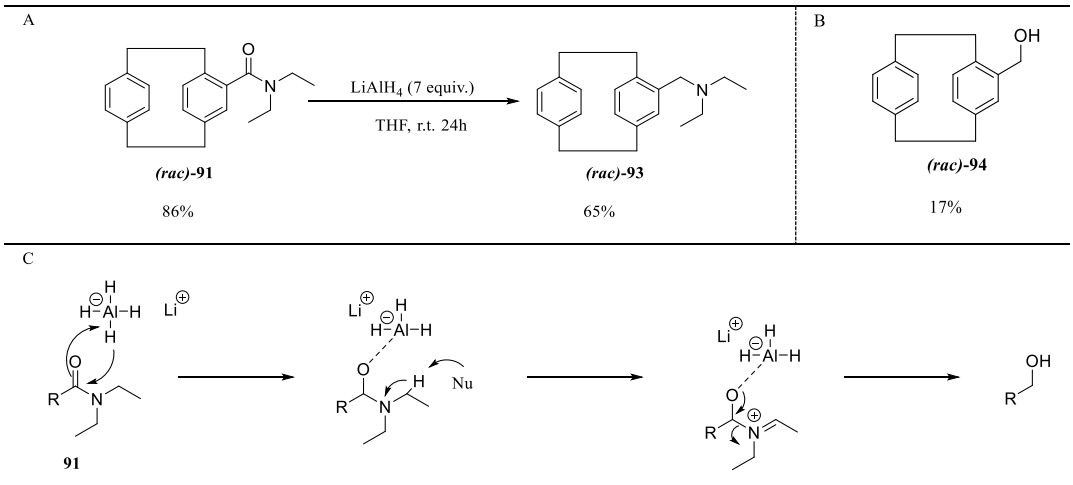

Scheme 28. A. reduction of amide **91** to the corresponding tertiary amine
B. Side product alcohol **94**. **C.** mechanism for obtaining the alcohol

The alkylation of the previously prepared tertiary amine **93** using 4 equiv. of haloalkanes in different solvents such as dichloromethane, THF, Acetonitrile, and DMF under reflux for 48 h didn't proceed (Scheme 29). However, using Methyl trifluoromethanesulfonate (CH_3OTf, 6 equiv.) in dichloromethane at room temperature favored the alkylation reaction of tertiary amine **93**, and the corresponding ammonium salt **71** was obtained with 90%. For purification, the prepared ammonium salt **71** was washed with distilled water and saturated solution of $NaHCO_3$.

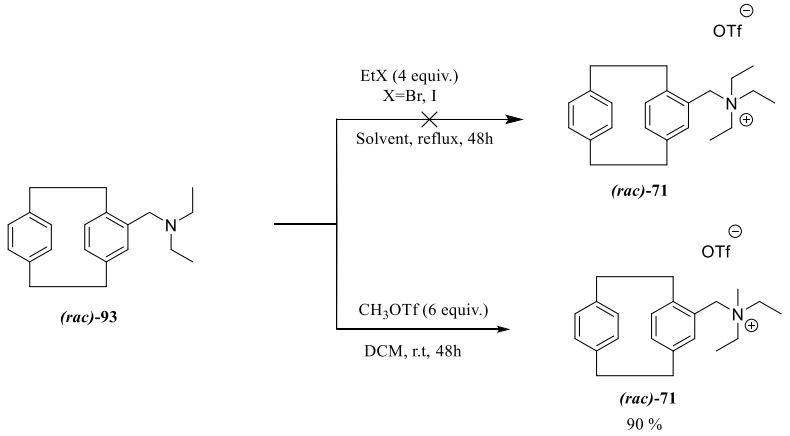

Scheme 29. Attempts to alkylate tertiary amine **71**

1.4.2. Synthesis of 4-phenylpyridinium and Mesitylene based ammonium salts.

Another ammonium salt **72** based on an aromatic group was synthesized, but this time instead of having the aromatic rings phasing each other, 4-phenylpyridine **(95)** was used having two aromatic rings in a linear position. The design of the aromatic ammonium salt **72** might favor the formation of a channel system instead of spherical ones and might favor the π–π stacking mode. The alkylation reaction of 4-phenylpyridine **95** with methyl iodide (26 equiv.) in acetonitrile, proceeded within 24 h at 80 ºC to afford the final product **72** with 99% yield (Scheme 30).

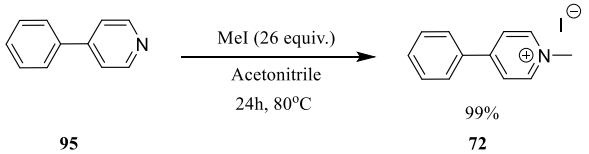

Scheme 30. Synthesis of ammonium salt **72** from 4-phenylpyridine **95**

The benzyltrimethylammonium salt **(96)** was used as SDA in the synthesis of ZSM-12 zeolite (Scheme 31. A). The obtained MTW topology has the largest ring size equal to 12 (T = 12) and the largest pore diameter of 0.608 nm.[95] Taking into consideration the ability of benzyl trimethylammonium salt **(96)** (Scheme 31) to favor the synthesis of zeolite with medium pore size, a new set of ammonium salts **73(a-c)** with modified alkyl groups was synthesized. The presence of three methyl groups on the benzene ring with different R groups on nitrogen may favor the crystallization of extra-large pore-size zeolites (Scheme 31). The three ammonium salts were synthesized by reacting tertiary amines **57(a-c)** (5 equiv.) with 2-(chloromethyl)-1,3,5-trimethylbenzene **(80g)** (1 equiv.) either in THF or acetonitrile at room temperature within 48h (Scheme 31, B). The excesses of trimethylamine **(57a)** and triethylamine **(57b)** were removed from products **73(a-b)** by heating under reduced pressure, and the final products **73(a**, **b)** were obtained quantitatively with a 99% yield. The ammonium salt **73c** still has some traces of tripropylamine **(57c)** even after washing several times with diethyl ether (Et_2O).

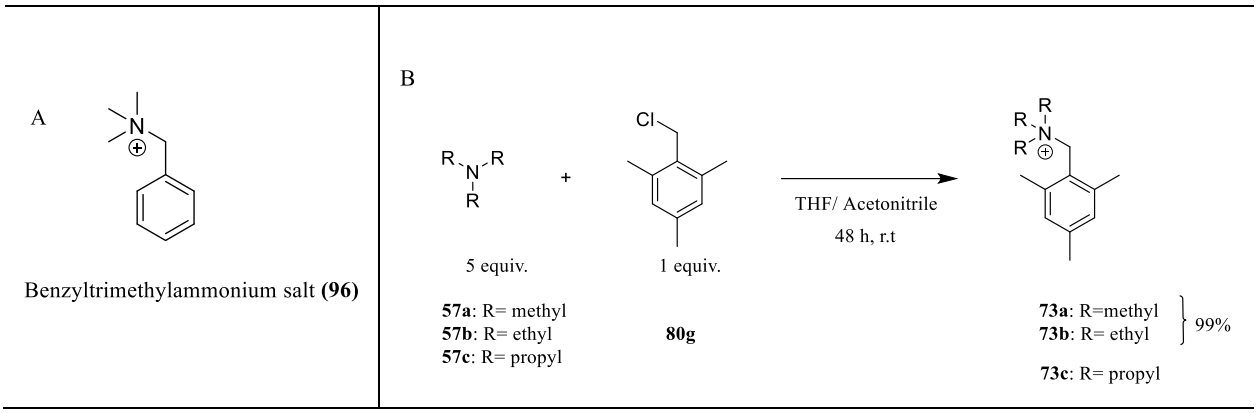

Scheme 31 A. SDA **96**
B. Synthesis of ammonium salts **73a-c**

2. Synthesis of phosphonium salts

2.1. Alkylated phosphonium salts with different alkyl and aryl chains.

The use of phosphonium-based SDAs in zeolite synthesis is flourishing, especially that SDAs with ammonium salts were extensively studied in the synthesis of zeolites and an alternative is required. Additionally, some ammonium salts have stability problems as they can undergo Hoffman elimination under basic conditions, making phosphonium-based SDAs a better alternative. Three different examples have been reported using phosonium-based SDAs in the synthesis of zeolites with extra-large pore sizes (Chapter 1, Scheme 15). Here, the synthesis of SDA **65a** was repeated to resynthesize ZEO-1, and the set is extended to include examples with different alkyl groups **65(b-c)** (Scheme 32). The starting material, **97**, was always weighed in a glove box, transferred to a Schlenk tube, and flushed with argon to avoid the formation of phosphorus oxide. Acetonitrile was then added, followed by electrophile **80**. The reaction proceeded within 48 h at room temperature when preparing **65(a-b)** and was heated at 70 ºC when preparing **65(c-d)**. A total of 147g of **65a** were prepared quantitatively on gram scale, and for each trial, 15g of **65a** were obtained with 98%. Additionally, phosphonium salt **65b** was also prepared quantitatively on a gram scale with 98%. Both phosphonium salts **65a** and **65b** were obtained pure after solvent evaporation and drying under reduced pressure. A 2.5g of pure phosphonium salt **65c** were obtained with good yield (89%) after they were dissolved at room temperature in distilled water and washed with pentane to remove traces of phosphine oxide. Moreover, 3.5 g phosphonium salt of **65d** were obtained quantitatively (98%) on gram scale after washing with pentane to remove benzyl bromide **(80d)**, followed by workup acetonitrile –pentane. The last example reported in this series was **65e**, similar to **65a** but having 3 phenyl groups instead of cyclohexyl groups. It was prepared by reacting **97b** with Methyl Iodide (4 equiv.) in acetonitrile at room temperature. The reaction proceeded within 48 h to afford 0.7g of **65e** with a 95% yield (Scheme 32). From the synthesized phosphonium salts **65a-e**, phosphonium salt **65a** was synthesized before and **65e** is commercially available.

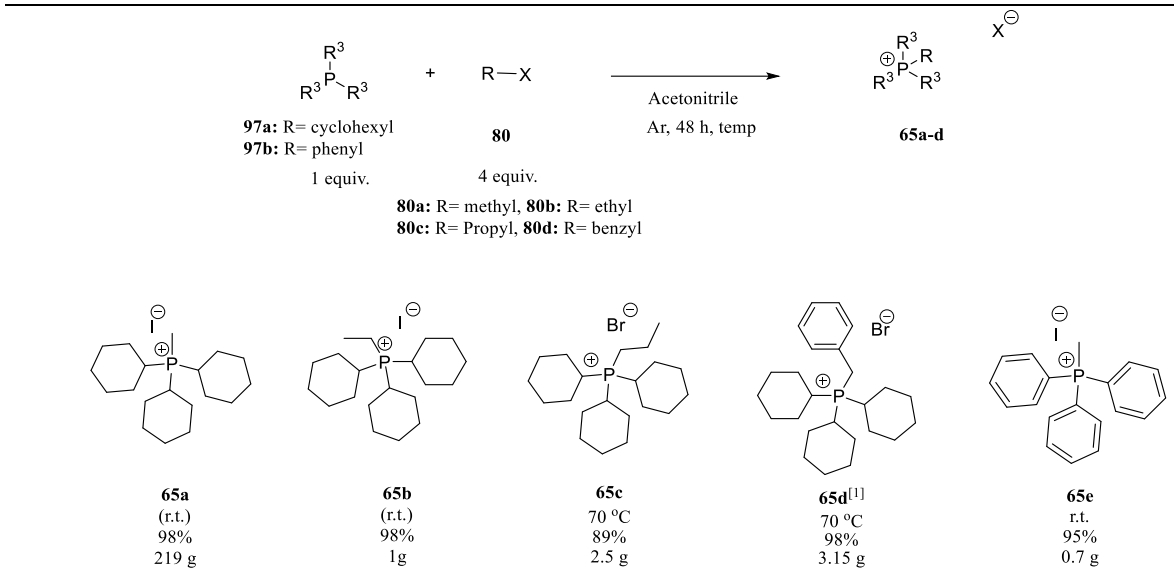

Scheme 32. Synthesis of phosphonium salts **65a-e**

Extending the phosphonium salt series, a phosphonium salt with three tricyclohexyl groups and one aryl group was prepared. The P- arylation of tricyclohexylphosphine **(97a)** to form SDA **65f** was first investigated following an approach reported by Dalla and Taillier in the literature for the Arylation of Phosphirane (Scheme 33A).[96] Tricyclohexyl phosphine **(97a)** and diaryiodonium salt **(98)** were dissolved in tetrachloroethane, and the reaction was studied at different temperatures in the presence and absence of copper metal and copper chloride. The results are shown in table 5. In the first two trials, 1 and 2, the reactions were done in the presence of copper chloride (10%) and copper metal.[96] In trial 1, the reaction was stirred for 1 h at 50 °C, and in trial 2, the reaction was stirred for 6 h at room temperature. In trials 3-5, the reactions were done in the absence of copper chloride and copper metal. In trial 3, the reaction was stirred at room temperature for 6h, trial 4, the reaction was stirred for 6h at 80 °C; and in trial 5 , the reaction was stirred 6h at 116 °C. The **^{31}P NMR** analysis of the solutions found in trials 1-5 at different times and temperatures showed the presence of side product **99** with a peak at 27.3 ppm with no traces of the expected product **65f** (Scheme 33).

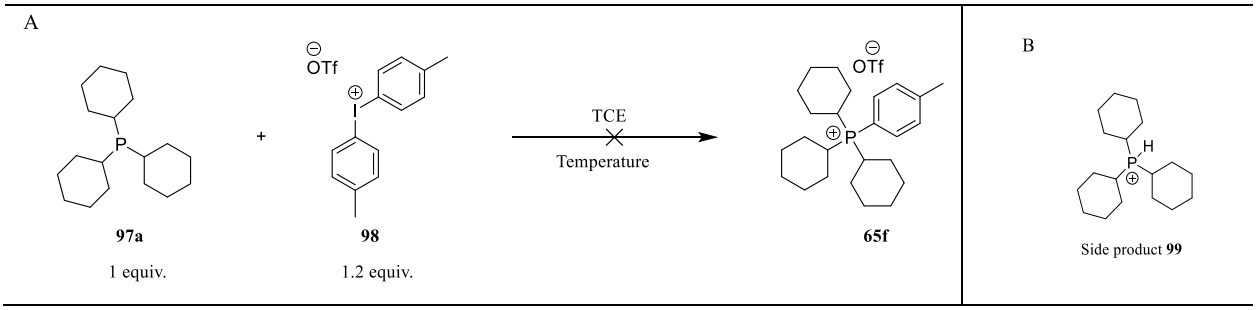

Scheme 33. A. Attempt to synthesize phosphonium salt **65f**
B. Side product **99**

Trial	Copper Chloride (10 %)	Copper metal	Monitoring
1	✓	✓	1h at 50 ^{O}C
2	✓	✓	6h at r.t
3	-	-	6h at r.t
4	-	-	6h at 80 ^{o}C
5	-	-	6h at 116 ^{o}C

Table 5. Attempts done for the preparation of **65f**

To further confirm that side product **99** was obtained, tricyclohexylphosphine **(97a)** was mixed with triflic acid (TfOH, 1 equiv.) at room temperature for 1h in tetrachloroethane (Scheme 34). The obtained solution was later concentrated under reduced pressure, followed by a water-dichloromethane workup. The **^{31}P NMR** decoupled analysis showed a peak at 27.7 ppm, which confirms that side product **99** was obtained (Figure 5). Additionally, the coupled **^{31}P NMR** analyses showed a peak of the doublet at the same position at 27.7 ppm, indicating the presence of a P-H bond. The first postulate about obtaining side product **99** could be due to the use of triflic acid in the preparation of diaryiodonium salt **98**. However, the **^{1}H NMR** and **^{13}C NMR** of diaryiodonium salt **98** were pure, and the **^{19}F NMR** of the product showed only one peak at -77.8 ppm referring to the counter anion OTf of the product with no other peaks referring to triflic acid (TfOH), unless the triflic acid (TfOH) peak and OTf counter anion peak of **98** superpose (Figure 6).

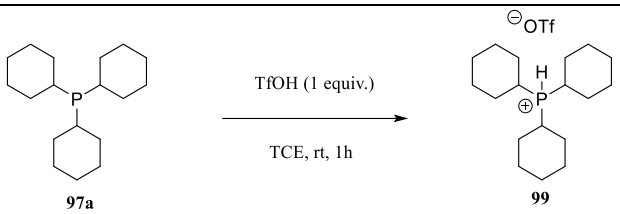

Scheme 34. Protonation of **97a** with TfOH

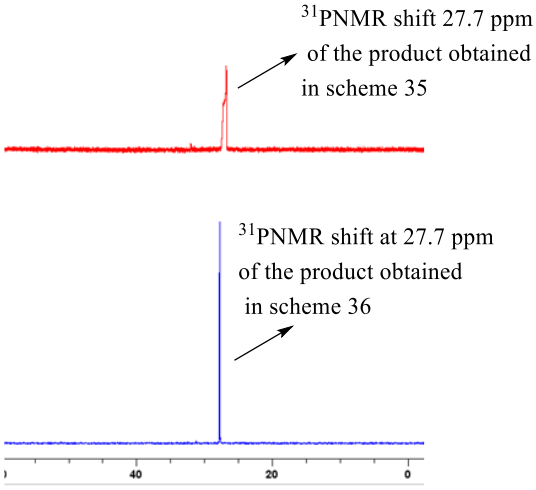

Figure 5. ^{31}PNMR spectra of the same product obtained in scheme 35 and scheme 36.

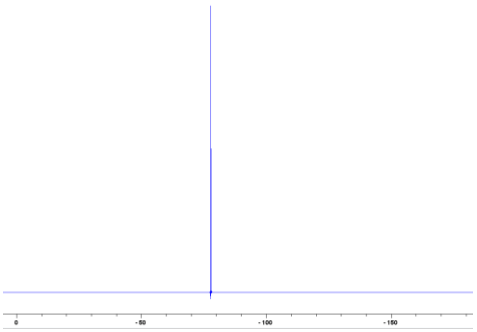

Figure 6. ^{19}FNMR spectrum for diaryiodonium salt 115.

As the approach used in Scheme 33 was not successful, another approach reported by Jugé for the synthesis of Phosphonium Triflates was followed (**65h** was reported with 89% yield). Tricyclohexyl phosphine **(97a)** or Triphenyl phosphine **(97b)** reacts with 2-(trimethyl s ilyl) phenyl trifluoromethanesulfonate **(100)** in the presence of CsF (6 equiv.) at room temperature. [97] within 15h in acetonitrile (Scheme 35). The products **65g** and **65h** were obtained with 80% and 60% yield, respectively, after purification by dissolving in acetonitrile and washing with pentane.

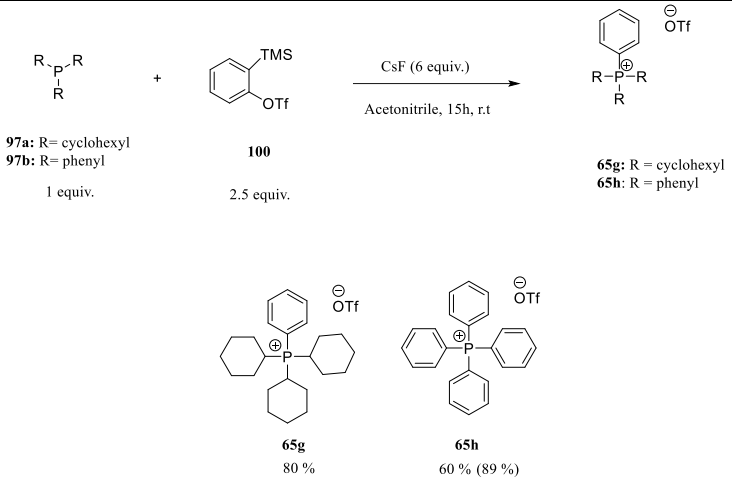

Scheme 35. Synthesis of phophonium salts **65g-h**

2.2. Phosphonium salts having two phosphorus groups linked with different alkyl chains.

SDA's formed of bis salts connected by an alkyl chain as a spacer were used in the preparation of zeolites with different pore sizes as mentioned in Chapter 1 (SDA **6** and **7** in Scheme 3, SDA **8** in Scheme 4, SDAs **9**, **10**, **11** in Scheme 5 etc. In this part, a set of bis tricyclohexyl phosphonium salts **74 (a-d)** were synthesized with different alkyl chain spacers **(n)** (Scheme 36). The first attempt to synthesize bistricyclohexylphosphonium salt with an n = 2 spacer did not proceed. So, the first spacer used was **101**, with n = 3. Tricyclohexyl phosphine **(97a)** was weighed in a glove box and transferred to a schlenk tube. Then, the tube was placed under argon, and acetonitrile was added, followed by electrophile **101**. The reaction proceeded with reflux for 48 h. The phosphonium salts **74(a-d)** were obtained with high purity and quantitatively on the gram scale after adding the salts separately to distilled water, followed by boiling the milky suspension until it became clear. The solution was left to cool down, followed by washing with diethyl ether (Et_2O) several times to afford the products **74a** (1.5 g, 99%), **74b** (2 g, 91%), **74c** (2g, 95%), and **74d** (2.6g, 93%), respectively.

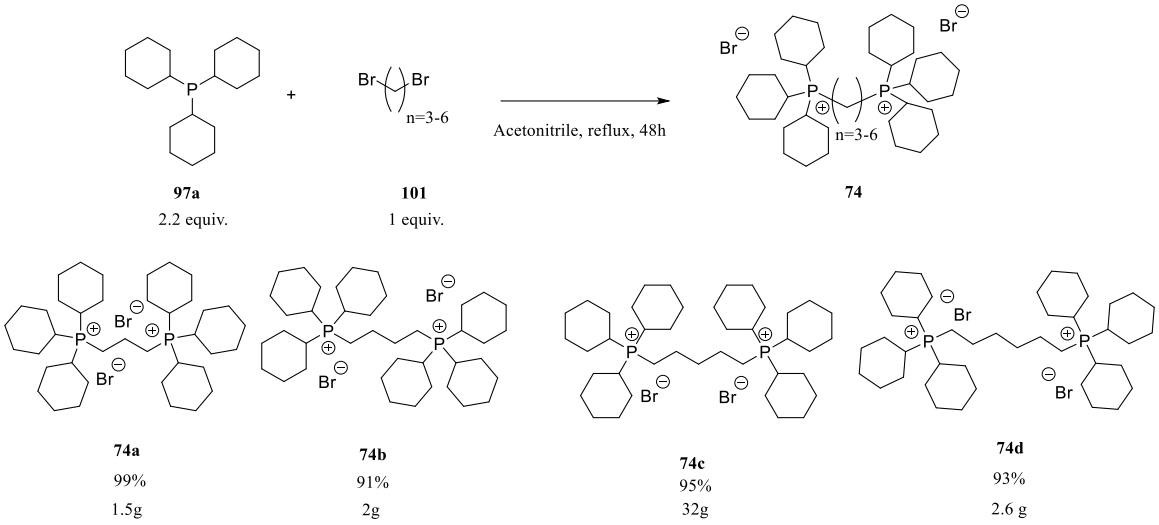

Scheme 36. Synthesis of bisphosphonium salts **74a-d**

3. Conclusion

This chapter showed the synthesis of two different categories of salts: ammonium and phosphonium salts. Within the ammonium salts category, compounds having alkyne unit(s), hexamethylenetetramine, imidazole, and aromatic moieties were synthesized on a gram scale. Additionally, phosphonium salts were also prepared, characterized by the presence of either one or two phosphonium units. Some of these synthesized salts were tested as SDAs in zeolite synthesis, as will be explained in the following chapter, while the others will be tested later. It is notable that the success of each structure-directing agent (SDA) is predicated upon a systematic trial-and-error approach. Consequently, each SDA should be used under different conditions and in multiple experimental trials to find the optimal parameters for zeolite crystallization.

Experimental Part

4. Experimental part

General description:

Solvents (THF, DCM, Et_2O, CH_3CN, and toluene) were dried using a double-cartridge solvent purification system. Anhydrous DMF was purchased from Sigma-Aldrich. The use of a glovebox was consistently used for the storage, weighing, and starting of reactions containing air-sensitive materials like tricyclohexylphosphine. Chromatographic purification processes employed Acros Organics silica gel Si 60 (40-60 μm) or Merck aluminum oxide 90 active neutral (60-200 μm, activity stage III) as stationary phases. Thin-layer chromatography (TLC) procedures were done on silica gel 60 plates (0.20 mm) or aluminium oxide 60 neutral plates (0.20 mm) with UV detection. Nuclear magnetic resonance (NMR) spectra were measured on either a Brucker Avance III (500 MHz) or a Brucker Neo (600 MHz) spectrometer. The chemical shifts (δ) of ^{1}H and ^{13}C NMR are denoted in parts per million (ppm) using the TMS signal (0 ppm) and the residual peak of chloroform-D (77.16 ppm) as internal references, respectively. Moreover, the coupled ^{13}C NMR was used for measurement with dept 135. Coupling constants are expressed in Hertz (Hz). Abbreviations are used as follows: s = singlet, d = doublet, t = triplet, q = quartet, qt = quintuplet, sext = sextuplet, m = multiplet, and br = broad. Infrared (IR) spectra were measured using a PerkinElmer instrument. Two spectrometers are equipped with an ATR device, and only the most significant or structurally relevant peaks are provided. High Resolution Mass Spectrometry (HRMS) and UPLC-MS analyses (Ultra Performance Liquid Chromatography coupled with Mass Spectrometry) were executed under electron spray ionization (ESI) mode utilizing an Acquity UPLC H-ClassXevo G2-XS QTof (WATERS) spectrometer. Melting points (Mp) were determined using an electrothermal apparatus, and are not corrected.

- Ammonium salts containing terminal and non-terminal alkyne unit(s)

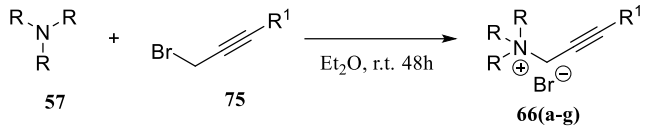

57 **75** **66(a-g)**

57a: R= Methyl
57b: R= Ethyl
57c: R= Propyl
57d: R= Butyl

75a: R= H
75b: R= Methyl
75c: R= Ethyl

General Procedure A:

To a dry flask containing the tertiary amine **57(a-d)** dissolved in diethyl ether, the bromoalkyne **75(a-c)** was added. The reaction mixture was stirred at room temperature for 48h,[85] and the obtained solution was concentrated under reduced pressure to afford the targeted product.

Triethyl(2-propynyl)ammonium bromide (66a)

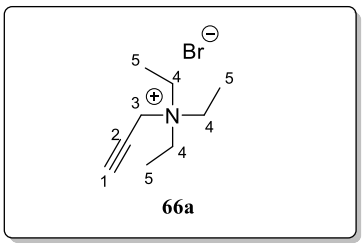

66a

Prepared according to general procedure **A** from triethylamine **(57b)** (5.64 g, 55.70 mmol, 1.2 equiv.) and propargyl bromide **(75a)** (5.52 g, 46.8 mmol, 1 equiv.). The reaction proceeded within 48h at room temperature, the organic phase was concentrated under reduced pressure, and the product obtained was purified by dissolving in water and washing with pentane to afford triethyl(2-propynyl)ammonium bromide **66a** (9.610 g, 43.7 mmol, Yield: 93%).

^{1}H NMR (500 MHz, D_2O) δ 4.11 (s, 2H, H-3), 3.40 (q, ^3J = 7.3 Hz, 6H, H-4), 1.29 (t, ^3J = 7.3 Hz, 9H, H-5).

^{13}C NMR (126 MHz, D_2O) δ 80.3 (Cq, C-1), 70.2 (Cq, C-2), 53.2 (CH_2, C-4), 47.4 (CH_2, C-3), 6.8 (CH_3, C-5).

HRMS (ESI+): Calcd for $C_9H_{18}N$ [M^+]: 140.1442; found: 140.1439.

Melting point: 196.0-196.9 2.5°C/min.

The ^{1}H and ^{13}C NMR data match those reported in the literature[98]

Tripropyl(2-propynyl) ammonium bromide (66b)

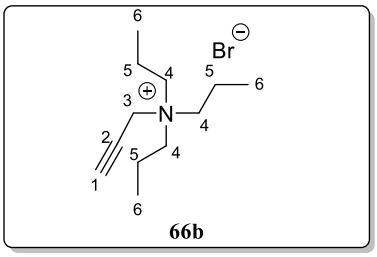

66b

Prepared according to general procedure **A** from tripropylamine **(57c)** (9.31 g, 65.0 mmol, 1.3 equiv.) and propargyl bromide **(75a)** (5.95 g, 50 mmol, 1 equiv.). The reaction proceeded within 48h at room temperature, the organic phase was concentrated under reduced pressure, and the product obtained was dissolved in water and washed with pentane to afford tripropyl(2-propynyl)ammonium bromide **66b** (10.9 g, 41.5 mmol, Yield: 83%).

^{1}H NMR (500 MHz, $CDCl_3$) δ 4.76 (d, ^4J = 2.6 Hz, 2H, H-3), 3.48 (m, 6H, H-4), 2.86 (t, ^4J = 2.6 Hz, 1 H, H-1), 1.86 (m, 6H, H-5), 1.07(t, ^3J = 7.4Hz, 9H, H-6).

^{13}C NMR (126 MHz, $CDCl_3$) δ 81.0 (Cq, C-1), 71.4 (Cq, C-2), 61.4 (CH_2, C-4), 50.8 (CH_2, C-3), 16.3 (CH_2, C-5), 10.9 (CH_3, C-6).

HRMS (ESI+): Calcd for $C_{12}H_{24}N$ [M^+]: 182.1914; found: 182.1909.

Melting point: 185.7-186.9 2.5 °C/min

IR (ATR, cm-1) v 3132, 2969, 2932, 2876, 2113, 1450, 1384

Trimethyl(2-butynyl)ammonium bromide (66c)

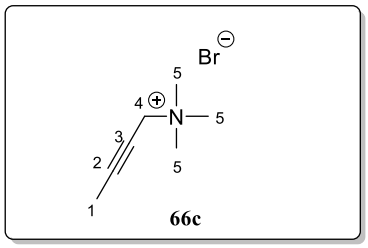

66c

Prepared according to general procedure **A** from trimethylamine **(57a)** (0.56 g, 9.40 mmol, 1.2 equiv.) and 1-bromo-2-butyne **(75b)** (1.04 g, 7.80 mmol, 1 equiv.). The reaction proceeded within 48h at room temperature, and the organic solution was concentrated under reduced pressure to afford trimethyl(2-butynyl)ammonium bromide **66c** (1.2 g, 6.25 mmol, Yield: 98%) without any further purification.

^{1}H NMR (500 MHz, D_2O) δ 4.18 (q, ^{5}J = 2.4 Hz, 2H, H-4), 3.20 (s, 9H, H-5), 1.96 (t, ^{5}J = 2.4 Hz, 3H, H-1).

^{13}C NMR (126 MHz, D_2O) δ 90.2 (Cq, C-2), 66.7 (Cq, C-3), 57.2 (CH_2, C-4), 52.6 (CH_3, C-5), 2.8 (CH_3, C-1).

HRMS (ESI+): Calcd for $C_7H_{14}N$ [M^+]: 112.1130; found: 112.1126

Melting point: 132.3-132.8 2.5ºC / min

IR (ATR, cm-1) v 3452, 3401, 2243, 1625, 1477, 905

Triethyl(2-butynyl)ammonium bromide (66d)

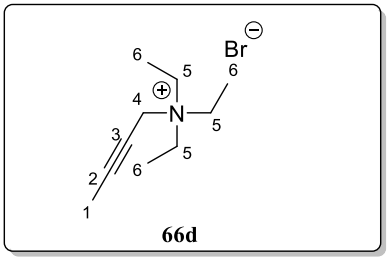

66d

Prepared according to general procedure **A** from triethylamine **(57b)** (0.48 g, 4.70 mmol, 1.1 equiv.) and 1-bromo-2-butyne **(75b)** (0.57 g, 4.27 mmol, 1 equiv.). The reaction proceeded within 48h at room temperature, the organic solution was concentrated under reduced pressure, and the obtained crude was dissolved in water and washed with pentane to afford triethyl(2-butynyl)ammonium bromide **(66d)** (0.97 g, 4.14 mmol, Yield: 97%).

^{1}H NMR (500 MHz, D_2O) δ 3.94 (q, ^{5}J = 2.5 Hz, 2H, H-4), 3.29 (q, ^{3}J = 7.2 Hz, 6H, H-5), 1.82 (t, ^{5}J = 2.5 Hz, 3H, H-1), 1.2 (t, ^{3}J = 7.2 Hz, 9H, H-6).

^{13}C NMR (126 MHz, D_2O) δ 89.1 (Cq, C-2), 66.1 (Cq, C-3), 53.0 (CH_2, C-5), 48.3 (CH_2, C-4), 7.0 (CH_3, C-6), 2.8 (CH_3, C-1).

HRMS (ESI+): Calcd for $C_{10}H_{20}N$ [M^+]: 154.1595; found: 154.1596.

Melting point: 127.0-128.3 2.5 ºC/min

IR (ATR, cm-1) v 3400, 2984, 2242, 1627, 1013.

Tripropyl(2- butynyl) ammonium bromide (66e)

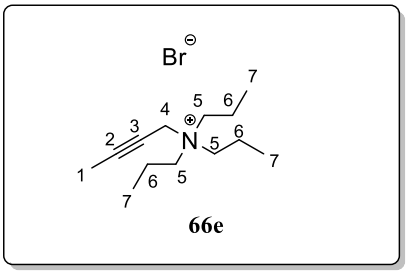

66e

Prepared according to procedure **A** from tripropylamine **(57c)** (1.06 g, 7.42 mmol, 1.3 equiv.) and 1-Bromo-2-butyne **75b** (0.76 g, 5.71 mmol, 1 equiv.). The reaction proceeded within 48h at room

temperature, the organic solution was concentrated under reduced pressure, and the obtained crude was dissolved in water and washed with pentane to afford tripropyl(2-butynyl)ammonium bromide **(66e)** (1.40 g, 5.07 mmol, Yield: 93%). For further purification, the product was heated under reduced pressure to remove traces of tripropylamine **(57c)**.

^{1}H NMR (500 MHz, D_2O) δ 4.08 (q, ^{5}J = 2.4 Hz, 2H, H-4), 3.28 (m, 6H, H-5), 1.92 (t, ^{5}J = 2.4 Hz, 3H, H-1), 1.73 (m, 6H, H-6), 0.98 (t, ^{3}J = 7.4 Hz, 9H, H-7).

^{13}C NMR (126 MHz, D_2O) δ 89.3 (Cq, C-2), 66.3 (Cq, C-3), 60.3 (CH_2, C-5), 50.0 (CH_2, C-4), 15.2 (CH_2, C-6), 10.0 (CH_3, C-7), 2.8 (CH_3, C-1).

HRMS (ESI+): Calcd for $C_{13}H_{26}N$ [M^+]: 196.2065; found: 196.2065.

Melting point: 96.4-97.8 2.5 °C/min

IR (ATR, cm-1) v 3200, 2938, 2250, 1400, 1320

Tributyl (2-butynyl)ammonium bromide (66f)

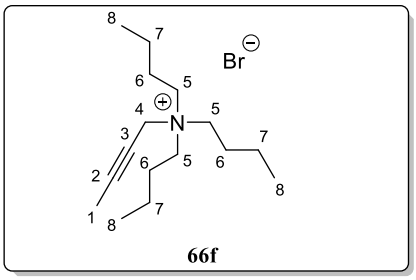

66f

Prepared according to general procedure **A** from tributylamine **(57d)** (1.51 g, 8.17 mmol, 1.3 equiv.) and 1-bromo-2-butyne **(75b)** (0.84 g, 6.28 mmol, 1 equiv.). The reaction proceeded within 48h at room temperature, the organic solution was concentrated under reduced pressure, and the product obtained was dissolved in water and washed with pentane to afford tributyl(2-butynyl)ammonium bromide **(66f)** (1.80 g, 5.65 mmol, Yield: 90%) as an oily compound.

^{1}H NMR (500 MHz, D_2O) δ 4.01 (q, ^{5}J = 2.2 Hz, 2H, H-4), 3.25 (m, 6H, H-5), 1.86 (t, ^{5}J = 2.2 Hz, 3H, H-1), 1.63 (m, 6H, H-6), 1.33 (sextet, ^{3}J = 7.3 Hz, 6H, H-7), 0.91 (t, ^{3}J = 7.3 Hz, 9H, H-8).

^{13}C NMR (126 MHz, D_2O) δ 89.1 (Cq, C-2), 66.1 (Cq, C-3), 58.3 (CH_2, C-5), 49.6 (CH_2, C-4), 23.3 (CH_2, C-6), 19.2 (CH_2, C-7),12.9 (CH_3, C-8), 2.8 (CH_3, C-1).

HRMS (ESI+): Calcd for $C_{16}H_{32}N$ [M^+]: 238.2534; found: 238.2535.

IR (ATR, cm-1) v 3410, 2960, 2874, 2243, 1620, 1477, 1378.

Tripropyl (2-pentynyl) ammonium bromide (66g)

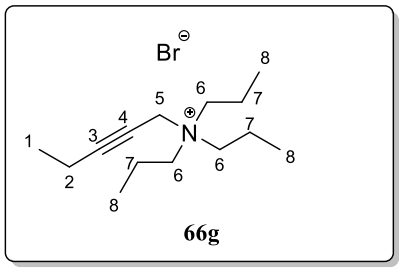

66g

Prepared according to general procedure **A** from tripropylamine **(57c)** (1.28 g, 8.96 mmol, 1.3 equiv.) and 1-bromo-2-pentyne **(75c)** (1.01 g, 6.89 mmol, 1 equiv.). The reaction proceeded within 48h at room temperature, the organic phase was concentrated under reduced pressure, and the product obtained was dissolved in water and washed with pentane to afford Tripropyl(2-pentynyl)ammonium bromide **66g** (1.98 g, 6.82 mmol, Yield: 98%). For further purification, the product was heated under reduced pressure to remove the traces of tripropylamine **(57c)**.

^{1}H NMR (500 MHz, D_2O) δ 4.05 (t, ^{5}J = 2.2 Hz, 2H, H-5), 3.23 (m, 6H, H-6), 2.27 (qt, ^{3}J = 7.5 Hz, ^{5}J = 2.2 Hz, 2H, H-2), 1.69 (m, 6H, H-7), 1.12 (t, ^{3}J = 7.5 Hz, 3H, H-1), 0.93 (t, ^{3}J = 7.3 Hz, 9H, H-8).

^{13}C NMR (126 MHz, D_2O) δ 94.6 (Cq, C-3), 66.4 (Cq, C-4), 60 (CH_2, C-6), 49.7 (CH_2, C-5), 15.0 (CH_2, C-7), 12.5 (CH_3, C-1), 11.8 (CH_2, C-2), 9.8 (CH_3, C-8).

HRMS (ESI+): Calcd for $C_{14}H_{28}N$ [M^+]: 210.2223; found: 210.2223.

Melting point: 130.8-132.7 2.5 ºC/min

IR (ATR, cm-1) v 3472, 2969, 2937, 2877, 2238, 1474, 749

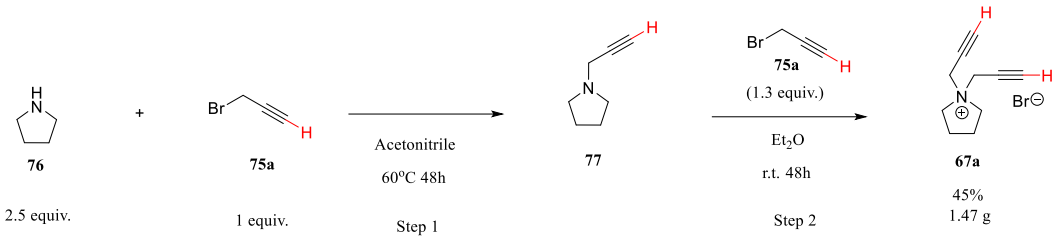

Di(2-propynyl)pyrrolidinium bromide (67a)

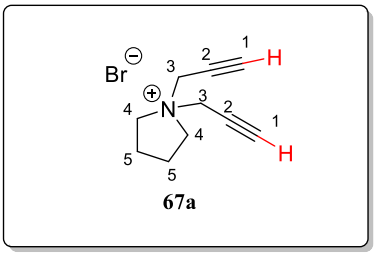

To a flask containing pyrrolidine **(76)** (1.64 g, 23 mmol, 2.5 equiv.) dissolved in acetonitrile, propargyl bromide **(75a)** (1.1g, 9.2 mmol, 1 equiv.) was added. The solution was heated at 60 °C for 48h, and the obtained product n-propargyl pyrrolidine **(77)** was purified by removing the excess of pyrrolidine salt using column chromatography (alumina oxide, pentane/ethyl acetate 95:5 (v/v)). The isolated compound **77** was further alkylated with propargyl bromide **(75a)** (1.42 g, 12.00 mmol, 1.3 equiv.) to afford the desired product di(2-propynyl)pyrrolidinium bromide **(67a)** (1.47 g, 6.47 mmol, Yield: 45%).

^{1}H NMR (500 MHz, D_2O) δ 4.38 (m, 4H, H-3), 3.73 (t, ^{3}J = 7.3 Hz, 4H, H-4), 3.19 (t, ^{4}J = 2.5 Hz, 1H, H-1), 2.22 (m, 4H, H-5).

^{13}C NMR (126 MHz, D_2O) δ 81.1 (CH, C-1), 71.6 (CH, C-1), 62.5 (CH_2, C-4), 51.4 (CH_2, C-3), 22.5 (CH_2, C-5)

HRMS (ESI+): Calcd for $C_{10}H_{14}N$ [M+]: 148.1128; found: 148.1126.

Melting Point: 225.6 - 226.3 2.5 °C/min

The ^{1}H and ^{13}C NMR data match those reported in the literature[99]

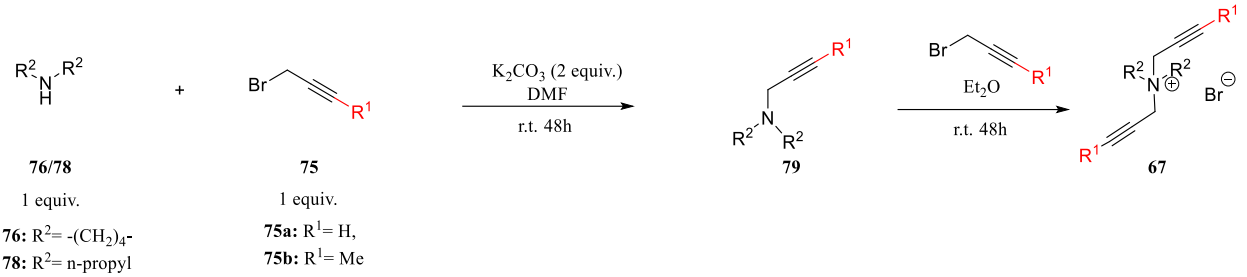

General Procedure B

To a mixture of dialkylamine **(76** or **78)** (1 equiv.) and K_2CO_3 (2 equiv.) in DMF, bromo alkyne **75(a-b)** (1 equiv.) was added. The reaction proceeded at room temperature within 48h.[86] After celite filtration, the solution was diluted with water, and compound **79** was extracted with Et_2O, dried over $MgSO_4$, and concentrated under reduced pressure. The obtained compound **79** was dissolved in dry Et_2O and further alkylated with bromoalkyne **75(a-b)** (1.2 equiv.) at room temperature within 48h. Upon reaction completion, the organic phase was concentrated under reduced pressure to afford ammonium salt **67(b-d)**.

Di(2-propynyl) dipropyl ammonium bromide (67b)

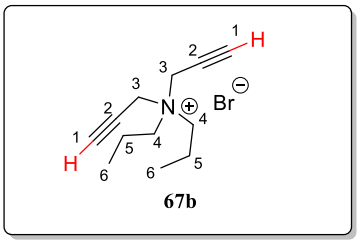

Prepared according to general procedure **B** from dipropylamine **(78)** (0.73 g, 7.20 mmol, 1 equiv.). In the first alkylation step, propargyl bromide **(75a)** (0.86 g, 7.20 mmol, 1 equiv.) was added. For the second alkylation step, extra propargyl bromide **(75a)** (1.03 g, 8.62 mmol, 1.2 equiv.) was added. The product obtained was dissolved in water and washed with pentane to afford di(2-propynyl) dipropyl ammonium bromide **(67b)** (1.60 g, 6.20 mmol, Yield: 87%). For purification, the product was crystallized from acetone.

^{1}H NMR (500 MHz, D_2O) δ 4.35 (d, ^{4}J = 2.5 Hz, 4H, H-3), 3.43 (m, 4H, H-4), 3.22 (t, ^{4}J = 2.5 Hz, 1H, H-1), 1.77 (m, 4H, H-5), 0.97 (t, ^{3}J = 7.3 Hz, 6H, H-6).

^{13}C NMR (126 MHz, D_2O) δ 81.2 (Cq, C-1), 69.9 (Cq, C-2), 60.7(CH_2, C-4), 49.5 (CH_2, C-3), 15.4 (CH_2, C-5), 9.7 (CH_3, C-6).

HRMS (ESI+): Calcd for $C_{12}H_{20}N$ [M^+]: 178.1596; found: 178.1596.

Melting point: 154.4 - 154.9 2.5^{o}C/min

IR (ATR, cm-1) v 3166, 2969, 2117, 1455, 719.

Di (2-butynyl) pyrrolidinium bromide (67c)

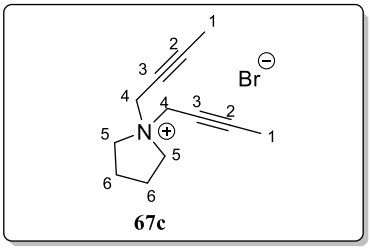

67c

Prepared according to general procedure **B** from pyrrolidine **(76)** (0.95 g, 12.20 mmol, 1 equiv.). In the first alkylation step, 1-bromo-2-butyne **(75b)** (1.6 g, 12.2 mmol, 1 equiv.) was added. For the second alkylation step, extra 1-bromo-2-butyne **(75b)** (1.94 g, 14.60 mmol, 1.2 equiv.) was added. The salt di(2-butynyl) pyrrolidinium bromide **(67c)** (1.3 g, 5.07 mmol, Yield: 43%) was obtained without any further purification.

^{1}H NMR (500 MHz, D_2O) δ 4.23 (q, ^{5}J = 2.5 Hz, 4H, H-4), 3.63 (t, ^{3}J = 7.3 Hz, 4H, H-5), 2.17 (m, 4H, H-6), 1.88 (t, ^{5}J = 2.5 Hz, 6H, H-1).

^{13}C NMR (126 MHz, D_2O) δ 88.8 (Cq, C-2), 66.8 (Cq, C-3), 61.3 (CH_2, C-5), 51.4 (CH_2, C-4), 22.0 (CH_2, C-6), 2.6 (CH_3, C-1).

HRMS (ESI+): Calcd for $C_{12}H_{18}N$ [M^+]: 176.1440; found: 176.1439

Melting point: 106.3-107.4 2.5 ^{o}C/min

IR (ATR, cm-1) v 3406, 2955, 2916, 2331, 2243, 1368, 879

Di (2-butynyl) dipropylammonium bromide (67d)

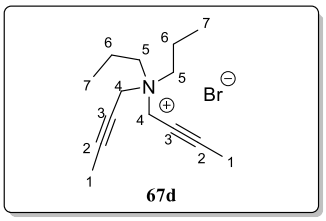

Prepared according to general procedure **B** from dipropylamine **(78)** (0.99 g, 9.79 mmol, 1 equiv.). In the first alkylation step, 1-bromo-2-butyne **(75b)** (1.30 g, 9.97 mmol, 1 equiv.) was added. For the second alkylation step, an extra 1-bromo-2-butyne **(75b)** (1.56g, 12 mmol, 1.2 equiv.) was added. The obtained salt di (2-butynyl) dipropylammonium bromide **(67d)** (2.40 g, 8.38 mmol, Yield: 86%) was dissolved in water and washed with pentane for further purification.

^{1}H NMR (500 MHz, D_2O) δ 4.13 (q, ^{5}J = 2.3 Hz, 4H, H-4), 3.31 (m, 4H, H-5), 1.88 (t, ^{5}J = 2.3 Hz , 6H, H-1), 1.71 (m, 4H, H-6), 0.94 (t, ^{3}J = 7.4 Hz, 6H, H-7).

^{13}C NMR (126 MHz, D_2O) δ 90.0 (Cq, C-2), 65.7 (Cq, C-3), 60.05 (CH_2, C-5), 49.8 (CH_2, C-4), 15.2 (CH_2,C-6), 9.8 (CH_3,C-7), 2.7 (CH_3,C-1).

HRMS (ESI+): Calcd for $C_{14}H_{24}N$ [M^+]: 206.1913; found: 206.1909.

Melting point: 135.7-136.4 2.5 ^{o}C/min

IR (ATR, cm-1) v 3405, 2970, 2939, 2907, 2869, 2329, 2240.

Di (propyl) pyrrolidinium Bromide (82)

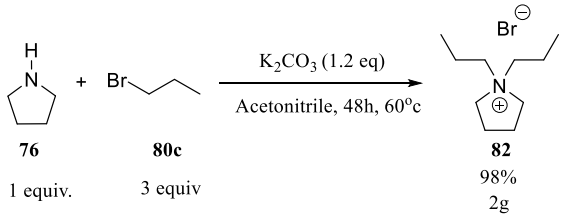

To a solution of pyrrolidine **(76)** (0.60 g, 8.50 mmol, 1 equiv.) and K_2CO_3 (1.40 g, 10.20 mmol, 1.2 equiv.) in acetonitrile, bromopropane **(80c)** (3.12 g, 25.4 mmol, 3 equiv.) was added. The solution was stirred for 48h at 60 °C. For purification, the obtained solution was condensed under reduced pressure, dissolved in ethanol, triturated, and then filtered to remove K_2CO_3. The final solution was condensed under reduced pressure to afford di(propyl)pyrrolidinium bromide **(82)** (2 g, 8.47 mmol, Yield 98%).

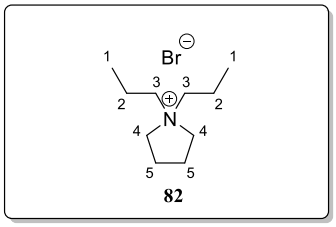

^{1}H NMR (500 MHz, D_2O) δ 3.37 (m, 4 H, H-4), 3.08 (m, 4 H, H-3), 2.03 (m, 4H, H-5), 1.61 (m, 4H, H-2), 0.83 (t, ^3J = 7.3 Hz, 6H, H-1).

^{13}C NMR (126 MHz, D_2O) δ 62.7 (CH_2, C-4), 61.1 (CH_2, C-3), 21.5 (CH_2, C-5), 16.2 (CH_2, C-2), 9.9 (CH_3, C-1).

HRMS (ESI+): Calcd for $C_{10}H_{22}N$ [M+]: 156.1752; found: 156.1752.

Melting Point: 263.6 - 264.5 2.5°C/min

IR (ATR, cm-1) v 3472, 2965, 2878, 1469, 949.

- Ammonium salts containing hexmethylenetetramine unit **68a-f**:

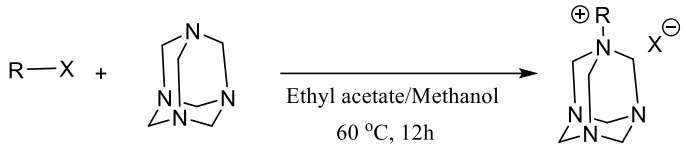

80 **83** **68a-f**

5 equiv. 1 equiv.

80a: R= methyl, **80b:** R= ethyl
80c: R= Propyl, **80d:** R= benzyl
80e: R= octanyl, **80f**: R= dodecyl
X= I, Br

General procedure C

To a flask containing hexamethylenetetramine **(83)** (1 equiv.) dissolved in ethyl acetate and methanol, electrophile **80(a-f)** was added (1 equiv.). The resulting mixture was stirred at 60°C for 12h, and the obtained product was filtered and washed with ethyl acetate.

1-methyl-1, 3, 5, 7- tetraazaadamantanium iodide (68a)

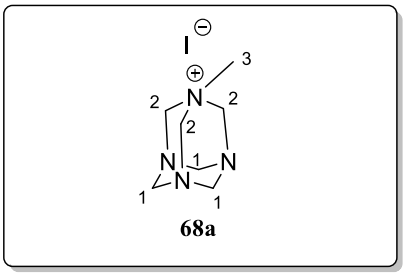

68a

Prepared according to general procedure **C** from methyl iodide **(80a)** (1.10 g, 7.60 mmol, 1 equiv.) and hexamethylenetetramine **(83)** (1.10 g, 7.60 mmol, 1 equiv.). The reaction mixture was refluxed for 12h in ethyl acetate (60 ml) and methanol (3 ml). The product obtained was filtered and washed with ethyl acetate to afford compound 1-methyl-1, 3, 5, 7-tetraazaadamantanium iodide **(68a)** (1.97 g, 6.98 mmol, Yield: 92%) as a white powder.

^{1}H NMR (500 MHz, $(CD_3)_2SO$) δ 5.10 (s, 6H, H-2), 4.62 (d, ^{2}J = 12.5 Hz, 3H, H-1), 4.42 (d, ^{2}J = 12.5 Hz, 3H, H-1), 2.49 (s, 3H, H-3).

^{13}C NMR (500 MHz, $(CD_3)_2SO$) δ 79.7 (CH_2, C-2), 70.2 (CH_2, C-1), 42.7 (CH_3, C-3).

HRMS (ESI+): Calcd for $C_7H_{15}N_4$ [M+]: 155.1298; found: 155.1297.

Melting point: 204.3 - 204.9 2.5 ºC/min

The ^{1}H and ^{13}C NMR data match those reported in the literature[100].

1-ethyl-1, 3, 5, 7-tetraazaadamantanium Iodide (68b):

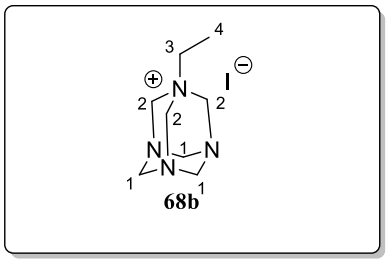

68b

Prepared according to general procedure **C** from ethyl iodide **(80b)** (2.07 g, 16.8 mmol, 1 equiv.) and hexamethylenetetramine **(83)** (0.47 g, 3.37 mmol, 1 equiv.). The reaction was refluxed for 12 h in ethyl acetate (30 ml) and methanol (1.4 ml). The crude mixture obtained was filtered and washed with ethyl acetate to afford compound 1-ethyl-1, 3, 5, 7-tetraazaadamantanium iodide **(68b)** (0.76 g, 2.56 mmol, Yield: 76%) as a white powder.

^{1}H NMR (500 MHz, D_2O) δ 5.02 (s, 6H, H-2), 4.66 (d, ^{2}J = 13.1 Hz, 3H, H-1), 4.50 (d, ^{2}J = 12.5 Hz, 3H, H-1), 2.95 (q, ^{3}J = 7.5 Hz, 2H, H-3), 1.22 (t, ^{3}J = 7.5 Hz, 3H, H-4).

^{13}C NMR (126 MHz, D_2O) δ 77.9 (CH_2, C-2), 70.3 (CH_2, C-1), 52.8 (CH_2, C-3), 5.01 (CH_3, C-4)

HRMS (ESI+): Calcd for $C_8H_{17}N_4$[M+]: 169.1454; found: 169.1453.

Melting Point: 140.8 - 141.4 2.5 ºC/min.

The ^{1}H and ^{13}C NMR data match those reported in the literature[101]

1-propyl-1, 3, 5, 7-tetraazaadamantanium bromide (68c)

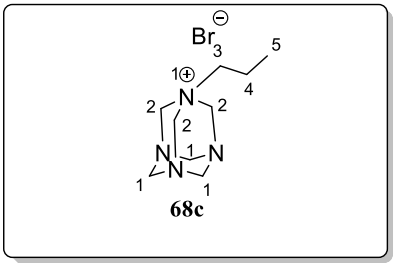

68c

Prepared according to general procedure **C** from bromopropane **(80c)** (4.70 g, 38 mmol, 5 equiv.) and hexamethylenetetramine **(83)** (1.06 g, 7.60 mmol, 1 equiv.). The reaction was refluxed for 12h in ethyl acetate (60 ml) and methanol (3 ml). The product obtained was filtered and washed with ethyl acetate to afford compound 1-propyl-1, 3, 5, 7-tetraazaadamantanium bromide **(68c)** (1.37 g, 5.21 mmol, Yield: 70%) as a white powder.

^{1}H NMR (500 MHz, $(CD_3)_2SO$) δ 5.12 (s, 6 H, H-2), 4.60 (d, ^{2}J = 12.5 Hz, 3H, H-1), 4.49 (d, ^{2}J = 12.5 Hz, 3H, H-1), 2.75 (m, 2H, H-3), 1.66 (m, 2H, H-4), 0.88 (t, ^{3}J = 7.3 Hz, 3H, H-5).

^{13}C NMR (500 MHz, $(CD_3)_2SO$) δ 78.2 (CH_2, C-2), 70.3 (CH_2, C-1), 57.7 (CH_2, C-3), 13.4 (CH_2, C-4), 11.5 (CH_3, C-5).

HRMS (ESI+): Calcd for $C_9H_{19}N_4$ [M+]: 183.1604; found: 183.1610.

Melting Point: 147.2 - 147.6 2.5 ^{o}C/min.

The ^{1}H and ^{13}C NMR data match those reported in the literature[102]

1-benzyl-1, 3, 5, 7-tetraazaadamantanium bromide (68d)

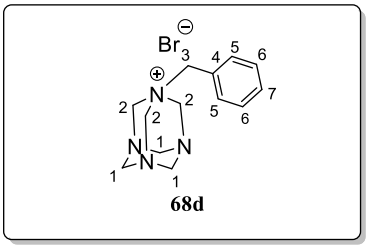

68d

Prepared according to general procedure **C** from benzyl bromide **(80d)** (1.65 g, 9.64 mmol, 1 equiv.) and hexamethylenetetramine **(83)** (1.35 g, 9.64 mmol, 1 equiv.). The reaction was refluxed

for 12h in ethanol (60 ml). The product was filtered and washed with ethanol and diethyl ether to afford compound 1-benzyl-1, 3, 5, 7-tetraazaadamantanium bromide **(68d)** (1.93 g, 6.20 mmol, Yield: 64%) as a white powder.

^{1}H NMR (500 MHz, $(CD_3)_2SO$) δ 7.52 (m, 5H, H-5, 6, 7), 5.11 (s, 6H, H-2), 4.59 (d, ^{2}J = 12.4 Hz, 3H, H-1), 4.43 (d, ^{2}J = 12.4 Hz, 3H, H-1), 4.12 (s, 2H, H-3)

^{13}C NMR (500 MHz, $(CD_3)_2SO$) δ 132.9 (CH, C-5), 130.6 (CH, C-7), 129.6 (CH, C-6), 126.1 (Cq, C-4), 78.1 (CH_2, C-2), 70.3 (CH_2, C-1), 59.6 (CH2, C-3).

HRMS (ESI+): Calc for $C_{13}H_{19}N_4$ [M+]: 231.1608; found: 231.1610.

Melting point: 173.1 - 173.9 2.5 ºC/min

The ^{1}H and ^{13}C NMR data match those reported in the literature.[87]

1-octyl-1, 3, 5, 7-tetraazaadamantanium bromide (68e)

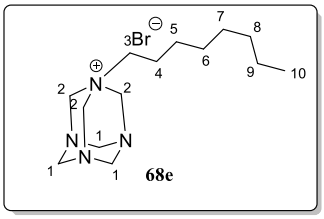

68e

Prepared according to general procedure **C** from bromooctane **(80e)** (7.34 g, 38 mmol, 5 equiv.) and hexamethylenetetramine **(83)** (1.06 g, 7.60 mmol, 1 equiv.). The reaction was refluxed for 12h in ethylacetate (60 ml) and methanol (3 ml). The product was filtered and washed with ethyl acetate to afford compound 1-octyl-1, 3, 5, 7-tetraazaadamantanium bromide **(68e)** (1.18 g, 3.54 mmol, Yield: 47%) as a white powder.

^{1}H NMR (500 MHz, D_2O) δ 5.10 (s, 6H, H-2), 4.72 (d, ^{2}J = 13 Hz, 3H, H-1), 4.58 (d, ^{2}J = 13 Hz, 3H, H-1), 2.9 (m, 2H, H-3), 1.7 (m, 2H, H-4), 1.28 (m, 10H, H-5, 6, 7, 8, 9), 0.85 (t, ^{3}J = 7.1 Hz, 3H, H-10).

^{13}C NMR (126 MHz, D_2O) δ 78.1 (CH_2, C-2), 70.1 (CH_2, C-1), 57.3 (CH_2, C-3), 30.9 (CH_2, C-4), 28.1 (CH_2, C-5), 28.0 (CH_2, C-6), 25.8 (CH_2, C-7), 22.0 (CH_2, C-8), 19.2 (CH_2, C-9), 13.4 (CH_3, C-10).

HRMS (ESI+): Calc for $C_{14}H_{29}N_4$ [M+]: 253.2392; found: 253.2392.

Melting point: 155.1 - 156.9 2.5 ^oC/min

The ^1H and ^{13}C NMR data match those reported in the literature[103]

1-dodecyl-1, 3, 5, 7-tetraazaadamantanium bromide (68f)

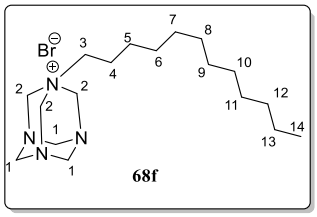

68f

Prepared according to general procedure **C** from bromododecane **(80f)** (9.50 g, 38 mmol, 5 equiv.) and hexamethylenetetramine **(83)** (1.06 g, 7.60 mmol, 1 equiv.). The reaction was refluxed for 12h in ethyl acetate (60 ml) and methanol (3 ml). The product was filtered and washed with ethyl acetate to afford compound 1-dodecyl-1, 3, 5, 7-tetraazaadamantanium bromide **(68f)** (1.6 g, 4.11 mmol, Yield: 54%) as a white powder.

^{1}H NMR (500 MHz, $(CD_3)_2SO$) δ 5.09 (s, 6H, H-2), 4.6 (d, ^2J = 12.4 Hz, 3H, H-1), 4.47 (d, ^2J = 12.4 Hz, 3H, H-1), 2.76 (m, 2H, H-3), 1.62 (m, 2H, H-4), 1.25 (m, 18H, H-5, 6, 7, 8, 9, 10, 11, 12, 13), 0.86 (t, ^3J = 7.2 Hz, 3H, H-12).

^{13}C NMR (126 MHz, $(CD_3)_2SO$) δ 79.7 (CH_2, C-2), 70.3 (CH_2, C-1), 42.6 (CH_2, C-3), 31.7 (CH_2, C-4, C-5, C-6, C-7), 29.4 (CH_2, C-8, C-9, C-10, C-11, C-12), 22.5 (CH_2, C-13), 14.6 (CH_3, C-14).

HRMS (ESI+): Calc for $C_{18}H_{37}N_4$ [M+]: 309.3018; found: 309.3018.

Melting point: 151.3 - 158.6 2.5 ^oC/min

IR (ATR, cm-1) v 3500, 2900, 2750, 1450, 1253, 1000

- Ammonium salts containing imidazole unit

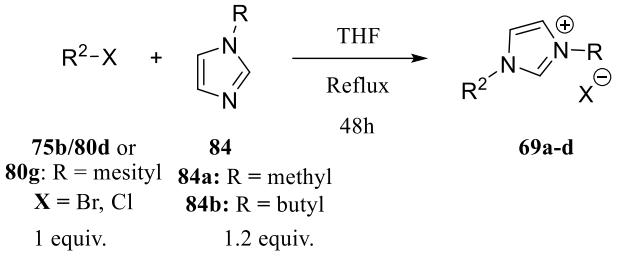

General procedure D

To a dry flask containing imidazole **84** (1.2 equiv.) in THF, electrophile **75b**/**80d/80g** (1 equiv.) was added. The solution was refluxed for 48h and the obtained product was filtered, washed with diethyl ether, and dried under reduced pressure to afford products **69a-d**.

1-(2-butynyl)-3-methylimidazolium bromide (69a)

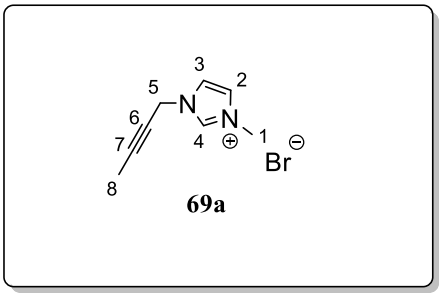

Prepared according to general procedure **D** from 1-bromo-2-butyne **(75b)** (0.46 g, 3.43 mmol, 1 equiv.) and 1-methylimidazole **(84a)** (0.33 g, 3.98 mmol, 1.2 equiv.). The reaction was refluxed for 48h and the obtained organic phase was concentrated under reduced pressure. For purification, the crude obtained was dissolved in water and washed with pentane and diethyl ether to afford 1-(2-butynyl)-3-methylimidazolium bromide **(69a)** (0.37 g, 1.72 mmol, Yield: 80%).

^{1}H NMR (500 MHz, $CDCl_3$) δ 10.23 (s, 1H, H-4), 7.62 (m, 2H, H-2, H-3), 5.24 (q, ^{5}J = 2.5 Hz, 2H, H-5), 1.91 (t, ^{5}J = 2.5 Hz, 3H, H-8).

^{13}C NMR (126 MHz, $CDCl_3$) δ 137.0 (CH, C-4), 123.7 (CH, C-2), 121.8 (CH, C-3), 86.4 (Cq, C-7), 69.4 (Cq, C-6), 40.5 (CH_2, C-5), 37.0 (CH_3, C-1), 3.8 (CH_3, C-8).

HRMS (ESI+): Calc for $C_8H_{11}N_2$ [M+]: 135.0922; found: 135.0922.

Melting point: 47.1 - 47.4 2.5 °C/min

The ^{1}H and ^{13}C NMR data match those reported in the literature[104]

1-benzyl-3-methylimidazolium chloride (69b)

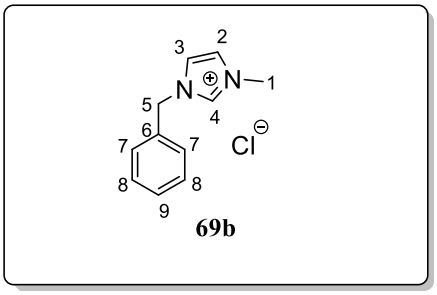

69b

Prepared according to general procedure **D** from benzyl bromide **(80d)** (1.35 g, 7.90 mmol, 1 equiv.) and 1-methylimidazole **(84a)** (0.75 g, 9.16 mmol, 1.2 equiv.). The reaction was refluxed for 48h and the obtained organic phase was concentrated under reduced pressure to afford the crude product. For purification, the product obtained was dissolved in water, washed with pentane, and further heated under reduced pressure to afford 1-benzyl-3-methylimidazolium chloride **(69b)** (1.95 g, 7.70 mmol, Yield: 78%).

^{1}H NMR (500 MHz, $CDCl_3$) δ 10.37 (s, 1H, H-4), 7.58 (t, ^{3}J = 1.9 Hz, 1 H, H-2), 7.50 (m, 2H, H-7), 7.46 (t, ^{3}J = 1.9 Hz, 1H, H-3), 7.36 (m, 3H, H-8, H-9), 5.59 (s, 2H, H-5), 4.10 (s, 3H, H-1).

^{13}C NMR (126 MHz, $CDCl_3$) δ 137.2 (CH, C-4), 133.1 (Cq, C-6), 129.5 (CH, C-9), 129.4 (CH, C-7), 128.9 (CH, C-8), 123.8 (CH, C-2), 122.0 (CH, C-3), 53.2 (CH_2, C-5), 36.8 (CH_3, C-1).

HRMS (ESI+): Calc for $C_{11}H_{13}N_2$ [M^+]: 173.1081; found: 173.1079

The ^{1}H and ^{13}C NMR data match those reported in the literature[105]

1-(mesityl)-3-methylimidazolium chloride (69c)

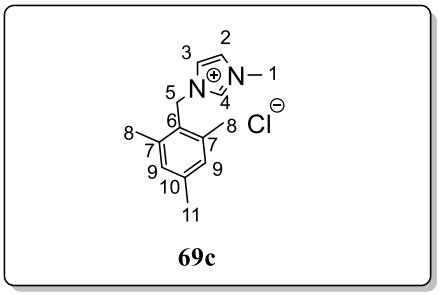

69c

Prepared according to general procedure **D** from 2, 4, 6-trimethylbenzyl chloride **(80g)** (2.00 g, 11.86 mmol, 1 equiv.) and 1-methylimidazole **(84a)** (1.13 g, 13.76 mmol, 1.2 equiv.). The reaction was refluxed for 48h and the obtained organic phase was concentrated under reduced pressure to afford 1-(mesityl)-3-methylimidazolium chloride **(69c)** (1.89g, 7.54 mmol, Yield: 64%) with no further purification.

^{1}H NMR (500 MHz, $CDCl_3$) δ 10.73 (s, 1H, H-4), 7.48 (t, ^{3}J = 1.6 Hz, 1H, H-2), 6.94 (s, 2H, H-9), 6.83 (t, ^{3}J = 1.6 Hz, 1H, H-3), 5.56 (s, 2H, H-5), 4.14 (s, 3H, H-1), 2.30 (s, 3H, H-11), 2.28 (s, 6H, H-8).

^{13}C NMR (126 MHz, $CDCl_3$) δ 139.9 (Cq, C-10), 138.1 (Cq, C-7), 137.7 (CH, C-4), 129.9 (CH, C-9), 125.2 (Cq, C-6), 123.7 (CH, C-2), 120.5 (CH, C-3), 47.7 (CH_2, C-5), 36.8 (CH_3, C-1), 21.0 (CH_3, C-11), 19.8 (CH_3, C-8).

HRMS (ESI+): Calc for $C_{14}H_{19}N_2$ [M^+]: 215.1548; found: 215.1548.

The ^{1}H and ^{13}C NMR data match those reported in the literature[89]

1-(mesityl)-3-butylimidazolium chloride (69d)

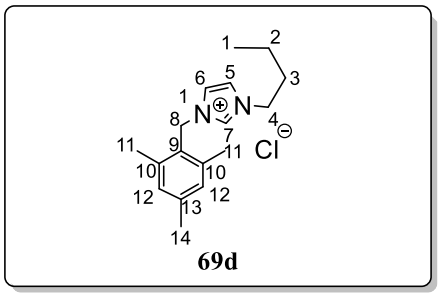

69d

Prepared according to general procedure **D** from 2, 4, 6-trimethylbenzyl chloride **(80g)** (2 g, 11.86 mmol, 1 equiv.) and 1-butylimidazole **(84b)** (1.71 g, 13.76 mmol, 1.2 equiv.). The reaction was refluxed for 48h and the obtained organic phase was concentrated under reduced pressure. For purification, the crude obtained was dissolved in water, washed with pentane, and further heated under reduced pressure to afford 1-(mesityl)-3-butylimidazolium chloride **(69d)** (3.20 g, 10.93 mmol, Yield: 92%) as an oily product.

^{1}H NMR (500 MHz, D_2O) δ 8.46 (s, 1H, H-7), 7.47 (t, ^{3}J = 1.9 Hz, 1H, H-5), 7.32 (t, ^{3}J = 1.9 Hz, 1H, H-6), 7.04 (s, 2H, H-12), 5.38 (s, 2H, H-8), 4.11 (t, ^{3}J = 7 Hz, 2H, H-4), 2.27 (s, 3H, H-14), 2.23 (s, 6H, H-11), 1.77 (pent, ^{3}J = 7.7 Hz, 2H, H-3), 1.22 (sextet, ^{3}J = 7.7 Hz, 2H, H-2), 0.85 (t, ^{3}J = 7.3 Hz, 3H, H-1)

^{13}C NMR (126 MHz, D_2O) δ 140.2 (Cq, C-13), 138.7 (Cq, C-10), 134.6 (CH, C-7), 129.4 (CH, C-12), 125.9 (Cq, C-9), 122.5 (CH, C-5), 122.1 (CH, C-6), 49.4 (CH_2, C-4), 47.2 (CH_2, C-8), 31.2 (CH_2, C-3), 20.0 (CH_3, C-14), 18.7 (CH_2, C-2), 18.5 (CH_3, C-11), 12.5 (CH_3, C-1).

HRMS (ESI+): Calc for $C_{17}H_{25}N_2$ [M^+]: 257.2018; found: 257.2018.

The ^{1}H and ^{13}C NMR data match those reported in the literature[106]

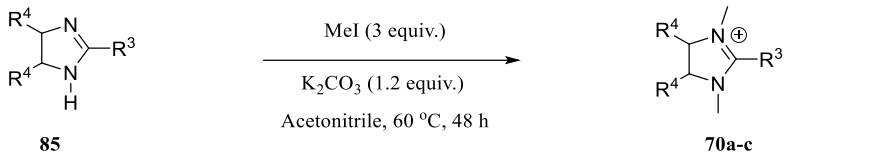

85

85c: R^3: phenyl; R^4: -CH=CH-CH=CH-
85d: R^3: H; R^4: Phenyl
85e: $R^3 = R^4$: Phenyl

70a-c

70a: R^3: phenyl; R^4: -CH=CH-CH=CH-
70b: R^3: H; R^4: Phenyl
70c: $R^3 = R^4$: Phenyl

General procedure E

To a solution of imidazole **85(c-e)** (1 equiv.) and K_2CO_3 (1.2 equiv.) in acetonitrile, MeI (3 equiv.) was added. The mixture was stirred for 48 h at 60°C, and the obtained solution was concentrated under reduced pressure to give a crude white powder. For purification, the crude product was added to an Erlenmeyer flask containing distilled water and stirred for 15 min at 100 °C to ensure the total dissolve of K_2CO_3. The solution was filtered through a Buchner funnel and further washed with distilled water until the pH of the water was neutral.

1, 3-dimethyl-2-phenyl-1H-benzo[d]imidazolium Iodide (70a)

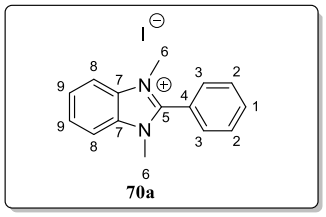

70a

Prepared according to general procedure **E** from 2-phenyl benzimidazole **(85c)** (10 g, 50 mmol, 1 equiv.) and MeI (21.92 g, 154 mmol, 3 equiv.) to afford 1, 3- dimethyl-2-phenyl-1H-benzo [d]imidazolium Iodide **(70a)** (14 g, 39.9 mmol, Yield: 80%).

^{1}H NMR (500 MHz, DMSO) δ 8.14 (dd, ^3J = 6.2, 3.1 Hz, 2H, H-2), 7.94 (d, ^3J = 7.0 Hz, 2H, H-3), 7.85–7.75 (m, 5H, H-8, H-9, H-1), 3.90 (s, 6H, H-6).
^{13}C NMR (126 MHz, DMSO) δ 150.8 (Cq, C-5), 133.4 (CH, C-8 or C-9), 132.2 (Cq, C-4), 131.3 (CH, C-3), 129.9 (CH, C-8 or C-9), 127.1 (CH, C-1), 121.4 (Cq, C-7), 113.9 (CH, C-2), 33.4 (CH_3, C-6).
HRMS (ESI+): Cal for $C_{15}H_{15}N^{2+}$[M+]: 223.1232; found: 223.1235

Melting point: 278.5 - 281.4 2.5 ºC/ min

The ^{1}H and ^{13}C NMR data match those reported in the literature[107]

4,5-diphenyl-1,3-dimethylimidazolium Iodide (70b):

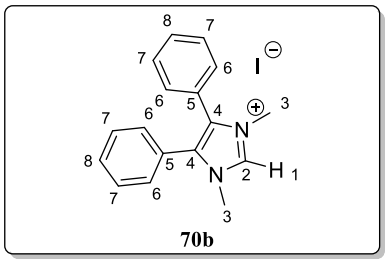

70b

Prepared according to general procedure **E** from 4,5-diphenylimidazole **(85d)** (10 g, 45.4 mmol, 1 equiv.) and MeI (19.30 g, 136 mmol, 3 equiv.) to afford 4,5-diphenyl-1,3-dimethylimidazolium Iodide **(70b)** (10 g, 42.5 mmol, Yield: 94%).

^{1}H NMR (500 MHz, DMSO) δ 9.41 (s, 1H, H-1), 7.50-7.41 (m, 10 H, H-6, 7, 8), 3.75 (s, 6H, H-3)

^{13}C NMR (126 MHz, DMSO) δ 137.2 (CH, C-1), 131.9 (Cq, C-4), 131.1 (CH, C-7), 130.5 (CH, C-8), 129.4 (CH, C-6), 125.6 (Cq, C-5), 34.9 (CH_3, C-3)

Melting Point: 204.4 - 204.9 ºC/min

HRMS (ESI+): Cal for $C_{17}H_{17}N^{2+}$ [M+]: 249.1393; found: 249.1392

The ^{1}H and ^{13}C NMR data match those reported in the literature[108]

2, 4, 5 triphenyl-1,3-dimethylimidazolium Iodide (70c)

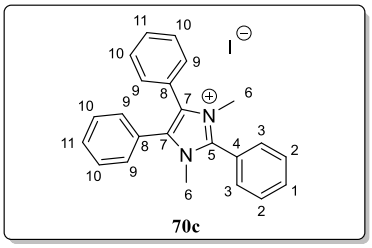

Prepared according to general procedure **E** from 2, 4, 5-triphenylimidazole **(85e)** (10 g, 33.7 mmol, 1 equiv.) and MeI (14.36 g, 101.2 mmol, 3 equiv.) to afford 2, 4, 5 triphenyl-1,3-dimethylimidazolium Iodide **70c** (14.6 g, 30.9 mmol, Yield: 92%).

^{1}H NMR (500 MHz, DMSO) δ 7.96 (dd, ^{3}J = 8 Hz, 1.9 Hz, 2H, H-3), 7.80 (m, 3H, H-2,1), 7.50 (m, 10H, H-9, 10, 11), 3.54 (s, 6H, H-6)

^{13}C NMR (126 MHz, DMSO) δ 144.6 (Cq, C-5), 133.0 (CH, C-2), 131.8 (Cq, C-7), 131.3 (CH, C-3), 131.2 (CH, C-9, 10, 11), 130.6 (CH, C-9, 10, 11), 130.0 (CH, C-1), 129.5 (CH, C-9, 10, 11), 126.1 (Cq, C-8), 122.4 (Cq, C-4), 35.0 (CH_3, C-6).

HRMS (ESI+): Cal for $C_{23}H_{21}N^{2+}$[M+]: 325.1702; found: 325.1705

Melting point: 255.6 - 257.1 2.5 ºC/min

The ^{1}H and ^{13}C NMR data match those reported in the literature[109]

- Ammonium salts containing aromatic units.

Preparation of amide **91** following path 1:

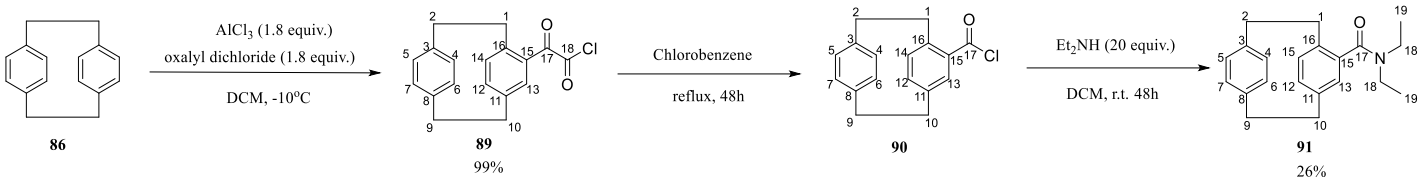

86 → **89** 99% → **90** → **91** 26%

4-Oxoacetyl chloride [2.2] paracyclophane (89)

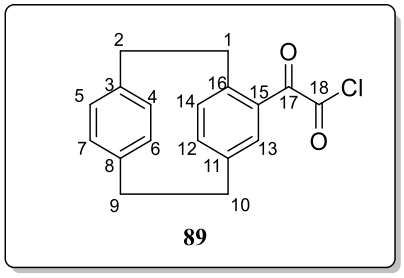

89

To a stirred solution of anhydrous aluminum chloride ($AlCl_3$) (1.15 g, 8.64 mmol, 1.8 equiv.) in dichloromethane (12 ml) at -10 °C, a solution of oxalyl chloride (1.09 g, 8.64 mmol, 1.8 equiv.) in dichloromethane (3 ml) was added dropwise within 5-10 min. The whole mixture was stirred for 10 min at -10 °C, followed by the addition of [2.2] Paracyclophane **(86)** to this suspension. The solution was stirred for an extra 15 min at – 10 °C, poured into ice, and extracted with dichloromethane (3 x 25 ml). The combined extracts were dried over $MgSO_4$ and concentrated under reduced pressure to afford 4-Oxoacetyl chloride [2.2] paracyclophane **(89)** (1.4 g, 4.8 mmol, Yield: 99%) without any further purification.

^{1}H NMR (500 MHz, $CDCl_3$) δ 6.93 (d, ^4J = 1.76 Hz, 1H), 6.83 (dd, ^3J = 7.89, ^4J = 1.61 Hz, 1H), 6.55 (m, 5H), 4.07 (m, 1 H), 3.11 (m, 7H).

^{13}C NMR (126 MHz, $CDCl_3$) δ 181.9 (Cq, C-18), 166.8 (Cq, C-17), 145.7 (Cq), 140.7 (Cq), 139.8 (Cq), 139.5 (CH), 139.4 (Cq), 137.3 (CH), 136.8 (CH), 133.1 (CH), 133.0 (CH), 132.4 (CH), 131.7 (CH), 129.5 (Cq), 35.8 (CH_2), 35.1 (CH_2), 35.0 (CH_2), 34.5 (CH_2).

The ^{1}H and ^{13}C NMR data match those reported in the literature.[92]

4-acetyl chloride [2.2] paracyclophane (90)[23]

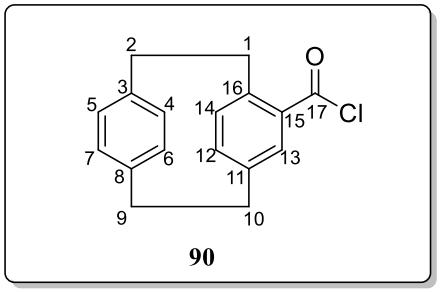

90

The prepared compound 4-oxoacetyl chloride [2.2] paracyclophane **(89)** (0.50 g, 1.67 mmol) was dissolved in chlorobenzene (10 ml) and refluxed for 48h . The obtained compound 4-acetyl chloride [2.2] paracyclophane **(90)** was used as it is in the next step (In situ) without distilling chlorobenzene.

4-N,N-diethylamido[2.2] paracyclophane (91)

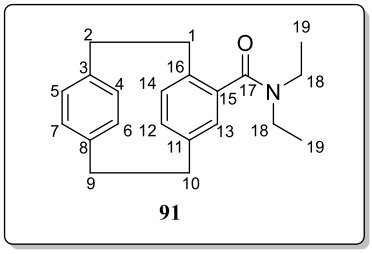

91

To a solution containing compound 4-acetyl chloride [2.2] paracyclophane **(90)** (0.45 g, 1.66 mmol, 1 equiv.) in dichloromethane (13 ml), diethylamine (2.43 g, 33.00 mmol, 20 equiv.) was added. The solution was stirred at room temperature for 48h. The organic phase was concentrated under reduced pressure, and the product obtained was purified by flash column chromatography (SiO_2, petroleum ether / EtOAc 80/20) to afford the titled compound 4-N,N-diethylamido[2.2]paracyclophane **(91)** (0.13 g, 0.43 mmol, Yield: 26% yield).

^{1}H NMR (500 MHz, $CDCl_3$) δ 7.19 (dd, ^4J = 8,2 Hz, 1H), 6.57-6.36 (6H, m), 3.60 (m, 1H), 3.40 (m, 1H), 3.25-2.78 (m, 10H), 1.23 (t, ^3J = 7.2 Hz, 3H), 0.81 (t, ^3J = 7.2 Hz, 3H) .

^{13}C NMR (126 MHz, $CDCl_3$) δ 170.8 (Cq), 139.8 (Cq), 139.3 (Cq), 139.1 (Cq), 136.9 (Cq), 134.8 (CH), 133.8 (CH), 133.6 (Cq), 133.0 (CH), 132.3 (CH), 131.7 (CH), 129.9 (CH), 42.4 (CH_2), 39.1 (CH_2), 35.3 (CH_2), 33.4 (CH_2), 13.9 (CH_3), 13.1 (CH_3)

The ^{1}H and ^{13}C NMR data match those reported in the literature. [94]

Preparation of amide **109** following path 2

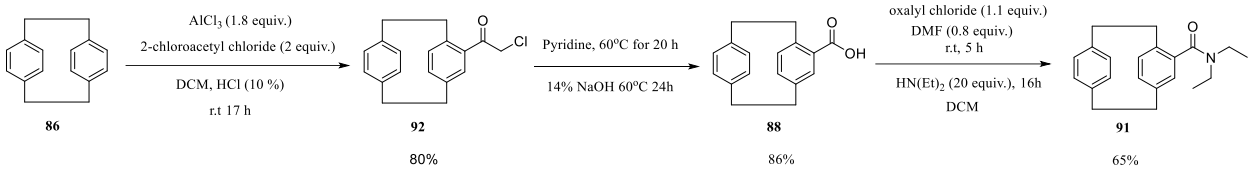

4-(chloroacetone)[2.2] paracyclophane (92)

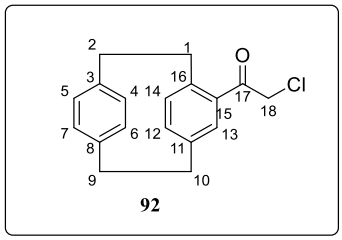

[2.2] Paracyclophane **(86)** (0.73 g, 3.51 mmol, 1 equiv.) was added in one portion to a stirred solution of powdered anhydrous aluminum chloride ($AlCl_3$) (0.84 g, 6.32 mmol, 1.8 equiv.) and 2-chloroacetyl chloride (0.79 g, 7.02 mmol, 2 equiv.) in dichloromethane at -30 ^{o}C. The resulting mixture was stirred for 20 min at a temperature between -15 ^{o}C and 20 ^{o}C, followed by the addition of HCl to the reaction mixture until the white precipitate was dissolved. The reaction mixture was allowed to slowly warm to room temperature and stirred for an extra 17 h. Upon reaction completion, the aqueous phase was separated and extracted with dichloromethane (3 x 15 ml). The combined organic phases were successively washed with a saturated aqueous solution of NaHCO3 (30 ml) and with water (30 ml). The resulting mixture was dried over $MgSO_4$, filtered, and evaporated in a vacuum. The obtained crude was purified by column chromatography (9-1 pentane / ethyl acetate) and (8-2 pentane / ethyl acetate) to afford the titled product 4-(chloroacetone)[2.2] paracyclophane **(92)** (0.74 g, 2.6 mmol, Yield: 74%).

^{1}H NMR (500 MHz, $CDCl_3$) δ 6.87 (d, ^{4}J = 1.8 Hz, 1H), 6.71 (dd, ^{3}J = 6.3 Hz, ^{4}J = 1.6 Hz, 1H), 6.57 (m, 2H), 6.51 (m, 2H), 6.36 (dd, ^{3}J = 7.9, ^{4}J = 1.9Hz, 1H), 4.63 (d, ^{2}J = 14.9 Hz, 1H), 4.33 (d, ^{2}J = 14.9 Hz, 1H), 3.85 (m, 1H), 3.28-2.85 (m, 7H)

^{13}C NMR (126 MHz, $CDCl_3$) δ 192.9 (Cq), 142.5 (Cq), 140.2 (Cq), 140.1 (Cq) 139.2 (Cq), 137.3 (CH), 136.7 (CH), 134.9 (Cq), 133.1 (CH), 132.9 (CH), 132.8 (CH), 132.3 (CH), 131.3 (CH), 47.3 (CH_2), 35.9 (CH_2), 35.2 (CH_2), 35.1 (CH_2) 35.0 (CH_2)

The ^{1}H and ^{13}C NMR data match those reported in the literature[110]

4-formic acid [2.2] paracyclophane (88)

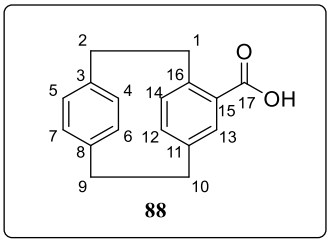

88

A mixture of 4-(chloroacetone)[2.2] paracyclophane **(92)** (0.50 g, 1.75 mmol) and pyridine (35 ml) was stirred for 20 h at 60 ^{o}C. The obtained solution was then condensed under reduced pressure, and the obtained residue was suspended in 14% NaOH (30 ml). The obtained mixture was further stirred for 24 h at 60 ^{o}C. The product 4-formic acid [2.2] paracyclophane **(88)** (0.38 g, 1.5 mmol, Yield: 86%) was isolated and purified by acid-base workup.

^{1}H NMR (500 MHz, $CDCl_3$) δ 7.30 (d, ^{4}J = 1.8 Hz, 1H), 6.72 (dd, ^{3}J = 7.7 Hz, ^{4}J = 1.9 Hz, 1H), 6.60 (m, 3H), 6.52 (m, 2H), 4.22 (m, 1H), 3.25-2.87 (m, 7H)

^{13}C NMR (150 MHz, $CDCl_3$) δ 172.1 (Cq), 143.8 (Cq), 140.1 (Cq), 140 (Cq), 139.5 (Cq), 137.4 (CH), 136.4 (CH), 136.2 (CH), 133.2 (CH), 132.8 (CH), 132.3 (CH), 131.8 (CH), 129.6 (Cq), 36.3 (CH_2). 35.3 (CH_2), 35.1 (CH_2), 34.9 (CH_2).

The ^{1}H and ^{13}C NMR data match those reported in the literature.[91]

4-N,N-diethylamido[2.2] paracyclophane (91)

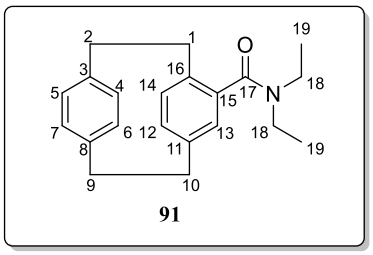

91

Oxalyl chloride (0.22 g, 1.75 mmol, 1.1 equiv.) was slowly added to a solution of carboxylic acid **(88)** (0.4 g, 1.59 mmol, 1 equiv.) dissolved in dichloromethane (13.8 ml). The obtained solution was stirred at room temperature for 10 min, followed by the addition of DMF (0.18 mL, 2 mmol, 0.73 equiv.) in a dropwise manner. The resulting mixture was stirred for 5 hours at room temperature, followed by the addition of diethylamine (2.33 g, 31.8 mmol, 20 equiv.). The reaction mixture was subsequently stirred for extra 16 hours. Upon reaction completion, the organic phase was separated and successively washed with a saturated aqueous solution of $NaHCO_3$ (10 mL) and with water (10 mL). The resulting organic phase was dried over $MgSO_4$, filtered, and evaporated in vacuo to afford a white powder. For purification, column chromatography on silica gel (80/20: petroleum ether/ethylacetate) was done to afford the title compound 4-N,N-diethylamido [2.2] paracyclophane **(91)** (0.31 g, 1 mmol, Yield: 65%).

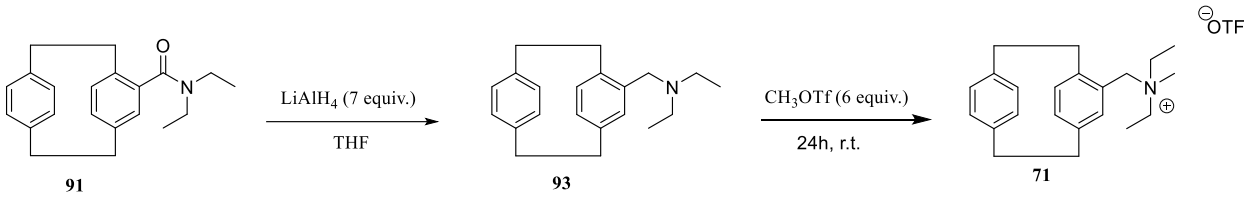

91 **93** **71**

4- N, N- diethylamino [2.2] paracyclophane (93)

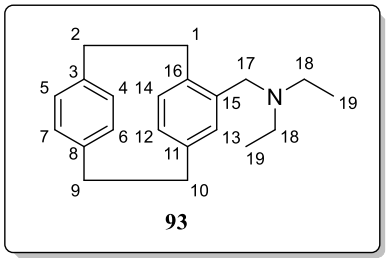

93

A solution of 4-N,N-diethylamido [2.2] paracyclophane **(91)** (0.25 g, 0.80 mmol, 1 equiv.) in anhydrous THF (5 ml) was added dropwise to a solution of lithium aluminum anhydride ($LiAlH_4$) (0.21 g, 5.60 mmol, 7 equiv.) in anhydrous THF (20 ml) at room temperature. After the addition was complete, the solution was stirred for 17 hours. The following day, the reaction was quenched with a 2M aqueous solution of HCl (15 ml) at 0 ^oC. The resulting aqueous layer was separated, extracted with dichloromethane (3x10 ml), basified with a 3M aqueous solution of NaOH (15 ml), and finally extracted with dichloromethane (5x10 ml). The combined organic layers were dried over $MgSO_4$, filtered, and evaporated in vacuum. The crude product was purified by column chromatography (Alumina, n-pentane/ethyl acetate 9:1 (v/v) to 7:3 (v/v)) to afford 4-N,N-diethylamino [2.2] paracyclophane **(93)** (142.3 mg, 0.48 mmol, Yield: 61%).

^{1}H NMR (500 MHz, $CDCl_3$) δ 6.64 (dd, ^3J = 6 Hz, ^4J = 1.9 Hz, 1H, H-5), 6.53 (dd, ^3J = 5.7 Hz, ^4J = 1.8 Hz, 1H, H-6), 6.48-6.45 (m, 2H, H-4, H-12), 6.41 (d, ^3J = 7.6 Hz, 1H, H-14), 6.38 (dd, ^3J = 6.02 Hz, ^4J = 1.9 Hz, 1H, H-7), 6.32 (d, ^4J = 1.34, 1H, H-13), 3.55 (d, ^3J = 13.4 Hz, 1H, H-17), 3.51 (m, 1H, H-1), 3.17- 2.92 (m, 7H, H-2, 9, 10, 17), 2.83-2.77 (m, 1H, H-1), 2.48-2.35 (m, 4H, H-18), 1.02 (t, ^3J = 7.01 Hz, 6H, H-19)

^{13}C NMR (126 MHz, $CDCl_3$) δ 139.5 (Cq, C-8), 139.44 (Cq, C-3), 139.41 (Cq, C-11), 138.9 (Cq, C-16), 138.5 (Cq, C-15), 135.2 (CH, C-13), 134.8 (CH, C-14), 133.3 (CH, C-6), 133.2 (CH,

C-4), 131.9 (CH, C-7), 131.1 (CH, C-12), 128.6 (CH, C-5), 56.4 (CH2, C-17), 47.1 (CH2, C-18), 35.3 (CH2, C-9), 35.0 (CH2, C-10), 34.5 (CH2, C-2), 33.4 (CH2, C-1), 11.6 (CH3, C-19)

HRMS (ESI+): Cal for $C_{21}H_{28}N[M+]$: 294.2221; found: 294.2222

4-N,N- diethyl-N-methyl ammonium Triflate [2.2] paracyclophane (71)

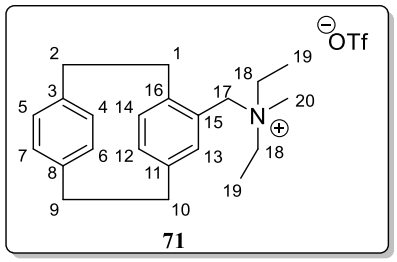

71

To a flask containing 4-N,N- diethylamino [2.2] paracyclophane **(93)** (0.15 g, 0.5 mmol, 1 equiv.) in dichloromethane (5 ml), methyl trifluoromethanesulfonate (CH_3OTf) (0.49 g, 2.98 mmol, 6 equiv.) was added. The solution was stirred for 72h at room temperature. The resultant solution was washed with water and saturated solution of $NaHCO_3$ to afford 4-N,N-diethyl-N-methyl ammonium Triflate [2.2] paracyclophane **(71)** (0.20 g, 0.43 mmol, Yield: 90%).

^{1}H NMR (500 MHz, $CDCl_3$) δ 6.61 (dd, ^3J = 7.9, ^4J = 1.62 Hz, 1H, H-14), 6.56-6.48 (m, 6H, H-12, 13, 4, 5, 6, 7), 4.39 (d, ^2J = 13.2 Hz, 1H, H-17), 4.27 (d, ^2J = 13.2 Hz, 1H, H-17), 3.46-2.95 (m, 12H, H-1, 2, 9, 10, 18), 2.70 (s, 3H, H-20), 1.34 (t, ^3J = 7.2 Hz, 3 H, H-19), 1.31 (t, ^3J = 7.2 Hz, 3H, H-19)

^{13}C NMR (126 MHz, $CDCl_3$) δ 141.9 (Cq, C-15), 141.2 (Cq, C-16), 139.7 (Cq, C-3), 139.5 (CH, C-13), 139.1 (Cq, C-8), 136.1 (CH, C-14), 135.7 (CH, C-12), 133.1 (CH, 4/ 5/ 6/ 7), 132.9 (CH, 4/ 5/ 6/ 7), 132.7 (CH, 4/ 5/ 6/ 7), 131.3 (CH, 4/ 5/ 6/ 7), 125.3 (Cq, C-11), 120.4 (q, OTf, J = 319 Hz), 63.7 (CH_2, C-17), 55.4 (CH_2, C-18), 55.1 (CH_2, C-1), 45.8 (CH_3, C-20), 35.1 (CH_2, C-1/ 2/ 9/ 10), 34.8 (CH_2, C-1/ 2/ 9/ 10), 34.7 (CH_2, C-1/ 2/ 9/ 10), 33.9 (CH_2, C-1/ 2/ 9/ 10), 8.03 (CH_3, C-19), 8.01 (CH_3, C-19)

HRMS (ESI+): Calc for $C_{22}H_{30}N^+$ [M+]: 308.2380; found: 308.2378

IR (ATR, cm-1) v 2987, 1252, 1028, 637.

1-methyl-4-phenylpyridinium Iodide (72)

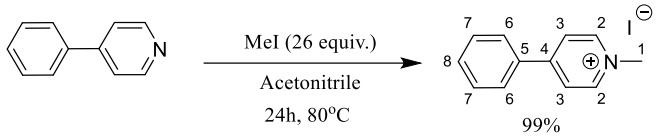

95 **72**

4-phenyl pyridine **(95)** (0.520 g, 3.37 mmol, 1 equiv.) and methyl iodide (12.4 g, 88 mmol, 26 equiv.) were added to a sealed Schlenk tube containing anhydrous acetonitrile. The solution was stirred at 80 °C for 24h. Upon reaction completion, the solvent and excess MeI were removed under reduced pressure to afford the final product 1-methyl-4-phenylpyridinium Iodide **(72)** (1.1 g, 3.7 mmol, Yield: 98%).

^{1}H NMR (500 MHz, $CDCl_3$) δ 9.35 (d, ^{3}J = 6.9 Hz, 2H, H-2), 8.26 (d, ^{3}J = 6.9 Hz, 2H, H-3), 7.80 (dd, ^{3}J = 6.6 Hz, ^{4}J = 1.7 Hz, 2H, H-6), 7.57 (m, 3H, H-7, H-8), 4.67 (s, 3H, H-1).
^{13}C NMR (126 MHz, $CDCl_3$) δ 156.2 (Cq, C-5), 145.7 (CH, C-2), 133.4 (Cq, C-4), 132.5 (CH, C-8), 130.0 (CH, C-7), 128.0 (CH, C-6), 125.0 (CH, C-3), 48.7 (CH_3, C-1).
The ^{1}H and ^{13}C NMR data match those reported in the literature[111]

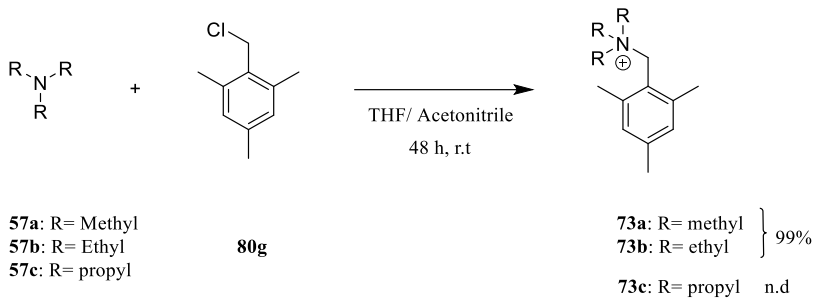

General procedure F

To a solution of trialkylamine **57(a-c)** (5 equiv.) in THF/Acetonitrile, 2-(chloromethyl)-1,3,5-trymethylbenzene **(80g)** (1 equiv.) was added. The resulting solution was stirred at room temperature for 48h. The obtained solution was evaporated under reduced pressure to afford the titled product **73(a-b)**.

Mesityl trimethyl ammonium chloride (73a)

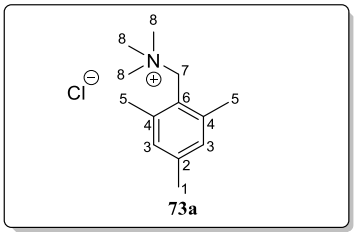

Prepared according to general procedure **F** from trimethylamine **(57a)** (0.78 g, 13.20 mmol, 1.5 equiv.) and 2, 4, 6-trimethylbenzyl chloride **(80g)** (1.50 g, 8.78 mmol, 1 equiv.) in THF. The obtained solution was condensed under reduced pressure, and the obtained crude salt was washed with dichloromethane to afford mesityl trimethyl ammonium chloride **(73a)** (1.90 g, 8.3 mmol, Yield: 95%).

^{1}H NMR (600 MHz, D_2O) δ 7.10 (s, 2H, H-3), 4.61 (s, 2H, H-7), 3.08 (s, 9H, H-8), 2.40 (s, 6H, H-5), 2.27 (s, 3H, H-1).

^{13}C NMR (150 MHz, D_2O) δ 140.90 (Cq, C-6),140.86(Cq, C-4), 130.1 (CH, C-3), 122.2 (Cq, C-2), 63.0 (CH_2, C-7), 52.6 (CH_3, C-8), 20.4 (CH_3, C-5), 20.0 (CH_3, C-1)

The ^{1}H and ^{13}C NMR data match those reported in the literature[112]

Mesityl triethyl ammonium chloride (73b)

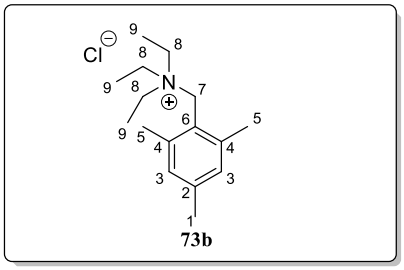

Prepared according to general procedure **F** from triethylamine **(57b)** (1.87 g, 19 mmol, 5 equiv.) and 2, 4, 6-trimethyl benzyl chloride **(80g)** (0.63 g, 3.70 mmol, 1 equiv.) in THF. For purification, the obtained crude salt was heated under reduced pressure to remove the traces of triethylamine **(57b)** and to afford Mesityl triethyl ammonium chloride **(73b)** (0.96 g, 3.5 mmol, Yield: 96%).

^{1}H NMR: (500 MHz, D_2O) δ 7.03 (s, 2H, H-3), 4.52 (s, 2H, H-7), 3.32 (q, ^{3}J = 7.2 Hz, 6H, H-8), 2.38 (s, 6H, H-5), 2.23 (s, 3H, H-1), 1.20 (t, ^{3}J = 7.2 Hz, 9H, H-9).

^{13}C NMR (126 MHz, D_2O) δ 140.7 (cq, C-6, C-4), 130.2 (CH, C-3), 123.0 (cq, C-2), 58.6 (CH_2, C-7), 54.2 (CH_2, C-8), 20.5 (CH_3, C-5), 19.9 (CH_3, C-1), 7.70 (CH_3, C-9).

Melting Point: 136.2-136.7 2.5 ^{O}C/min

HRMS (ESI+): Calcd for $C_{16}H_{28}N$[M+]= 234.2216; found= 234.2222

IR (ATR, cm-1) v 3391, 2945, 1608, 1455, 1017.

Mesityl tripropyl ammonium chloride (73c)

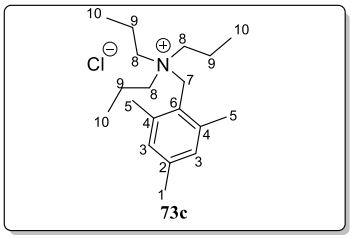

Prepared according to general procedure **F** from tripropylamine **(57c)** (2.30 g, 16 mmol, 5 equiv.) and 2, 4, 6-trimethyl benzyl chloride **(80g)** (0.54 g, 3.2 mmol, 1 equiv.) in acetonitrile. The solvent was evaporated under reduced pressure, and the obtained salt was washed several times with diethyl ether (Et_2O) to afford Mesityl tripropyl ammonium chloride **(73c)** (1g, 3.2 mmol, nd).

^{1}H NMR (600 MHz, $CDCl_3$) δ 6.95 (s, 2H, H-3), 4.91 (s, 2H, H-7), 3.43 (m, 6H, H-8), 2.49 (s, 6H, H-5), 2.30 (s, 3H, H-1), 1.69 (m, 6H, H-9), 0.99 (t, ^3J = 7.3 Hz, H-10).

^{13}C NMR (150 MHz, $CDCl_3$) δ 140.4 (Cq, C-6), 140.1 (Cq, C-2), 130.6 (CH, C-3), 123.0 (Cq, C-4), 61.7 (CH_2, C-8), 60.8 (CH_2, C-7), 21.7 (CH_3, C-5), 20.8 (CH_3, C-1), 16.6 (CH_2, C-9), 11.03 (CH_3, C-10)

HRMS (ESI+): Cal for $C_{19}H_{34}N^+[M^+]$: 276.2689; found: 276.2691

Melting point: 60.2-61.4 2.5 ^{O}C/min

IR (ATR, cm-1) v 3409, 2968, 1644, 1609, 1381.

- Synthesis of phosphonium salts

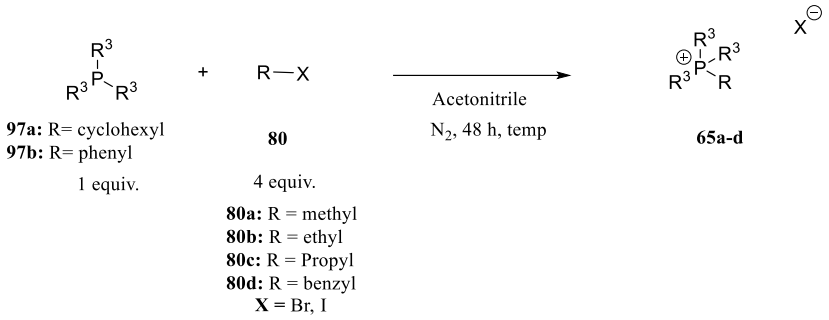

General procedure G

Phosphine **97(a/b)** (1 equiv.) and electrophile **80** (4 equiv.) were dissolved with anhydrous acetonitrile in a sealed Schlenk tube. The obtained solution was stirred at room temperature or heated at 70°C for 48h under an inert atmosphere (Ar). The solvent and sometimes excess of **80** were removed under reduced pressure to afford the final product **65a-d**.

Methyl tricyclohexyl phosphonium Iodide (65a)

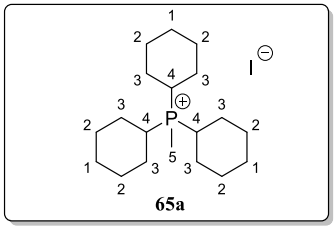

Prepared according to general procedure **G**, from tricyclohexyl phosphine **(97a)** (10 g, 35.6 mmol, 1 equiv.) and methyl iodide **(80a)** (19.58g, 138 mmol, 3.87 equiv.). The reaction proceeded within 48h at room temperature and the obtained solution was concentrated under reduced pressure to afford the final product methyl tricyclohexyl phosphonium Iodide **(65a)** (15g, 35.5 mmol, Yield: 98%).

^{1}H NMR (600 MHz, $CDCl_3$) δ 2.62 (qt, *J* = 12.1 Hz, *J* = 2.9 Hz, 3H, H-4), 2.02 (m, 9H, H-2, H-5), 1.94 (m, 6H, H-3, H-5), 1.80 (m, 3H, H-1), 1.50 (m, 12H, H-3, H-2, H-1), 1.32 (qt, *J* = 12.9, *J* = 3.4 Hz, 3H, H-1).

^{13}C NMR (150 MHz, $CDCl_3$) δ 30.2 (CH, d, $^{1}J_{(c-p)}$ = 42.2 Hz, C-4), 26.9 (CH_2, d, $^{3}J_{(c-p)}$ = 3.8 Hz, C-2), 26.3 (CH_2, d, $^{2}J_{(c-p)}$ = 12.2 Hz, C-3), 25.3 (CH_2, d, $^{4}J_{(C-p)}$ = 1.4 Hz, C-1), 0.1 (CH_3, d, $^{1}J_{(c-p)}$ = 49.1 Hz, C-5).

HRMS (ESI+): Calc for $C_{19}H_{36}P$ [M+]: 295.2555; found: 295.2555.

^{31}P NMR (243 MHz, $CDCl_3$) δ 33.9 ppm

Melting point: 186.7 - 187.9 2.5 ºC/min

The ^{1}H and ^{13}C NMR data match those reported in the literature[113]

Ethyl tricyclohexyl phosphonium Iodide (65b)

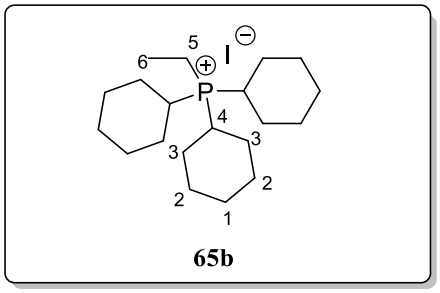

65b

Prepared according to general procedure **G**, from tricyclohexyl phosphine **(97a)** (0.64 g, 2.29 mmol, 1 equiv.) and ethyl iodide **(80b)** (1 g, 8.87 mmol, 3.87 equiv.). The reaction proceeded within 48h at room temperature and the obtained solution was concentrated under reduced pressure to afford the final product ethyl tricyclohexyl phosphonium Iodide **(65b)** (0.92 g, 2.09 mmol, Yield: 92%).

^{1}H NMR (500 MHz, $CDCl_3$) δ 2.63 (q, *J* = 12.3 Hz, 3H, H-4), 2.53 (Sext, *J* = 4.7 Hz, 2H, H-5), 2.05 (d, *J* = 9 Hz, 6H, H-2), 1.95 (d, *J* = 11 Hz, 6H, H-3), 1.8 (d, *J* = 13 Hz, 3H, H-1), 1.53 (Sept, *J* = 11.7 Hz, 12 H, H-2, H-3), 1.35 (m, 6H, H-1, H-6).

^{13}C NMR (126 MHz, $CDCl_3$) δ 29.9 (CH, d, $^{1}J_{(c-p)}$ = 40.3 Hz, C-4), 27.3 (CH_2, $^{3}J_{(c-p)}$ = 3.9 Hz, C-2), 26.5 (CH_2, $^{2}J_{(c-p)}$ = 11.7 Hz, C-3), 25.4 (CH_2, $^{4}J_{(c-p)}$ = 1.4 Hz, C-1), 10.1 (CH_2, $^{1}J_{(c-p)}$ = 44.6 Hz, C-5), 7.5 (CH_3, $^{2}J_{(c-p)}$ = 7.5 Hz, C-6)

^{31}P NMR (243 MHz, $CDCl_3$) δ 33.3 ppm

HRMS (ESI+): Calc for $C_{20}H_{38}P^+$ [M+]: 309.2709; found: 309.2711

Melting point: 187.7 - 194.6 2.5°C/min

IR (ATR, cm-1) v 2958, 2926, 1066.

Propyl tricyclohexyl phosphonium bromide (65c)

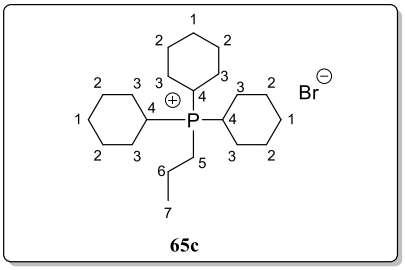

65c

Prepared according to general procedure **G**, from tricyclohexyl phosphine **(97a)** (2 g, 7.13 mmol, 1 equiv.) and bromopropane **(80c)** (4.4 g, 35.65 mmol, 5 equiv.). The reaction proceeded within 48h at 70 °C, and the obtained solution was concentrated under reduced pressure to afford propyl tricyclohexyl phosphonium bromide **(65c)** (2.5 g, 6.20 mmol, Yield: 89%). Traces of phosphine oxide were removed by acetonitrile-pentane workup.

^{1}H NMR (500 MHz, $CDCl_3$) δ 2.39 (qt, *J* = 12.6 Hz, *J* = 2.6 Hz, 3H, H-4), 20.8 (m, 2H, H-5), 1.83 (dd, *J* = 39.8 Hz, *J* = 11.50 Hz, 12 H, H-3, H-2), 1.62 (m, 5H, H-1, H-7), 1.48 (tq, *J* = 12.5 Hz, *J* = 3.3 Hz, 6H, H-2), 1.24 (m, 10H, H-3), 0.98 (td, *J* = 7.3 Hz, *J* = 1.9 Hz, 3H, H-6)

^{13}C NMR (125 MHz, $CDCl_3$) δ 29.1 (CH, d, $^{1}J_{(c\text{-}p)}$ = 41.4 Hz, C-4), 26.4 (CH_2, d, $^{3}J_{(c\text{-}p)}$ = 3.8 Hz, C-2), 26.1 (CH_2, d, $^{2}J_{(c\text{-}p)}$ = 12.9 Hz, C-3), 25.1 (CH_2, d, $^{4}J_{(C\text{-}P)}$ = 1 Hz, C-1), 16.7 (CH_2, d, $^{1}J_{(C\text{-}P)}$ = 43.5 Hz, C-5), 15.8 (CH_3, d, $^{3}J_{(C\text{-}P)}$ = 4.8 Hz, C-7), 15.10 (CH_2, d, $^{2}J_{(c\text{-}p)}$ = 15.5 Hz, C-6)

^{31}P NMR (243 MHz, $CDCl_3$) δ 31.2 ppm

HRMS (ESI+): Cal for $C_{21}H_{40}P^+$[M+]: 323.2861; found: 323.2868

Melting point: 75.3 - 76.3 2.5 °C/min

IR (ATR, cm-1) v 2928, 2852, 1619, 1447.

Benzyl tricyclohexyl phosphonium bromide (65d)[114]

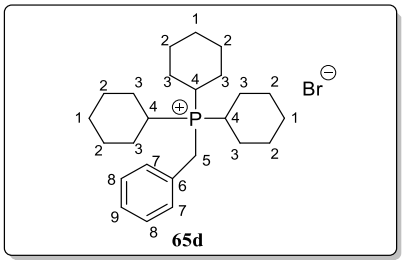

Prepared according to general procedure **G**, from tricyclohexyl phosphine **(97a)** (2g, 7.13 mmol, 1 equiv.) and benzyl bromide **(80d)** (6.10 g, 35.6 mmol, 5 equiv.). The reaction proceeded within 48h at 70 °C, and the obtained solution was concentrated under reduced pressure. For purification, pentane was added to precipitate the product. The obtained white salt was further washed with pentane to remove traces of benzyl bromide. Moreover, traces of phosphine oxide were removed by acetonitrile-pentane workup to afford the final product benzyl tricyclohexyl phosphonium bromide **(65d)** (3.15 g, 6.97 mmol, Yield: 98%).

^{1}H NMR (500 MHz, $CDCl_3$) δ 7.44 (m, 2H, H-7), 7.35 (m, 3H, H-8, H-9), 4.30 (d, 2H, H-5), 2.74 (qt, *J* = 13 Hz, *J* = 2.7 Hz, 3H, H-4), 1.89 (m, 16H, H-3, H-2, H-1), 1.45 (m, 12H, H-3, H-2), 1.25 (qt, *J* = 13 Hz, *J* = 3.7 Hz, 3H, H-1).

^{13}C NMR (125 MHz, $CDCl_3$) δ 130.4 (CH, d, $^{3}J_{(C\text{-}P)}$ = 4.9 Hz, C-7), 129.5 (Cq, C-6), 129.4 (CH, d, $^{4}J_{(c\text{-}p\ )}$ = 2.5 Hz, C-8), 128.4 (CH, d, $^{5}J_{(C\text{-}P)}$ = 2.9 Hz, C-9), 31.0 (CH, d, $^{1}J_{(C\text{-}P)}$ = 38.8 Hz, C-4), 27.2 (CH_2, d, $^{3}J_{(C\text{-}P)}$ = 4.1 Hz, C-2), 26.6 (CH_2, d, $^{2}J_{(C\text{-}p)}$ = 11.7 Hz, C-3), 25.5 (CH_2, d, $^{4}J_{(c\text{-}p)}$ = 1.3 Hz, C-1), 23.3 (CH_2, d, $^{1}J_{(C\text{-}P\ )}$ = 41.2 Hz, C-5).

^{31}P NMR (243 MHz, $CDCl_3$) δ 29.3 ppm

HRMS (ESI+): Calc for $C_{25}H_{40}P^{+}$[M+]: 371.2867; found: 371.2868

Melting Point: 242.2 - 242.8 2.5 °C/min

Methyl triphenyl phosphonium Iodide (65e):

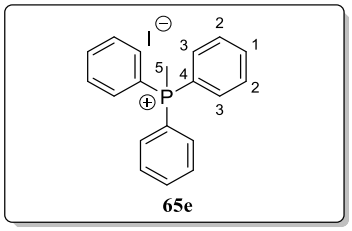

65e

Prepared according to general procedure **G**, from triphenyl phosphine **(97b)** (0.5g, 1.91 mmol, 1 equiv.) and methyl iodide **(80a)** (1.1g, 7.6 mmol, 4 equiv.). The reaction proceeded within 48h at room temperature and the obtained solution was concentrated under reduced pressure to afford the final product methyl triphenyl phosphonium Iodide **(65e)** (0.73 g, 1.8 mmol, Yield: 95%); no further purification was needed.

^{1}H NMR (500 MHz, $CDCl_3$) δ 7.83-7.69 (m, 15 H, H-3, 2, 1), 3.20 (d, ^{3}J = 13.1 Hz, 3H, H-5).
^{13}C NMR (126 MHz, $CDCl_3$) δ 135.3 (CH, d, $^{4}J_{(c\text{-}p)}$ = 3.0 Hz, C-1), 133.4 (CH, d, $^{3}J_{(c\text{-}p)}$ = 10.7 Hz, C-2), 130.6 (CH, d, $^{2}J_{(c\text{-}p)}$ = 12.9 Hz, C-3), 118.9 (Cq, d, $^{1}J_{(c\text{-}p)}$ = 88.8 Hz, C-4), 11.7 (CH3, d, $^{1}J_{(c\text{-}p)}$ = 57.1 Hz, C-5).
^{31}P NMR (243 MHz, $CDCl_3$) δ 21.6 ppm
Melting point: 169.2 - 169.7 2.5 ºC/min
The ^{1}H and ^{13}C NMR data match those reported in the literature[115]

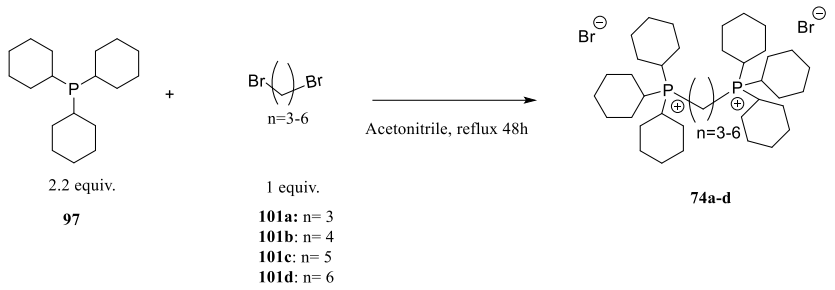

2.2 equiv.

97

1 equiv.

101a: n= 3
101b: n= 4
101c: n= 5
101d: n= 6

74a-d

General procedure H

To a dry Schlenk tube purged with argon containing tricyclohexyl phosphine **97a** (3 equiv.), acetonitrile and electrophile **101(a-d)** (1 equiv.) were added. The solution was refluxed for 48 h, and the obtained solution was condensed under reduced pressure. For purification, the salts were added separately to distilled water, followed by boiling the milky suspension with continuous stirring until it became clear. The clear solution obtained is then left to cool down, followed by washing with diethyl ether (Et_2O) several times to afford the targeted products **74(a-d).**

1,3-di(tricyclohexyl phosphonium) propane dibromide (74a)

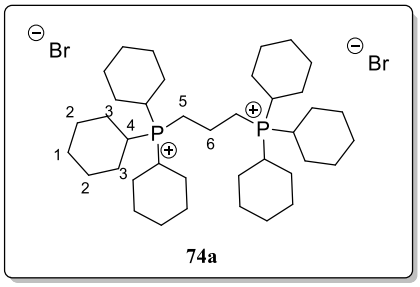

74a

Prepared according to general procedure **H** from tricyclohexyl phosphine **(97a)** (1.5g, 4.92 mmol, 2.5 equiv.) and 1,3-dibromo propane **(101a)** (0.4g, 1.97 mmol, 1 equiv.). The reaction proceeded within 48h, and the obtained solution was concentrated under reduced pressure to afford the product as a white salt 1,3-di(tricyclohexyl phosphonium) propane dibromide **(74a)** (1.5g, 19.67 mmol, Yield: 99%).

^{1}H NMR (500 MHz, $CDCl_3$) δ 2.95 (m, 10 H, H-4, H-5), 2.34 (m, 2 H, H-6), 2.07 (bs, 12 H, H-3), 1.9 (bs, 12 H, H-3) 1.81 (d, 6H, H-1), 1.57 (m, 24H, H-2, H-3), 1.29 (m, 6 H , H-1).

^{13}CNMR(125 MHZ, $CDCl_3$) δ CdecP 30.6 (CH, C-4), 27.7 (CH_2, C-2), 26.3 (CH_2, C-3), 25.6 (CH_2, C-1), 18.1 (CH_2, C-6), 17.5 (CH_2, C-5)

^{31}P NMR (243 MHz, $CDCl_3$) δ 31.8 ppm

HRMS (ESI+): Calculated for $C_{39}H_{72}P_2Br$ $[M]^+$= 681.4293; Found: 681.4290

Melting point: 147.8 - 155.3 2.5 ^oC/min

IR (ATR, cm-1) v 2927, 2852, 1444.

1,4- di(tricyclohexyl phosphonium) butane dibromide (74b)

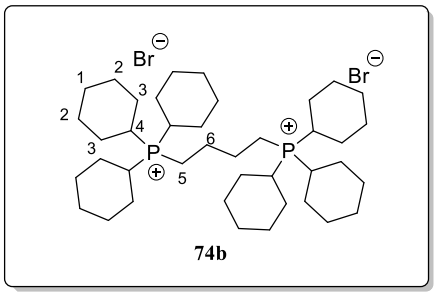

74b

Prepared according to general procedure **H**, from tricyclohexyl phosphine **(97a)** (3.0 g, 10.7 mmol, 3 equiv.) and 1,4-dibromobutane **(101b)** (0.77g, 3.56 mmol, 1 equiv.). The reaction proceeded within 48h, and the obtained solution was concentrated under reduced pressure to afford the product 1,4-di(tricyclohexyl phosphonium) butane dibromide **(74b)** (2.5g, 3.2 mmol, Yield: 93%) as a white salt.

^{1}H NMR (500 MHz, $CDCl_3$) δ 2.80 (m, 4H, H-5), 2.52 (qt, *J* = 12.6 Hz, *J* = 2.2 Hz, 6H, H-4), 2.16- 1.78 (m, 40H, H-6, H-2, H-3, H-1), 1.61 (q, *J* = 12.7 Hz, 6 H, H-2), 1.48- 1.31 (m, 18H, H-3, H-1).

^{13}C NMR(125 MHZ, $CDCl_3$) δ 30.2 (CH, d, $^1J_{(c-p)}$ = 40.6 Hz, C-4), 27.2 (CH_2, d, $^3J_{(c-p)}$ = 3.8 Hz, C-2), 26.6 (CH_2, d, $^2J_{(c-p)}$ = 11.9 Hz, C-3), 25.4 (CH_2, s, C-1), 24.1 (CH_2, dd, $^2J_{(c-p)}$ = 16.6 Hz, $^3J_{(c-p)}$ = 4.6 Hz, C-6), 15.7 (CH_2, d, $^1J_{(c-p)}$ = 43.2 Hz, C-5)

^{31}P NMR (243 MHz, $CDCl_3$) δ 32.3 ppm

HRMS (ESI+): Calculated for $C_{40}H_{74}P_2Br$ $[M]^+$= 695.4449; found: 695.4446

Melting Point: 280.0-284.2 2.5^{o}C/min

IR (ATR, cm-1) v 2924, 2851, 1444.

1,5-di (tricyclohexyl phosphonium) pentane dibromide (74c)

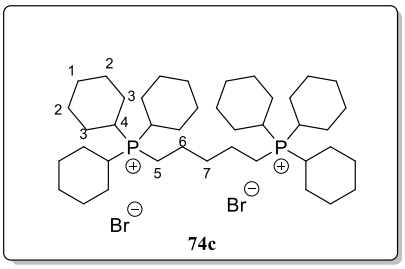

74c

Prepared according to general procedure **H**, from Tricyclohexyl phosphine **(97a)** (10g, 35.6 mmol, 3 equiv.) and 1,5-dibromopentane **(101c)** (2.73 g, 11.8 mmol, 1 equiv.). The reaction proceeded within 48h, and the obtained solution was concentrated under reduced pressure to afford the product 1,5-di (tricyclohexyl phosphonium) pentane dibromide **(74c)** (29 g, 36.7 mmol, Yield: 95%) as a white salt.

^{1}H NMR (600 MHz, $CDCl_3$) δ 2.56 (tq, *J* = 12.6 Hz, *J* = 2.3 Hz, H-4), 2.55-2.49 (m, 4 H, H-5), 1.98-1.71(m, 42 H, H-2, H-1, H-3), 1.50 (qt, *J* = 12.5 Hz, 3.0 Hz, 12H, H-2), 1.41 (q, *J* = 13 Hz, H-3), 1.26 (qt, *J* = 13.1 Hz, 3.1, H-1)

^{13}C NMR (150 MHz, $CDCl_3$) δ 30.2 (CH_2, t, $^{3}J_{(C-P)}$ = 14.5 Hz, C-7), 28.0 (CH, d, $^{1}J_{(C-P)}$ = 40.8 Hz, C-4), 25.2(CH_2, $^{3}J_{(C-P)}$ = 3.82 Hz, C-2), 24.5 (CH_2, d, $^{2}J_{(C-P)}$ = 11.8 Hz, C-3), 23.5 (CH_2, C-1), 19.72 (CH_2, d, $^{2}J_{(C-P)}$ = 4.3 Hz, C-6), 13.9 (CH_2, d, $^{1}J_{(C-P)}$ = 43.5 Hz, C-5)

HRMS (ESI+): Calculated for $C_{41}H_{76}P_2^{2+}$ $[M]^+$= 315.2711; found: 315.2683

Melting Point: 74.6-75.32.5 ^{o}C/min

IR (ATR, cm-1) v 2928, 2853, 1620, 1445

1,6- di(tricyclohexyl phosphonium) hexane dibromide (74d)

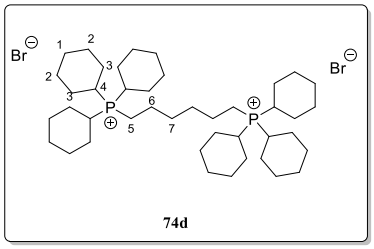

Prepared according to general procedure **H** from tricyclohexyl phosphine **(97a)** (2.5 g, 10.6 mmol, 3 equiv.) and 1,6-dibromohexane **(101d)** (0.87 g, 3.56 mmol, 1 equiv.). The reaction proceeded within 48h and the obtained solution was concentrated under reduced pressure to afford 1,6-di(tricyclohexyl phosphonium) hexane dibromide **(74d)** (2.6 g, 3.2 mmol, Yield: 93%) as a white salt.

^{1}H NMR (500 MHz, $CDCl_3$) δ 2.61 (m, 4H, H-5), 2.55 (qt, *J* = 12.5 Hz, *J* = 2.6 Hz, 6H, H-4), 1.98 (m, 24 H, H-2, H-3), 1.81 (m, 6 H, H-1), 1.74 (m, 8 H, H-7, H-6), 1.56 (qt, *J* = 12.5 Hz, *J* = 3.2 Hz, 12 H, H-2), 1.45 (qt, *J* = 12.9 Hz, *J* = 2.8 Hz, 12 H, H-3), 1.32 (qt, *J* = 12.9 Hz, *J* = 3.6 Hz, 6H, H-1)

^{13}CNMR (150 MHZ, $CDCl_3$) δ 30.1 (CH, d, $^{1}J_{(c\text{-}p)}$ = 40.5 Hz, C-4), 29.8 (CH_2,d, $^{2}J_{(c\text{-}p)}$ = 14.8 Hz, C-6), 27.2 (CH_2, d, $^{3}J_{(c\text{-}p)}$ = 3.9 Hz, C-2), 26.5 (CH_2, d,$^{2}J_{(c\text{-}p)}$ = 11.7 Hz, C-3), 25.5 (CH_2, d, $^{4}J_{(c\text{-}p)}$ = 0.9 Hz, C-1), 22.4 (CH_2, d, $^{3}J_{(c\text{-}p)}$ = 5 Hz, C-7), 15.9 (CH_2, d, $^{1}J_{(c\text{-}p)}$ = 42.9 Hz, C-5).

^{31}P NMR (243 MHz, $CDCl_3$) δ 31.8 ppm

HRMS (ESI+): Calculated for $C_{42}H_{78}P_2^{2+}[M]^+$= 322.2789; found = 322.2773

Melting Point: 122.4-123.3 2.5 ºC/min

IR (ATR, cm-1) v 2927, 3852, 1447.

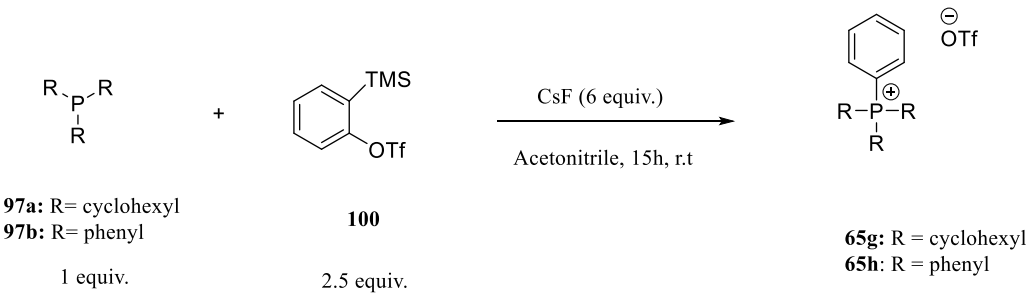

97a: R= cyclohexyl
97b: R= phenyl

1 equiv.

100

2.5 equiv.

65g: R = cyclohexyl
65h: R = phenyl

General procedue I

To a solution of phosphine **(97a/97b)** (0.2 g, 0.7 mmol, 1 equiv.) in acetonitrile (5 ml), cesium chloride (0.65 g, 4.28 mmol, 6 equiv.) and 1-(Trifluoromethyl sulfonyl)-2-(trimethyl silyl) benzene **(100)** (0.53 g, 1.78 mmol, 2.5 equiv.) were successively added. The reaction mixture was stirred at room temperature for 15h, and the obtained solution was then concentrated under reduced pressure to afford the crude product. For purification, the product was dissolved in DCM, washed with water, and then condensed under reduced pressure. Finally, an acetonitrile-pentane workup was performed to yield the final product **65**.

Phenyl tricyclohexyl phosphonium trifluoromethanesulfonate (65g)

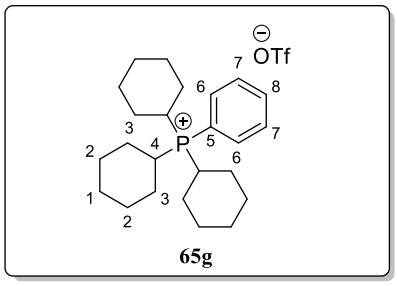

65g

Prepared according to general procedure **I** from tricyclohexyl phosphine **(97a)** (0.2 g, 0.7 mmol, 1 equiv.) and 1-(Trifluoromethyl sulfonyl)-2-(trimethyl silyl) benzene **(100)** (0.53 g, 1.78 mmol, 2.5 equiv.) to afford phenyl tricyclohexyl phosphonium trifluoromethanesulfonate **(65g)** (0.28 g, 0.55 mmol, Yield: 80%).

^{1}H NMR (500 MHz, $CDCl_3$) δ 7.73 (d, *J* = 7.6 Hz, 2 H, H-7), 7.61 (t, *J* = 7.5 Hz, 1 H, H-8), 7.53 (t, *J* = 7.5 Hz, 2 H, H-6), 2.93 (t, *J* = 11.1 Hz, 3H, H-4), 1.67-1.44 (m, 16H, H-2,3,1), 1.20 (septet, *J* = 11.4 Hz, 13 H, H-2,3), 1.00 (q, *J* = 12.8, 4H, H-1)

^{13}C NMR (125 MHz, $CDCl_3$) δ 134.5 (d, $^{4}J_{(c\text{-}p)}$ =3 Hz, CH, C-8), 133.9 (d, $^{3}J_{(c\text{-}p)}$ = 7.2 Hz, CH, C-7), 130.4 (d, $^{2}J_{(c\text{-}p)}$ = 10.6 Hz, CH, C-6), 114.2 (d, $^{1}J_{(c\text{-}p)}$ = 72.7 Hz, Cq, C-5), 28.6 (d, $^{1}J_{(c\text{-}p)}$ = 41.7 Hz, CH, C-4), 26.4 (d, $^{3}J_{(c\text{-}p)}$ = 3.3 Hz, CH_2, C-2), 26.2 (d, $^{2}J_{(c\text{-}p)}$ = 12.6 Hz, CH_2, C-3), 25.5 (s, CH_2, C-1)

^{31}P NMR (243 MHz, DMSO) δ 30.9 ppm

HRMS (ESI+): Calc for $C_{24}H_{38}P^{+}$ [M+]: 357.2708; found: 357.2711

Melting Point: 274.1 - 275.8 2.5 °C/min

IR (ATR, cm-1) v 2971, 2937, 1256, 1028, 363

Tetraphenylphosphonium trifluoromethanesulfonate (65h)

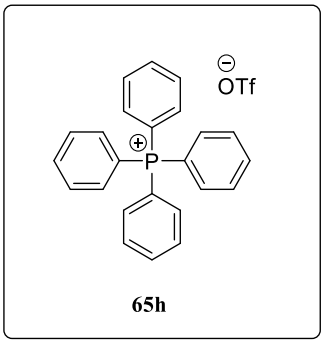

65h

Prepared according to general procedure **I** from triphenyl phosphine **(97b)** (0.2 g, 0.76 mmol, 1 equiv.) and 1-(Trifluoromethyl sulfonyl)-2-(trimethyl silyl) benzene **(100)** (0.56 g, 1.9 mmol, 2.5 equiv.) to afford Tetraphenylphosphonium trifluoromethanesulfonate **(65h)** (0.22 g, 0.45 mmol, Yield: 60%).

^{1}H NMR (600 MHz, $CDCl_3$) δ 7.52-7.60 (m, 8H), 7.67-7.74 (m, 8H), 7.80-7.86 (m, 4H)

^{13}C NMR (150 MHz, $CDCl_3$) δ 135.8 (d, $^{4}J_{(C\text{-}P)}$ = 1.23 Hz, CH), 134.4 (d, $^{3}J_{(C\text{-}P)}$ = 10.4 Hz, CH), 130.8 (d, $^{2}J_{(C\text{-}P)}$ = 13 Hz, CH), 117.5 (d, $^{1}J_{(C\text{-}P)}$ = 89.8 Hz, Cq)

The ^{1}H and ^{13}C NMR data match those reported in the literature**Error! Bookmark not defined.**

5. References:

[85] J. Luo, A. G. Oliver, J. S. McIndoe, A Detailed Kinetic Analysis of Rhodium-Catalyzed Alkyne Hydrogenation. *Dalton Trans.* **2013**, *42*, 11312–11318. https://doi.org/10.1039/C3DT5121 2F.

[86] T. Sugiishi, H. Nakamura, Zinc(II)-Catalyzed Redox Cross-Dehydrogenative Coupling of Propargylic Amines and Terminal Alkynes for Synthesis of N-Tethered 1,6-Enynes. *J. Am. Chem. Soc.* **2012**, *134*, 2504–2507. https://doi.org/10.1021/ja211092q.

[87] L.-J. Xu, S. Lee, X. Lin, L. Ledbetter, M. Worku, H. Lin, C. Zhou, H. Liu, A. Plaviak, B. Ma, Multicomponent Organic Metal Halide Hybrid with White Emissions. *Angew. Chem. Int. Ed.* **2020**, *59*, 14120–14123. https://doi.org/10.1002/anie.202006064.

[88] X. Li, O. J. Curnow, J. Choi, A. C. K. Yip, Recent Advances in the Imidazolium-Based Ionic Liquid-Templated Synthesis of Microporous Zeolites. *Materials Today Chemistry* **2022**, *26*, 101133. https://doi.org/10.1016/j.mtchem.2022.101133.

[89] Z. R. Gao, J. Li, C. Lin, A. Mayoral, J. Sun, M. A. Camblor, HPM-14: A New Germanosilicate Zeolite with Interconnected Extra-Large Pores Plus Odd-Membered and Small Pores. *Angew. Chem. Int. Ed.* **2021**, *60*, 3438–3442. https://doi.org/10.1002/anie. 202011801.

[90] E. A. Truesdale, D. J. Cram, Macro rings. 49. Use of transannular reactions to add bridges to [2.2]paracyclophane, *J. Org. Chem.* **1980**, *45*, 3974-3981 https://doi.org/10.1021/jo01308a005.

[91] D. J. Cram, N. L. Allinger, Macro Rings. XII. Stereochemical Consequences of Steric Compression in the Smallest Paracyclophane1. *J. Am. Chem. Soc.* **1955**, *77*, 6289–6294. https://doi.org/10.1021/ja01628a067.

[92] M. Psiorz, R. Schmid, I. Cyclophane, Ein einfacher Zugang zu funktionalisierten [2.2] Paracyc lophanen. *Chem. Ber.* **1987**, *120*, 1825–1828. https://doi.org/10.1002/cber.19871201109.

[93] L. C. King, The Reaction of Iodine with Some Ketones in the Presence of Pyridine. *J. Am. Chem. Soc.* **1944**, *66*, 894–895. https://doi.org/10.1021/ja01234a015.

[94] N. Dendele, F. Bisaro, A.-C. Gaumont, S. Perrio, C. J. Richards, Synthesis of a [2.2]Paracyclo phane Based Planar Chiral Palladacycle by a Highly Selective Kinetic Resolution/C–H Activation Reaction. *Chem. Commun.* **2012**, *48*, 1991–1993. https://doi.org/10.1039/C2CC16864 B.

[95] D. F. Shantz, J. Schmedt auf der Günne, H. Koller, R. F. Lobo, Multiple-Quantum 1H MAS NMR Studies of Defect Sites in As-Made All-Silica ZSM-12 Zeolite. *J. Am. Chem. Soc.* **2000**, *122*, 6659–6663. https://doi.org/10.1021/ja000374s.

[96] J. Gasnot, C. Botella, S. Comesse, S. Lakhdar, C. Alayrac, A.-C. Gaumont, V. Dalla, C. Taillier, Access to Stable Quaternary Phosphiranium Salts by P-Alkylation and P-Arylation of Phosphiran es. *Synlett* **2020**, *31*, 883–888. https://doi.org/10.1055/s-0040-1708000.

[97] E. Rémond, A. Tessier, F. R. Leroux, J. Bayardon, S. Jugé, Efficient Synthesis of Quaternary and P-Stereogenic Phosphonium Triflates. *Org. Lett.* **2010**, *12*, 1568–1571. https://doi.org/10.1021/ol100304c.

[98] H. Sun, J. Han, C. Gao, High yield production of high molecular weight poly(ethylene glycol)/α-cyclodextrin polyrotaxanes by aqueous one-pot approach, Polymer **2012**, *53*, 2884–2889. https://doi.org/10.1016/j.polymer.2012.04.038

[99] J. Haque, M. A. Jafar Mazumder, M. A. Quraishi, S. A. Ali, N. A Aljeaban, Pyrrolidine-based quaternary ammonium salts containing propargyl and hydrophobic C-12 and C-16 alkyl chains as corrosion inhibitors in aqueous acidic media, *J. Mol. Liq.* **2020**, *320*, 114473. https://doi.org/10.1016/j.molliq.2020.114473

[100] H. Xue, H. Gao, B. Twamley, J. Shreeve, Energetic Nitrate, Perchlorate, Azide and Azolate Salts of Hexamethylenetetramine *Eur. J. Inor. Chem.* **2006**, 2959-2965. https://doi.org/10.1002/ejic.20 0600148

[101] C. -B. Li, L. -S. Huang, R. -S. Wu, D. -Z. Xu, Bridged Alkyl Ionic Liquid-Catalyzed Tandem Reaction for Synthesis of Spiro[4H-pyran-3,3′-oxindoles] in Aqueous Ethanol Solution ChemistrySelect **2019**, *4*, 1635–1639. https://doi.org/10.1002/slct.201803905

[102] T. Poreba, M. Swiatkowski, M. Ernst, P. Macchi, N. Casati, Pressure-Aided Stabilization of Pyramidal Polyiodides *J. Phys. Chem. C.*, **2021**, *125*, 24105-24114 https://doi-org.inc.bib.cnrs.fr/10.1021/acs.jpcc.1c06324

[103] W. Pei, W. Yang, L. Sun. (2009). A process for preparing N-alkylhexamethylenetetramine fluorides (China, CN101519406).

[104] S. Schneider, G. Drake, L. Hall, T. Hawkins, M. Rosander, *Z. Anorg*, Alkene- and Alkyne-substituted Methylimidazolium Bromides: Structural Effects and Physical Properties *Allg. Chem.* **2007**, *633*, 1701-1707 https://doi-org.inc.bib.cnrs.fr/10.1002/zaac.200700234

[105] E. Chardon, G. Dahm, G. Guichard, S. Laponnaz, Derivatization of Preformed Platinum N-Heterocyclic Carbene Complexes with Amino Acid and Peptide Ligands and Cytotoxic Activities toward Human Cancer Cells *Organometallics*, **2012**, *31*, 7618-7621. https://doi-org.inc.bib.cnrs.fr/10.1021/om300806g

[106] R. Firinci, M. Gunay, A. GoKce, Synthesis, characterization and catalytic activity in Suzuki–Miyaura coupling of palladacycle complexes with n-butyl-substituted N-heterocyclic carbene ligands, *Appl. Organomet. Chem.* **2018**, *32*, 4109-4119 https://doi-org.inc.bib.cnrs.fr/10.1002/aoc.4109

[107] R. Iakovenko Hlaváč, Visible light-mediated metal-free double bond deuteration of substituted phenylalkenes, *J. Green Chem.* **2021**, *23*, 440–446. https://doi-org.inc.bib.cnrs.fr/10.1039/D0GC03081C

[108] S. N. P. Ndlovu, H. Ibrahim, M. D. J. Bala, Sterically Hindered N-Heterocyclic Salts Utilized as Antimicrobial Agents *Heterocycl. Chem*, **2017**, *54, 3646–3655.* https://doi-org.inc.bib.cnrs.fr/10.1002/jhet.2992

[109] T. Peppel, P. Thiele, M.-B. Tang, J.-T. Zhao, Köckerling, Low-Melting Imidazolium-Based Salts with the Paramagnetic Reineckate-Analogue Anion [Cr(NCS)4(bipy)]− (bipy = 2,2′-Bipyridine): Syntheses, Properties, and Structures *M. Inorg. Chem.* **2015**, 54, 982–988. https://doi-org.inc.bib.cnrs.fr/10.1021/ic502358b

[110] R. Rajan, D. Schepmann, R. Steigerwald, J. A. Schreiber, E. El-Awaad, J. Jose, G. Seebohm, B. Wünsch, [2.2]Paracyclophane-Based TCN-201 Analogs as GluN2A-Selective NMDA Receptor Antagonists *ChemMedChem* **2021**, *16*, 3201–3209. https://doi.org/10.100 2/cmdc.202100400

[111] Y. Zhang, T. Zhou, K. Zhang, J. Dai, Y. Zhu, X. Zhao, Encapsulation Enhanced Dimerization of a Series of 4-Aryl-N-Methylpyridinium Derivatives in Water: New Building Blocks for Self-Assembly in Aqueous Media *Chem. Asian. J.* **2014**, *9*, 1530-1534 https://doi-org.inc.bib.cnrs.fr/10.1002/asia.201400006

[112] S. W. Kantor, C. R. Hauser, Rearrangements of Benzyltrimethylammonium Ion and Related Quaternary Ammonium Ions by Sodium Amide Involving Migration into the Ring, *J. Am. Chem. Soc.* **1951**, *73*, 4122–4131. https://doi-org.inc.bib.cnrs.fr/10.1021/ja01153a022

[113] Q. Lin, Z. Gao, C. Lin, S. Zhang, J. Chen, Z. Li, X. Liu, W. Fan, J. Li, X. Chen, M. Camblor, F. Chen, A stable aluminosilicate zeolite with intersecting three-dimensional extra-large pores, *Science*, **2021**, *374*, 1605-1608. DOI:10.1126/science.abk3258

[114] H. J. Bestmann, S. Dötzer, Synthese von Tricyclohexylphosphoniumbromiden aus einem luftsta- bilen Phosphinderivat, *Synthesis* **1989**, *3*, 204–205. DOI: 10.1055/s-1989-27198

[115] George Wittig and U. Schoellkop, METHYLENECYCLOHEXANE *Org. Synth.* **1960**, *40*, 66 DOI:10.15227/orgsyn.040.0066

Chapter Three

1. General introduction about the characterization technique used for zeolite structure determination (PXRD)[116]

Powder X-Ray Diffraction (PXRD) is a technique that is used to analyze the crystal structures of solid materials. It uses a beam of X-rays that is directed at a powdered sample of the material. For example, in the case of zeolites, which are mostly crystalline aluminosilicate materials that are widely used for adsorption and catalytic purposes, PXRD can provide important information about their crystalline structure, including their size, shape, and dimension. By analyzing the diffraction pattern created by the X-rays, scientists and researchers can determine the specific crystal structure of the zeolite, its properties and potential uses.

The PXRD process begins by preparing a powdered sample of the zeolite, which is then placed onto a flat sample holder, typically a glass or silicon slide. The sample is then bombarded with a beam of X-rays, which causes the atoms in the sample to scatter the X-rays in different directions. As the X-rays scatter, they interfere with each other, creating a unique pattern of peaks that is collected by a detector.

To perform the analysis, the diffraction pattern produced by the X-rays is compared to known patterns for different crystal structures using a software program. This allows researchers to identify the specific zeolite crystal structure and determine its properties, such as its porosity or catalytic activity.

In general, PXRD is an important tool for the analysis of zeolites and other solid materials, enabling scientists and researchers to gain a better understanding of their properties and potential uses.

2. Attempts to synthesize zeolites using ammonium salts

2.1. Attempts to synthesize zeolites using ammonium salts with terminal and non-terminal alkyne unit(s)

All the PXRD measurements were conducted by my colleague in the LCS laboratory. Ludox HS-40 was used as a silica source, sodium aluminate was used as alumina source (Al), and hydrogen fluoride (40 %) was used as a fluoride source.

- Attempts to synthesize zeolites using SDA's with one alkyne group:

The ammonium salts **66(a, b)** were used as SDA's in fluoride or hydroxide media with different silica-to-alumina ratios (Si:Al) at two temperatures (Table 6). All of the reaction mixtures contain a constant silica-to-SDA ratio of Si:SDA = 10 and a silica-to-water ratio of Si:H_2O = 20. The ammonium salts **66(a, b)** were added separately to two different mixtures containing Si:Al = 20 and OH:Si = 0.185 each. The gel mixtures were heated at 140 ^oC for 10 days (Table 6, Entries 1 and 7). The PXRD analysis of the two reaction mixtures showed the presence of a single peak around 2θ = 5.7 and the absence of any other peaks up to 2θ = 25, indicating the presence of only layered material (2d material). The isolated solutions from the two reaction mixtures were subjected to ^1H NMR analyses. The results showed that some of the ammonium salts lost some of their alkyl groups. To avoid the decomposition of the SDA's used, the reactions using **66(a, b)** were repeated again, this time at 100 ^oC. (Table 4, Entries 2 and 8). The PXRD analysis of the two mixtures again showed layered materials. The synthesis procedures using ammonium salts **66(a,b**) were also repeated with a higher silica to alumina ratio of Si:Al = 40. The reactions were run at two different temperatures: 140 ^oC (Entries 3 and 9) and 100 ^oC (Entries 4 and 10) for 10 days each. The PXRD analysis showed that the high silica amount didn't help in forming zeolites, and only layered materials were obtained. Another approach was followed by replacing hydroxide ions with fluoride ions in the reaction mixtures. The ammonium salts **66(a, b)** were mixed separately in two different media with Si:Al = 40 and F:Si = 0.5, and then the two media were heated at 140 ^oC for 10 days. The use of both ammonium salts **66(a, b)** as SDA's in media with fluoride ions was repeated again at 100 ^oC (Table 6: Entries 6 and 12). The PXRD analysis showed that the

fluoride medium didn't help in forming a zeolite under the used conditions.

SDA	Entry	Si:Al	OH:Si	F:Si	Temperature
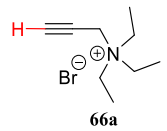 66a	1	20	0.185	-	140
	2	20	0.185	-	100
	3	40	0.185	-	140
	4	40	0.185	-	100
	5	40	-	0.5	140
	6	40	-	0.5	100
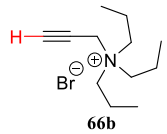 66b	7	20	0.185	-	140
	8	20	0.185	-	100
	9	40	0.185	-	140
	10	40	0.185	-	100
	11	40	-	0.5	140
	12	40	-	0.5	100

Table 6. Attempts to synthesize zeolites using **66a** and **66b**. Ludox HS-40 was used as a silica source, sodium aluminate was used as an alumina source (Al), and hydrogen fluoride (40 %) was used as a fluoride source.

Due to the unstable character of the synthesized ammonium salts with terminal alkyne group, a new set of ammonium salts with non-terminal alkyne groups was synthesized and used in zeolite synthesis **66c-f** (Table 7). In this part, Si:H_2O = 20, F:Si = 0.5, T = 140 ^oC, and time = 21 days were kept constant in all experimental trials. The SDA's **66c**, **66d**, **66e,** and **66f** were mixed separately in different solutions having Si:Al = 40 and Si:SDA = 2 (Table 7: Entries 1, 3, 5, and 7). The ammonium salts **66c**, **66d**, and **66f** were also mixed separately in solutions containing Si:Al= 20 and Si:SDA= 2 (Entries 2, 4, and 8). The ammonium salt **66e** was also mixed in a solution containing a mixture of Si:Al = 40 and Si:SDA = 10 (Table 7, Entry 6). After 21 days, the PXRD analysis showed the formation of MFI zeolite in all trials when using **66d** and **66e** as SDA's. The characteristic peaks of MFI zeolite are shown mainly in the region between 10 (2θ) and 30 (2θ) when compared to the spectra found on zeolite data base (Figure 7). The other experiments using **66c** and **66f** as templates only gave dense phases (2D material). The pores of MFI zeolite are not considered extra-large. However, these SDAs (**66d** and **66e**) demonstrated their ability to favor the formation of MFI zeolite. Thus, further investigation should be done to use this approach in inserting metal atoms in zeolite pores.

SDA	Entry	Si:Al	Si:SDA
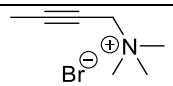 **66c**	**1**	40	2
	2	20	2
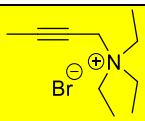 **66d**	**3**	40	2
	4	20	2
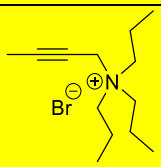 **66e**	**5**	40	2
	6	40	10
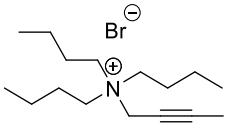 **66f**	**7**	40	2
	8	20	2

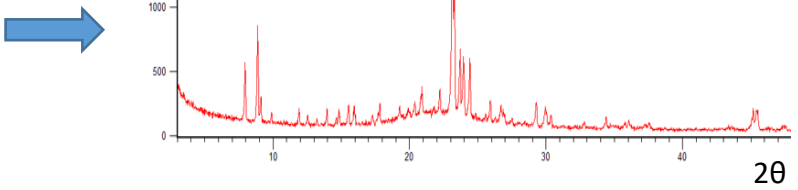

Figure 7: PXRD analysis of an MFI zeolite

Table 7. Attempts so synthesize zeolites using **66(c-f)**. Ludox HS-40 was used as a silica source, sodium aluminate was used as an alumina source (Al), and hydrogen fluoride (40 %) was used as a fluoride source.

- Attempts to synthesize zeolites using SDA's with two alkyne substituents:

The synthesized compound **67d** was used as SDA in two trials: the first trial contained Si:Al = 40, Si:SDA = 2, OH:Si = 0.5, and Si:H_2O = 20. Second trial containing Si:Al = 20, Si:SDA = 2, OH:Si = 0.5 and Si:H_2O = 20. Both mixtures were heated at 140 ^oC for 21 days. The PXRD analysis showed the presence of a broad peak around the region (2θ) = 20, indicating the presence of amorphous material only (Figure 8).

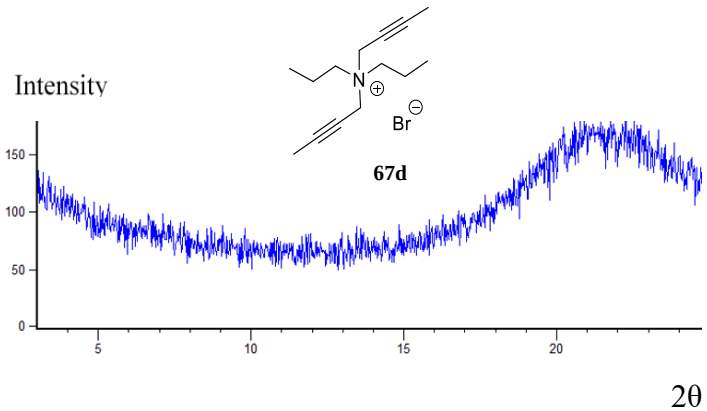

Figure 8. The PXRD analysis showing an amorphous phase when using **67d**.

2.2. Attempts to synthesize zeolite using ammonium salts with hexamethylenetetramine unit.

So far, **68(a**, **c**, and **d)** hexamethylenetetramine-based ammonium salts have been used as SDA's in zeolite synthesis. The media used in all experiments in Table 8 were done at constant ratio of $Si:H_2O$ = 20 and were heated for 10 days. At first, **68a** was used as SDA in two different trials, each containing Si:SDA = 10 and NaOH:Si = 0.185. In entry 1, the Si:Al was 20 and the mixture was heated at 140 ^oC (Table 8). In entry 2, the Si:Al ratio was increased to 40, and the mixture was also heated to 140 ^oC. Secondly, **68a** was used as SDA in two different mediums, each containing Si:SDA = 10 and F:Si = 0.5 (Entries 3 and 4). In entry 3, the Si:Al = 40, and in entry 4 the Si:Al = 7. Both procedures were heated to 140 ^oC. The PXRD analysis of the experiments done using **68a** as SDA showed the presence of amorphous material only.

SDA	Entry	Si:Al	Si:SDA	NaOH:Si	F:Si	LiOH:Si	Temperature (^oC)
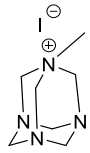	1	20	10	0.185	-	-	140
	2	40	10	0.185	-	-	140
	3	40	10	-	0.5	-	140
68a	4	7	10	-	0.5	-	140
	5	40	5	0.5	-	-	140
	6	40	5	0.5	-	-	160
	7	excess	5	0.5	-	-	140
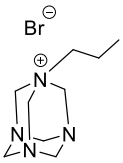	8	excess	5	0.5	-	-	160
	9	40	5	-	0.5	-	140
	10	40	5	-	0.5	-	160
	11	20	10	0.185	-	-	140
68c	12	40	10	0.185	-	-	140
	13	20	5	0.5	-	-	140
	14	40	5	0.5	-	-	140
	15	40	5	-	-	0.5	140
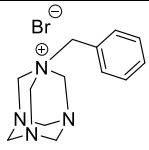	16	20	10	0.185	-	-	140
68d	17	40	10	0.185	-	-	140

Table 8. Attempts to synthesize zeolites using **68(a-d)**. Ludox HS-40 was used as a silica source, sodium aluminate was used as an alumina source (Al), and hydrogen fluoride (40 %) was used as a fluoride source.

The hexamethylenetetramine-based ammonium salt **68c** was used as SDA in 11 different trials (Table 8, Entries 5-15). In the first four trials, entries 5, 6, 7, and 8, the Si:SDA and NaOH:Si ratios were kept the same (Si:SDA = 10 and NaOH:Si = 0.5). In entries 5 and 6, the Si:Al = 40 and the two trials were heated at 140 ^{o}C and 160 ^{o}C, respectively. In entries 7 and 8, we used an excess amount of silica, and the two trials were heated at 140 ^{o}C and 160 ^{o}C, respectively. In entries 9 and 10, the Si:SDA = 5 but this time the reactions were run in fluoride media (F:Si = 0.5) and not in hydroxide media. The two trials were run in a medium containing Si:Al = 40 at 140 ^{o}C and 160 ^{o}C, respectively. In entries 11 and 12, the **68c** was added to a media containing constant Si:SDA and NaOH:Si ratios (Si:SDA = 10 and NaOH:Si = 0.185). The two trials were run using a ratio of Si:Al = 20 and Si:Al = 40, respectively. The conditions in entries 11 and 12 are repeated again using a ratio of 0.5 instead of 0.185 NaOH:Si entries 13 and 14. In entry 15, the **68c** SDA was added to a medium containing Si:Al = 40, Si:SDA = 5, and LiOH:Si = 0.5. We used LiOH instead of NaOH to see if the counteranion would affect the synthesis used. The PXRD analysis of the 11 trials showed the presence of amorphous materials only.

The hexamethylenetetramine-based ammonium salt **68d** was used as SDA in 2 trials (Table 8, Entries 16 and 17). The Si:SDA, NaOH:Si, and temperature were kept the same in both trials (Si:SDA = 10, NaOH:Si = 0.185 and T = 140 ^{o}C). The difference between the two trials is that the ratio of Si:Al in entry 16 was half of the ratio used in entry 17. After 10 days, the PXRD analysis of the two trials using **68d** as SDA showed the presence of amorphous materials only.

2.3. Attempts to synthesize zeolites using ammonium salts with imidazole unit

The ammonium salt **69a** was used as SDA in 4 experimental procedures, each containing a constant ratio of silica to SDA of Si:SDA = 10, fluoride to silica F:Si = 0.5, and silica to water of Si:H_2O = 20. Two of the experiments were run in a medium containing Si:Al = 40 at two different temperatures: 140 ^oC and 100 ^oC. The other two reactions were run in a medium containing Si:Al = 7 at two different temperatures, 140 ^oC and 100 ^oC. The PXRD analysis for the four procedures showed only an amorphous layer. Secondly, the imidazole-based ammonium salt **69b** was used as SDA in 2 experimental procedures, each containing a constant ratio of Silica to SDA of Si:SDA = 10, hydroxide to silica of OH:Si = 0.185, and Si to H_2O of Si:H_2O = 20 at 140 ^oC. In the first procedure, Si:Al = 20, and in the second Si:Al = 40. The PXRD analysis also showed the presence of an amorphous layer. The last ammonium salt in this series, **69d** was used in three different trials, all having a constant ratio of Si:SDA, Fi:Si, and H_2O:Si (Si:SDA = 2, Si:SDA = 0.0335, and H_2O:Si = 10-15). In trial one, the Si: Al = 25, In trial 2 the Si:Al = 50, and in trial 3, the Si:Al = infinity, These trials were run at 190 ^oC for 30 days. The PXRD pattern of **69a-d** shows the absence of any peak in the fingerprint of zeolitic material between 2θ = 3-10°, and the presence of a broad peak between 2θ = 16-25° which confirms that the material is amorphous (Figure 9).

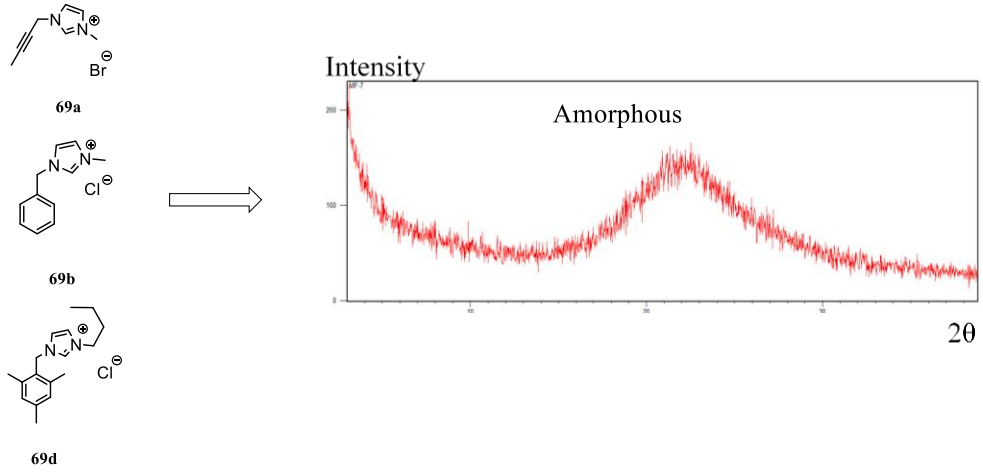

Figure 9. The PXRD analysis showing an amorphous phase when using **69(a**, **b** and **d).**

2.4. Attempts to synthesize zeolite using ammonium salts with aromatic units.

In the series of ammonium salts with aromatic units, only 1-methyl-4-phenylpyridinium salt **(72)** was used in zeolite synthesis. Three separate trials were run using ammonium salt **72** with consistent ratios of Si:SDA, Fi:Si, and H_2O:Si (Si:SDA = 2, Fi:Si = 0.0335, and H_2O:Si = 10-15). In trial 1, the Si:Al ratio was 25. In trial 2, the Si:Al ratio was 50, and in trial 3, the Si:Al ratio was approaching infinity. All trials were run in oven at a temperature of 190 ^oC for a duration of 30 days. Analysis using powder X-ray diffraction (PXRD) revealed the presence of amorphous material only. It should be noted that the ammonium salt **72** had low solubility in water until the iodide (I^-) counter anions was exchanged with hydroxide anions (OH^-).

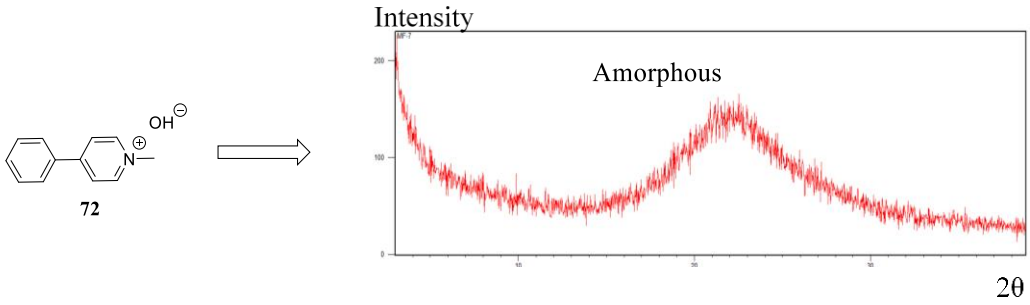

Figure 10. The PXRD analysis showing an amorphous phase when using **72**.

The other prepared ammonium salt series **73(a-c)**, showed low solubility in water even after exchanging chlorine (Cl^-) with hydroxide (OH^-) and only a milky heterogeneous solution was obtained. The low solubility of these SDAs limits their use in zeolite synthesis.

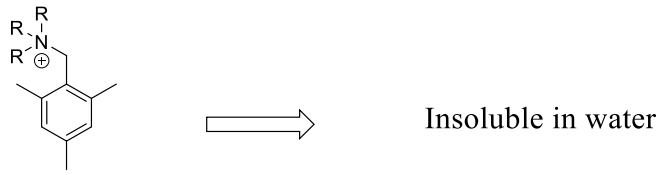

73 (a-c)

Figure 11. The low solubility of **73(a-c)** in water.

3. Attempts to synthesize zeolites using phosphonium salts

3.1. Attempts to resynthesize ZEO-1 zeolite using tricyclohexyl(methyl)phosphonium hydroxide with results

3.1.1. Stability of tricyclohexyl(methyl)phosphonium hydroxide under the used conditions

The counter anion (I^-) of the prepared tricyclohexyl(methyl)phosphonium Iodide was exchanged with hydroxide (OH^-) using Dowex Monosphere 550 A UPW OH in distilled water to afford SDA **65a**. The exchange goes well, and the product is stable as long as the amount of water is not totally removed. Otherwise, if distilled water is removed, the product decomposes to give tricyclohexyl phosphine oxide **(102)** and the ylide **103**.

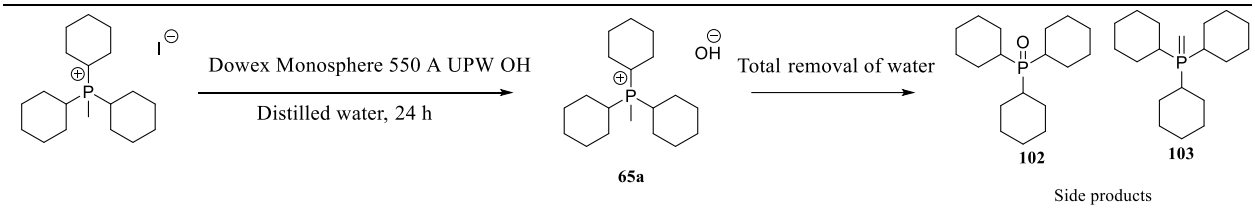

Scheme 37. The total decomposition of the ion exchanged SDA **65a** to **102** and **103** after the total removal of water

Moreover, to confirm that the prepared SDA methyl tricyclohexyl phosphonium hydroxide **(65a)** directed the crystallization of ZEO-1 zeolite and no side product was generated insitu, to play the role of SDA, a stability test was done. The synthesized SDA **65a** was checked by **^{31}P NMR** before its use in zeolite synthesis, as shown by the blue Spectra (Figure 12). The spectra shows only one peak at 33.8 ppm ($\delta P = 33.8$ ppm), which refers to the prepared SDA **65a**. Then, the prepared SDA was used in zeolite synthesis at T = 190 ºC. After 7 days, a sample of the solution mixture containing SDA **65a** was taken, and **^{31}P NMR** was measured. The results confirm the stability of SDA after 7 days, as shown by the red spectra in figure 12; there is a characteristic peak at 32.8 ppm referring to SDA **65a**. However, in addition to this characteristic peak, two extra peaks appeared between 60 and 65 ppm with ratios of 0.3 and 0.07 compared with the original peak at 32.8 ppm of SDA **65a**. These two peaks indicate the presence of other phosphorus containing products, which could result from the decomposition of SDA **65a** to the corresponding ylide **103**

and/or decomposition to other phosphorus-containing compounds. Moreover, there is a possibility that the phosphorus impurities could also be found in the water used for synthesis. Furthermore, the stability test was repeated after 14 days as shown by green spectra. The results also confirmed the SDAs stability. Additionally, the peaks found in the region between 60 and 65 ppm were also found in this sample with the same ratios found in the first sample with no changes. The tricyclohexyl phosphine oxide spectra, which appears in purple at 51.0 ppm (δP = 51.0 ppm), is only used for comparing. The absence of this peak at 51.0 ppm in all other spectra (Green, Red and Blue) is an indication of the stability of the SDA.

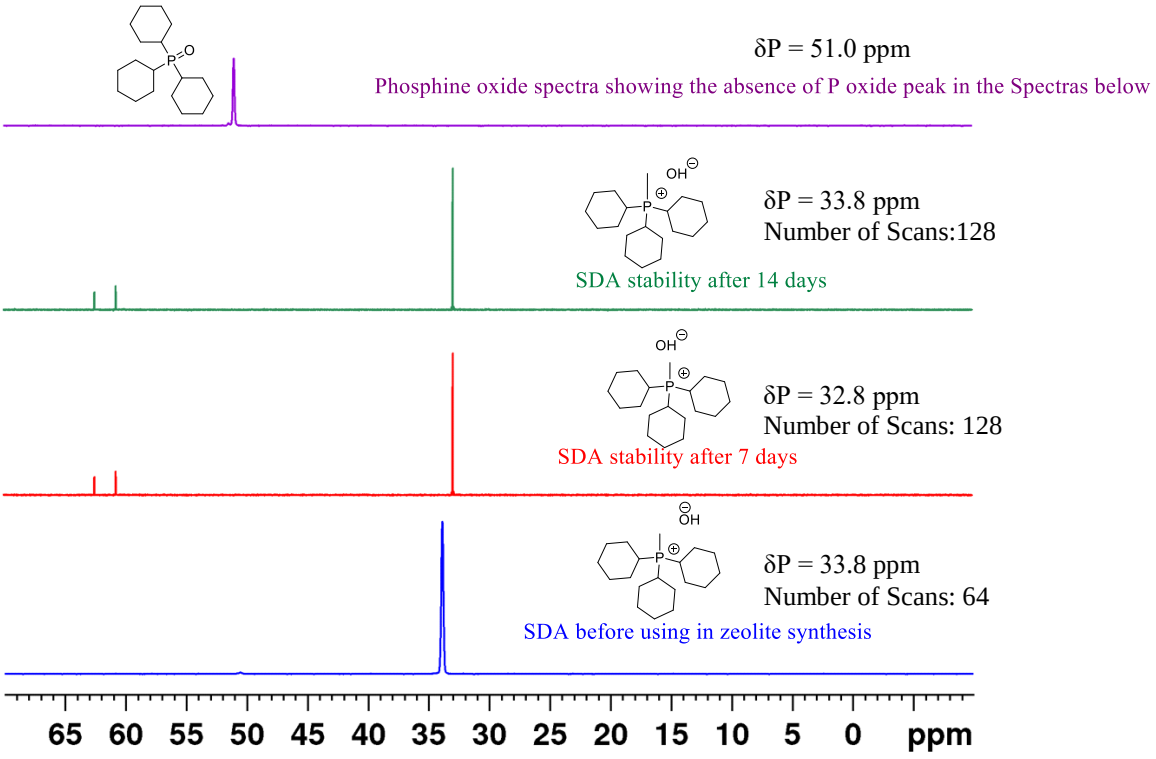

Figure 12. The **^{31}PNMR** analysis showing the stability of SDA **79a** at different days during zeolite synthesis.

3.1.2. Conditions used for the synthesis of ZEO-1 with the time needed

ZEO-1 zeolite was obtained when using Si:SDA = 0.5, Si:F = 0.5, Si:Al = 0.04, and H_2O:Si = 5 within 15 days at 190 ºC, using Al(i-PrO)$_3$ as alumina source and Si(OEt)$_4$ as silica source.[113] In our case the ZEO-1 zeolite couldn't be obtained when repeating the same conditions. Thus, different variables and chemical sources where used to resynthesize ZEO-1 as shown in the following tables.

In the first two tables 9 and 10, aluminium isopropoxide and Ludox HS-40 were used as an aluminium and silica source, respectively. In table 9, the ratios Si:Al = 25 and H_2O:Si = 7 were held constant. The ratio of Si:SDA and Si:F were used as variables. When using a ratio of Si:F = 20, the ZEO-1 zeolite was obtained within 16 days regardless the ratio of Si:SDA used (Si:SDA = 2, 3, 4) (Figure 13A). The PXRD simulated pattern in figure 13B is used as reference to compare the Zeo-1 finger print with the PXRD obtained in figure 13A in our group. The characteristic peaks according to figure 13 are shown in the area below 10 (2θ), specifically at 4 (2θ) and 7 (2θ). Increasing the ratio of Si:F to 30 or decreasing it to 10 didn't improve the synthesis time. Moreover, the use of Si:SDA = 3 and Si:F = 30 only gave amorphous phase.

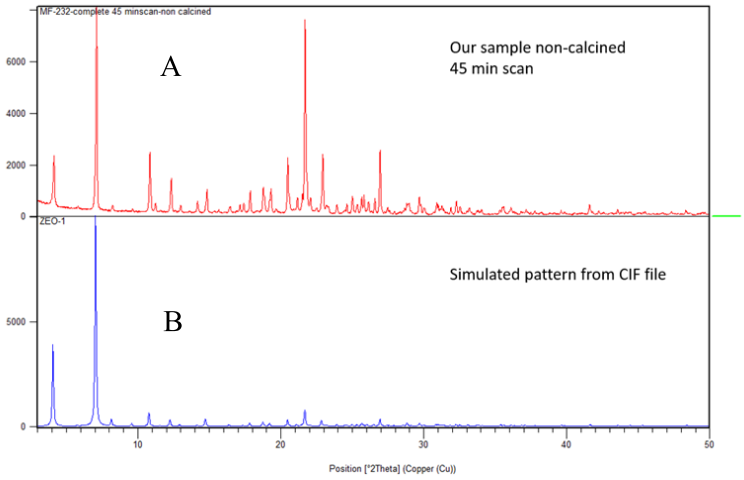

Figure 13. The PXRD analysis of ZEO-1 zeolite. **A.** The PXRD analysis of ZEO-1 obtained in our group. **B.** The PXRD analysis of ZEO-1 in the published paper.

Constant: Si:Al = 25 / H_2O:Si = 7 / 190 °C				
		Ratio of Si:SDA		
		2	3	4
Ratio of Si:F	10	n.a.	29 days	n.a.
	20	16 days	16 days	16 days
	30	50 days	Amorphous	n.a.

Table 9: The duration in days needed to synthesize ZEO-1 using aluminium isopropoxide as an aluminium source and Ludox HS-40 as a silica source when having constant ratios of Si:Al and H_2O:Si. n.a. = not available and * Modernite impurity.

In table 10, the Si:F = 20 and Si:SDA = 3 ratios were kept constant, and the Si:Al and H_2O:Si were changed. The ZEO-1 was obtained within 16 days at the shortest time upon using Si:Al = 25 and H_2O:Si = 7.

Constant: Si:F = 20 / Si:SDA = 3 / 190 °C				
		Ratio of Si:Al		
		15	20	25
Ratio of H_2O:Si	7	31 days*	23 days	16 days
	15	n. a.	n. a.	31 days

Table 10: The duration in days needed to synthesize ZEO-1 using aluminium isopropoxide as an aluminium source and Ludox HS-40 as a silica source when having constant ratios of Si:F and Si:SDA. n.a. = not available and * Modernite impurity.

In the following two tables 11 and 12, sodium aluminate was used as aluminium source and ludox HS-40 as a silica source. In table 11, The best duration for ZEO-1 formation (8 days) was obtained upon using Si:F = 20, regardless the amount of Si:Al used (15, 20, or 25).

Si:SDA = 3 / H_2O:Si = 7 / 190 °C				
		Ratio of Si:Al		
		15	20	25
Ratio of Si:F	0	n.a.	n.a.	12 days*
	20	8 days*	8 days*	8 days*

Table 11: The duration in days needed to synthesize ZEO-1 using sodium aluminate as an aluminium source and Ludox HS-40 as a silica source when having constant ratios of Si:SDA and H_2O:Si. n.a. = not available and * Modernite impurity.

Moreover, in table 12, the Si:Al, Si:SDA and Si:F were kept constant. However, H_2O:Si and temperature were changed. The ZEO-1 was obtained within 8 days upon using H_2O:Si = 7 at 190 °C

Si:Al = 25 / Si:SDA = 3 / Si:F = 20				
		Temperature °C		
		150	170	190
Ratio of H_2O/Si	7	38*	21*	8*
	15	n.a.	n.a.	21

Table 12: The duration in days needed to synthesize ZEO-1 using sodium aluminate as an aluminium source and Ludox HS-40 as a silica source when having constant ratios of Si:Al, Si:SDA and Si:F. n.a. = not available and * Modernite impurity.

3.2. Attempts to synthesize zeolites using mono and bis phosphonium salts

Phosphonium salts **65c**, **65d**, and **74d** were utilized in the synthesis of zeolites, as indicated in table 13. These structure-directing agents (SDAs) were individually employed in solutions with Si:Al = 25, Si:SDA = 4, Si:F = 2, and H_2O:Si = 15. Subsequently, the three samples were subjected to a 40-day heating period at 190°C in an oven. The X-ray powder diffraction (PXRD) analysis revealed the presence of only an amorphous phase.

SDAs	Si/Al	Si/SDA	Si/F	H_2O/Si	Temperature
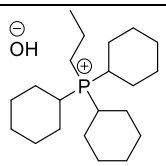 **65c**	25	4	2	15	190 °C
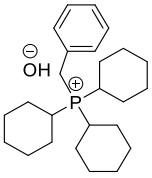 **65d**	25	4	2	15	190 °C
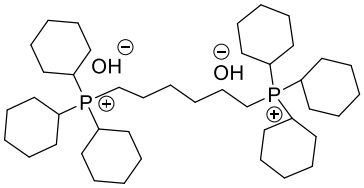 **74d**	25	4	2	15	190 °C

Table 13. Attempts to synthesize zeolites using SDAs **65c, 65d** and **74d**. Ludox HS-40 was used as a silica source, sodium aluminate was used as an alumina source (Al), and hydrogen fluoride (40 %) was used as a fluoride source.

4. Conclusion

In conclusion, the use of ammonium salts with terminal alkynes (**66a** and **66b**) in media containing Si:Al = 20 and 40 in hydroxide medium (OH:Si = 0.185) or fluoride medium (F:Si = 0.5) gave only a dense phase, indicating their low stability under the harsh conditions used (high temperature and pH). Two of the prepared ammonium salts with non-terminal alkyne unit (**66d** and **66e**) demonstrated the ability to direct the synthesis of MFI zeolite at 140 ^{o}C within 21 days. The SDA **66d** favored MFI formation when used in media containing Si:Al = 20 and 40 and Si:SDA = 2. Also, SDA **66e** favored MFI formation when used in media containing Si:Al = 40 and Si:SDA = 2 and 10. Other ammonium salts (**73a-c**) that were tested displayed low solubility in water, especially those that were based on aromatic compounds, even after the substitution of the halogen anion with the hydroxide anion. Furthermore, the resynthesis of ZEO-1 zeolite was challenging, and using the same experimental procedure did not favor the crystallization of ZEO-1. Thus, a new investigation was done to find other suitable conditions. The results showed that the synthesis of ZEO-1 was mostly favored when using aluminium isopropoxide and Ludox-40 as aluminium and silica sources, respectively. More precisely, upon using ratios of Si:Al = 25, H_2O:Si = 7, Si:F = 20, and Si:SDA = 2, 3, and 4. Also, when using Si:F = 20, Si:SDA = 3, Si:Al = 25 and H_2O:Si = 7. These conditions favored ZEO-1 crystallization within 16 days at 190 ^{o}C. Other ammonium and phosphonium salts were found to have an amorphous phase, which requires further adjusting of the synthesis conditions to achieve a zeolitic product.

5. References

[116] R. E. Morris, P. S. Wheatley, in *Studies in Surface Science and Catalysis* (Eds.: J. Čejka, H. van Bekkum, A. Corma, F. Schüth), Elsevier, **2007**, pp. 375–401. https://doi.org/10.1016/S0167-2991(07)80799-3

Chapter Four

Chapter 4: Synthesis of indoles and aryl phosphine oxides starting from N-aryl ynamides.

1. Indole Synthesis

1.1. General Introduction

Nitrogen-containing heterocyclic compounds such as indoles are widely present in nature. Indoles play an essential role as bioactive substances in treating a wide range of diseases. For example, indoles are used in the development of anti-tumor agents.[117] Moreover, indoles are also present in many commercial products like agrochemicals, dyes, cosmetics, essential oils, and fragrances.[118] Indole synthesis has been studied for over a century resulting in numerous classical methods for their formation named after their discoverers, such as Fischer,[119] Bischler,[120] Reissert,[121] Madelung,[122] Sundberg,[123] Hemetsberger,[124] Gassman,[125] Leimgruber-Batcho,[126] Julia,[127] Bartoli,[128] Larock,[129] and Fukuyama.[129]

1.2. Use of ynamides in the preparation of indoles

Ynamides, a class of organic compounds having an N-triple bond, are considered versatile reagents for many reactions. The use of ynamides in the formation of indoles is a relatively new approach compared to other traditional approaches. This approach has many advantages over other methods, since it allows the modification of both the substituents present on the aromatic ring and the ynamide. Therefore, allowing access to a wide set of indole derivatives. Additionally, such reactions don't require harsh conditions, making it suitable to the synthesis of sensitive compounds. The synthesis of indoles starting from ynamides can proceed through 5 different retrosynthetic paths: **a**, **ad**, **edc**, **d**, and **ac** (Scheme 40). In most of these reactions, the transformation occurs in the presence of gold catalysis through the formation of carbenes. Path **ad**: Skrydstrup (2009, reaction 6),[130] Liu (2019, reaction 7),[131] Ballesteros (2019, reaction 8),[132] Hashmi (2020, reaction 9),[133] Cai (2023, reaction 11).[134] Following path **ac**: Long-Wu (2015, reaction 3),[135] and Hasmhi (2019, reaction 4),[136] Ye (2022, reaction 14). Following path **a**, Cai (2018, reaction 13)[137]

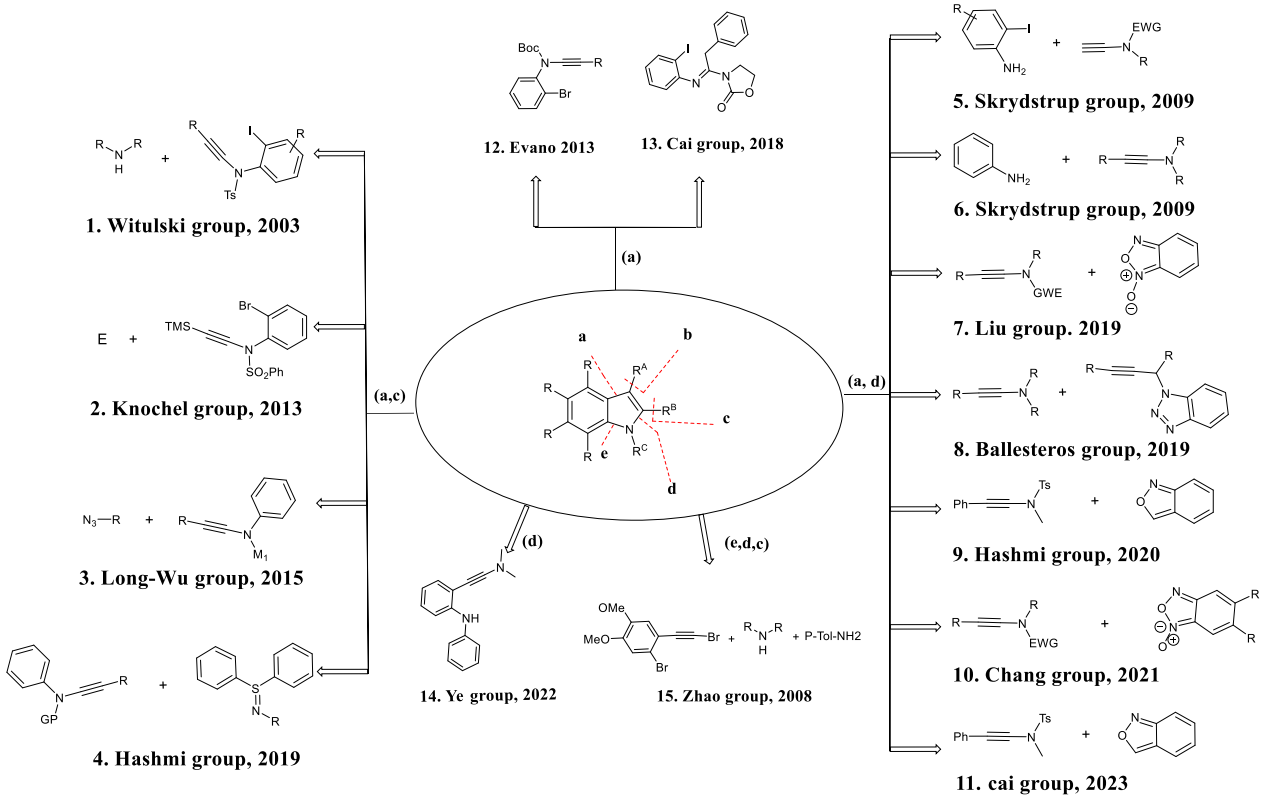

Scheme 38. Previously reported approaches for the synthesis of indoles starting from ynamides

Other than the use of gold catalysis, two different methods were reported following path **ad**. The first example was in 2009 by Skrydstrup's group (Scheme 39),[137] in which a palladium-catalyzed one-pot procedure is reported starting from an ynamide and an o-iodoanilines. The interesting feature of this method is that after the Sonogashira reaction, the intramolecular cyclization to form the indole occurs spontaneously without activation of the alkyne (Reaction 5).

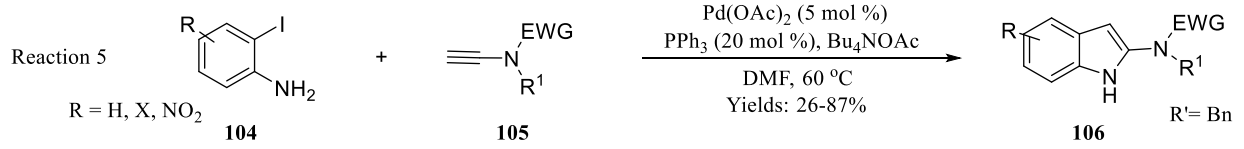

Scheme 39. Skrydstrups's approach for the preparation of the indole **106.**

The second example was reported by Chang's group in 2021 (reaction 10), a novel metal-free [3+2] annulation of ynamides with anthranils (Scheme 40). [138] The procedure provides a facile,

environmentally friendly, and atom-economical route to 2-aminoindoles. This synthetic process proceeds with excellent regio selectivity and has a wide functional group tolerance under mild reaction conditions.

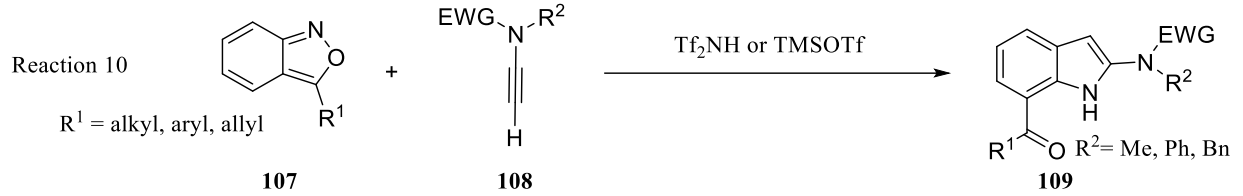

Scheme 40. Chang's approach for the preparation of the indole **109**

Following path **a**, a method for indole synthesis was reported by Evano's group in 2013 (Scheme 40), it is based on an intramolecular 5-endo-dig carbocupration to afford indoles in moderate to good yields (Reaction 12). [139]

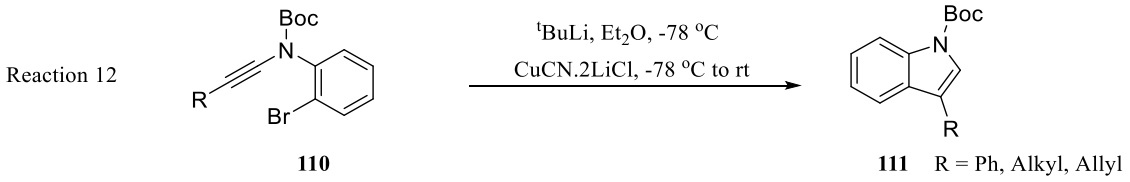

Scheme 41. Evano's approach for the preparation of indole **111**

Following path **d**, in 2022, the Ye group reported a method that allows access to axially chiral *N*-heterocycles, which is achieved by chiral Brønsted acid-catalyzed 5-endo-dig cyclization of ynamides (reaction 14). This approach represents the first metal-free protocol for the construction of axially chiral compounds starting from ynamides (Scheme 42). [140] This method allows the practical and atom-economical synthesis of valuable *N*-arylindoles in excellent yields with generally excellent enantio selectivities. Moreover, organocatalysts and ligands based on such axially chiral *N*-aryl indole skeletons are demonstrated to be usable in asymmetric catalysis.

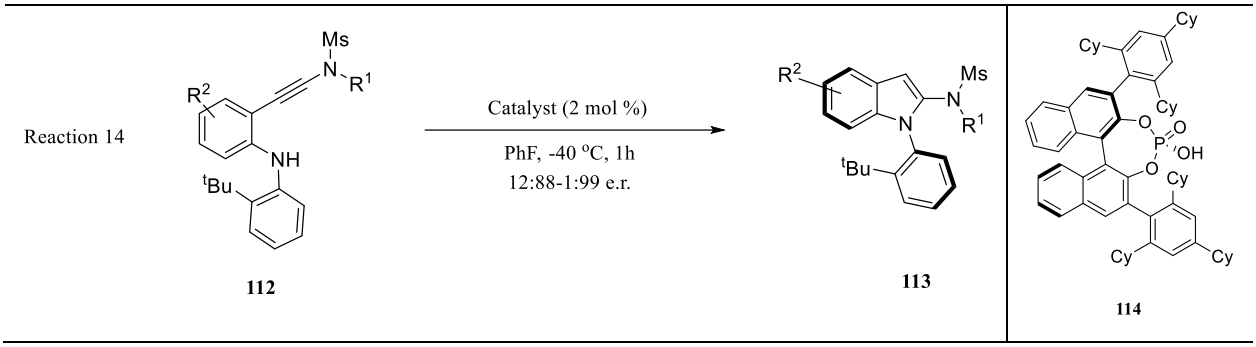

Scheme 42. Ye's approach for the preparation of indole **113**

Following path **edc** by Zhao group (2008),[141] a metal-catalyzed C-N bond formation with *ortho*-haloaryl acetylinic bromide was followed by 5-endo-dig cyclization to form the targeted indole(s) (Reaction 15) (Scheme 43).

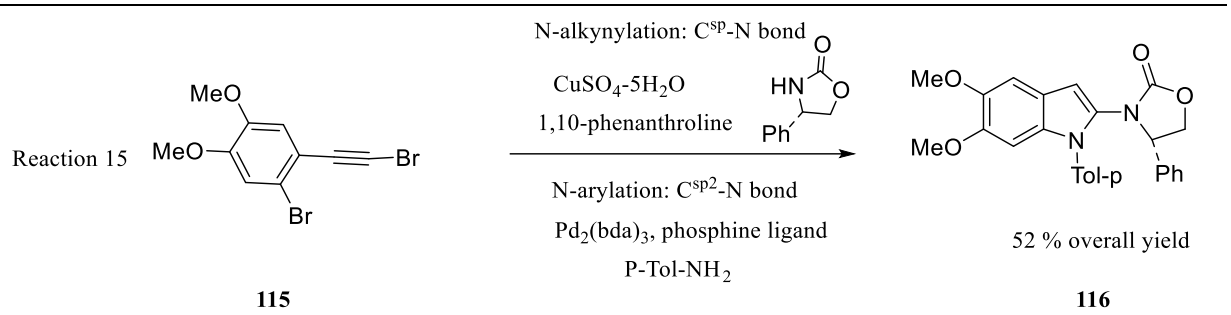

Scheme 43. Zhao's approach for the preparation of the indole **116.**

The first report on the preparation of indole starting from ynamide was discovered by the Witulski group in 2003 following path **ac** (Reaction 1),[142] a straight-forward approach for the preparation of 2-aminoindoles based on palladium-catalyzed heteroanulation reaction (Scheme 44).

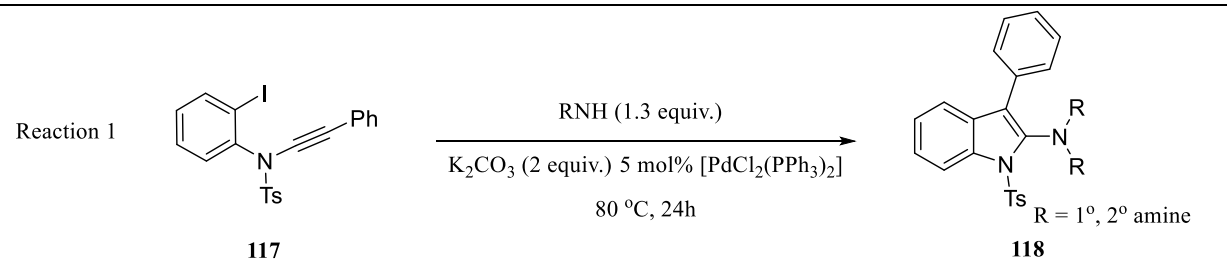

Scheme 44. Witulski's approach for the preparation of the indole **118**.

Using the same path **a,c**, another example was reported by Knochel group (2013).[143] They reported the preparation of indoles using an ynamide similar to the one used by Wituslki's group but contains bromide substituent instead of iodine and using electrophile instead of a nucleophile (Reaction 2) (Scheme 45). The reaction proceeded in a one-pot endo-dig approach, in which copper metal is used to form an intramolecular catalytic carbo-cupration reaction, and the obtained intermediate was later quenched with various electrophiles to afford the targeted indoles.

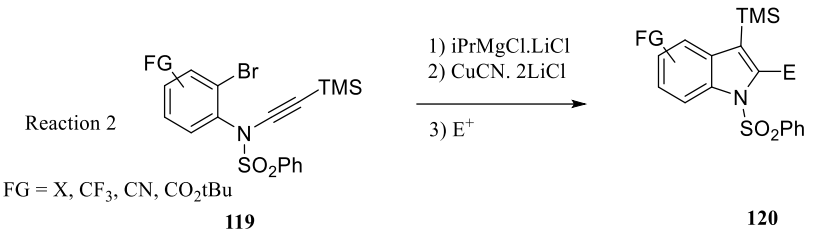

Scheme 45. Knochel's approach for the preparation of indole **120**.

The formation of indoles, following Witulski's approach, is more clarified by the mechanism shown in Scheme 46A. The key step in this mechanism is the formation of σ,π-chelated palladium bond, followed by the addition of a secondary amine as a nucleophile on the α-position (Scheme 46A, Step 2). In step 3, the base used will extract the acidic proton, and the final step involves reductive elimination to afford the targeted indole (Scheme 46A, Step 4). On the other hand, following the Knochel approach (Scheme 46B), a Grignard-like ynamide is formed in step 1'. This is followed by 5-endo-dig copper-mediated intramolecular carbometelation of the Grignard derivative to afford a cuprated heterocyclic intermediate in step 2'. The final step involves quenching the obtained intermediates with different electrophiles (E) (Scheme 46 B, step 3') .

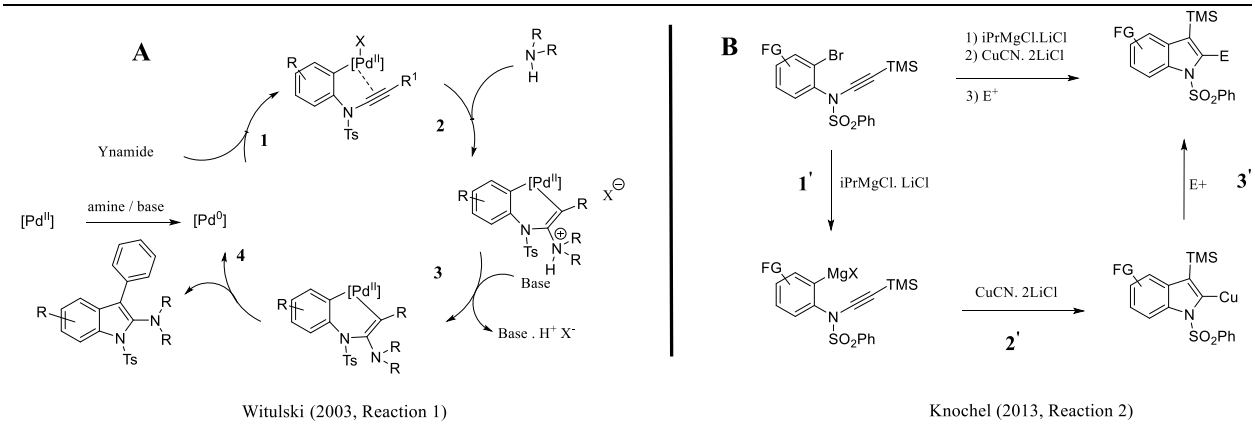

Scheme 46. Difference between witulski's and knochel's approach for the preparation of indoles.

2. Palladium-Catalyzed C-P cross coupling

The synthesis of organophosphorus compounds, such as triaryl phosphine oxides, is an essential area of chemical research. These compounds are widely present in bioactive pharmaceutical products,[144] coordination complexes,[145] organic synthesis,[146] and functional materials.[147] The synthetic community has shown great interest in the preparation of triaryl phosphines or triaryl phosphine oxides due to their significance for instance as ligands. Various methods involving palladium-catalyzed coupling of secondary phosphine (or oxides) with different SP2 aryl partners have been developed in recent decades. An approach for cross-coupling H-phosphinate esters **121** with chloroarenes or chloroheteroarenes was reported by Montchamp's group in 2011 (Scheme 47). The reaction proceeded in the presence of palladium catalyst (2 mol%) and *i*-Pr_2NEt base (DIPEA, 1.3 equiv.) in toluene/Ethylene glycol (EG) (9:1) at 110 ^oC to afford a set of phosphinate **122** in good yields (50-86 %).[148]

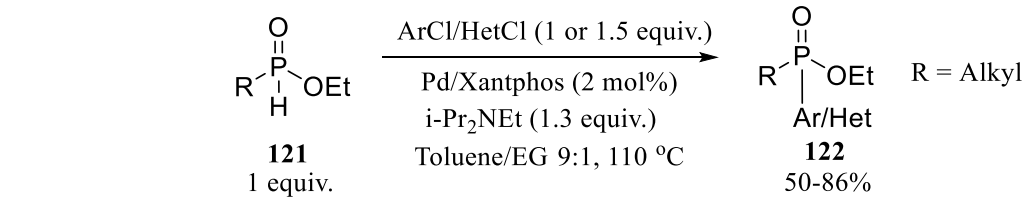

Scheme 47. Montchamp's approach for the preparation of phoshinate **122**

One year later, in 2012, Herzon group reported the use of phosphine oxide **123** and aryl iodide **124** for the preparation of product **125** in the presence of 1 mol% of a catalyst formed *in situ* from tris(dibenzylideneacetone)dipalladium and Xantphos (Scheme 48). The reaction proceeded within 2 h in the presence of triethylamine (TEA) in 1,4-dioxane at 24 ^oC to afford a wide set of aryl phosphine oxides **125** with high yields (64-97%). [149]

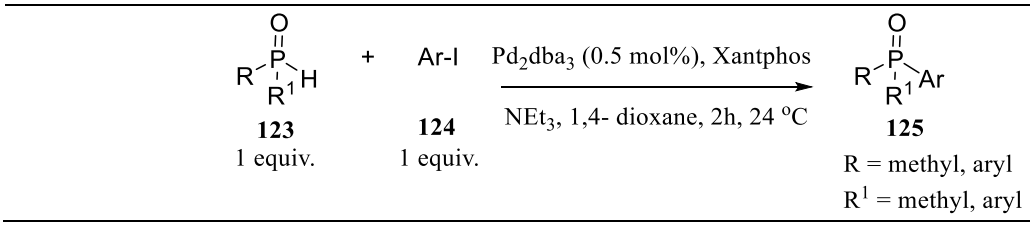

Scheme 48. Herzon's approach for the preparation of **125**

Four years later, in 2016, Cai's group reported an enantioselective C–P cross-coupling reaction of diarylphosphine oxides **126** with ortho-substituted aryl iodides **127** . The reaction proceeded at 70 ^{o}C within 20h via kinetic resolution strategy in the presence of 5 mol% $Pd(CF_3CO_2)_2$, ligand **129** and NMM base (3 equiv.) in acetonitrile. The resulting chiral triarylphosphine oxides were obtained in high yields up to 96 % and with moderate to high enantioselectivity.[150]

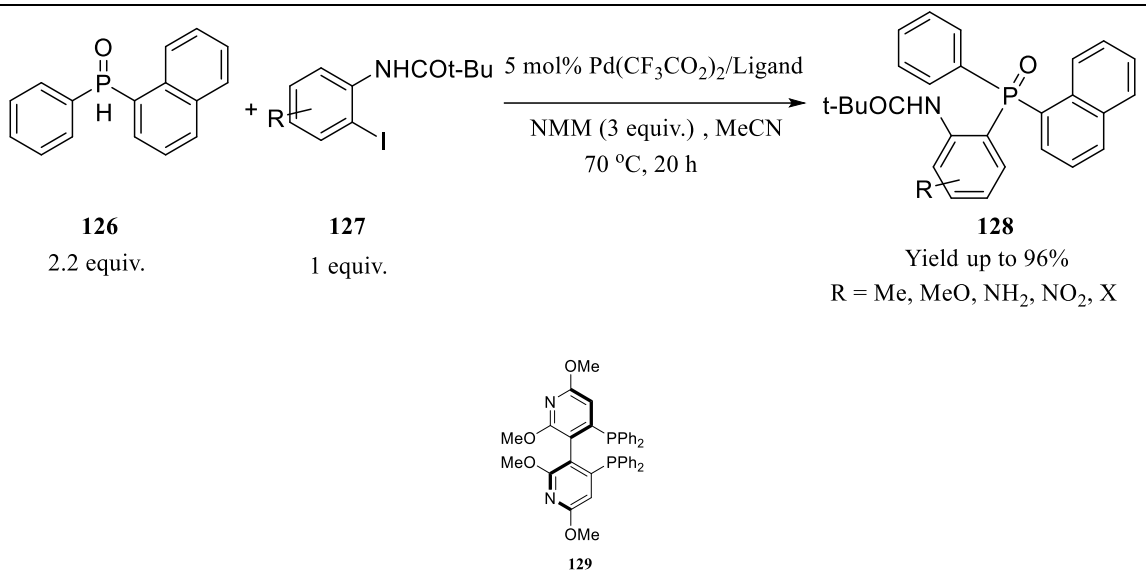

Scheme 49. Cai's approach for the preparation of phosphine oxide **128**

Three years later, in 2019, Zhou's group reported an oxidative C /P decarbonylative cross-coupling between P(O)H compounds **131** and aroylhydrazides **130** via $Pd(OAc)_2$ (10-30%) in the presence of $Na_2S_2O_8$ (2 equiv.) and $PhSO_2OH$ (2 equiv.) (Scheme 50). The reaction medium, which involves the use of Brønsted acid and bidentate phosphine ligand, enables the activation of the unreactive CC bond while preventing the undesired oxidation and coordination of P(O)H compounds, leading to a general oxidative synthesis of aryl phosphorus compounds from available substrates.[151]

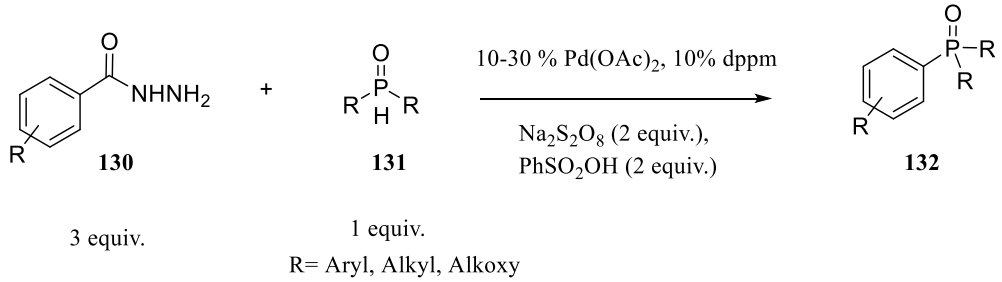

Scheme 50. Zhou's approach for the preparation of phosphine oxide **132**

The last reported example, to the best of our knowledge, was described in 2023 by Yu-Chang's research group.[152] In the presence of a Pd(II) catalyst and Cs_2CO_3 (2 equiv.), a Hirao cross-coupling reaction occurred between phenyl bromide **133** and di-p-tolylphosphine oxide **134** within one hour at 90°C in ethanol (Scheme 51). The used catalyst **136**, demonstrated successful conversion of aryl bromides containing both electron-donating and electron-withdrawing groups. Additionally, nucleophile-sensitive compounds such as 2-bromopyridine, 2-bromothiophene, and 4-bromobenzonitrile were tolerated when the reaction was performed in a toluene/ethylene glycol (EG) solvent mixture at a ratio of 9:1.

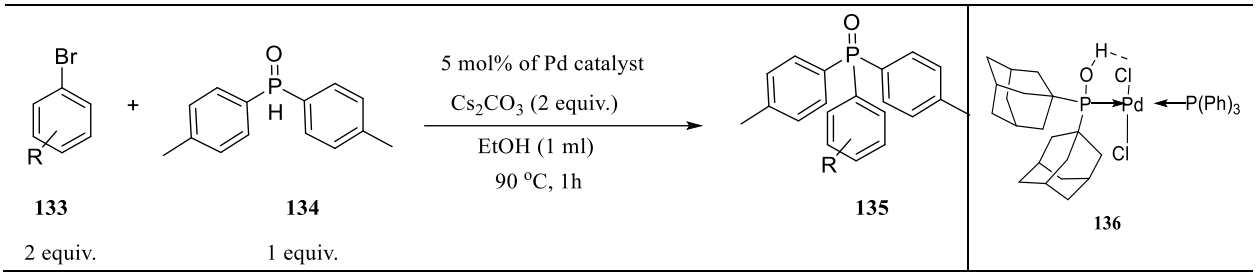

Scheme 51. Yu-Chang's approach for the preparation of phosphine oxides **135**

3. Synthesis of Indoles and aryl phosphine oxides starting from N-aryl ynamides (results and discussion)

3.1 Project description

The aim of this project is to extend the work presented by the Witulski group in 2003 (Reaction 1 scheme 44) by using phosphorus compounds as nucleophiles instead of amines. Specifically, the reaction involves the use of H-diethylphosphonate along with N-aryl ynamide as starting materials, tetrakis (triphenylphosphine) palladium ($Pd(PPh_3)_4$) as a catalyst, and potassium carbonate (K_2CO_3) as the base in THF. The reaction proceeds to afford the targeted indole with an excellent yield. Furthermore, this research highlighted the significance of substituents on ynamides, where by changing the substituents can influence the reactions outcome and promote the formation of distinct products through cross-coupling of *N*-tosylated ynamides with H-phosphonates instead of indole formation.

3.2 Results and Discussion: Palladium-catalyzed synthesis of indoles using N-aryl ynamide, H-phosphonate, and a base

3.2.1 Starting Materials: Synthesis of N-aryl ynamide

- Preperation of Iodonium salts **139** and **140**

Iodonium salts **139** and **140** were synthesized and used in ynamide synthesis having two different substituents on the beta position. These alkynyl- iodonium salts which act as electrophilic acetylenes were first reported in 1995 by P. Stang. [153] A gram-scale preparation of iodosylbenzene **(138)** was obtained with a quantitative yield of 87% by mixing diacetoxyiodobenzene **(137)** with water under basic conditions. The resulting iodosylbenzene **(138)** was then reacted with either Ph-TMS (1 equiv.) or TMSCCTMS (1 equiv.) in the presence of TMSOTF, resulting in the formation of iodonium salts **139** and **140** with 74% and 89% yields, respectively.

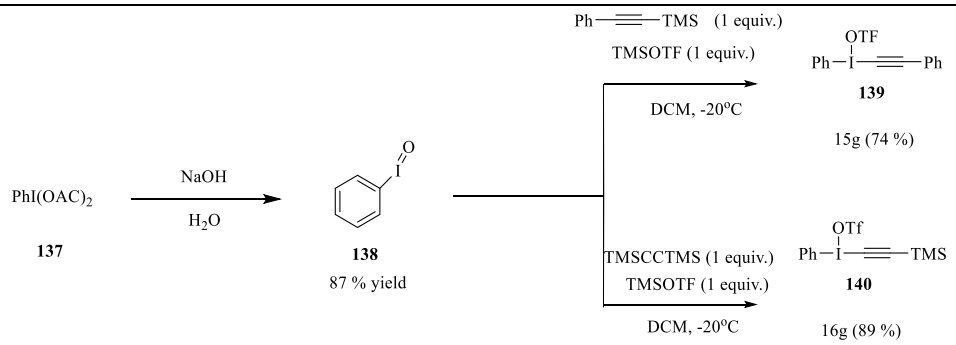

Scheme 52. Synthesis of iodonium salts **139** and **140**

- Synthesis of N-aryl ynamide [154]

Two different methods were used for the synthesis of ynamides **142(a-c)**. In the first method, cesium carbonate (Cs_2CO_3) was used in a mixture of *N*,*N*-dimethylformamide (DMF) and dichloromethane (DCM) (Scheme 42, A). The reaction between an iodonium salt with a phenyl group **139** and a *N*-tosylated iodo aniline **141** resulted in the formation of ynamide **142a** with a 46% yield. However, when iodonium salt with a trimethylsilyl (TMS) group **140** was used, the reaction produced a terminal alkyne side product **142b** due to the loss of the TMS group under these reaction conditions. The products were purified using column chromatography (SiO_2, n-pentane/Ethyl acetate 9:1 (v/v) to 8:2 (v/v)). Further purification of the samples was achieved by

trituration with a 9:1 mixture of pentane and ethyl acetate (v/v), resulting in the precipitation of the product as a white solid.

In the second method, potassium bis(trimethylsilyl)amide (KHMDS) was used as the base in toluene. The reaction between iodonium salts **139** or **140** and tosylated iodoaniline **141** proceeded within 24 hours at room temperature. The purification of the products was carried out using column chromatography (silica gel, 9:1 to 8:2 (v/v) n-pentane-ethyl acetate). The reactions resulted in the formation of **142a** and **142c** with 70% and 73% yields, respectively (Scheme 53, A). The synthesis of N-aryl ynamides starting from *N*-tosylated iodoaniline, proceeds via the formation of a carbene intermediate. In the presence of a base, the deprotonated tosylated aniline will attack the iodonium salt from the same side of the R group, eliminating the phenyl iodine and forming the carbene intermediate. Lastly, the migration of the R group leads to the formation of the targeted ynamide (Scheme 53 b).

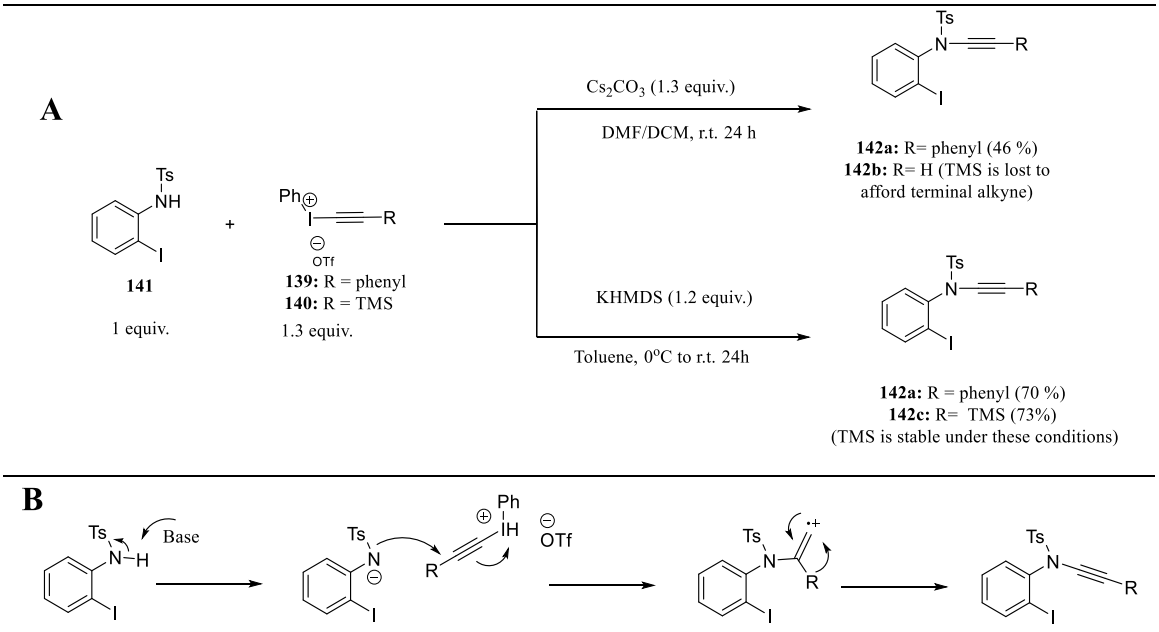

Scheme 53. A Synthesis of N-aryl ynamides using two different approaches. **B**. Reaction mechanism

3.2.2. Optimizing reaction conditions of indole synthesis

The reaction between Ynamide **142a** and diethyl phosphite was studied using different catalysts, solvents, and bases (Scheme 54). The results of the optimization studied involving different conditions are summarized in the table (Table 14).

In entries 1-3, ynamide **142a** (1 equiv.), diethyl phosphite (5 equiv.), $Pd(PPh_3)_4$ (10 mol%), and K_2CO_3 (2 equiv.) were added to three different solvents (DMF, THF, and Acetonitrile). The reaction proceeded to afford the highest yield (95%) upon using THF as a solvent (Entry 2). However, the reaction was less favored in acetonitrile and DMF, as the yields were 50% (Entry 3) and 35% (Entry 1), respectively. As the reaction was mostly favored when using the conditions of entry 2, a similar reaction was followed in entry 4 but using $Pd(Cl)_2(PPh_3)_2$ (10 mol%) instead of $Pd(PPh_3)_4$ (10 mol%). The reaction did not proceed well, and indole **143** was obtained with a 46% yield only, accompanied by the presence of impurities.

In entry 5, the conditions of entry 2 were applied in the absence of phosphorous compounds. The reaction proceeded to afford the indole product with a 13% yield. The use of triphenyl phosphine instead of diethyl phosphite in the presence of $Pd(PPh_3)_4$ (10 mol%) and K_2CO_3 (2 equiv.) in THF afforded the indole with 27% yield. The presence of a base is critical in this type of chemistry, in which the reaction does not proceed in the absence of a base and only the starting material is retrieved (Entry 7). Moreover, the reaction did not proceed when using triethyl phosphine (Entry 9), $NiBr_2$dppe (Entry 10), $Pd(OAC)_2$ (Entry 11), and diphenyl phosphine oxide (Entry 12). As a result, only the starting material was retrieved in all of the previous cases. Moreover, using DIPEA instead of potassium carbonate did not improve the yield, and only 36% of the product was obtained (Entry 13).

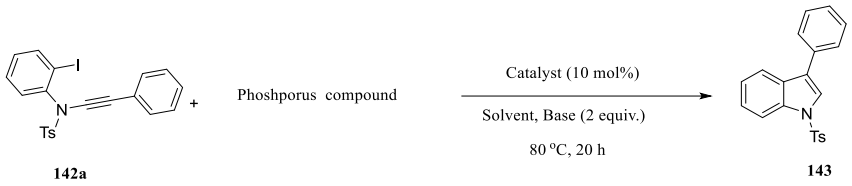

Scheme 54. Reaction followed for the preparation of indole

Entry	Phosphorus Compound (5 Equiv.)	Catalyst (10 mol%)	Solvent	Base (2 equiv.)	Yield
1	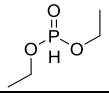	$Pd(PPh_3)_4$	DMF	K_2CO_3	35%
2	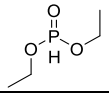	$Pd(PPh_3)_4$	THF	K_2CO_3	95%
3	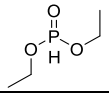	$Pd(PPh_3)_4$	Acetonitrile	K_2CO_3	50 %
4	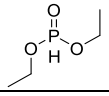	$Pd(Cl)_2(PPh_3)_2$	THF	K_2CO_3	46 %
5	-	$Pd(PPh_3)_4$	THF	K_2CO_3	13 %
6		$Pd(PPh_3)_4$	THF	K_2CO_3	27 %
7	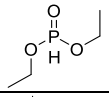	$Pd(PPh_3)_4$	THF	-	Starting material
9	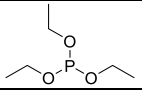	$Pd(PPh_3)_4$	THF	K_2CO_3	Starting material
10	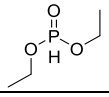	$NiBr_2dppe$	THF	K_2CO_3	Starting material
11	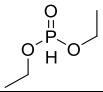	$Pd\ (OAC)_2$	THF	K_2CO_3	Starting material
12	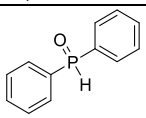	$Pd(PPh_3)_4$	THF	K_2CO_3	Starting material
13	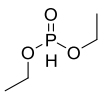	$Pd(PPh_3)_4$	THF	DIPEA	36 %

Table 14. Optimizing reaction conditions

3.2.3 Isotope labelling experiment

In order to confirm that the source of hydrogen on the indole molecule is primarily originating from diethyl phosphite, a deuteration experiment was performed using a previously described method.[155] The deuterated diethyl phosphite **(144)** was prepared by refluxing triethyl phosphite and D_2O (1.5 equiv.) in acetonitrile for 2 hours. The resulting product was obtained with a 70% yield after distillation (Scheme 55).

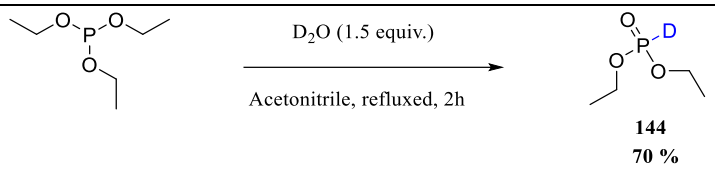

Scheme 55. Synthesis of deuterated diethyl phosphonate

The **^{31}P NMR** analysis showed the presence of a triplet around 7 ppm referring to the deuterated product **144**. The intensity of the middle peak is higher than the other two due to the presence of non-deuterated diethyl phosphite (Figure 14).

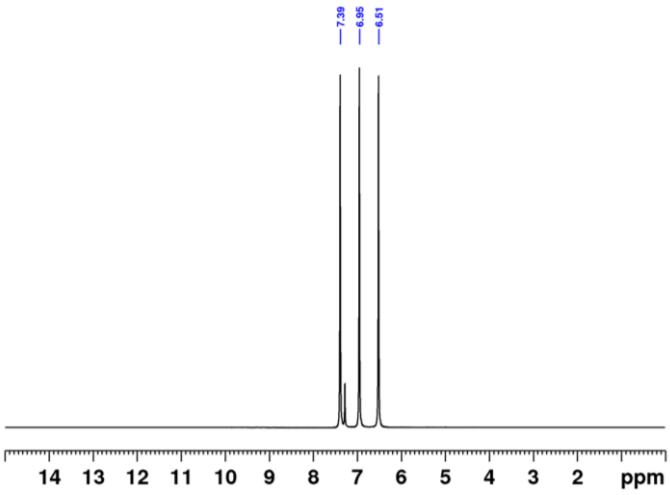

Figure 14. ^{31}P NMR of **144**

The prepared deuterated diethyl phosphite **144** was used in the synthesis of indole **145** (Scheme 56). The reaction proceeded to afford indole **145** with 52% yield. The **^{1}H NMR** of the obtained deuterated indole showed a peak at 7.62 ppm; the integration of the peak is 0.2<1 which means

that the deuterium is found at this position. Therefore, this result validates that the proton is coming from phosphorous compound (Figure 15). The presence of a small peak referring to H and not to deuterium is due to the presence of traces of diethyl phosphite in the previously prepared deuterated diethyl phosphite (Fig 14). Also, H can be generated from traces of water found in THF. According to the ratio obtained, 80% of the deuterated product is obtained and the remaining 20% refers to the formation of indole with proton instead of deuterium.

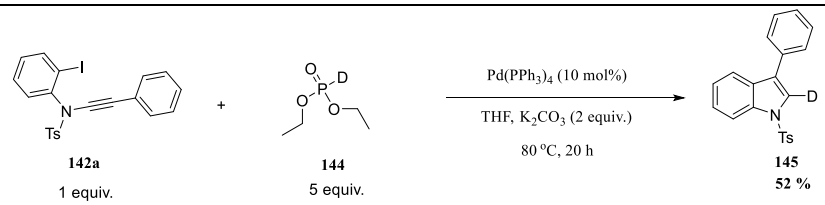

Scheme 56. Synthesis of indole using deuterated diethyl phosphite

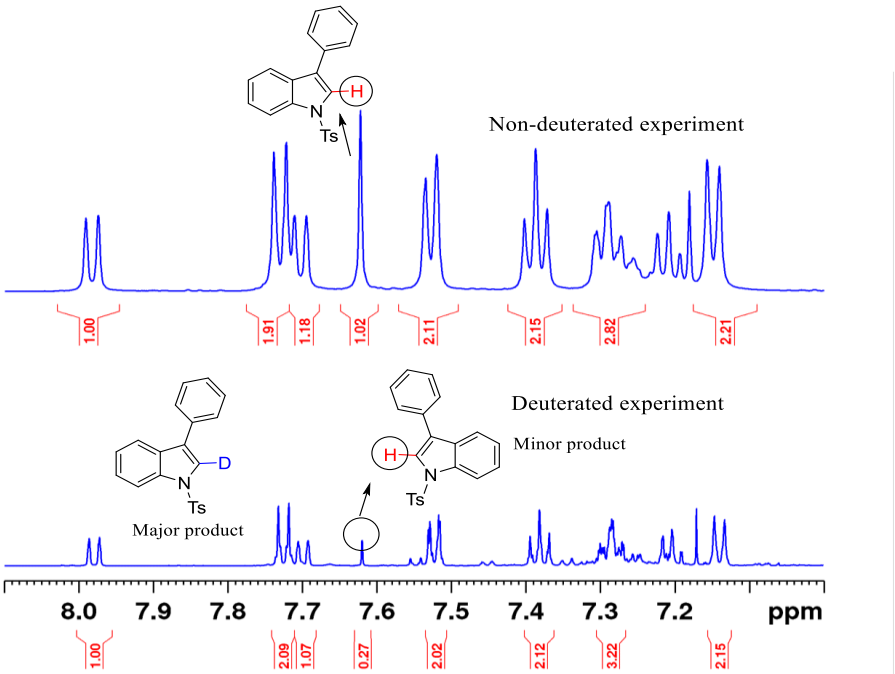

Figure 15. ^{1}H NMR analysis of non-deuterated and deuterated indole

3.2.4 Proposed Mechanism:

A proposed mechanism for indole formation is shown in Scheme 57. In step 1, the Pd (0) center inserts into the aryl-halogen bond of **142a** via the oxidative addition step to afford a palladium s,p-chelated intermediate. Followed by 5-Endo-dig cyclizations and σ-vinylpalladium intermediate formation as shown in step 2. And finally the obtained intermediate will extract the acidic H from the phosphorus compound to afford the targeted product.

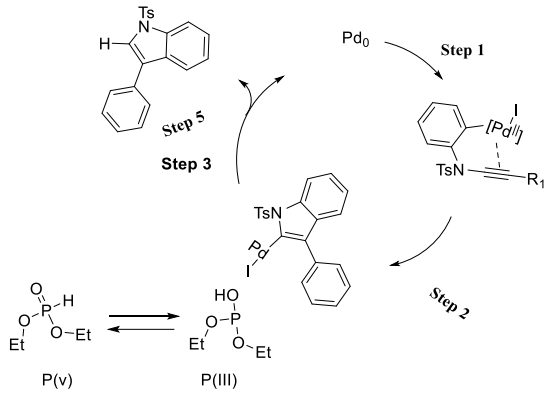

Scheme 57. Proposed mechanism of Indole formation

3.3. Palladium-Catalyzed cross coupling of tosylated 2-Iodo-trimethylsilylynamide with H-phosphonate in the presence of a base.

The previously reported examples in section 2 page 149 reveal certain limitations in the preparation of aromatic compounds containing phosphorus, as they possess minimal or nonexistent reactive functional groups on their aromatic rings apart from halogens. Furthermore, this could limit their efficacy as building blocks for the formation of molecules and their role in the synthesis of pharmaceutical or material compounds. In this study, we present a new methodology for the synthesis of phosphonates and phosphine oxide compounds having a ynamide group, with excellent yields. The presence of the ynamide group can favor the synthesis of more complex compounds. The results of this investigation are detailed below.

3.3.1 Optimizing reaction conditions.

N-(2-iodophenyl)-4-methyl-N-((trimethylsilyl)ethynyl)benzenesulfonamide **(142c)**, H-diethylphosphonate and diphenylphosphine oxide were taken as model substrates. The optimization of the reaction conditions was done using different bases, palladium catalysts, and reaction temperatures. The results are summarized in Table 15.

When using ynamide **142c** instead of ynamide **142a**, a different reaction occurred, and product **146** was obtained instead of the indole (Scheme 58). The reason behind obtaining the new product could be due to the stabilized intermediate (Scheme 58, A), which favors the coupling and prevents cyclization, leading to the formation of the indole product. The obtained product is new, and so far, a cross-coupling reaction in the presence of an ynamide has not been yet reported. In this section, different conditions were tested for the preparation of **146** using variable reaction conditions. In Table 15, entry 1, when using diethyl phosphite (5 equiv.), $Pd(PPh_3)_4$ (10 mol%), and K_2CO_3 (2 equiv.) as a base, the reaction proceeded to afford product **146** with 76% yield. However, when using $Pd(Cl)_2(PPh_3)_2$ instead of $Pd(PPh_3)_4$, the reaction didn't proceed, and the starting material was recovered (Entry 2). Moreover, the reaction didn't proceed in the absence of a base, and the starting material was retrieved, too (Entry 3). When using DIPEA (2 equiv.) instead of K_2CO_3 (2 equiv.), the reaction proceeded with 99% yield (entry 4). Following the conditions of entry 4, and using diphenyl phosphite instead of diethyl phosphite, the reaction resulted in an 88% yield to afford the corresponding phosphine oxide.

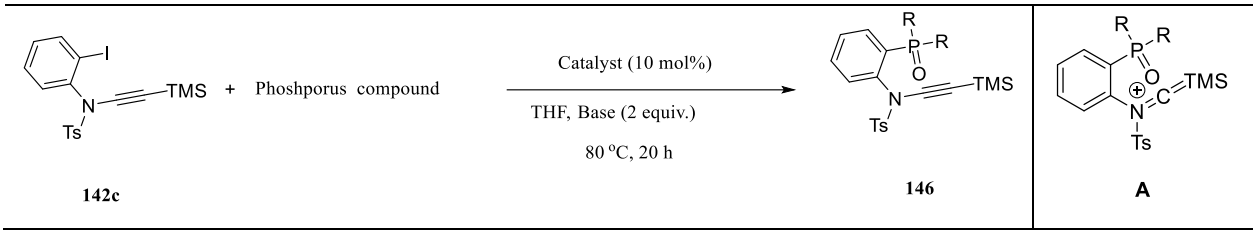

Scheme 58. Reaction followed for the preparation of **146**

Entry (Ref)	Phosphorous Compound (Equiv)	Catalyst (10 mol%)	Base	Yield of 146
1	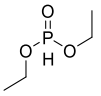 (5 equiv)	$Pd(PPh_3)_4$	K_2CO_3	76 %
2	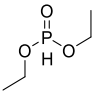 (5 equiv)	$Pd(Cl)_2(PPh_3)_2$	K_2CO_3	Starting material
3	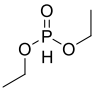 (5 equiv)	$Pd(PPh_3)_4$	-	Starting material
4	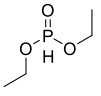 (5 equiv)	$Pd(PPh_3)_4$	DIPEA	99%
5	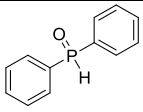 (3 equiv)	$Pd(PPh_3)_4$	DIPEA	88 %

Table 15. Optimizing reaction conditions

One example was performed on ynamide **142b**, which has terminal alkyne group, in the presence of diethyl phosphite (5 equiv.), $Pd(PPh_3)_4$ (10 mol%), and K_2CO_3 (2 equiv.) as a base in THF. The reaction proceeded and the C-P coupling was observed. However, the cleavage of ynamide occurred, which afforded the tosylated aniline (Figure 16).

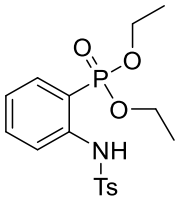

Figure 16. Tosylated aniline

3.3.2. Proposed Mechanism

A proposed mechanism for SP2 C-P coupling is shown in scheme 53. In step 1, the Pd (0) center inserts into the aryl-halogen bond of **142c** via oxidative addition. In step 2, a ligand substitution occurs, replacing the halogen (I) with H-phophonate or phophine oxide (H-phophonate is shown in this case). Followed by the last step 3, the reductive elimination of product **146**, and the regeneration of palladium catalyst.

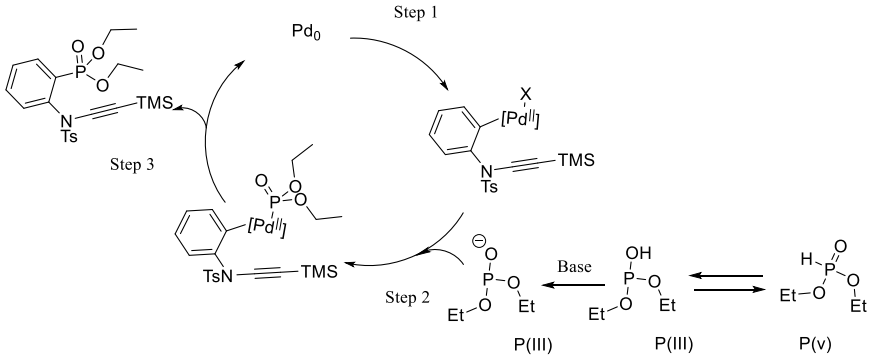

Scheme 59. Proposed mechanism

4. General Conclusion

The optimization of reaction conditions for the preparation of indoles resulted in the following findings: The use of diethylphosphonate was found to favor the reaction. Moreover, the use of triethyl phosphite and phosphine oxide did not lead to indole formation but instead resulted in retrieving starting material. Moreover, the reaction was more favored in the presence of the palladium catalyst $Pd(PPh_3)_4$ and also proceeded with a lower yield upon using $Pd(Cl)_2(PPh_3)_2$ as a catalyst. However, the use of catalysts such as $NiBr_2$dppe or $Pd(OAC)_2$ did not promote the reaction and only resulted in the retrieval of starting material. It is worth noting that indole formation did not occur in the absence of a base. Furthermore, the use of potassium carbonate (K_2CO_3) demonstrated greater enhancement of the reaction compared to the use of diisopropylethylamine (DIPEA) as the base.

While the optimization of reaction conditions for the C-P coupling reaction resulted in the following findings: The reaction is favored when using H-diethyl phosphonate or diphenyl oxide with N-(2-iodophenyl)-4-methyl-N-((trimethylsilyl)ethynyl)benzenesulfonamide **142c**. In the absence of a base, the reaction didn't proceed. Moreover, the use of potassium carbonate (K_2CO_3) or diisopropylethylamine (DIPEA) both favors the proceed of the reaction. However, the yield was higher when using diisopropylethyl amine (DIPEA). The use of $Pd(Cl)_2(PPh_3)_2$ instead of $Pd(PPh_3)_4$ didn't favor the reaction, and only starting material was retrieved. Finally, the use of terminal ynamide **142b** favored the C-P coupling, however, the cleavage of ynamide was observed.

In conclusion, a new approach for indole synthesis or C-P coupling is reported based on the ynamide substituent. The use of ynamide with a phenyl group **(142a)**, diethyl phosphite, $Pd(PPh_3)_4$ (10 mol%), and K_2CO_3 as a base in THF favored the synthesis of indoles with quantitative yields as the presence of an electron rich substrate like benzene will favor the cyclization. However, when using ynamide with a TMS group **(142c)** instead of ynamide with a phenyl group **(142a)**, the C-P coupling reaction was favored, especially, when using DIPEA base instead of K_2CO_3. In this case the cyclization is not favored due to the presence of poor electron substituent (TMS).

Experimental Part

5. Experimental part

General Procedure J

To a dried schlenk tube purged with argon, ynamide **142a-c** (1 equiv.), base (2 equiv.) and catalyst (10 mol %) were added. Argon gas was flushed several times to the medium, and removed using vacuum pump to ensure that the reaction proceeds under inert atmosphere. THF was added then to the medium followed by the addition of phosphorous compound. The tube was closed well and placed in a preheated oil bath at 80 ^{o}C for 20 h.

Purification:

The obtained solution was passed over celite, condensed and purified by column chromatography (SiO_2, EtOAc/n-pentane 1:9 (v/v) to 2:8 (v/v))

3-phenyl-1-tosyl-1H-indole (143)

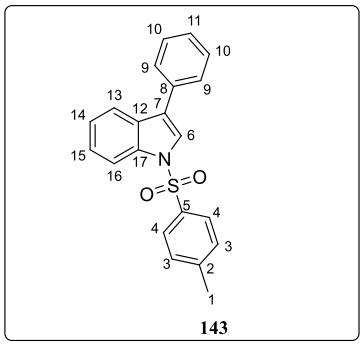

Prepared according to general procedure **J** from N-(2-Iodophenyl)-4-methyl-N-(2-phenylethynyl)benzene sulfonamide **(142a)** (0.1 g, 0.2 mmol, 1 equiv.) and H-diethyl phosphite (0.15 g, 1.1 mmol, 5 equiv.) to afford 3-phenyl-1-tosyl-1H-indole **(143)** (0.07g, 0.2 mmol, Yield: 95%)

^{1}H NMR: (500 MHz, $CDCl_3$) δ 8.06 (d, *J* = 8.4 Hz, 1H, H-16), 7.80 (d, *J* = 8.5 Hz, 2H, H-4), 7.77 (d, *J* = 7.9 Hz, 1H, H-13), 7.69 (s, 1H, H-6), 7.59 (d, *J* = 7.0 Hz, 2H, H-9), 7.46 (t, *J* = 7.7 Hz, 2 H, H-10), 7.36 (t, *J* = 7.9 Hz, 2 H, H-14, H-15), 7.27 (t, *J* = 7.7 Hz, 1 H, H-11), 7.21 (d, *J* = 8.2 Hz, 2H, H-3), 2.32 (s, 3H, H-1)

^{13}C NMR (126 MHz, $CDCl_3$) δ 145.0 (Cq, C-2), 135.6 (Cq, C-17), 135.3 (Cq, C-5), 133.1 (Cq, C-7), 129.9 (CH, C-3), 129.4 (Cq, C-12), 128.9 (CH, C-10), 127.9 (CH, C-9), 127.6 (CH, C-15), 126.9 (CH, C-4), 124.9 (CH, C-14), 124.0 (Cq, C-8), 123.6 (CH, C-11), 123.0 (CH, C-6), 120.5 (CH, C-13), 113.9 (CH, C-16), 21.6 (CH_3, C-1)

The ^{1}H and ^{13}C NMR data match those reported in the literature[156]

Di Ethyl 2-(4-methyl-N-(trimethylsilyl)ethynylbenzenesulfonamido)phenylphosphonate (146a)

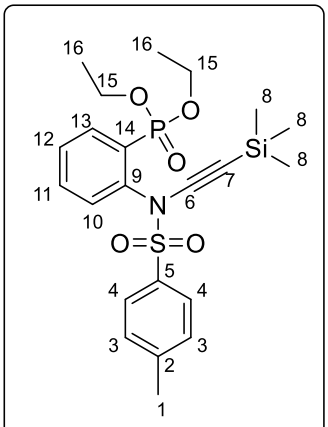

146a

Prepared according to general procedure from N-(2-Iodophenyl)-4-methyl-N-[2-(trimethyl silyl)ethynyl]benzene sulfonamide **(142c)** (0.05 g, 0.1 mmol, 1 equiv.) and H-diethyl phosphonate (0.073 g, 0.53 mmol, 5 equiv.) to afford di ethyl 2-(4-methyl-N-(trimethylsilyl)ethynyl benzene su lfonamido)phenylphosphonate **(146a)** (0.05 g, 0.1 mmol, Yield: 99 %)

^{1}H NMR (600 MHz, $CDCl_3$) δ 8.03 (m, 1H, H-13), 7.72 (d, *J* = 8.4 Hz, 2H, H-4), 7.38 (m, 2H, H-11, H-12), 7.27 (d, *J* = 8 Hz, 2H, H-3), 6.80 (m, 1H, H-10), 4.11 (d, *J* = 59.2 Hz, 4H, H-15), 2.39 (s, 3H, H-1), 1.28 (dt, *J* = 25 Hz, 6.8 Hz, 6 H, H-16), 0.0 (S, 9H, H-8)

^{13}C NMR (150 MHz, $CDCl_3$) δ 145.2 (Cq, C-2), 140.6 (Cq, d, $^2J_{(C-P)}$ = 2.4 Hz, C-9), 136.2 (CH, d, $^2J_{(C-P)}$ = 8.1 Hz, C-13), 133.9 (Cq, C-5), 133.6 (CH, d, $^4J_{(C-P)}$ = 2.3 Hz, C-11), 129.7 (Cq, d, $^1J_{(c-p)}$ = 186.1 Hz, C-14), 129.42 (CH, $^3J_{(C-P)}$ = 14.2 Hz, C-12), 129.41 (CH, C-3), 129.2 (CH, s, C-4), 128.0 (CH, d, $^3J_{(C-P)}$ = 9.7 Hz, C-10), 96.2 (Cq, C-6), 72.5 (Cq, C-7), 62.7 (CH_2, dd, $^2J_{(C-P)}$ = 29.5, 5.2 Hz, C-15), 21.8 (CH_3, C-1), 16.3 (CH_3, d, $^3J_{(C-P)}$ = 18.5, 6.7 Hz, C-16), 0.0 (CH_3, C-8)

HRMS (ESI+): Calculated for $C_{19}H_{23}NO_5PS$ [M+]: 408.1035; found: 408.1035

IR (ATR, cm-1) v 3675, 2976, 2158, 1372, 1020

^{31}P NMR (243 MHz, $CDCl_3$) δ 13.98 ppm

N-(diphenylphosphoryl)-4-methyl-N-(trimethylsilyl)benzenesulfonamide (146b)

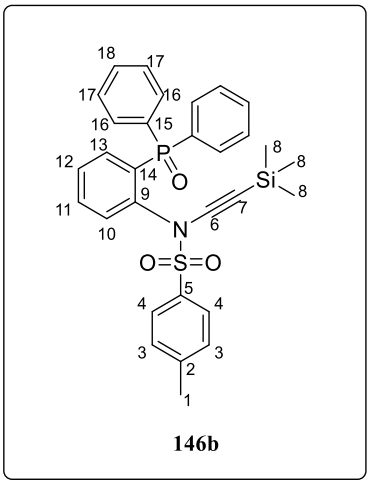

146b

Prepared according to procedure **J** from N-(2-Iodophenyl)-4-methyl-N-[2-(trimethylsilyl) ethynyl] benzene sulfonamide **(142c)** (0.05 g, 0.1 mmol, 1 equiv.) and diphenylphosphine oxide (0.06 g, 0.3 mmol, 3 equiv.) to afford N-(diphenylphosphoryl)-4-methyl-N-(trimethylsilyl) benzene sulfonamide **(146b)** (0.05g, 0.09 mmol, Yield: 88%).

^{1}H NMR (600 MHz, $CDCl_3$) δ 7.75-7.70 (m, 6H, H-13, H-16, H-4), 7.50-7.42 (m, 8H, H-11, H-12, H-17, H-18), 7.29 (d, *J* = 8.2 Hz, 2H, H-3), 6.97 (qd, *J* = 3.1 Hz, 1.3 Hz, 1H, H-10), 2.44 (s, 3H, H-1), 0.0 (s, 9H, H-8).

^{13}C NMR (150 MHz, $CDCl_3$) δ 145.2 (Cq, C-2), 141.3 (Cq, $^{2}J_{(c-p)}$ = 3.5 Hz, C-9), 135.8 (CH, d, $^{3}J_{(c-p)}$ = 8.7 Hz, C-13), 133.9 (Cq, $^{1}J_{(c-p)}$ = 98.6 Hz, C-15), 133.3 (CH, d, $^{4}J_{(c-p)}$ = 1.84 Hz, C-11), 133.2 (Cq, C-5), 132.5 (Cq, $^{1}J_{(c-p)}$ = 29 Hz, C-16), 132.4 (Cq, d, $^{1}J_{(c-p)}$ = 108.2 Hz, C-14), 131.91 (CH, $^{4}J_{(c-p)}$ = 2.5 Hz, C-18), 129.8 (CH, C-3), 129.5 (CH, d, $^{2}J_{(c-p)}$ = 11.1 Hz, C-12), 129.3 (CH, C-4), 129.0 (CH, d, $^{4}J_{(c-p)}$= 6.9 Hz, C-10), 128.4 (Bs, CH, C-17), 95.8 (Cq, C-6), 72.8 (Cq, C-7), 21.9 (CH_3. C-1), 0.0 (CH_3, C-8)

IR (ATR, cm-1) v 3675, 2969, 2162, 535.

HRMS (ESI+): Calcd for $C_{30}H_{31}NO_3SSiP$[M+] = 544.1539; found = 544.1532.

^{31}P NMR (243 MHz, $CDCl_3$) δ 26.6 ppm.

6. Reference

[117] (a) T. P. Singh, O. M. Singh, Recent Progress in Biological Activities of Indole and Indole Alkaloids. *Mini.Rev.Med. Chem.* **2018**, *18*, 9–25. https://doi.org/1 0.2174/13895 57517666170 8 07123201. (b) S. Suzen, Recent Studies and Biological Aspects of Substantial Indole Derivatives with Anti-Cancer Activity. *Curr. Org. Chem.* **2017**, *21*, 2068 - 2076 https://doi.org/10.2174/ 13852 728216 66170809143233. (c) Y.-M. Ma, X.-A, Liang, Y. Kong, B. Jia, Structural Diversity and Biological Activities of Indole Diketopiperazine Alkaloids from Fungi. *J. Agric. Food Chem.* **2016**, *64*, 6659–6671. https:// doi.org/10.1021/acs.jafc.6b01772. (d) S.-M. Li, Prenylated Indole Derivatives from Fungi: Structure Diversity, Biological Activities, Biosynthesis and Chemoenzymatic Synthesis. *Nat. Prod. Rep.* **2009**, *27*, 57–78. https://doi.or g/10.1039/B9 09987 P. (e) S. Kumar, A. Ritika Brief Review of the Biological Potential of Indole Derivatives. *Future J. Pharm. Sci.* **2020**, *6*, 1-19. https://doi.org/10.1186/s43094-020-00141-y. (f) Y. Han, W. Dond, Q. Guo, X. Li, L. Huang, The importance of indole and azaindole scaffold in the development of antitumor agents, *Eur. J. Med. Chem.* **2020**, *203*, 112506. https://doi.org/10.1016/j.ejmech.2020. 112506 (g) J. Dhuguru, R. Skouta, Role of Indole Scaffolds as Pharmacophores in the Development of Anti-Lung Cancer Agents, *Molecules* **2020**, *25*, 1615.https://doi.org/10.3390 /molecules25071615. (h)A. Kumari, R. K. Singh, Medicinal chemistry of indole derivatives: Current to future therapeutic prospectives *Bioorganic Chemistry* **2019**, *89*, 103021. https://doi.or g/10.1016/j.bioorg.2019.103021.

[118] (a)P. Sun, Y. Huang, S. Chen, X. Ma, Z. Yang, J. Wu, Indole derivatives as agrochemicals: An overview, *Chin Chem Lett* **2023**, 109005. https://doi.org/10.1016/j.cclet.2023.109005. (b)P. R. Nitha, S. Soman, J. John, Indole fused heterocycles as sensitizers in dye-sensitized solar cells: an overview *Mater. Adv.* **2021**, *2*, 6136–6168. DOI: 10.1039/D1MA00499A (c) Barden, T.C. (2010). Indoles: Industrial, Agricultural and Over-the-Counter Uses. Topics in Heterocyclic Chemistry, Vol. 26. Gribble, G. (Ed.). Springer, Berlin, Heidelberg. https://doi.org/10.100 7/7081201048.

[119] E. Fischer, F. Jourdan, Ueber Die Hydrazine Der Brenztraubensäure. *Ber. Dtsch. Chem. Ges.* **1883**, *16*, 2241–2245. https://doi.org/10.1002/cber.188301602141.

[120] Aug. Bischler, Ueber Die Entstehung Einiger Substituirter Indole. *Ber. Dtsch. Chem. Ges.* **1892**, *25*, 2860–2879. https://doi.org/10.1002/cber.189202502123.

[121] A. Reissert, Einwirkung von Oxalester Und Natriumäthylat Auf Nitrotoluole. Synthese Nitrirter Phenylbrenztraubensäuren. *Ber. Dtsch. Chem. Ges.* **1897**, *30*, 1030–1053. https:// doi.org/ 10.1 00 2/cber.189703001200.

[122] W. Madelung, Über Eine Neue Darstellungsweise Für Substituierte Indole. Ber. Dtsch. Chem. Ges. **1912**, *45*, 1128–1134. https://doi.org/10.1002/cber.191204501160.

[123] R. J. Sundberg, T. Yamazaki, Rearrangements and Ring Expansions during the Deoxygenation of Beta, Beta.-Disubstituted o-Nitrostyrenes. *J. Org. Chem.* **1967**, *32*, 290–294. https://doi.org/10.1021/jo01288a009.

[124] H. Hemetsberger, D. Knittel, Synthese und Thermolyse von α-Azidoacrylestern. *Monatsh. Chem.* **1972**, *103*, 194–204. https://doi.org/10.1007/BF00912944.

[125] P. G. Gassman, T. J. Van Bergen, G. Gruetzmacher, Use of Halogen-Sulfide Complexes in the Synthesis of Indoles, Oxindoles, and Alkylated Aromatic Amines. *J. Am. Chem. Soc.* **1973**, *95*, 6508–6509. https://doi.org/10.1021/ja00800a088.

[126] A. D. Batcho and W. Leimgruber, INDOLES FROM 2-METHYLNITROBENZENES BY CONDENSATION WITH FORMAMIDE ACETALS FOLLOWED BY REDUCTION: 4-BENZYLOXYINDOLE, *Org. Synth.*, **1985**, *63*, 214–220. DOI: 10.15227/orgsyn.063.0214

[127] J.-B. Baudin, S. A. Julia, Synthesis of Indoles from N-Aryl-1-Alkenylsulphinamides. *Tetrahedron Lett.* **1986**, *27*, 837–840. https://doi.org/10.1016/S0040-4039(00)84114-3.

[128] G. Bartoli, G. Palmieri, M. Bosco, R. Dalpozzo, The Reaction of Vinyl Grignard Reagents with 2-Substituted Nitroarenes: A New Approach to the Synthesis of 7-Substituted Indoles. *Tetrahedron Lett.* **1989**, *30*, 2129–2132. https://doi.org/10.1016/S0040-4039(01)93730-X.

[129] R. C. Larock, E. K. Yum, Synthesis of Indoles via Palladium-Catalyzed Heteroannulation of Internal Alkynes. *J. Am. Chem. Soc.* **1991**, *113*, 6689–6690. https://doi.org/10.1021/ja00017a059.

[130] S. Kramer, K. Dooleweerdt, A. T. Lindhardt, M. Rottländer, T. Skrydstrup, Highly Regioselective Au(I)-Catalyzed Hydroamination of Ynamides and Propiolic Acid Derivatives with Anilines. *Org. Lett.* **2009**, *11*, 4208–4211. https://doi.org/10.1021/ol901565p.

[131] W. Xu, Y. Chen, A. Wang, Y. Liu, Benzofurazan N-Oxides as Mild Reagents for the Generation of α-Imino Gold Carbenes: Synthesis of Functionalized 7-Nitroindoles. *Org. Lett*. **2019**, *21*, 7613–7618. https://doi.org/10.1021/acs.orglett.9b02893.

[132] D. Allegue, J. González, S. Fernández, J. Santamaría, A. Ballesteros, Regiodivergent Control in the Gold(I) Catalyzed Synthesis of 7-Pyrazolylindoles from 1-Propargyl-1H-Benzotriazoles and Ynamides through α-Imino Gold(I) Carbene Complexes. Adv. Synth. Catal. **2019**, *361*, 758–768. https://doi.org/10.1002/adsc.201801484.

[133] X. Tian, L. Song, K. Farshadfar, M. Rudolph, F. Rominger, T. Oeser, A. Ariafard, A. Hashmi, A. S. K. Acyl Migration versus Epoxidation in Gold Catalysis: Facile, Switchable, and Atom-Economic Synthesis of Acylindoles and Quinoline Derivatives. *Angew. Chem. Int. Ed*. **2020**, *59*, 471–478. https://doi.org/10.1002/anie.201912334.

[134] Z. Xu, J. Zeng, M. Cai, An MCM-41-Immobilized Dichloro(Pyridine-2-Carboxylato)Gold(III) Complex: An Efficient and Recyclable Catalyst for the Annulation of Anthranils and Ynamides. *Dalton Trans.* **2023**, *52*, 806–817. https://doi.org/10.1039/D2DT03733E.

[135] C. Shu, Y. –H. Wang, B. Zhou, X.-L. Li, Y.-F. Ping, X. Lu, L. –W. Ye, Generation of α-Imino Gold Carbenes through Gold-Catalyzed Intermolecular Reaction of Azides with Ynamides. *J. Am. Chem. Soc.* **2015**, *137*, 9567–9570. https://doi.org/10.1021/jacs.5b06015.

[136] X. Tian, L. Song, M. Rudolph, F. Rominger, A. S. K. Hashmi, Synthesis of 2-Aminoindoles through Gold-Catalyzed C–H Annulations of Sulfilimines with N-Arylynamides. Org. Lett. **2019**, *21*, 4327–4330. https://doi.org/10.1021/acs.orglett.9b01501.

[137] K. Dooleweerdt, T. Ruhland, T. Skrydstrup, Application of Ynamides in the Synthesis of 2-Amidoindoles. *Org. Lett.* **2009**, *11*, 221–224. https://doi.org/10.1021/ol802477d.

[138] J. Zhang, Y. Li, C. Zhang, X.-N. Wang, J. Chang, Metal-Free [3+2] Annulation of Ynamides with Anthranils to Construct 2-Aminoindoles. *Org. Lett.* **2021**, *23*, 2029–2035. https://doi.org/10.1021/acs.orglett.1c00158.

[139] Gati, W.; Couty, F.; Boubaker, T.; Rammah, M. M.; Rammah, M. B.; Evano, G. Intramolecular Carbocupration of N-Aryl-Ynamides: A Modular Indole Synthesis. *Org. Lett.* **2013**, *15*, 3122–3125. https://doi.org/10.1021/ol4013298.

[140] Z.-S.Wang, L.-J. Zhu, C.-T. Li, B.-Y. Liu, X. Hong, L.-W. Ye, Synthesis of Axially Chiral N-Arylindoles via Atroposelective Cyclization of Ynamides Catalyzed by Chiral Brønsted Acids. *Angew. Chem. Int. Ed.* **2022**, *61*, e202201436. https://doi.org/10.1002/anie.202201436.

[141] P.-Y. Yao, Y. Zhang, R. P. Hsung, K. Zhao, A Sequential Metal-Catalyzed C-N Bond Formation in the Synthesis of 2-Amido-Indoles. *Org. Lett.* **2008**, *10*, 4275–4278. https://doi.org/10.1021/ol801711p.

[142] B. Witulski, C. Alayrac, L. Tevzadze-Saeftel, Palladium-Catalyzed Synthesis of 2-Aminoindoles by a Heteroanulation Reaction. *Angew. Chem. Int. Ed.* **2003**, *42*, 4257–4260. https://doi.org/10.1002/anie.200351977.

[143] A. Frischmuth, P. Knochel, Preparation of Functionalized Indoles and Azaindoles by the Intramolecular Copper-Mediated Carbomagnesiation of Ynamides. *Angew. Chem. Int. Ed.* **2013**, *52*, 10084–10088. https://doi.org/10.1002/anie.201304380.

[144] (a) P. Finkbeiner, J. P. Hehn, C. Gnamm, Phosphine Oxides from a Medicinal Chemist's Perspective: Physicochemical and in Vitro Parameters Relevant for Drug Discovery, *J. Med. Chem.* **2020**, *63*, 7081–7107. DOI:10.1021/acs.jmedchem.0c00407 (b) K. Moonen, I. Laureyn, C.V. Stevens, Synthetic methods for azaheterocyclicphosphonates and their biological activity. *Chem. Rev.* **2004**, *104*, 6177−62155. https://doi-org.inc.bib.cnrs.fr/10.1021/cr030451c

[145] (a) A. L. Schwan, Palladium catalyzed cross-coupling reactions for phosphorus–carbon bond formation *Chem. Soc. Rev.* **2004**, *33*, 218–224. https://doi-org.inc.bib.cnrs.fr/10.1039/B307538A. (b) E. Manoury, R. Poli, in *Phosphorus Compounds: Advanced Tools in Catalysis and Material Sciences* (Eds.: M. Peruzzini, L. Gonsalvi), Springer Netherlands, Dordrecht, **2011**, pp. 121–149. (c) A. Romerosa, L. Gonsalvi, Phosphorus Coordination Chemistry: A Special Issue in Honor of Maurizio Peruzzini, *Coordination Chemistry Reviews* **2021**, *441*, 213990.

[146] (a) Quin, L. D. A Guide to Organophosphorus Chemistry; John Wiley & Sons: New York, 2000. (b) Demmer, C. S.; KrogsgaardLarsen, N.; Bunch, L. Review on Modern Advances of Chemical Methods for the Introduction of a Phosphonic Acid Group. Chem. Rev. 2011, 111, 7981−8006. (c) A. A. Zagidullin, I. F. Sakhapov, V. A. Miluykov, D. G. Yakhvarov, *Molecules* **2021**, *26*, 5283.

[147] (a) D. Joly, P.-A. Bouit, M. Hissler, Organophosphorus derivatives for electronic devices, *J. Mater. Chem. C.* **2016**, *4*, 3686–3698. DOI https://doi-org.inc.bib.cnrs.fr/10.1039/C6TC00590J (b) Y. Zhang, T. Fan, S. Yang, F. Wang, S. Yang, S. Wang, J. Su, M. Zhao, X. Hu, H. Zhang, T. Zhai, Decarbonylative Phosphorylation of Carboxylic Acids via Redox-Neutral Palladium Catalysis, *Small Methods* **2021**, *5*, 2001068. https://doi-org.inc.bib.cnrs.fr/10.1002/smtd.202001068

[148] E.L. Deal, C. Petit, J.-L. Montchamp, Palladium-Catalyzed Cross-Coupling of H-Phosphinate Esters with Chloroarenes *Org. Lett*. **2011**, *13*, 3270–3273 https://doi-org.inc.bib.cnrs.fr/10.1021/ol201222n

[149] A.J. Bloomfield, S.B. Herzon, Room Temperature, Palladium-Mediated P–Arylation of Secondary Phosphine Oxides *Org. Lett*. **2012**, *14*, 4370–4373 https://doi-org.inc.bib.cnrs.fr/10.1021/ol301831k

[150] Y. Zhang, H. He, Q. Wang, Q. Cai, Asymmetric synthesis of chiral P-stereogenic triaryl phosphine oxides via Pd-catalyzed kinetic arylation of diaryl phosphine oxides *Tetrahedron Lett.* **2016**, 57, 5308–5311 https://doi.org/10.1016/j.tetlet.2016.10.048

[151] J. Dong, L. Liu, X. Ji, Q. Shang, L. Liu, L. Su, hydrazides, R. Kan, Y. Zhou, S.-F. Yin, L.- B. Han, General Oxidative Aryl C–P Bond Formation through Palladium-Catalyzed Decarbonylative Coupling of Aroylhydrazides with P(O)H Compounds, Org. Lett. **2019**, 21, 3198–3203 https://doi.org/10.1021/acs.orglett.9b00922

[152] L. -H. Hong, W. –J. Feng, W. -C. Chen, Y. -C. Chang, Highly Efficient and Well-Defined Phosphinous Acid-Ligated Pd(II) Precatalysts for Hirao Cross-Coupling Reaction. *Dalton Trans.* **2023**, *52*, 5101–5109. https://doi-org.inc.bib.cnrs.fr/10.1039/D3DT00033H

[153] P. J. Stang, In Modern Acetylene Chemistry; P. J. Stang, F. Diederich, Eds.; VCH: Weinheim, 1995

[154] B. Witulski, T. Stengel, N-Functionalized 1-Alkynylamides: New Building Blocks for Transition Metal Mediated Inter- and Intramolecular [2+2+1] Cycloadditions. *Angew. Chem. Int. Ed.* **1998**, *37*, 489–492. https://doi.org/10.1002/(SICI)1521-3773(19980302)37:4<489::AID-ANIE489>3 .0 .CO;2-N.

[155] J.-L. Clément, J.-P. Finet, C. Fréjaville, P. Tordo, Deuterated analogues of the free radical trap DEPMPO: synthesis and EPR studies, *Org. Biomol. Chem.* **2003**, *1*, 1591–1597. DOI:10.1039/b300870c

[156] T. O. Vieira, L. A. Meaney, Y.-L. Shi and H. Alper, Tandem Palladium-Catalyzed N,C-Coupling/Carbonylation Sequence for the Synthesis of 2-Carboxyindoles, Org. Lett., 2008, 10, 4899- 4901 https://doi-org.inc.bib.cnrs.fr/10.1021/ol801985q.

Supplementary

Annexes

Tripropyl(2-propynyl) ammonium bromide (66b)

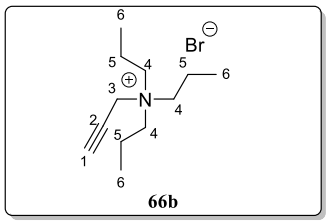

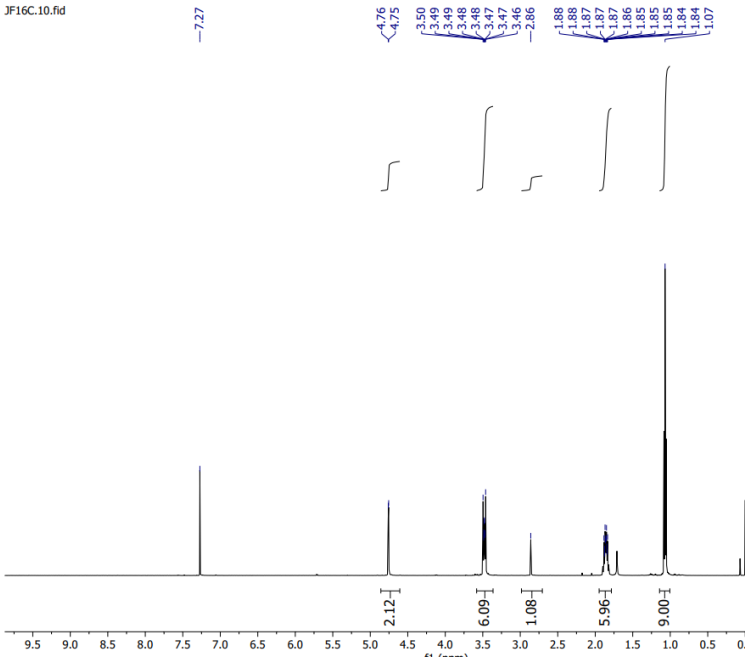

^{1}H NMR (500 MHz, $CDCl_3$) of **66b**

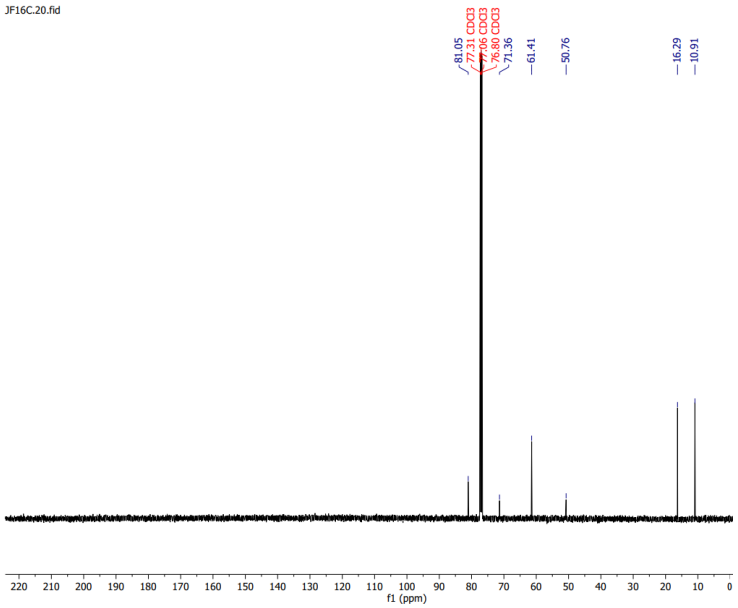

^{13}C NMR (126 MHz, $CDCl_3$) of **66b**

Trimethyl(2-butynyl)ammonium bromide (66c)

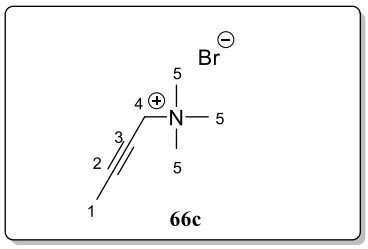

66c

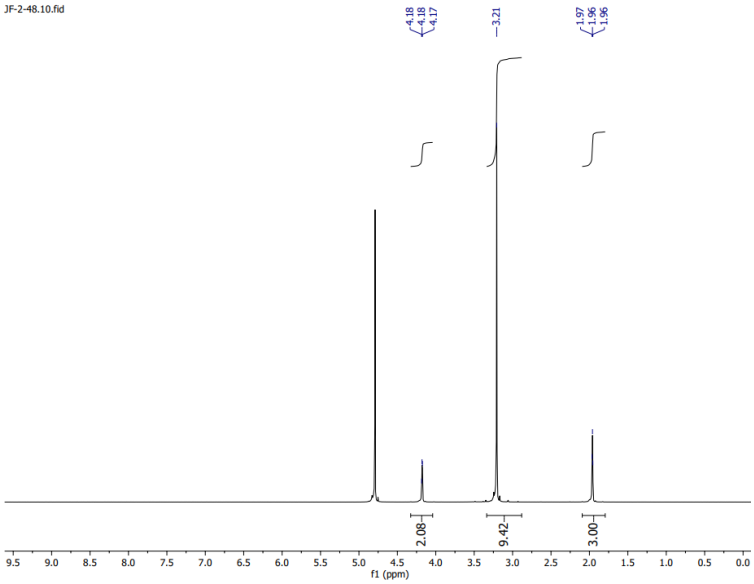

^{1}H NMR (500 MHz, D_2O) of **66c**

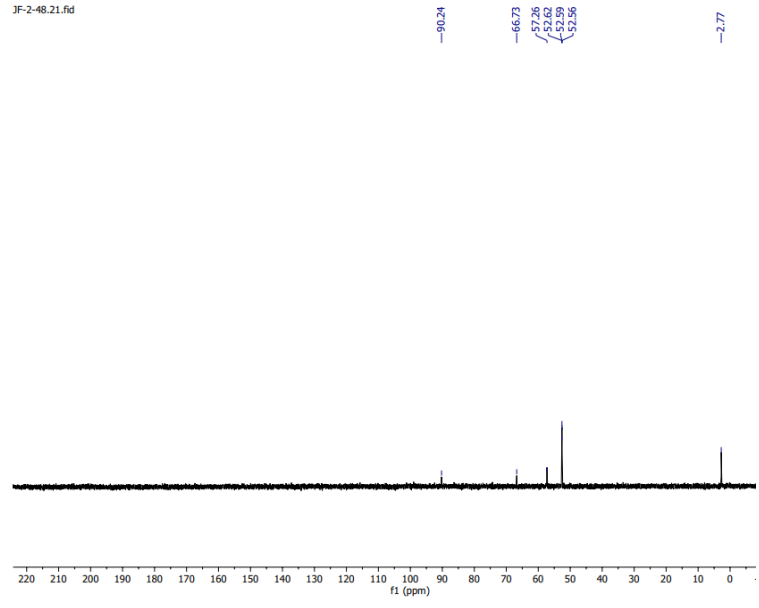

^{13}C NMR (126 MHz, D_2O) of **66c**

Triethyl(2-butynyl)ammonium bromide (66d)

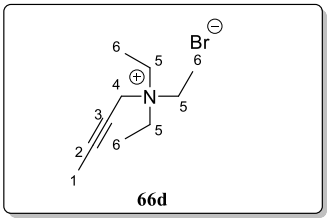

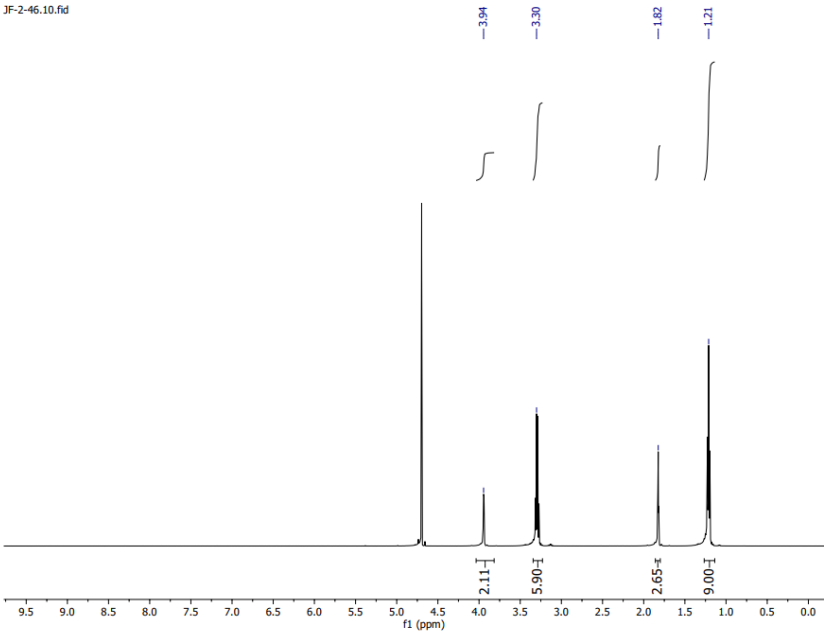

^{1}H NMR (500 MHz, D_2O) of **66d**

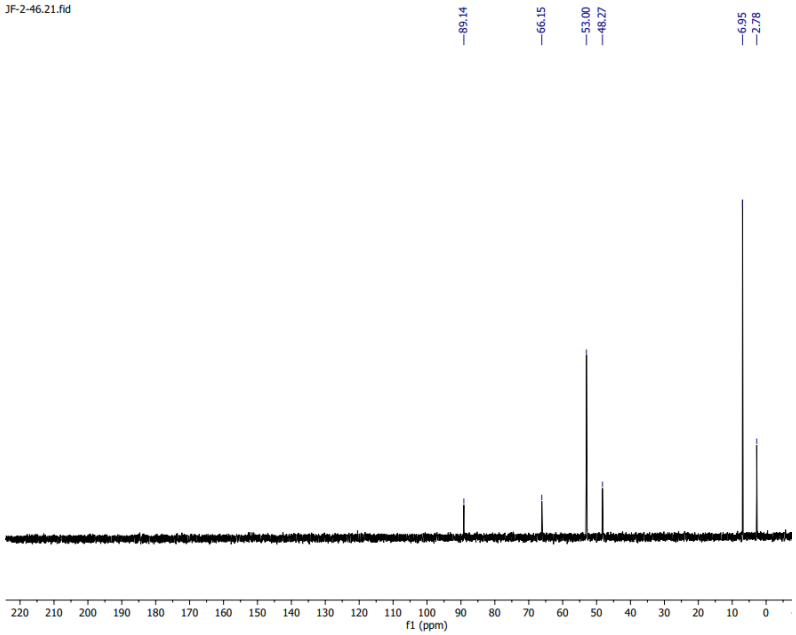

^{13}C NMR (126 MHz, D_2O) of **66d**

Tributyl (2-butynyl)ammonium bromide (66f)

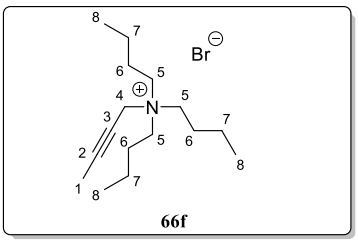

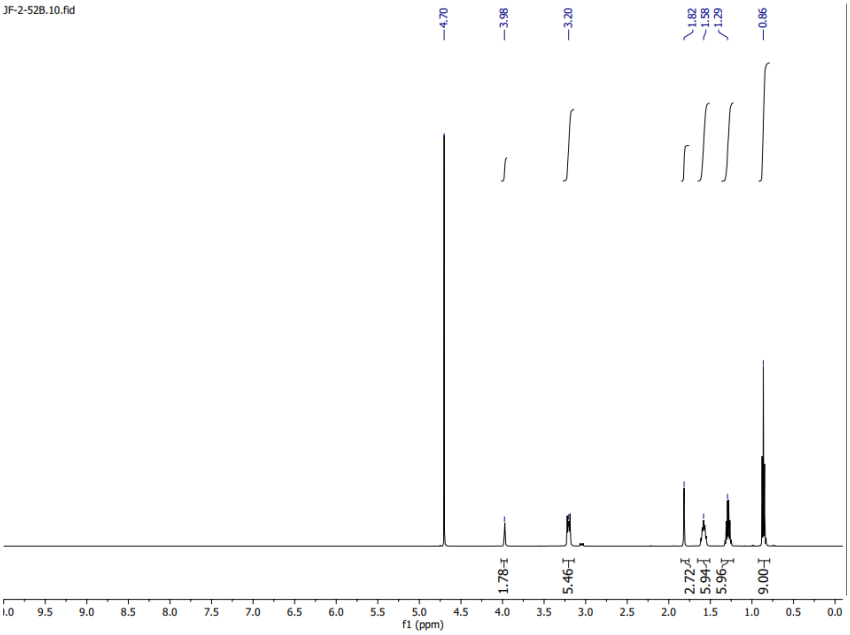

^{1}H NMR (500 MHz, D_2O) of **66f**

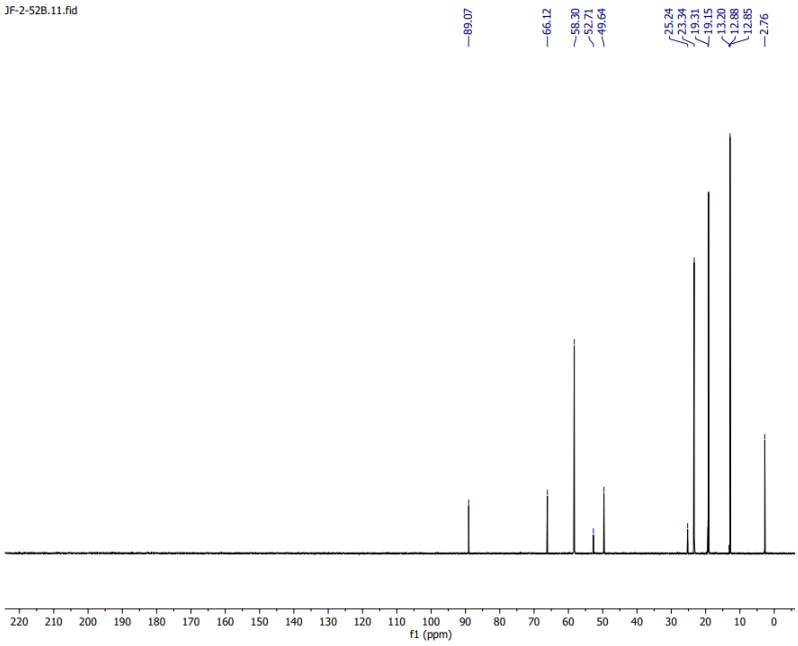

^{13}C NMR (126 MHz, D_2O) of **66f**

Tripropyl (2-pentynyl) ammonium bromide (66g)

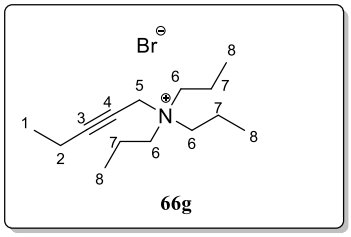

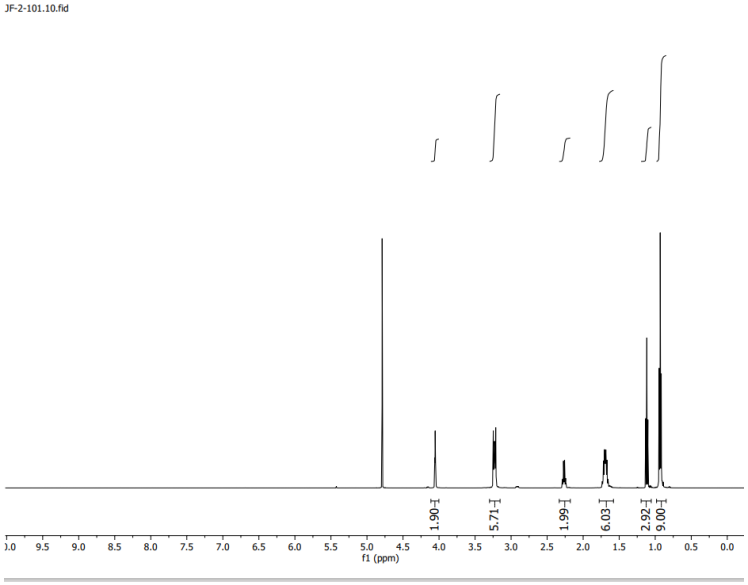

^{1}H NMR (500 MHz, D_2O) of **66g**

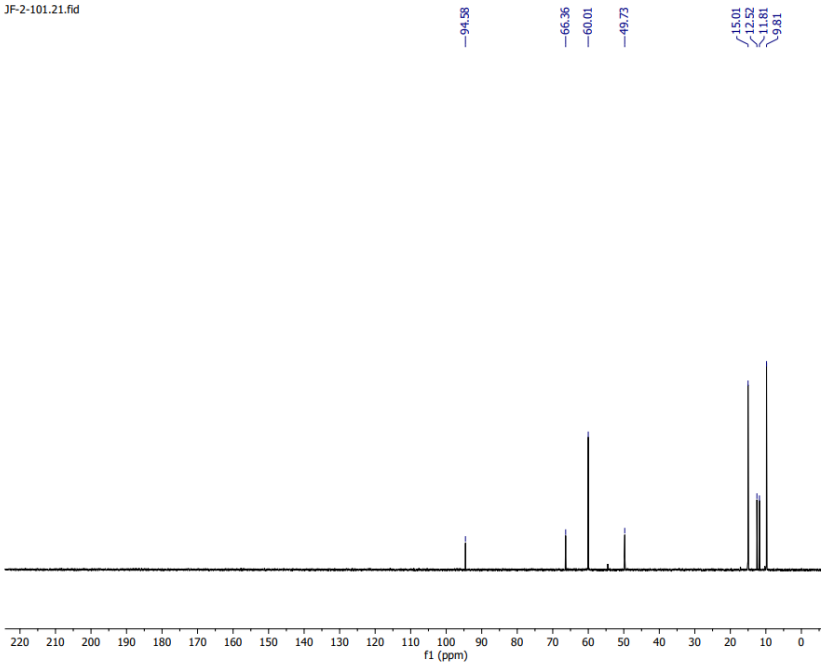

^{13}C NMR (126 MHz, D_2O) of **66g**

Di (2-butynyl) dipropylammonium bromide (67d)

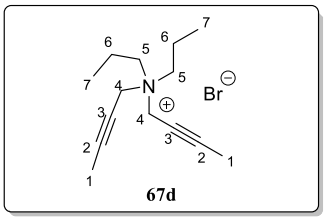

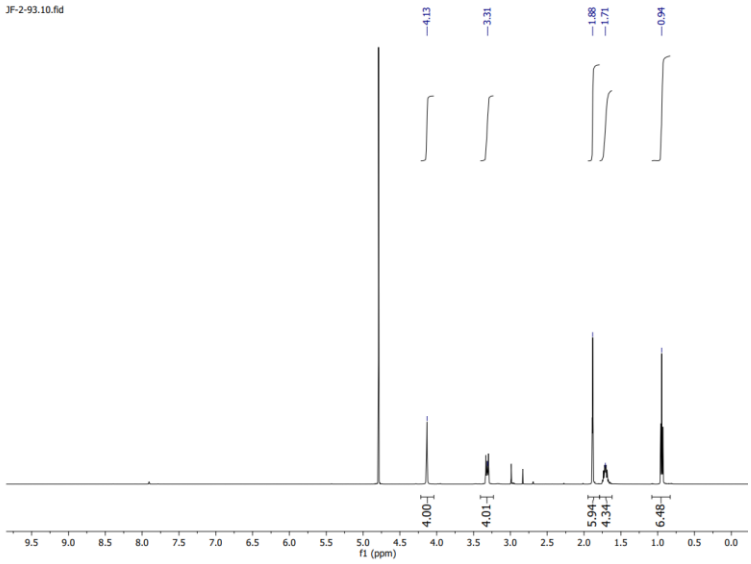

^{1}H NMR (500 MHz, D_2O) of **67d**

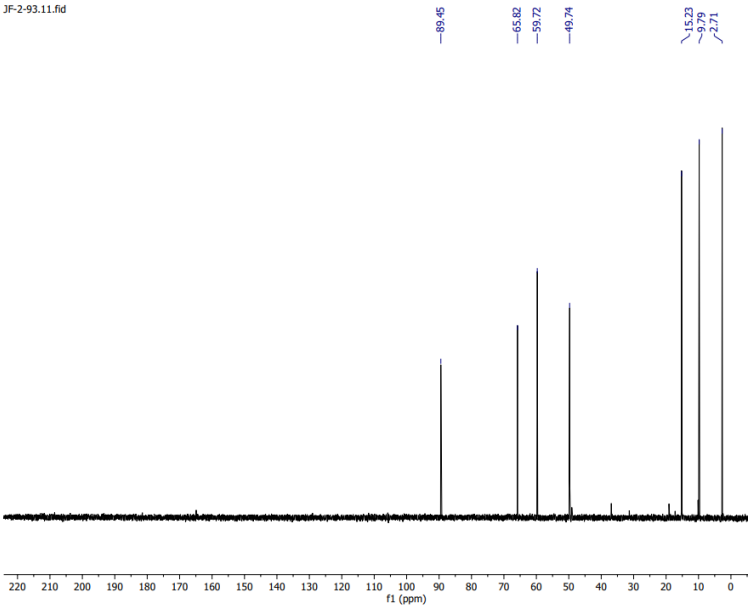

^{13}C NMR (126 MHz, D_2O) of **67d**

Di (2-butynyl) pyrrolidinium bromide (67c)

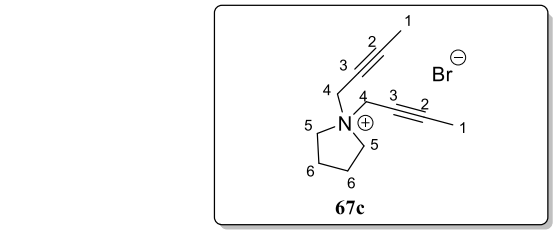

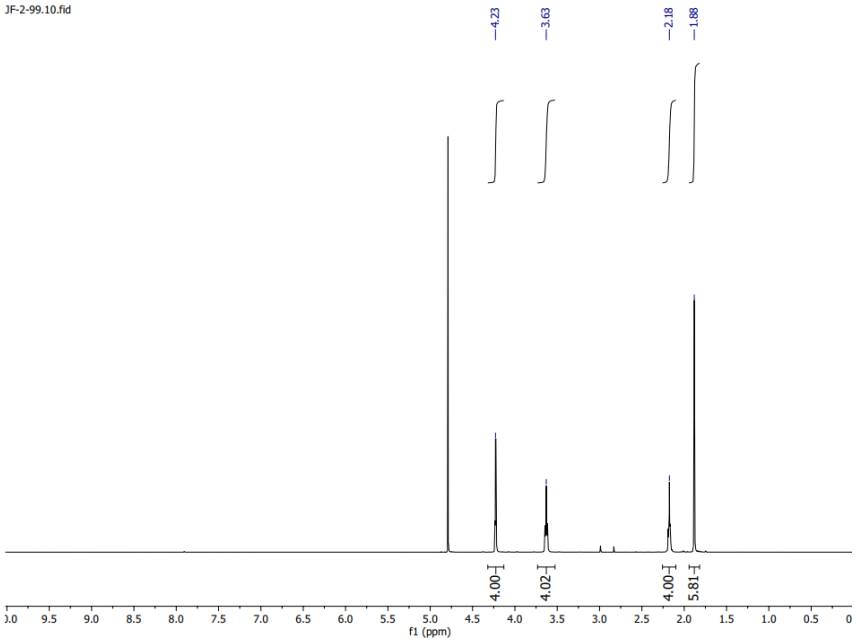

^{1}H NMR (500 MHz, D_2O) of **67c**

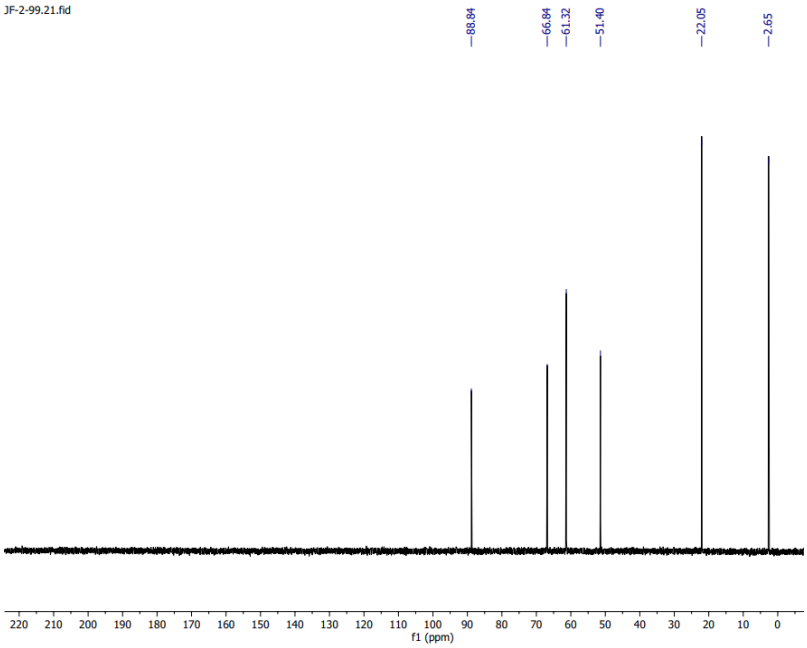

^{13}C NMR (126 MHz, D_2O) of **67c**

Tripropyl (2- butynyl) ammonium bromide (66e)

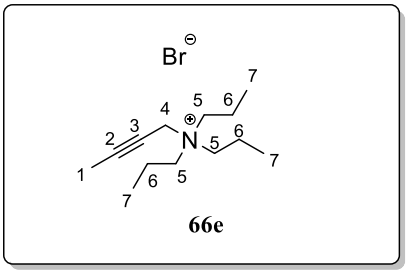

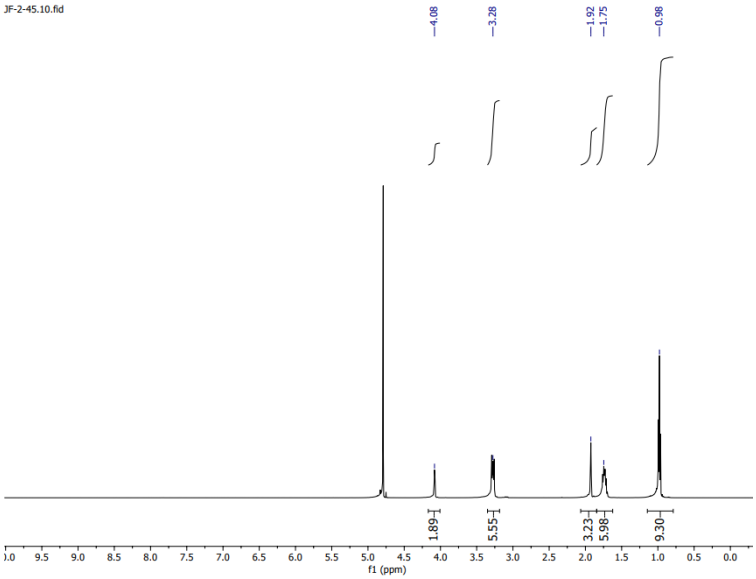

^{1}H NMR (500 MHz, D_2O) of **66e**

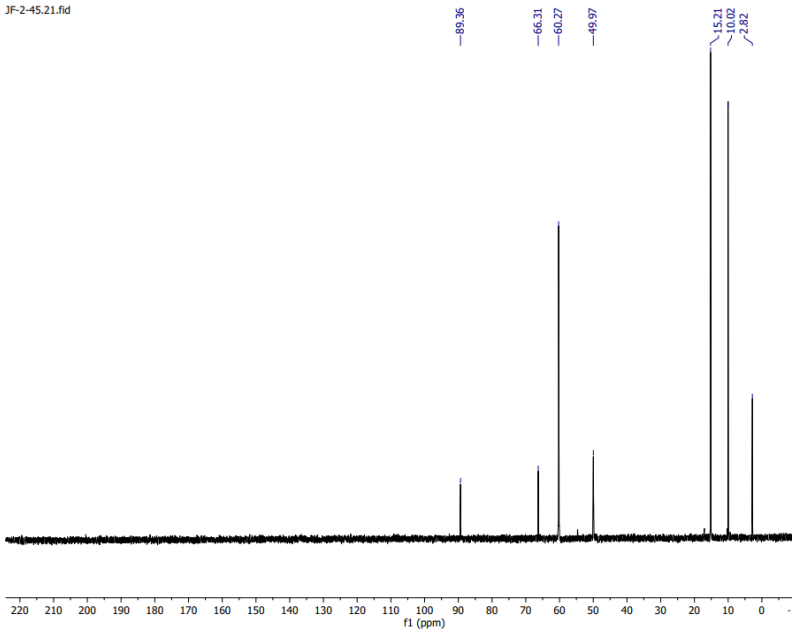

^{13}C NMR (126 MHz, D_2O) of **66e**

Di (propyl) pyrrolidinium Bromide (82)

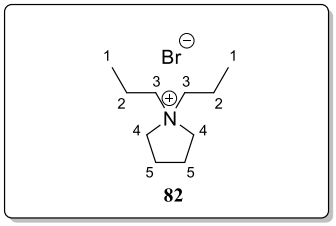

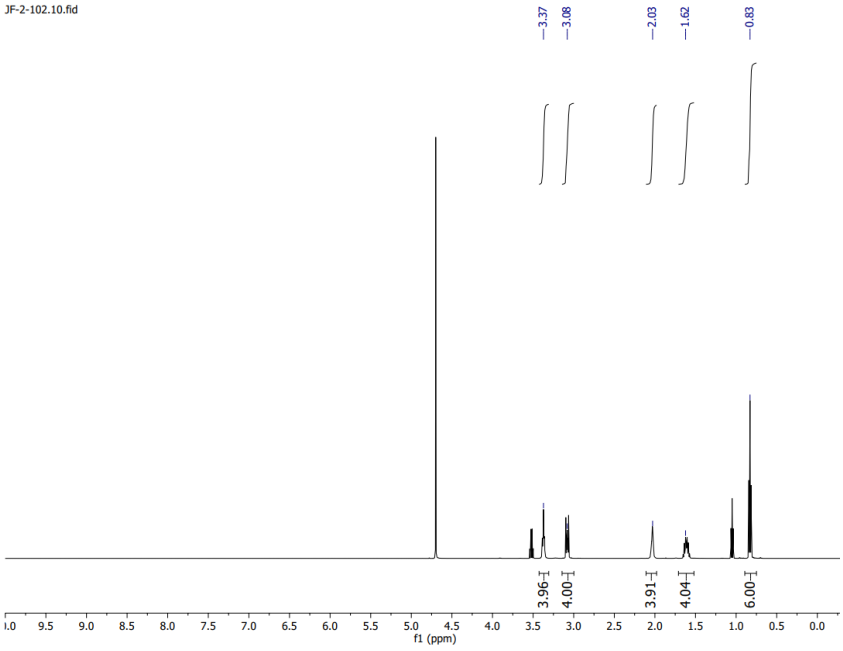

^{1}H NMR (500 MHz, D_2O) of **82**

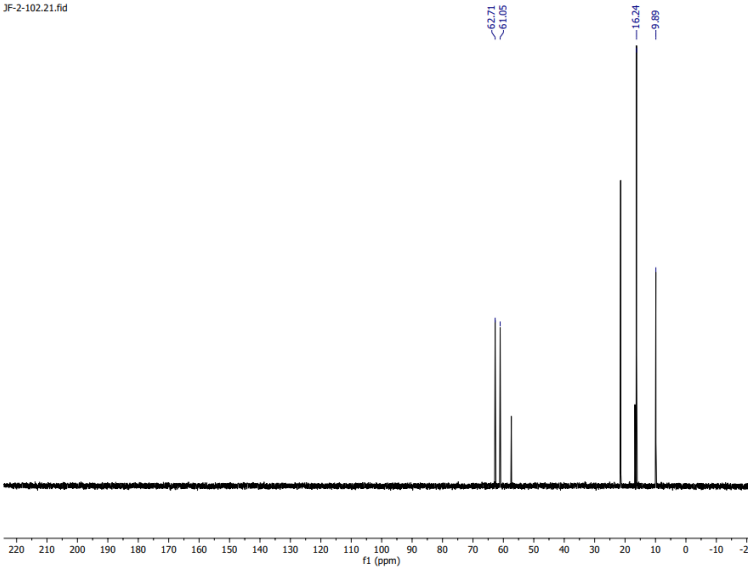

^{13}C NMR (126 MHz, D_2O) of **82**

4- N, N- diethylamino [2.2] paracyclophane (93)

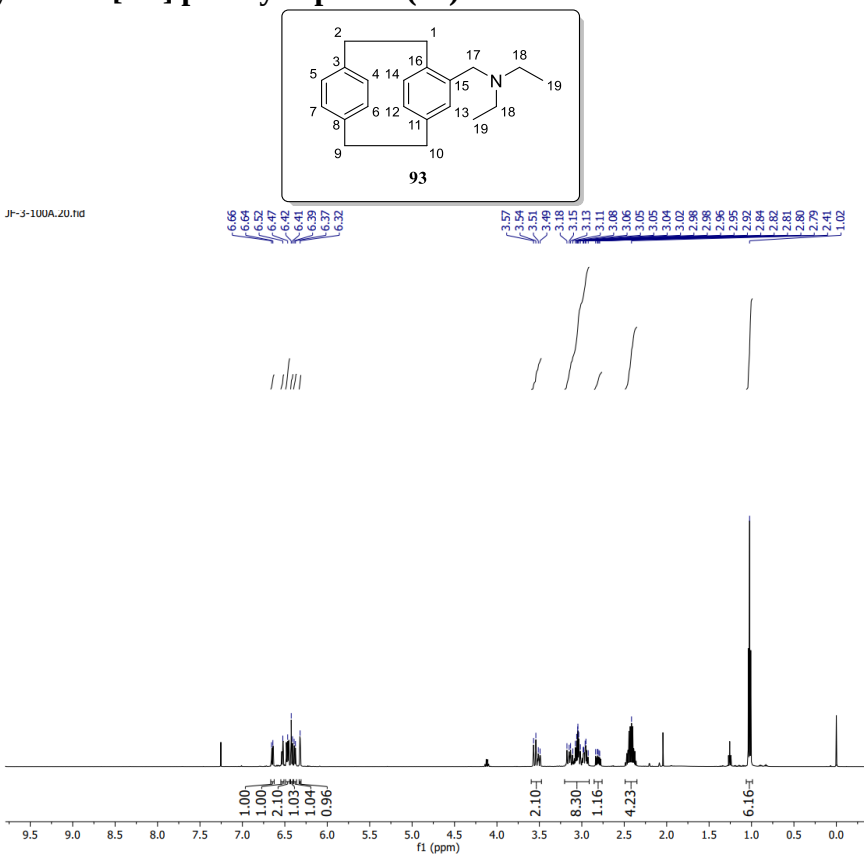

^{1}H NMR (500 MHz, $CDCl_3$) of **93**

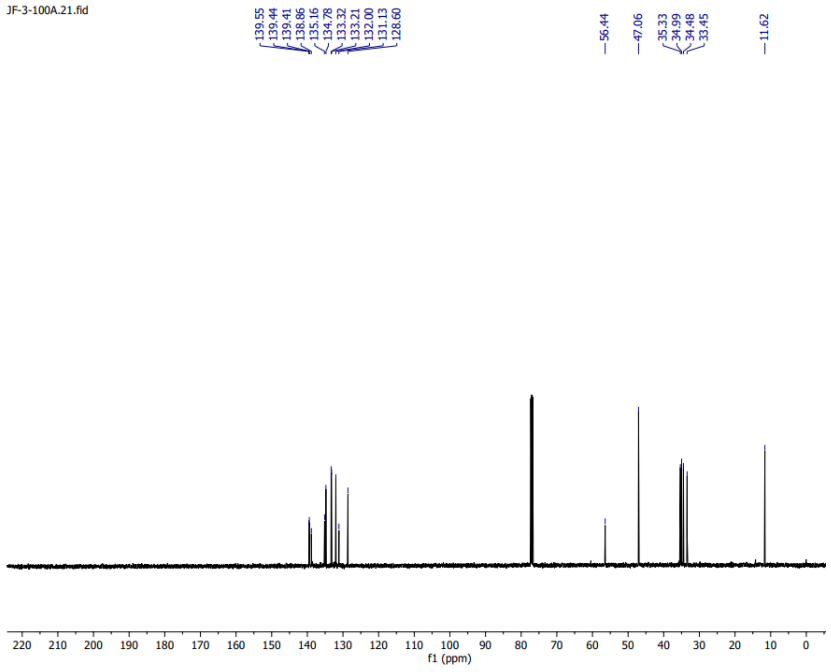

^{13}C NMR (126 MHz, $CDCl_3$) of **93**

Mesityl triethyl ammonium chloride (73b)

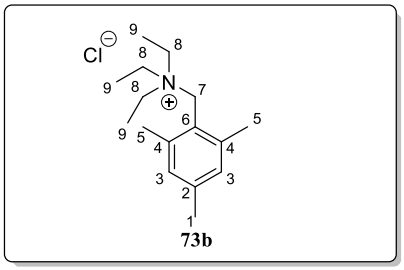

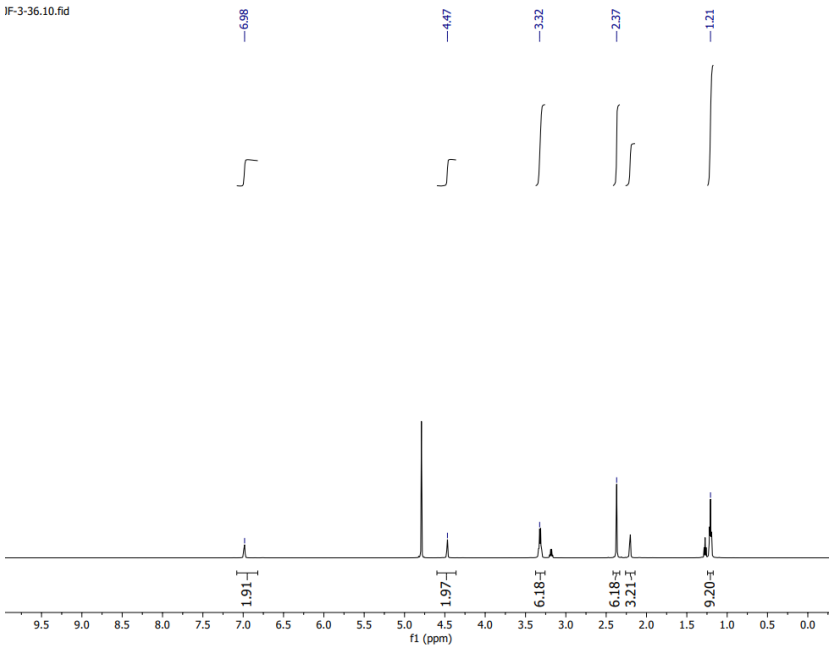

^{1}H NMR (500 MHz, D_2O) of **73b**

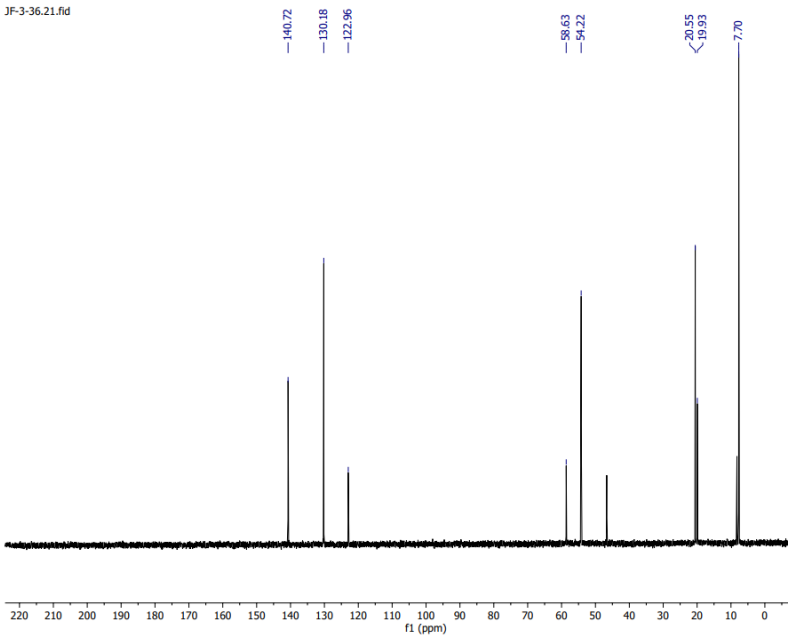

^{13}C NMR (126 MHz, D_2O) of **73b**

tricyclohexyl(propyl)phosphonium (65c)

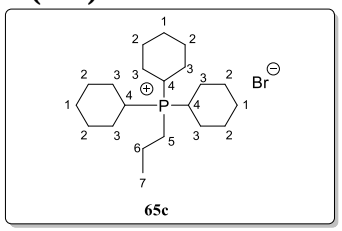

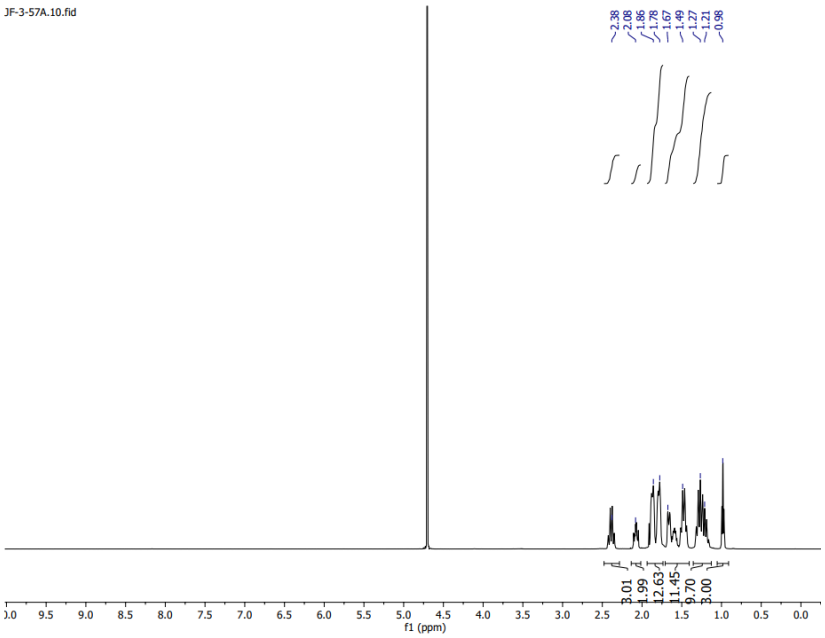

^{1}H NMR (500 MHz, $CDCl_3$) of **65c**

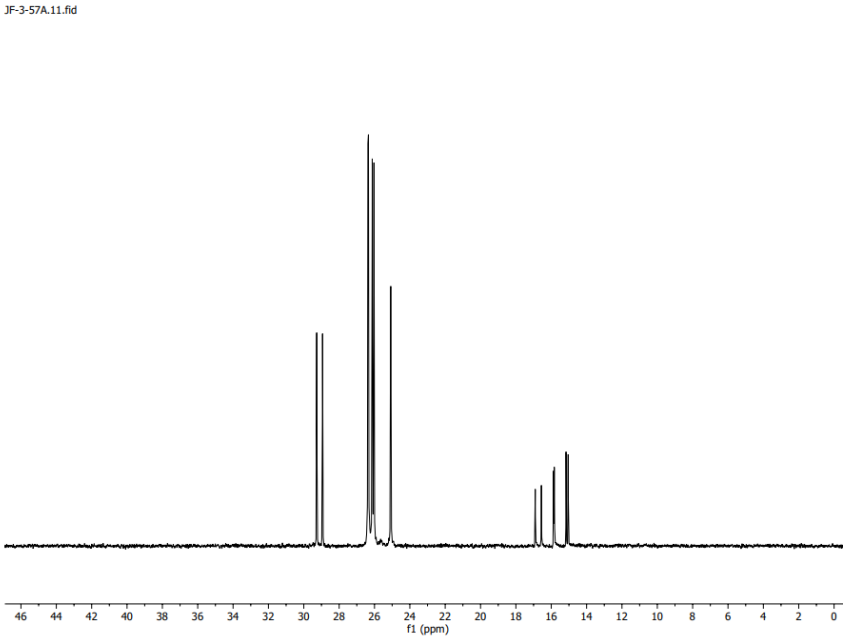

^{13}C NMR (125 MHz, $CDCl_3$) of **65c**

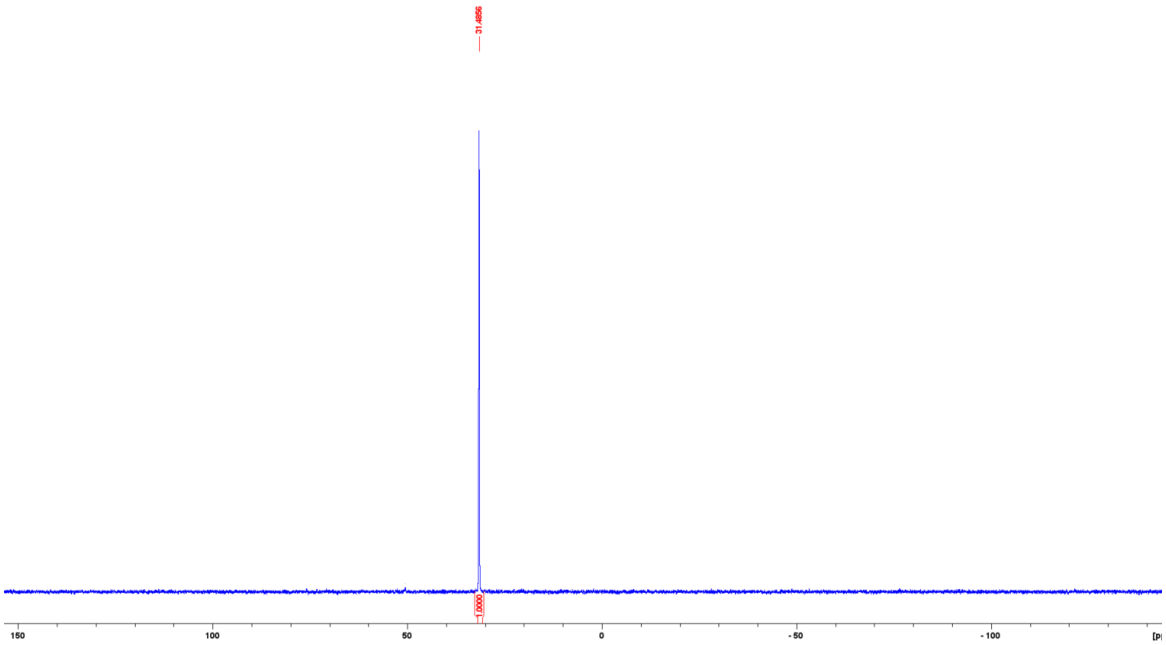

^{31}P NMR (243 MHz, $CDCl_3$) of **65c**

1,4- di(tricyclohexyl phosphonium) butane dibromide (74b)

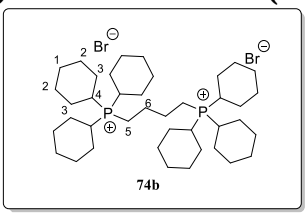

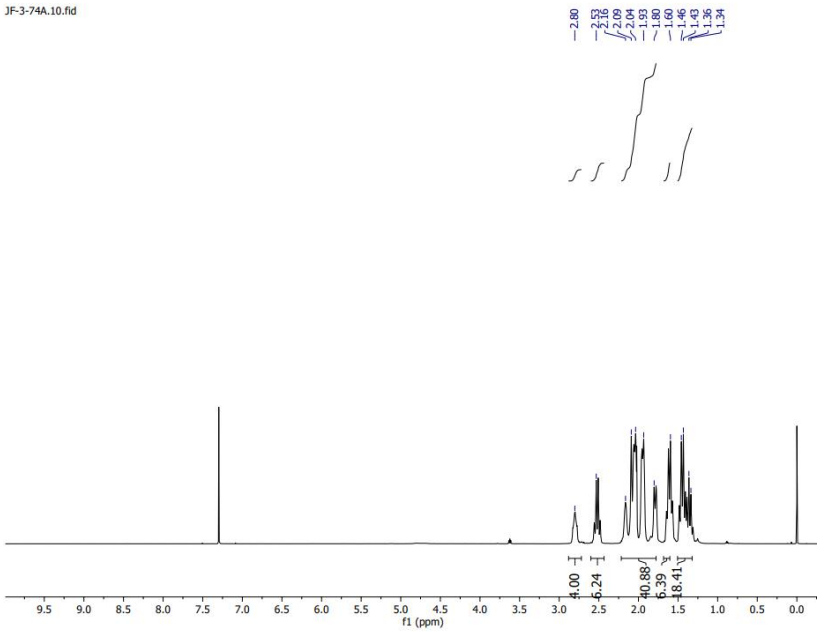

^{1}H NMR (500 MHz, $CDCl_3$) of **74b**

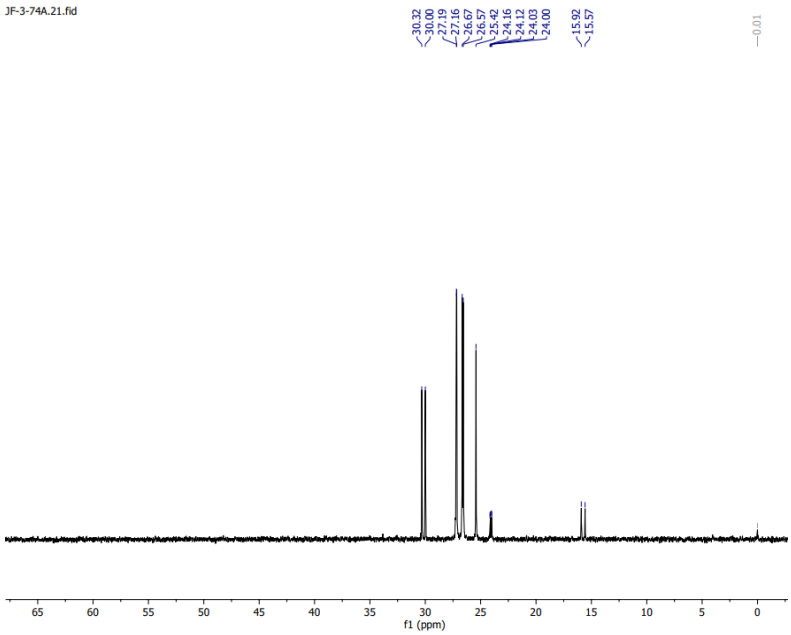

^{13}CNMR(125 MHZ, $CDCl_3$) of **74b**

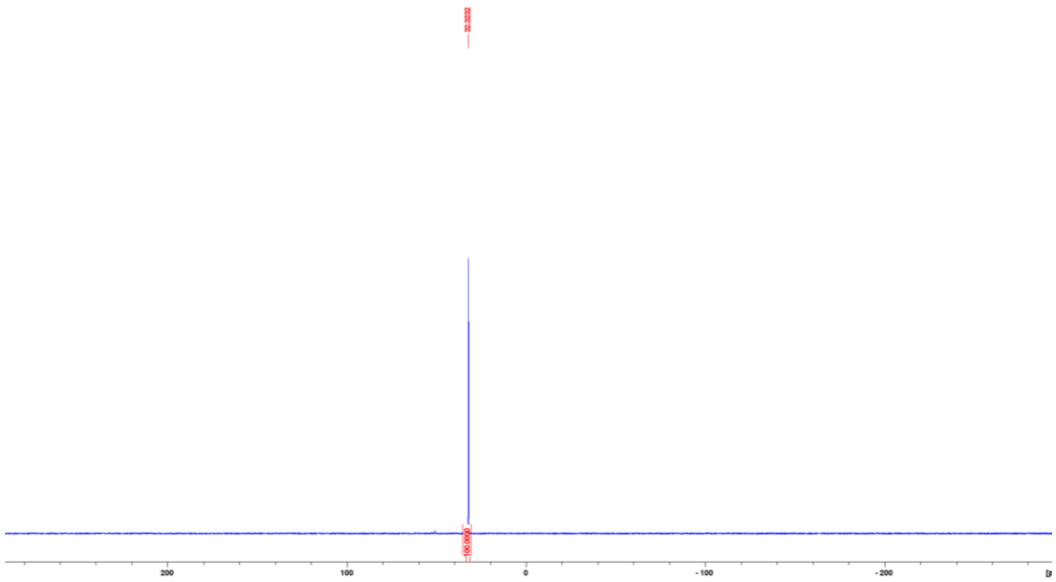

^{31}P NMR (243 MHz, $CDCl_3$) of **74b**

1,3-di(tricyclohexyl phosphonium) propane dibromide (74a)

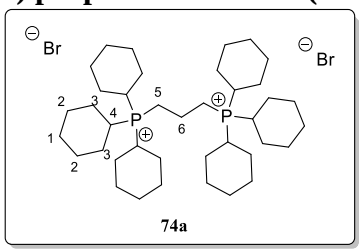

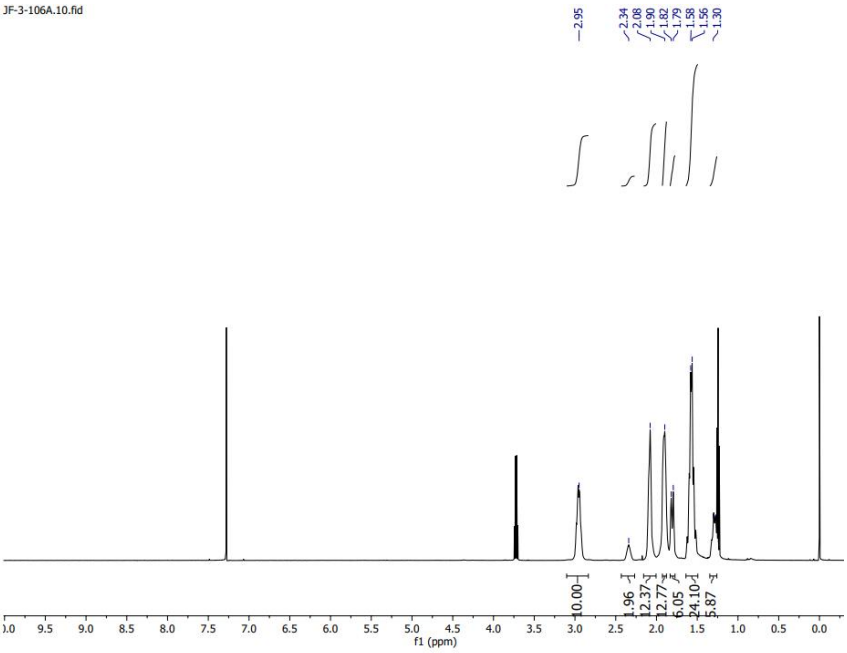

^{1}H NMR (500 MHz, $CDCl_3$) of **74a**

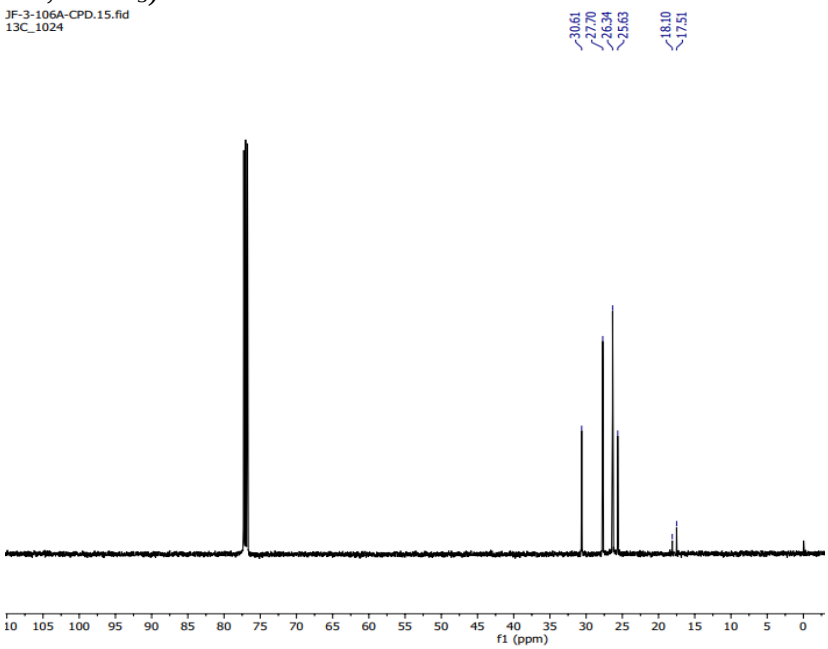

^{13}CNMR(125 MHZ, $CDCl_3$) of **74a**

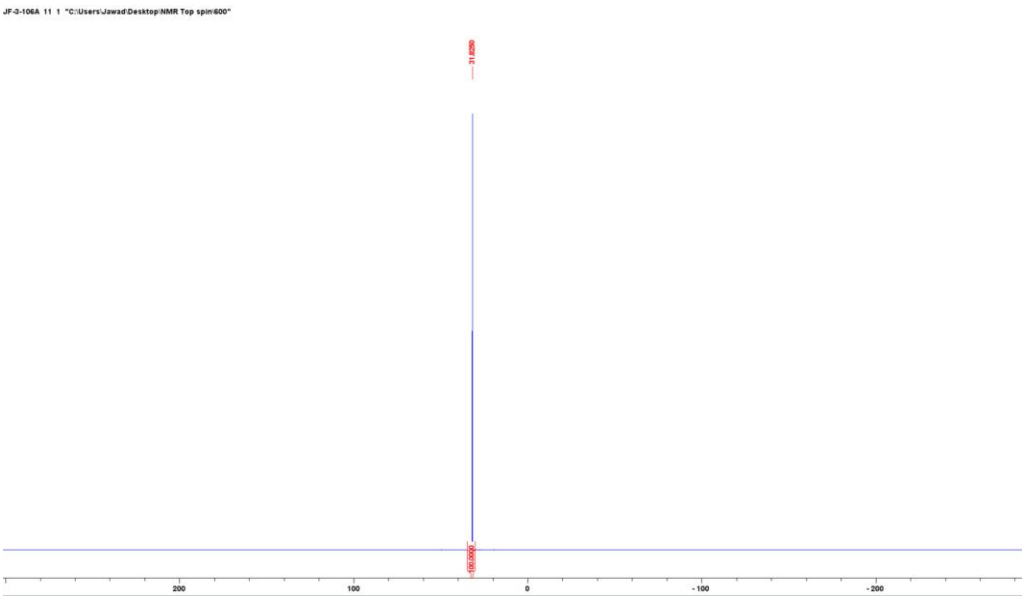

^{31}P NMR (243 MHz, $CDCl_3$) of **74a**

1,6- di(tricyclohexyl phosphonium) hexane dibromide (74d)

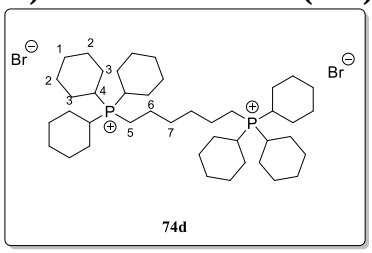

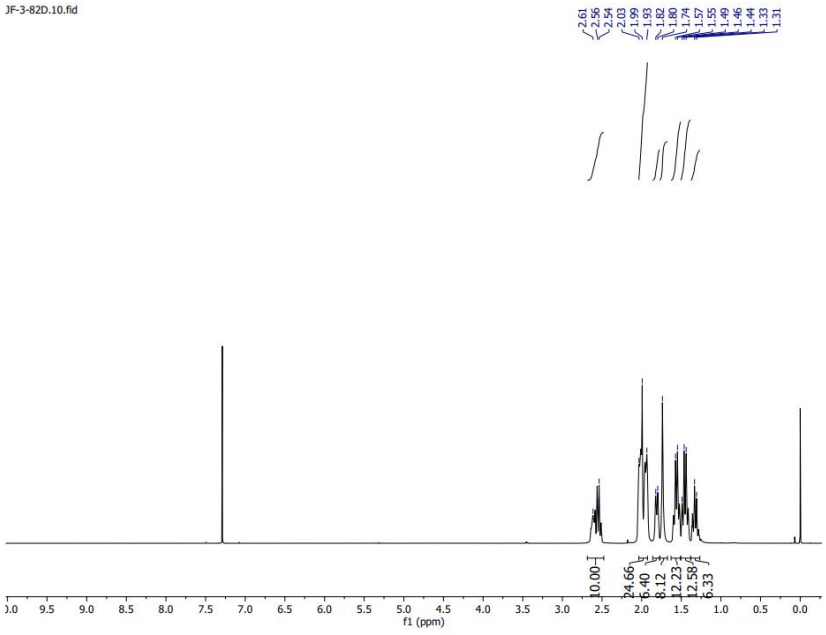

^{1}H NMR (500 MHz, $CDCl_3$) of **74d**

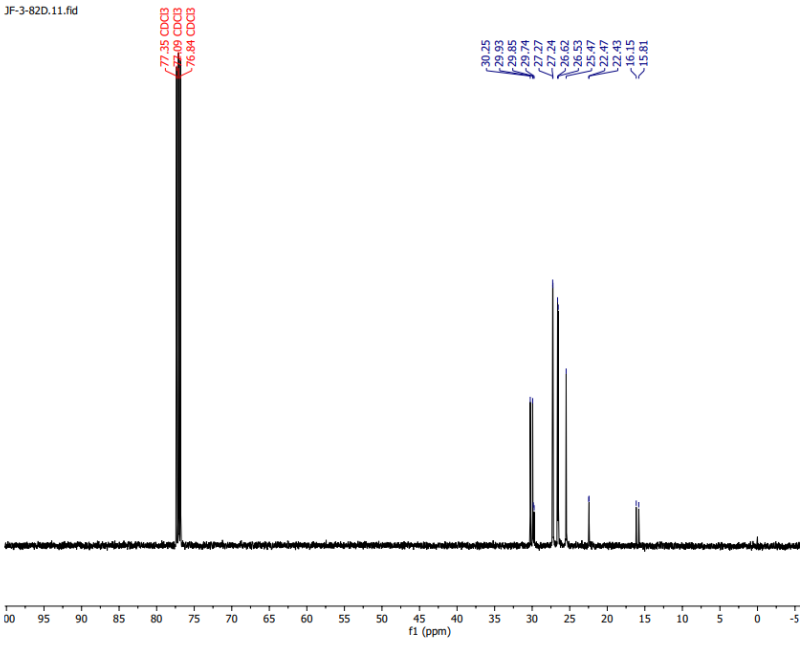

^{13}CNMR (150 MHZ, $CDCl_3$) of **74d**

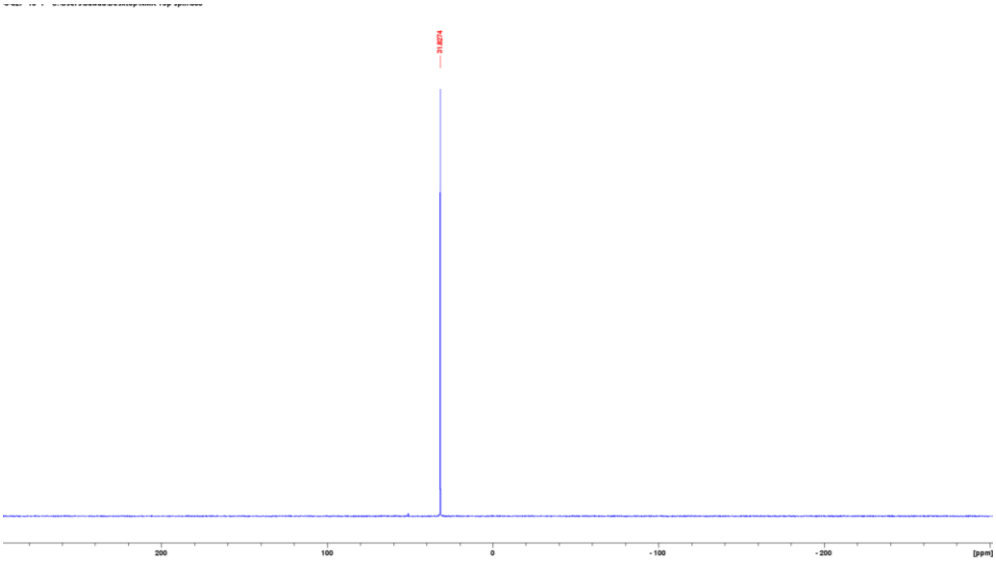

^{31}P NMR (243 MHz, $CDCl_3$) of **74d**

4-N,N- diethyl-N-methyl ammonium Triflate [2.2] paracyclophane (71)

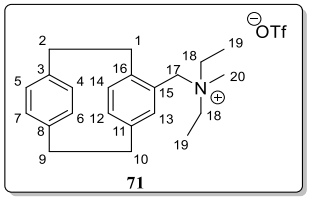

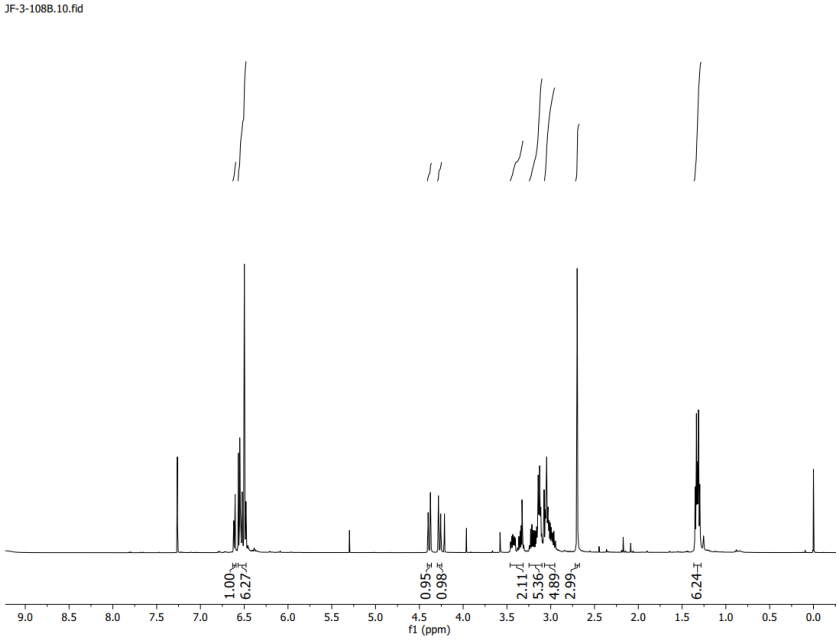

^{1}H NMR (500 MHz, $CDCl_3$) of **71**

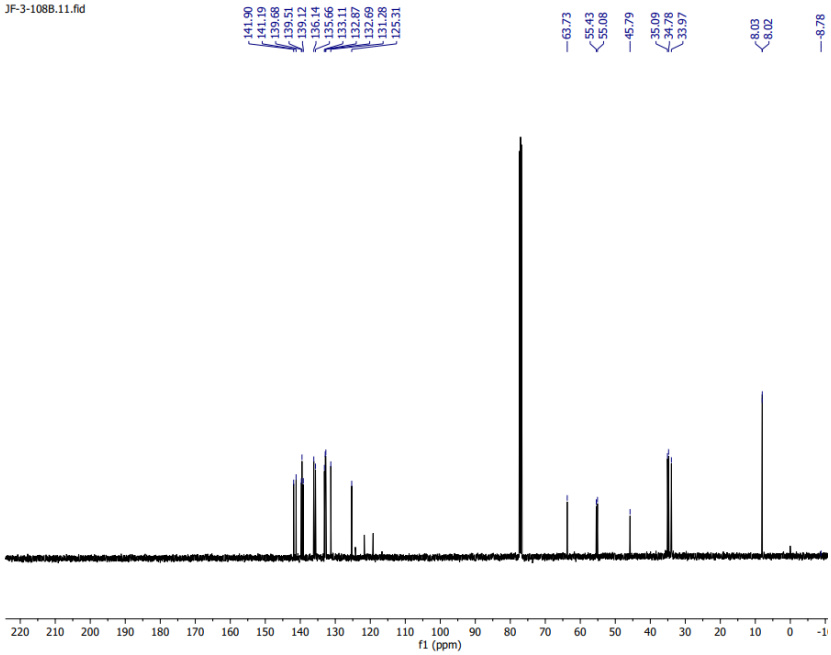

^{13}C NMR (126 MHz, $CDCl_3$) of **71**

Tricyclohexyl(phenyl)phosphonium trifluoromethanesulfonate (65g)

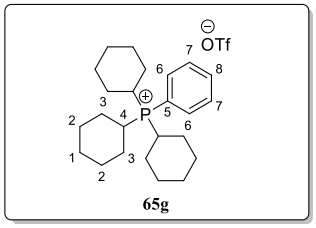

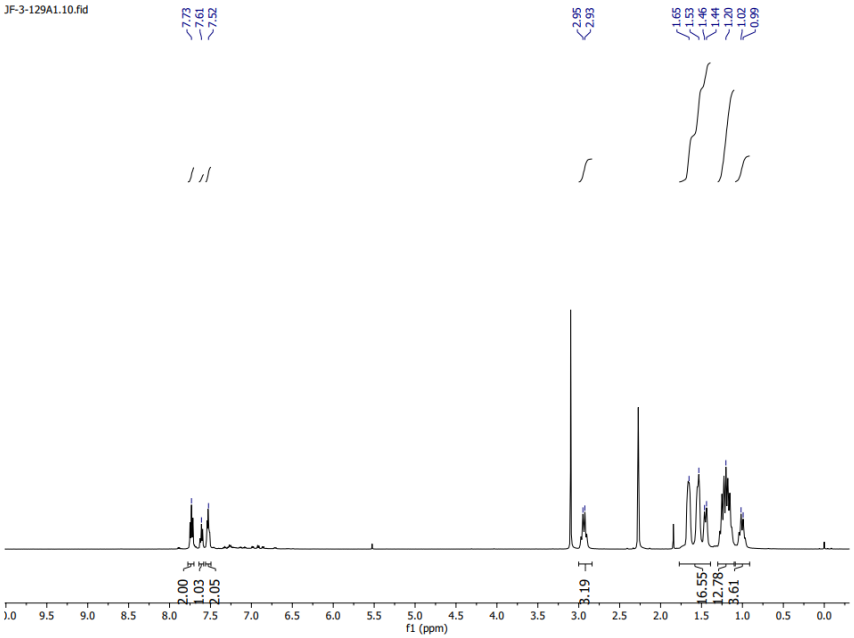

^{1}H NMR (500 MHz, $CDCl_3$) of **65g**

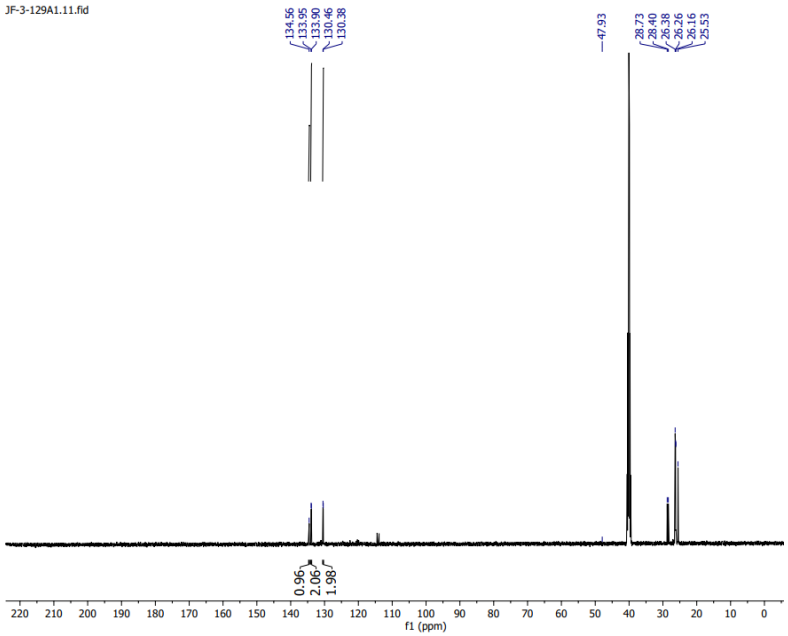

^{13}C NMR (125 MHz, $CDCl_3$) of **65g**

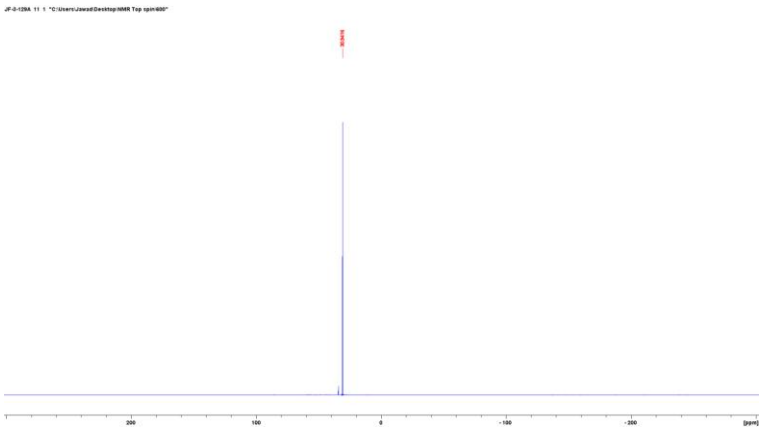

^{31}P NMR (243 MHz, DMSO) of **65g**

tricyclohexyl(ethyl)phosphonium Iodide (65b):

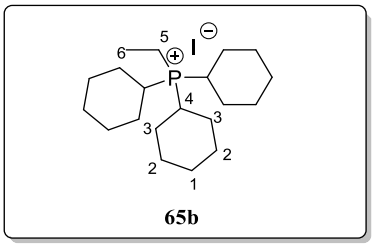

65b

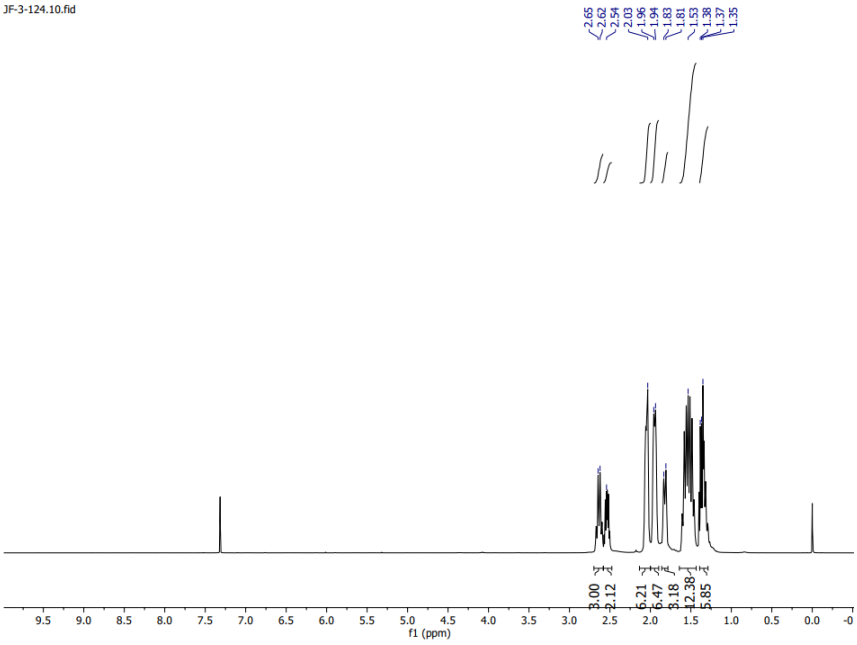

^{1}H NMR (500 MHz, $CDCl_3$) of **65b**

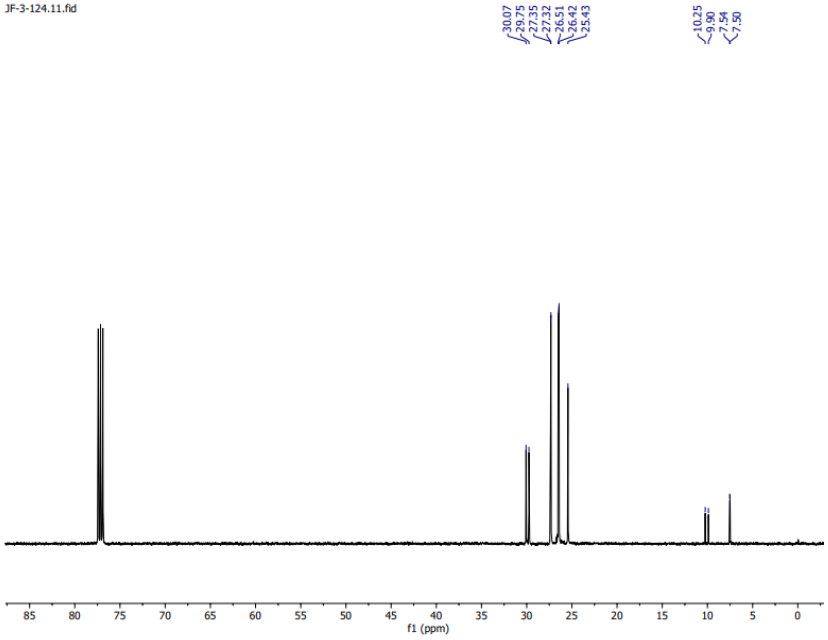

^{13}C NMR (126 MHz, $CDCl_3$) of **65b**

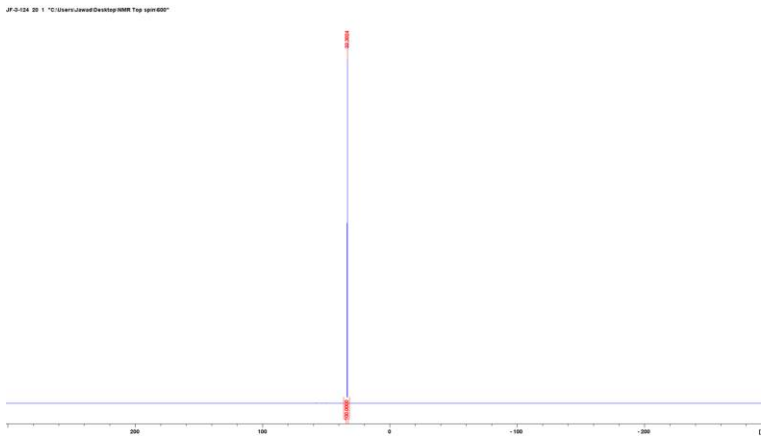

^{31}P NMR (243 MHz, $CDCl_3$) of **65b**

Diethyl (2-((4-methyl-N-((trimethylsilyl)ethynyl)phenyl)sulfonamido)phenyl)phosphonate (146a)

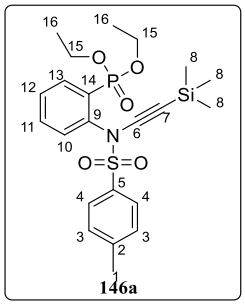

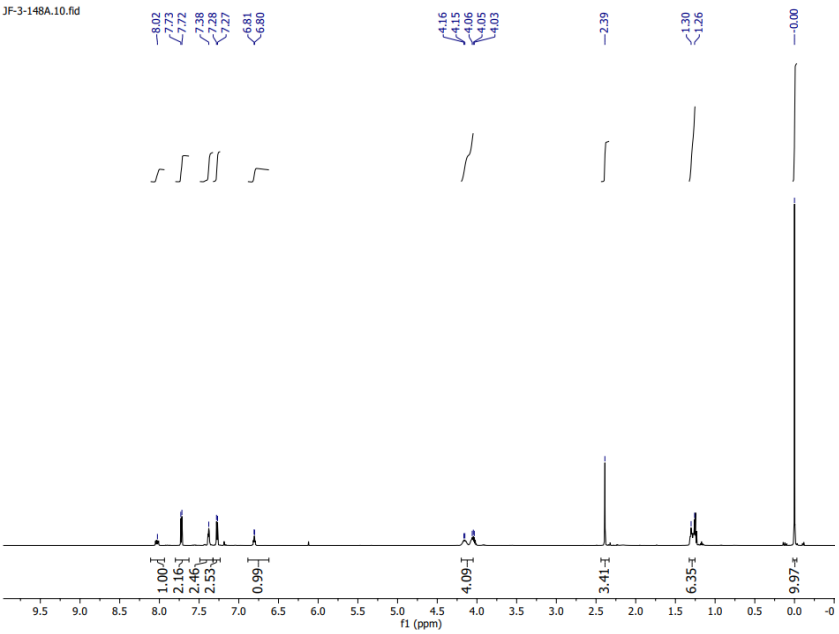

^{1}H NMR (600 MHz, $CDCl_3$) of **146a**

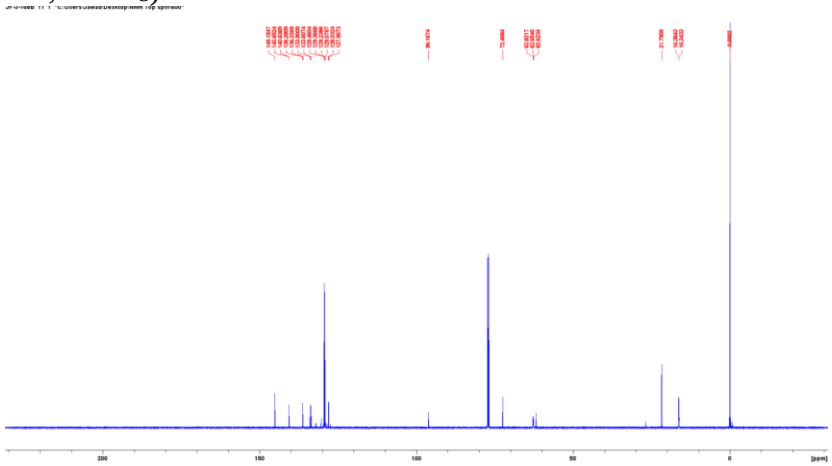

^{13}C NMR (150 MHz, $CDCl_3$) of **146a**

N-(diphenylphosphoryl)-4-methyl-N-(trimethylsilyl)benzenesulfonamide (146b)

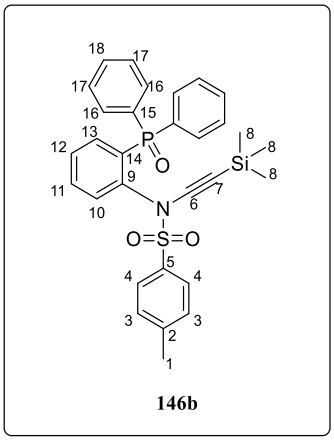

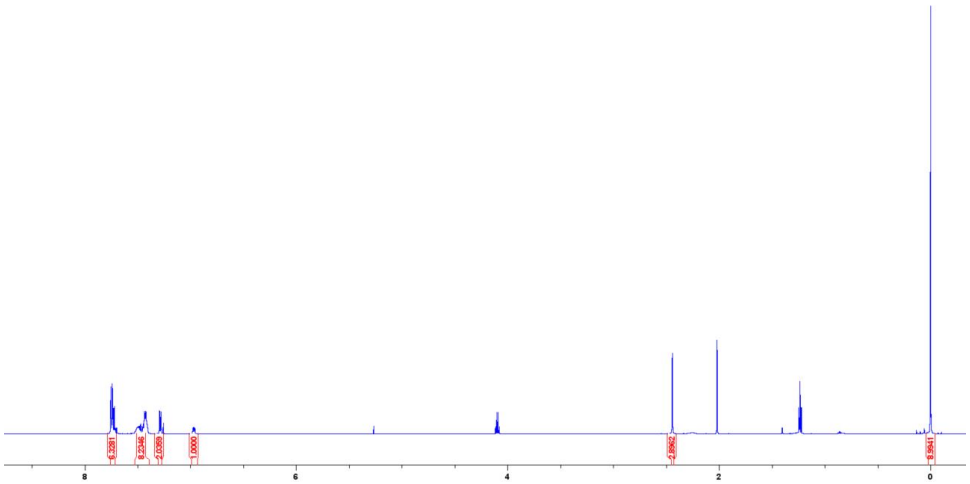

^{1}H NMR (600 MHz, $CDCl_3$) of **146b**

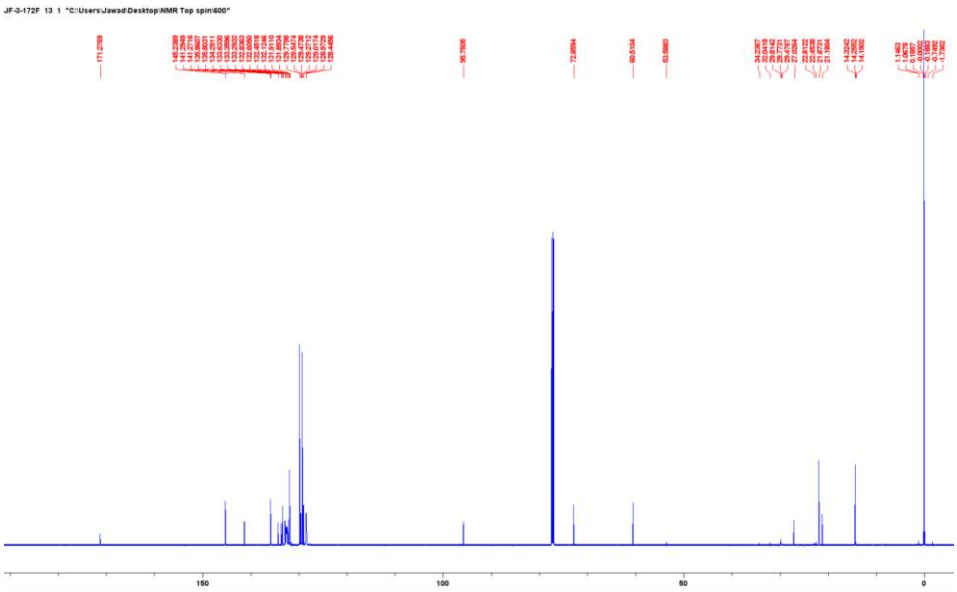

^{13}C NMR (150 MHz, $CDCl_3$) of **146b**

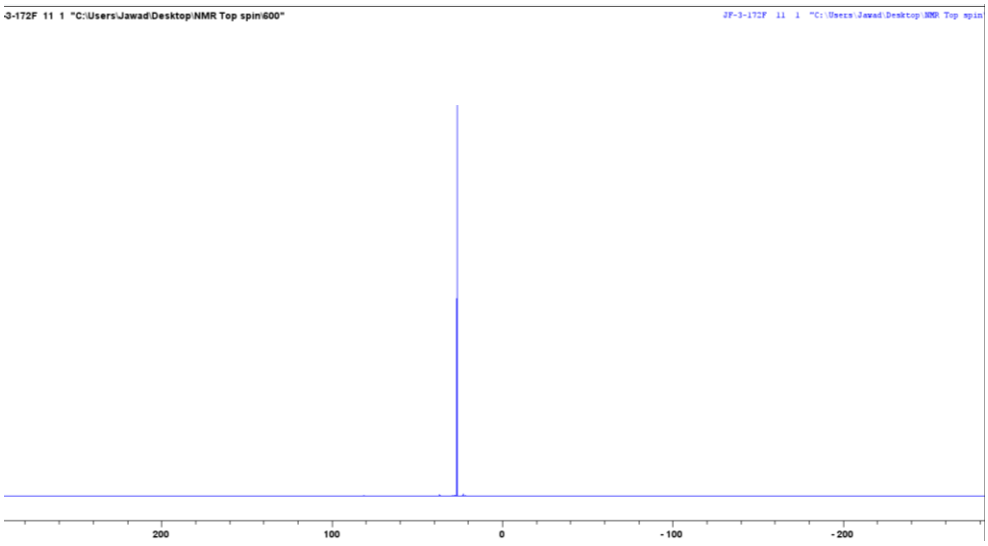

^{31}P NMR (243 MHz, $CDCl_3$) of **146b**

Abstract

Zeolites are uniformly crystalline porous materials formed of a vertex sharing TO_4 units (T= Si, Al, Ge, etc.). They are prepared under hydrothermal conditions, by mixing a suitable structure directing agent (SDA) with a gel containing inorganic components such as silica, alumina or germanium. At specific pH and temperature, the SDA induces nucleation, seed formation and crystal growth to obtain zeolites with specific size, shape and dimension. Extra-large pore size zeolites with pore aperture larger than 0.75 nm aroused increasing interest from researchers due to their promising activity in processing bulkier molecules, improving diffusion rate, prolonging the catalyst lifetime and changing product selectivity. Our goal is to prepare SDA's having different alkyl substituents following size expansion approach, by synthesizing-ammonium salts containing either one or two alkyne moieties. Furthermore, ammonium salts based on imidazole, hexamethyl-enetetramine and 4-phenylpyridine compounds – as well as synthetic paths for the preparation of [2.2] paracyclophane based ammonium salts using King's reaction were explored. Additionally, organic salts based on phosphorous were synthesized. Preparation, purification and preliminary results of their use as SDAs in zeolite synthesis will be shown in this thesis.

Keywords: Zeolites; Extra Large pore; ZEO-1; Synthesis; Ammonium salts; Phosphonium salts; SDA's

Résumé

Les zéolites sont des matériaux poreux cristallins uniformesformés d'unités TO_4 partageant un sommet (T = Si, Al, Ge, etc.). Ils sont préparés sous des conditions hydrothermales, en mélangeant un agent directeur de structure (SDA) approprié avec un gel contenant des composants inorganiques tels que la silice, l'alumine ou le germanium. À un pH et une température spécifiques, le SDA induit la nucléation et la croissance cristalline pour obtenir des zéolites de taille, de forme et de dimension spécifiques. Les zéolites à pores de taille extra-large avec une ouverture de pore supérieure à 0,75 nm suscitent un intérêt croissant de la part des chercheurs en raison de leur activité prometteuse dans le traitement de molécules plus volumineuses, de l'amélioration de la vitesse de diffusion, de la prolongation de la durée de vie du catalyseur et du changement de la sélectivité du produit.

Notre objectif est de préparer des SDA avec des substitutions alkyliques différentes en suivant une approche d'expansion de taille, en synthétisant des sels d'ammonium contenant une ou deux entités alcyne. De plus, des sels d'ammonium à base d'imidazole, d'hexaméthylénétanétramine et de composés de 4-phénylpyrridine - ainsi que des voies de synthèse pour la préparation de sels d'ammonium à base de [2.2] paracyclophane en utilisant la réaction de King ont été explorées. En outre, des sels organiques à base de phosphore ont été synthétisés. La préparation, la purification et les premiers résultats de leur utilisation comme SDA dans la synthèse des zéolites seront présentés dans cette thèse.

Mots-clés : Zéolites; Pore extra-large; ZEO-1; Synthèse; Sels d'ammonium, Sels de phosphonium; SDA.